



**HYBRID CONTROL FOR POSE STABILIZATION USING DUAL
QUATERNIONS**

HUGO TADASHI MUNIZ KUSSABA

**TESE DE DOUTORADO EM ENGENHARIA DE SISTEMAS ELETRÔNICOS E
AUTOMAÇÃO
DEPARTAMENTO DE ENGENHARIA ELÉTRICA**

**FACULDADE DE TECNOLOGIA
UNIVERSIDADE DE BRASÍLIA**

UNIVERSIDADE DE BRASÍLIA
FACULDADE DE TECNOLOGIA
DEPARTAMENTO DE ENGENHARIA ELÉTRICA

**CONTROLE HÍBRIDO PARA ESTABILIZAÇÃO DE POSE USANDO
QUATERNIONS DUAIS**

**HYBRID CONTROL FOR POSE STABILIZATION USING DUAL
QUATERNIONS**

HUGO TADASHI MUNIZ KUSSABA

ORIENTADOR: PROF. DR. JOÃO YOSHIYUKI ISHIHARA

TESE DE DOUTORADO EM ENGENHARIA DE SISTEMAS
ELETRÔNICOS E AUTOMAÇÃO

PUBLICAÇÃO: PPGEA.TD-128/2018

BRASÍLIA/DF: MARÇO - 2018

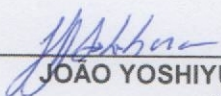
UNIVERSIDADE DE BRASÍLIA
FACULDADE DE TECNOLOGIA
DEPARTAMENTO DE ENGENHARIA ELÉTRICA

HYBRID CONTROL FOR POSE STABILIZATION USING DUAL
QUATERNIONS

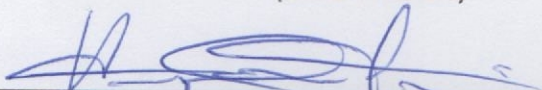
HUGO TADASHI MUNIZ KUSSABA

TESE DE DOUTORADO SUBMETIDA AO DEPARTAMENTO DE ENGENHARIA ELÉTRICA DA
FACULDADE DE TECNOLOGIA DA UNIVERSIDADE DE BRASÍLIA, COMO PARTE DOS
REQUISITOS NECESSÁRIOS PARA A OBTENÇÃO DO GRAU DE DOUTOR.

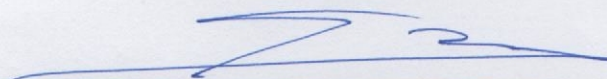
APROVADA POR:



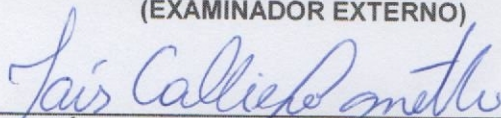
JOAO YOSHIYUKI ISHIHARA, Dr., ENE/UNB
(ORIENTADOR)



HENRIQUE CEZAR FERREIRA, Dr., ENE/UNB
(EXAMINADOR INTERNO)



FERNANDO CESAR LIZARRALDE, Dr., UFRJ
(EXAMINADOR EXTERNO)



TAÍS CALLIERO TOGNETTI, Dra., FGA/UNB
(EXAMINADORA EXTERNA)

Brasília, 26 de março de 2018.

FICHA CATALOGRÁFICA

KUSSABA, HUGO TADASHI M.,

Hybrid control for pose stabilization using dual quaternions [Distrito Federal] 2018.

viii+128 p., 210 x 297 mm (ENE/FT/UnB, Doutor, Engenharia de Sistemas Eletrônicos e Automação, 2018).

TESE DE DOUTORADO – Universidade de Brasília, Faculdade de Tecnologia.

Departamento de Engenharia Elétrica

1. Sistemas dinâmicos

2. Grupos de Lie

3. Controle não-linear

4. Sistemas híbridos

I. ENE/FT/UnB

II. Título (série)

REFERÊNCIA BIBLIOGRÁFICA

KUSSABA, H. T. M. (2018). Hybrid control for pose stabilization using dual quaternions, TESE DE DOUTORADO, Publicação PPGEA.TD-128/2018, Departamento de Engenharia Elétrica, Universidade de Brasília, Brasília, DF, viii+128.

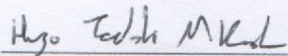
CESSÃO DE DIREITOS

AUTOR: Hugo Tadashi Muniz Kussaba

TÍTULO: Hybrid control for pose stabilization using dual quaternions.

GRAU: Doutor ANO: 2018

É concedida à Universidade de Brasília permissão para reproduzir cópias desta tese de doutorado e para emprestar ou vender tais cópias somente para propósitos acadêmicos e científicos. O autor reserva outros direitos de publicação e nenhuma parte dessa tese de doutorado pode ser reproduzida sem autorização por escrito do autor.



Hugo Tadashi Muniz Kussaba

Departamento de Eng. Elétrica (ENE) - FT

Universidade de Brasília (UnB)

Campus Darcy Ribeiro

CEP 70919-970 - Brasília - DF - Brasil

ACKNOWLEDGMENTS

Agradeço a Deus, pela vida e pela graça e amor de Jesus Cristo. Agradeço também aos familiares pelo amor incondicional, em especial meu pai e minha mãe.

Sou grato aos professores da UnB, sobretudo os professores João Ishihara, Renato Borges e Eduardo Tognetti: essa tese não seria possível sem a orientação do sensei Ishihara, 1° dan em publicações científicas de automação e controle. Muito aprendi com seus ensinamentos e com sua análise detalhista e precisa. Com os professores Renato Borges e Eduardo Tognetti também tive muitas discussões frutíferas, em especial sobre a técnica e a arte das desigualdades matriciais lineares.

Agradeço aos amigos, pelos bons momentos e companheirismo, principalmente aos colegas do LARA. Gostaria de agradecer especialmente aos colegas e amigos Henrique Menegaz, Luis Figueredo e Paulo Pércio, com os quais tive o privilégio de trabalhar junto e escrever vários resultados durante o período de doutorado.

Finalmente, agradeço com muita satisfação os participantes da banca de qualificação e da defesa final desta tese: prof. Edson Roberto de Pieri, prof. Fernando Lizarralde, prof. Henrique Cezar Ferreira e profa. Taís Calliero Tognetti. Os conselhos e sugestões são de fundamental importância para este trabalho.

Pelos vários suportes financeiros, agradeço as agências de fomento à pesquisa CAPES, CNPq, DPP/UnB e FAP-DF. Também agradeço ao IMA (Institute for Mathematics and Applications) pelo apoio financeiro para minha participação no workshop “Distributed Control and Decision Making Over Networks” e pela sociedade de controle da IEEE, IEEE CSS, que me apoiou financeiramente para participação no congresso “54th IEEE Conference on Decision and Control”. Pude aprender bastante nesses dois congressos e tive vários insights para vários trabalhos. Não obstante, agradeço aos desenvolvedores dos softwares Inkscape e do LyX, ferramentas que facilitaram bastante a redação desta tese.

RESUMO

Título: Hybrid control for pose stabilization using dual quaternions

Autor: Hugo Tadashi Muniz Kussaba

Orientador: Prof. Dr. João Yoshiyuki Ishihara

Motivado tanto pelas vantagens da representação em dual quatérnios duais e por problemas relativos à obstrução topológica de se ter um equilíbrio assintótico globalmente estável, esse trabalho visa usar o formalismo de quaternion dual e as ferramentas de sistemas dinâmicos híbridos para tratar o problema de estabilização de pose de corpos rígidos. O grupo de Lie dos quatérnios duais proporciona um modo eficiente de representar a cinemática linear e rotacional de um corpo rígido sem singularidades. Algumas estratégias híbridas são propostas para lidar com o problema de “chattering” presente em todos os controladores por realimentação descontínuos enquanto ao mesmo tempo garantindo atratividade global da pose de estabilização do corpo rígido.

ABSTRACT

Title: Controle híbrido para estabilização de pose usando quaternions duais

Author: Hugo Tadashi Muniz Kussaba

Supervisor: Prof. Dr. João Yoshiyuki Ishihara

Motivated both by the advantages of the dual quaternion representation and by the problems concerning the topological obstruction to global asymptotic stability, this work addresses the rigid body pose stabilization problem using dual quaternion formalism and dynamic hybrid systems tools. The Lie group of unit dual quaternions provides a computationally efficient way to represent coupled linear and rotational kinematics without singularities. Some hybrid control strategies are proposed to overcome the chattering problem present in all discontinuous-based feedback controllers while at same time also guaranteeing global attractivity of the stabilization pose of the rigid body.

CONTENTS

SYMBOLS LIST	VI
1 INTRODUCTION	1
1.1 POSE CONTROL OF RIGID-BODIES	1
1.1.1 WHY TO USE QUATERNIONS AND DUAL-QUATERNIONS?	2
1.1.2 WHY TO USE HYBRID CONTROL?	4
1.2 CONTRIBUTIONS	5
1.2.1 PUBLISHED AND SUBMITTED PAPERS	6
1.3 MANUSCRIPT ORGANIZATION	7
2 PRELIMINARIES	8
2.1 SET-VALUED ANALYSIS	8
2.1.1 SET-VALUED FUNCTIONS	9
2.1.2 DIFFERENTIAL AND DIFFERENCE INCLUSIONS	12
2.2 DYNAMICAL HYBRID SYSTEMS	13
2.2.1 SOLUTIONS TO HYBRID SYSTEMS	15
2.2.2 STABILITY OF HYBRID SYSTEMS	17
2.2.3 GENERALIZED SOLUTIONS AND ROBUSTNESS OF HYBRID SYSTEMS	19
2.3 QUATERNIONS	23
2.3.1 UNIT QUATERNIONS	25
2.3.2 ROTATION KINEMATICS	27
2.4 DUAL QUATERNIONS	27
2.4.1 UNIT DUAL QUATERNIONS	29
2.4.2 RIGID BODY KINEMATIC EQUATIONS	31
2.4.3 RIGID BODY DYNAMIC EQUATIONS	32
3 CHALLENGES OF RIGID-BODY POSE STABILIZATION AND PRIOR WORK	35
3.1 INTRODUCTION	35
3.2 A TOPOLOGICAL OBSTRUCTION TO GLOBAL STABILIZATION BY CONTINUOUS FEEDBACK	35
3.3 THE UNWINDING PHENOMENA	36
3.4 DISCONTINUOUS CONTROLLERS AND THE VULNERABILITY TO SMALL AMPLITUDE MEASUREMENT NOISES PROBLEM	37
4 FIRST PROPOSED HYBRID SOLUTION FOR A ROBUST KINEMATIC CONTROLLER	41
4.1 INTRODUCTION	41
4.2 KINEMATIC HYBRID CONTROL LAW FOR ROBUST GLOBAL POSE STABILITY	41
4.3 NUMERICAL SIMULATIONS	47
4.4 CHAPTER CONCLUSIONS	51
5 BIMODAL KINEMATIC CONTROLLER WITH EXPONENTIAL CONVERGENCE	54
5.1 INTRODUCTION	54
5.2 BIMODAL CONTROLLER WITH EXPONENTIAL CONVERGENCE	54
5.3 STABILITY ANALYSIS OF THE BIMODAL KINEMATIC CONTROLLER	56

5.4 NUMERICAL SIMULATIONS	59
5.5 CHAPTER CONCLUSIONS	63
6 HYBRID DYNAMIC CONTROLLER.....	64
6.1 INTRODUCTION	64
6.2 DYNAMICS OF THE POSE TRACKING PROBLEM.....	64
6.2.1 DUAL QUATERNION ERROR KINEMATICS	65
6.2.2 DYNAMICS OF THE TWIST ERROR.....	67
6.2.3 FULL DYNAMICS OF TRACKING PROBLEM	68
6.3 PROPOSED BIMODAL HYBRID DYNAMIC POSE TRACKING CONTROLLER	69
6.4 DYNAMICS STABILITY ANALYSIS	70
6.5 STABILIZING CONTROLLER	73
6.6 NUMERICAL SIMULATIONS	74
6.7 CHAPTER CONCLUSIONS	76
7 CONCLUSION	78
A ALGEBRAIC STRUCTURES	80
B RESULTS ON TOPOLOGY.....	87
B.1 THE IMPOSSIBILITY OF A GLOBAL THREE DIMENSIONAL PARAMETERIZATION FOR $SO(3)$ WITHOUT SINGULAR POINTS.....	87
B.2 A TOPOLOGICAL OBSTRUCTION TO GLOBAL STABILITY	87
B.3 POINCARÉ-HOPF INDEX THEOREM	92
C PUBLISHED ARTICLES RELATED TO THE THESIS	95
BIBLIOGRAPHY.....	121
INDEX	128

List of Figures

1.1	Some examples where pose control is crucial: (a) Pointing a satellite antenna to a ground station. (b) While welding, a robotic manipulator has to control not only the position of the welding tool, but also its orientation. (c) An unmanned aerial vehicle holding a camera to record a sport game or making a surveillance of an area must have both position and orientation precisely controlled in order to achieve its objectives.	1
2.1	Regularization of a scalar discontinuous function f . (a) Graph of f near a neighborhood of x^* . (b) Image of f near a neighborhood of x^* . (c) Krasovskii regularization of f evaluated at the point x^*	13
2.2	Hybrid trajectory. The blue trajectory represents a continuous evolution (the <i>flow</i> of the system) and the red trajectory represents a discrete evolution (the <i>jump</i> of the system).	14
2.3	Example of a non-robust hybrid system. The blue continuous arrow represents the flow of the solution and the red dashed arrow represents the jumps of the solution. (a) The origin is globally asymptotically stable in hybrid system given by (2.6). (b) After taking the closure of the jump set, the origin is not more globally asymptotically stable: there is a solution starting at 1 that remains at 1 through an infinite number of jumps.	20
2.4	Enlarged set \hat{C} generated by Krasovskii regularization.	21
2.5	Illustration of the practical stability of Theorem 2.9. (a) Nominal hybrid system \mathcal{H} . (b) Perturbed hybrid system by a constant δ -perturbation.	23
2.6	Rotation represented by a unit quaternion $\mathbf{r} = \cos(\theta/2) + \sin(\theta/2)\mathbf{n}$. The vector v is rotated an angle θ about the axis (n_1, n_2, n_3) resulting in the vector v'	26
3.1	Illustration of unwinding problem using a continuous controller. The unit-norm quaternion $\mathbf{q} = \eta + \boldsymbol{\mu}$ represents the current attitude of the satellite illustrated in the figure. Since $\eta^2 + \ \boldsymbol{\mu}\ ^2 = 1$, this quaternion is in the unit half-circle of the figure. Supposing that the initial attitude of the satellite is described by quaternion A and point 1 is unstable, the satellite will rotate towards the further equilibrium point -1 , although the quaternions -1 and 1 describe the same attitude.	37
3.2	Illustration of chattering problem when using a discontinuous vector field to control the attitude of a satellite. The unit-norm quaternion $\mathbf{q} = \eta + \boldsymbol{\mu}$ represents the current attitude of the satellite illustrated in the figure. Since $\eta^2 + \ \boldsymbol{\mu}\ ^2 = 1$, this quaternion is in the unit half-circle of the figure. (a) In this state, the real attitude of satellite is described by quaternion A . However, due to noise, the measurement sensor outputs that the satellite is quaternion B , causing it to rotate in the wrong direction. (b) In this state, the real attitude of satellite is described by quaternion B . However, due to noise, the measurement sensor outputs that the satellite is quaternion A , causing it to rotate again in the wrong direction.	38
3.3	Time-simulation of discontinuous control law (3.2) in presence of a random measurement noise (note that the measurement noise is turned off after 20 seconds of simulation). (a) Trajectory of the rotation unit quaternion $\mathbf{r} = \eta + \boldsymbol{\mu} = \eta + \mu_1\hat{i} + \mu_2\hat{j} + \mu_3\hat{k}$ and switches $s(t)$ along time t . (b) Trajectory of the three-dimensional translation elements $\mathbf{p} = p_1\hat{i} + p_2\hat{j} + p_3\hat{k}$	40

4.1	Illustration of the hysteretic control strategy. The unit-norm quaternion $\mathbf{q} = \eta + \boldsymbol{\mu}$ represents the current attitude of the satellite illustrated in the figure. Since $\eta^2 + \ \boldsymbol{\mu}\ ^2 = 1$, this quaternion is in the unit half-circle of the figure. The discrete variable h indicates if the target equilibrium should be -1 or 1 . The state variable h will only change according to the hysteretic curve of Fig. 4.2(a).	42
4.2	Curves illustrating how the state h changes according to the state variable η . (a) Hysteresis curve for $\delta > 0$. (b) When δ tends to 0, the hysteresis curve will behave as the graph of the sgn function, that is, without memory and with a discontinuity on $\eta = 0$	43
4.3	Numerical example for the hybrid controller: (a) Trajectory of the rotation unit quaternion \mathbf{r} in terms of η and $\boldsymbol{\mu}$ (dashed line). (b) Trajectory of the three-dimensional translation elements $\mathbf{p} = p_1\hat{i} + p_2\hat{j} + p_3\hat{k}$	48
4.4	Trajectory of η with hybrid feedback controller (4.1) and discontinuous controller (3.2) over time.	48
4.5	The number of switches with regard to the hysteresis parameter δ is shown in (a), while the switches along time $s(t)$ are illustrated in (b) for different values of δ	49
4.6	Influence of the hysteresis parameter δ on unwinding— η converges to the farther stable point when the value of δ increases.	50
4.7	Trajectory of the rotation unit quaternion \mathbf{r} in terms of η and $\boldsymbol{\mu}$ using the proposed hybrid controller (<i>left</i>), the discontinuous controller (<i>center</i>), and the continuous feedback controller (<i>right</i>). The unwinding phenomenon arises only on the continuous feedback controller.	50
4.8	Trajectory of the three-dimensional translation error using the hybrid (<i>solid line</i>), the discontinuous (<i>red dashed line</i>) and the continuous controller (<i>magenta dashed line</i>).	51
4.9	Simulation snapshots of the robotic manipulator using the continuous controller. When the dual quaternion representing the desired robot pose is changed from $\underline{\mathbf{q}}$ to $-\underline{\mathbf{q}}$ (both represents the same pose), the unwinding phenomenon can be observed. In contrast to maintaining the desired pose, the robotic manipulator goes through unexpected and unnecessary longer motions. In all snapshots, the light red robot represents the initial robot configuration. ¹	52
4.10	The left figure shows the trajectory of the rotation error in terms of the scalar part η using the hybrid (<i>solid line</i>) and the discontinuous controller (<i>red dashed line</i>). The right figure shows the trajectory of the three-dimensional translation elements $\mathbf{p} = p_1\hat{i} + p_2\hat{j} + p_3\hat{k}$ with reference given in dotted blue line.	52
5.1	State space representation of the quaternionic part of the bimodal controller. Arrows indicate the direction of the rotation. (Figure based on Fig. 5.2 of [1]).	55
5.2	Block diagram of the closed-loop system.	59
5.3	Trajectory of the real primary part of the dual quaternion $\underline{\mathbf{q}}$	60
5.4	Evolution of the norm of angular velocity $\boldsymbol{\omega}$	61
5.5	Evolution of the norm of position expressed in the reference frame.	62
5.6	Evolution of the norm of position expressed in the reference frame.	63
6.1	Comparison between dynamic controllers in the presence (red dashed line) and absence (blue solid line) of disturbances. The left graphics show the time evolution of the dynamic controller proposed in [2] and the right graphics show the time evolution of the proposed dynamic controller.	75
6.2	Compared total control effort (force and torque) between proposed dynamic hybrid controller (right plot) and the memoryless discontinuous controller of [2] (left plot).	76

B.1	Homotopy mapping H induced by the semi-flow of the system in a neighborhood of the global equilibrium point x_0 . The map is illustrated for points x_1, \dots, x_5 at times $t = 0$ and $t = 0.5$. At time $t = 1$, the map $x \mapsto H(1, x)$ is equal to the constant map x_0	89
B.2	Example of a vector bundle: the trivial bundle given by $\mathcal{S}^1 \times \mathbb{R}$	90
B.3	Möbius bundle.	90
B.4	Cutting Möbius strip along the base circle.	91
B.5	Semi-flow induced in the base space by the semi-flow on the bundle.	91
B.6	Vector fields on \mathbb{R}^2 and computation of its indices. All of the vector fields has an unique isolated equilibrium point in $(0, 0)$. (a) Vector field defined by $f_1(x, y) := (x, y)$. The equilibrium point can be seen to be unstable and source-like. (b) Vector field defined by $f_2(x, y) := (-x, y)$. The equilibrium point can be seen to be unstable and saddle-like. (c) Computation of $\text{ind}_{f_1}(0, 0)$: following the vector field f_1 counterclockwise along a circle gives a single complete revolution counterclockwise, thus $\text{ind}_{f_1}(0, 0) = 1$. (d) Computation of $\text{ind}_{f_2}(0, 0)$: following the vector field f_2 counterclockwise along a circle gives a single complete revolution clockwise, thus $\text{ind}_{f_2}(0, 0) = -1$	93

SYMBOLS LIST AND NOTATION

\emptyset	the empty set;
\mathbb{R}	set of real numbers;
\mathbb{R}_+^*	set of non-negative real numbers;
\mathbb{N}	set of natural numbers $(\{0, 1, \dots\})$;
\mathbb{B}	closed unit ball in \mathbb{R}^n , where n should be clear by context;
\mathbb{H}	set of quaternions;
\mathbb{H}_0	set of pure imaginary quaternions;
$\underline{\mathbb{H}}$	set of dual quaternions;
$\underline{\mathbb{H}}_0$	set of pure imaginary dual quaternions;
$\text{SO}(3)$	3-dimensional Lie group of rotations;
$\text{SE}(3)$	3-dimensional Lie group of rigid body motions;
$\text{Spin}(3)$	Lie group of unit norm quaternions;
$\text{Spin}(3) \times \mathbb{R}^3$	Lie group of unit norm dual quaternions;
S^n	n -dimensional sphere in \mathbb{R}^n ;
S^3	underlying manifold of unit norm quaternions;
\underline{S}	underlying manifold of unit norm dual quaternions;
\mathcal{KL}	class of continuous functions $\beta : \mathbb{R}_+^* \times \mathbb{R}_+^* \rightarrow \mathbb{R}_+^*$ such that for each fixed s , the function $\beta(r, s)$ is strictly increasing and $\beta(0, s) = 0$ and for each fixed r , the function $\beta(r, s)$ is decreasing and $\lim_{s \rightarrow \infty} \beta(r, s) = 0$;
$\mathbf{u} \cdot \mathbf{v}$	dot product between pure imaginary quaternions \mathbf{u} and \mathbf{v} ;
$\mathbf{u} \times \mathbf{v}$	cross product between pure imaginary quaternions \mathbf{u} and \mathbf{v} ;
$[\boldsymbol{\omega}]_{\times}$	matrix representation of the cross product $\boldsymbol{\omega} \times \cdot$;
$\text{Re}(\mathbf{q})$	real component of quaternion \mathbf{q} ;
$\text{Im}(\mathbf{q})$	imaginary component of quaternion \mathbf{q} ;
$\underline{\mathbf{Re}}(\mathbf{q})$	dual number component of dual quaternion \mathbf{q} ;
$\underline{\mathbf{Im}}(\mathbf{q})$	dual vector component of dual quaternion \mathbf{q} ;
$\mathcal{P}(\mathbf{q})$	primary part of dual quaternion \mathbf{q} ;
$\mathcal{D}(\mathbf{q})$	dual part of dual quaternion \mathbf{q} ;
$\overset{+}{\mathbf{H}}_4$	Hamilton operator for quaternions;
$\overset{+}{\mathbf{H}}$	Hamilton operator for dual quaternions;
\overline{S}	topological closure of set S ;
$\overline{\text{co}}(\cdot)$	closure of the convex hull;
$X + Y$	Minkowski sum between the sets X and Y ;
$\ x\ $	Euclidean norm of $x \in \mathbb{R}^n$;
$\ x\ _{\mathcal{A}}$	The distance of $x \in \mathbb{R}^n$ to the set $\mathcal{A} \subset \mathbb{R}^n$, that is, $\ x\ _{\mathcal{A}} := \inf_{y \in \mathcal{A}} \ x - y\ $.
$\text{Gr}(F)$	Graph of the set-valued function F ;
$\text{Gr} \upharpoonright_S (F)$	Graph of the set-valued function F restricted to set S ;
x^+	denotes the next state of the hybrid system after a jump;

1

INTRODUCTION

1.1 POSE CONTROL OF RIGID-BODIES

The control of rigid body motion consists of attitude (or orientation) and position control. Applications of this type of control are vast, ranging from control of mechanical systems, such as robotic manipulators, to satellites and spacecraft. Because of this, rigid-body motion control has been extensively investigated by the control and systems community [3, 4, 5, 6, 7, 8]. For instance, maintaining a specific orientation and position, or changing the orientation and translation with time in a specific manner is crucial for mission effectiveness of most spacecraft, such as pointing a satellite to a ground station (see Fig. 1.1(a)). The same is valid for unmanned vehicles and robotic systems which rely on precise coupled attitude and positioning control. In a welding robotic manipulator, the end-effector must not only position the welding tool in the desired trajectory of welding, but also in a specific orientation to weld correctly (see Fig. 1.1(b)). The global control arises when arbitrary changes in attitude and angular velocity are allowed or desired [9]. Such feature is highly desirable for spacecraft systems, for instance, to enhance the flight envelope [10] and to allow agile maneuvers [11]. This has applications, for example, in surveillance missions and in the recording of sports games with an unmanned quadrotor equipped with a camera, as illustrated in Fig. 1.1(c).

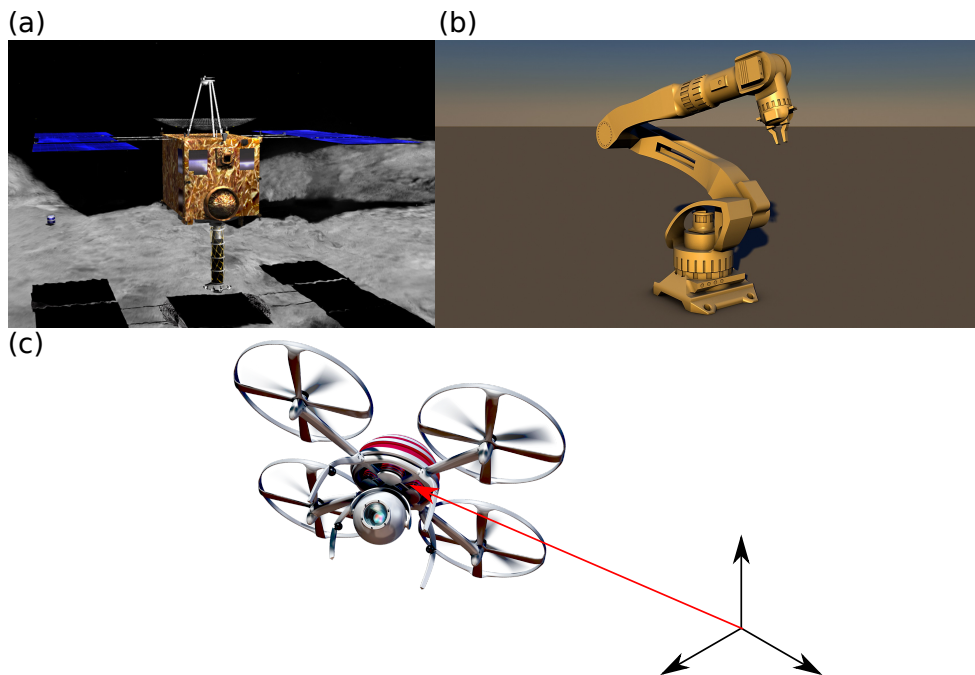


Fig. 1.1: Some examples where pose control is crucial: (a) Pointing a satellite antenna to a ground station. (b) While welding, a robotic manipulator has to control not only the position of the welding tool, but also its orientation. (c) An unmanned aerial vehicle holding a camera to record a sport game or making a surveillance of an area must have both position and orientation precisely controlled in order to achieve its objectives.

The attitude and the orientation of a rigid body is known as pose, and the coupled control of attitude and position of a rigid-body is known as pose control of rigid-bodies, or simply, pose control. The aforementioned problems of pose control can be classified in a **stabilization** problem or a **tracking** problem. In the case of stabilization, one desires to maintain the rigid body in a specific pose. In the tracking problem, one desires that the rigid body follows (that is, tracks) a desired reference attitude and a reference spatial trajectory. Moreover, depending on how the actuation is done to the controlled system, the problem can be classified as a **kinematic control problem** or a **dynamic control problem**. In the former case, the control inputs to the system are the angular and linear velocity, while in the latter case the control inputs are the resulting force and torque expressed in the rigid-body frame (more details will be seen in the end of Chapter 2).

In all of these scenarios, the configuration space of the system is not the Euclidean space \mathbb{R}^n , but a space of states that is a non-Euclidean differentiable manifold \mathcal{M} : in the case that the state-space of the system is the orientation of a rigid body, \mathcal{M} is the manifold $SO(3)$ of proper rotations, and in the case that the state-space of the system is the pose of a rigid body, \mathcal{M} is the manifold of rigid body motions $SE(3)$. These manifolds are special in the sense that they are also an algebraic structure named group (more details can be seen on Appendix A), whose group operation is the composition: a rotation followed by a rotation gives another rotation, and a rigid body motion followed by another rigid body motion gives another rigid body motion. The group operation is compatible with the smooth structure on the manifold and we call these Lie groups. Another important Lie groups are the unit quaternion group $Spin(3)$ [6] and the unit dual quaternion Lie group $Spin(3) \times \mathbb{R}^3$ [12]. Those can be used to algebraically express rotations and rigid body motions in a simpler way, analogously to the way complex numbers can be used to express rotations in the plane and dual numbers translations in the planes [13]. In this thesis, we propose hybrid controllers for the rigid body pose stabilization and tracking in the unit dual quaternion Lie group $Spin(3) \times \mathbb{R}^3$, while dealing with the problems of topological obstructions to global stabilization, unwinding and vulnerability of the stability to small measurement noises.

1.1.1 Why to use quaternions and dual-quaternions?

The control and modeling of mechanical systems are intrinsically connected with the study of the efficient descriptions of rigid-body transformations. While the tridimensional position of a rigid body—for example, the end-effector of a rigid body, a mobile robot, etc.—can be easily described by a vector with the Cartesian coordinates, the rigid-body orientation has multiple descriptions. Among the most used, it is worth mentioning the use of rotation matrices, unit norm quaternions and the Euler angles [14]. Among these descriptions, it should be emphasized that the latter description is a minimal parameterization for the group $SO(3)$: any parameterization of $SO(3)$ requires at least three parameters, since it is a three-dimensional manifold. Nevertheless, Euler angles is not a global parameterization of $SO(3)$: there are some points where the rank (that is, the degrees of freedom) of this parameterization is less than three, making occur a problem known as *gimbal lock* [14]. This implies that Euler angles are kinematically singular in the sense that transformation from their time rates of change to the angular velocity vector is not globally defined. Therefore, continuous control laws using these three-parameter representation cannot be globally defined, and, as such, the use of Euler angles are limited to local attitude maneuvers—this is a particular concern when deploying in safety-critical environments. This problem is not exclusive to Euler angles, but for any three dimensional parameterization of $SO(3)$: while $SO(3)$ is a three dimensional manifold and it is only required three parameters to describe a rotation, there does not exist a *global* 3-dimensional parameterization *without* singular points for the rotation group. This fact is a corollary to Brouwer’s theorem on the invariance of domain [15] (see Section B.1 of Appendix B for more

details). It is interesting to remark that this impossibility can also be understood algebraically in the sense that is impossible to extend the complex numbers to a three dimensional algebra (see Theorem A.1 of Appendix A for details).

The impossibility of embedding $SO(3)$ topologically in \mathbb{R}^4 was proved by Hopf in 1940 [16]. It is possible, however, to embed $SO(3)$ in \mathbb{R}^5 [15]. This parameterization, however, leads to nonlinear differential equations and an undesirable amount of computation is necessary to obtain a rotation as an output. Another alternative is to use many-to-one correspondences, such as the unit quaternions. This method has advantages of leading to linear equations while using only one redundant parameter while representing the most general possible rotation of the rigid body, that is, having no singular points. It would be reasonable to ask whether it might be possible to obtain a many-to-one representation, using only three parameters, but still possessing the property of being a local homeomorphism, and having no singular points. The answer is no, for this would force the parameter set to be a covering space of $SO(3)$, and it is known that the 3-sphere, which cannot be represented topologically by less than 3 parameters, is the only covering space of $SO(3)$ (in fact, it is the universal covering space of $SO(3)$).

To represent a complete rigid-body transformation, that is, rotation and translation, the Cartesian vector of position can be directly combined with one of the descriptions of rotation. This manner to represent a rigid-body transform, however, ignores the natural coupling between translation and rotation, and in general, results in a poor representation for the control [17]. To describe a rigid-body coupled movement in a global manner, the homogeneous transformation matrices (HTM) to represent elements of $SE(3)$ and the unit dual quaternions stand out [18]. Recently, this last representation received a growing interest from the scientific community because it is more compact than HTM (it uses only eight parameters against twelve parameters), it allows an easy extraction of geometric parameters, and allows the use of control rules directly in the defined in a vector field, eliminating the need to build controllers with matrix structure.

In summary, while it is possible to directly design attitude and rigid motion controllers for mechanical systems respectively using rotation matrices and homogeneous transformation matrices (HTM) [4, 19, 20], using the unit quaternion group $Spin(3)$ for rotations and the unit dual quaternions $Spin(3) \times \mathbb{R}^3$ for rigid motions can bring computational advantages because of the smaller number of parameters utilized to describe a movement. In fact, it has been noted by some authors the following advantages: [21] concludes that employing quaternions are more efficient and more compact than using homogeneous transformation matrices, [6] notes that normalizing quaternion to unit-norm quaternions is easier than using Gram-Schmidt to matrix orthogonalization, [18] compares dual quaternions against homogeneous matrices and against Lie algebra approach and concludes that for manipulators with high number of degree of freedoms and specially for redundant manipulators, the dual quaternion based method are more cost effective than the homogeneous transformation, [22] shows a comparative study on the proportional control algorithms based on the logarithmic mapping of the HTM and the unit dual quaternion and shows that the unit dual quaternion-based control law is higher in computational efficiency, [23] compares computation of forward kinematics and Jacobian matrix for any serial manipulator based on HTM and the dual quaternion framework and [24] compares the computation of forward kinematics and Jacobian matrix for any serial manipulator, based on product of exponentials formula and unit dual quaternion algebra, concluding that the latter method is in general more efficient in terms of computational operations and storage. Finally, it is also interesting to remark that the quaternion and dual quaternion kinematic equations (which will be detailed in Chapter 2) can be used to exploit the inherent passivity of rigid-body dynamics to design control laws that does not need direct angular or linear measurements [25, 26].

1.1.2 Why to use hybrid control?

Stabilizing a system whose state-space is not the Euclidean space \mathbb{R}^n , but it is one of the Lie groups $SO(3)$, $SE(3)$, $Spin(3)$, $Spin(3) \times \mathbb{R}^3$ or it is a vector bundle over these groups, poses several challenges. In particular (see Appendix B for more details), there does not exist a continuous vector field with a global asymptotically stable equilibrium point defined on the groups $SE(3)$ and $Spin(3) \times \mathbb{R}^3$ (and on any vector bundle over these groups) [27], or defined on the groups $SO(3)$ and $Spin(3)$ (and on any vector bundle over these groups) [17]. Due to this (as will be seen in more details on Chapter 3), continuous feedback controllers proposed on the literature sums up to controllers guaranteeing only almost global stability, which has an undesired equilibrium manifold that even being of null measure can lead to undesirable effects (see [28] for more details), or continuous controllers that guarantees global stability of the set of dual quaternions representing the same pose, but suffers from unwinding. To achieve global stabilization of pose control using dual quaternions and at the same time mitigating the unwinding problem, one can resort to a memoryless discontinuous feedback or to resort to a hybrid strategy with memory. As will be detailed in Chapter 3, the discontinuous-based solutions are extremely sensitive to noise and cause undesired chattering in the system, and even worse, to turn the system into an unstable system. The fragility of discontinuous-based feedback to small amplitude measurement noises stems from the non-feasibility of achieving robust global stabilization of a disconnected set of points from a pure non-hybrid state feedback [29].

Control design using hybrid systems, however, has extra capabilities: for example, sample and hold control (a special type of hybrid feedback) can be used to achieve stabilization that is robust to measurement noise and fast sensor/actuator dynamics, even if such robustness is impossible using purely continuous-time feedback [30, p. 68]. A hybrid mechanism that has been used to induce robustness with respect to measurement noise is hysteresis switching based control [28, 31], and its extension, bimodal control [32]. Hysteresis is a property of a system that relates its input and output through a mechanism that keeps track of the previous input and output values, i.e. it has memory. The framework of dynamical hybrid systems is very useful to model these type of controllers and also to assess its robustness. Hysteresis switching control can stabilize large classes of nonholonomic systems even though stabilization is impossible using time-invariant continuous state feedback [33], and *robust* stabilization is impossible using time-invariant locally bounded feedback [34].

Summing up, despite the solid contributions in the literature on dual quaternion-based controllers in the context of rigid body motion stabilization and tracking, existing pose controllers are either only almost global, global but suffers from unwinding, or have lack of robustness in the sense that they are sensitive to arbitrarily small measurement noises, or use a hybrid solution that mitigates the unwinding and chattering problems while still being global: for the kinematic control scenario, [35, 36] present a discontinuous control law to avoid unwinding, but this control law is prone to measurement noises of arbitrarily small amplitudes and chattering; the controller proposed in [17] uses a hybrid solution based on the hysteresis approach of [37] mitigating the chattering and unwinding problem, while still guaranteeing global stability; in [38] this controller is improved by using the bimodal technique of [1]. For the dynamic control scenario, [39, 36, 2] present a controller based on feedback linearization that uses a memoryless discontinuous-based approach and thus prone to measurement noises of arbitrarily small amplitudes; [40] proposes a sliding-mode controller, but the tracking error is not null; [26] proposes a controller based on the passivity technique of the attitude-only control of [25], but it suffers from unwinding; [41] proposes an adaptive controller, but the stability of the closed-loop system is not global; [42] presents a passivity-based solution for the finite-time stabilization of pose control, but it is not global (only almost global); [43] proposes an adaptive solution that allows uncertainties in the inertial parameters of the system, but this controller is not global.

Table 1.1 summarizes the solutions proposed in the literature. It is important to remark that some of these works which are not unwinding-free propose the use of a memoryless discontinuous approach to eliminate the unwinding, but as will be seen in Subsection 3.4, this leads to the chattering problem.

Table 1.1: Summary of pose control strategies for the dynamic control scenario and its features. The symbol \checkmark means yes, the symbol \circ means partially and the symbol \times means no.

Controller	Global	Unwinding-free	Chattering-free	Stabilization/Tracking	Kinematic/Dynamic
[35, 36]	\checkmark	\times	\checkmark	Tracking	Kinematic
Chapter 4	\checkmark	\circ	\circ	Stabilization	Kinematic
[38]	\checkmark	\circ	\circ	Stabilization	Kinematic
Chapter 5	\checkmark	\circ	\circ	Stabilization	Kinematic
[40]	\times	\checkmark	\times	Tracking	Dynamic
[39, 36, 2]	\checkmark	\checkmark	\times	Tracking	Dynamic
[26]	\checkmark	\times	\checkmark	Stabilization	Dynamic
[41]	\checkmark	\times	\checkmark	Tracking	Dynamic
[42]	\circ	\checkmark	\times	Tracking	Dynamic
[43]	\circ	\times	\checkmark	Tracking	Dynamic
Chapter 6	\checkmark	\circ	\circ	Tracking	Dynamic

1.2 CONTRIBUTIONS

In this work, hybrid control strategies for rigid-body pose control within the framework of dual quaternions are proposed for the kinematic and dynamic control scenario. The hybrid strategies stem from the idea of the hybrid kinematic control law with hysteresis switching proposed in [28] for the attitude-only control using quaternions. This strategy is used to solve the vulnerability to small amplitude measurement noises problem present in discontinuous control laws [29].

It is important to emphasize that, albeit some algebraic identities in quaternion algebra can be easily carried over to the dual quaternion algebra by the principle of transference [44, 6], the proposed generalizations do not follow by the principle of transference: the necessity of different procedures for quaternion and dual quaternion stems from their different topologies and group structures. For example, the unit quaternion group is a compact manifold, whereas the unit dual quaternion group is not a compact manifold. This reflects in the use of distinct approaches to controller design (see for instance [4] and [45]). The unit dual quaternion group is not a subgroup from $\text{Spin}(3)$ —it is indeed the other way around—and boundedness, geodesic distance, norm properties, and other manifold features that are valid on S^3 cannot be directly carried to $\text{Spin}(3) \times \mathbb{R}^3$.

In particular, it is worth to point out the following contributions:

- A proof that the topological obstruction for global stabilization by continuous feedback for compact manifolds are also present in $\text{SE}(3)$ and in the group of the unit dual quaternions (see corollaries B.2 and B.3).
- A hybrid kinematic controller [17] which extends the hybrid kinematic controller proposed in [28] for kinematic stabilization of quaternions to dual quaternions (see Chapter 4).

Table 1.2: Summary of proposed controllers in this thesis.

Controller	Hybrid strategy	Convergence rate	Control problem
Kinematic [17]	Hysteretic	Asymptotic	Stabilization
Kinematic [32]	Bimodal	Exponential	Stabilization
Dynamic [32]	Bimodal	Asymptotic	Tracking

After the qualification exam of this thesis, the following contributions were also done:

- A novel hybrid kinematic controller using a novel Lyapunov function and the bimodal strategy from [32]. Compared with the kinematic controllers proposed in [17, 38], the proposed solution to address kinematic stabilization has an exponential convergence (see Chapter 5).
- A novel dual-quaternion controller which considers the entire dynamics of the rigid body for the stabilization and tracking problem (see Chapter 6).

Table 1.2 summarizes the proposed controllers in this thesis and each one of its characteristics.

1.2.1 Published and submitted papers

During the doctorate, the following papers related to the theme of the thesis have been published:

- H. T. Kussaba, L. F. Figueredo, J. Y. Ishihara, and B. V. Adorno, “Hybrid Kinematic Control for Rigid Body Pose Stabilization using Dual Quaternions,” *Journal of the Franklin Institute*, vol. 354, no. 7, pp. 2769–2787, 2017
- P. P. M. Magro, H. T. M. Kussaba, L. F. Figueredo, and J. Y. Ishihara, “Dual quaternion-based bimodal global control for robust rigid body pose kinematic stabilization,” in *Proceedings of 2017 American Control Conference*, Seattle, USA, 2017, pp. 1205–1210

Not directly related to the thesis, the following papers also have been done and published during the doctorate:

- H. T. M. Kussaba, R. A. Borges, and J. Y. Ishihara, “A new condition for finite time boundedness analysis,” *Journal of the Franklin Institute*, vol. 352, no. 12, pp. 5514–5528, dec 2015
- H. T. M. Kussaba, J. Y. Ishihara, and R. A. Borges, “Uniform versions of Finsler’s lemma,” in *Proceedings of the 54th IEEE Conference on Decision and Control*. IEEE, dec 2015, pp. 7292–7297
- —, “Finite time boundedness and stability analysis of discrete time uncertain systems,” in *Proceedings of the 54th IEEE Conference on Decision and Control*. IEEE, dec 2015, pp. 5972–5977
- H. T. M. Kussaba, R. A. Borges, and J. Y. Ishihara, “Parameter-Dependent Filter with Finite Time Boundedness Property for Continuous-Time LPV Systems,” in *Proceedings of XVII Latin American Conference on Automatic Control*, Medellín, Colombia, 2016, pp. 189–194
- J. Y. Ishihara, H. T. M. Kussaba, and R. A. Borges, “Existence of continuous or constant Finsler’s variables for parameter-dependent systems,” *IEEE Transactions on Automatic Control*, vol. 62, no. 8, pp. 4187–4193, aug 2017

1.3 MANUSCRIPT ORGANIZATION

An introduction to quaternion and dual quaternion algebra is given in Chapter 2. The hybrid framework used in this work, along the basic tools that it will use it will also be given in Chapter 2. A brief explanation of the problems arising in the control of the pose of rigid bodies is given in Chapter 3.

The main results of this work are proved and presented in chapters 4, 5 and 6: Chapter 4 presents the kinematic controller introduced in [17]. Chapter 5 presents another kinematic controller that was obtained after the qualification exam of this thesis. This novel kinematic controller is based in a Lyapunov function which guarantees an exponential rate of convergence and also uses a bimodal strategy introduced in [32]. Both kinematic controllers does not considers the full dynamics of the system. In Chapter 6 is proposed a controller which considers the full dynamics of rigid-body pose: both the pose and the twist as a state of system, and actuating force and torque on the system are the control inputs. The conclusion of this research is presented in Chapter 7.

A summary of the algebraic structures used in this work is present in Appendix A. Topological results related to obstruction of global stabilization are presented and explained in more details in Appendix B. Copies of the published papers directly related to the thesis can be found in Appendix C.

2

PRELIMINARIES

2.1 SET-VALUED ANALYSIS

Taking into account uncertainties, disturbances and modeling errors leads naturally to set-valued maps and differential inclusions: for instance, it is usual in robust control problems that only the ranges of a parameter α of the model is known, but the exact value of α is not known. These problems can be modeled by the family of parametrized differential equations

$$\dot{x}(t) = f(x(t), \alpha), \alpha \in S,$$

which leads to the differential inclusion

$$\dot{x}(t) \in F(x(t)), F(x) := \{f(x, \alpha) : \alpha \in S\},$$

where S is the set of possible values of the unknown parameter α .

Differential inclusions are generated, for example, by problems concerning functions which satisfy a differential equation to within required accuracy, by differential inequalities, by implicit differential equations, by differential equations with discontinuous right-hand side and by problems in the theory of optimal and robust control [51]. A system of differential inequalities

$$\dot{x}_i \leq f_i(x_1, \dots, x_n), i = 1, \dots, n,$$

for example, can also be considered as a differential inclusion. In the context of control and systems, we have dynamical systems of the form [52]

$$\dot{x}(t) = A(x(t)) \frac{d}{dt} [B(x(t)) + C(x(t))], x(0) = x_0,$$

in which the velocity of the state of the system depends not only upon the state $x(t)$ of the system at time t , but also on variations of observations $B(x(t))$ of the state, This leads to an implicit differential equation

$$f(x, \dot{x}) = 0,$$

which is equivalent to the differential inclusion $\dot{x} \in F(x)$ with $F(x) = \{v \mid f(x, v) = 0\}$.

Differential inclusions are also used to study ordinary differential equations with an inaccurately known right-hand side: if the right-hand side of a differential equation is in an ε -neighborhood of a given function $f(x)$, then any solution of the differential equation is a solution to the differential inclusion

$$\dot{x} \in f(x) + \varepsilon\mathbb{B},$$

where \mathbb{B} is a unit ball in \mathbb{R}^n centered at zero.

Moreover, differential inclusions play a crucial role in the theory of differential equations with a discontinuous right-hand side, that is, differential equations $\dot{x}(t) = f(x(t), t)$ with a discontinuous function f . The investigation of such equations is of great importance since they model the performance of various mechanical and electrical devices as well the behavior of automatic control systems [53]. By embedding $f(x, t)$ into a set-valued map $F(t, x)$ then it is possible to develop a rigorous mathematical theory of discontinuous systems [51, 52].

Since the dynamics of economical, social, and biological macrosystems is multivalued, differential inclusions serve as natural models in macrosystem dynamics. Moreover, differential inclusions of first-order (in particular, the Moreau's sweeping process) encompasses several practical situations in Mechanics, such as water falling in a cavity, the dynamics of systems with perfect unilateral constraints, and plasticity and the evolution of elastoplastic systems [54]. Differential inclusions are also used to describe some systems with hysteresis. In particular, the controller developed in this thesis will be based on a hybrid hysteresis technique to avoid chattering problems.

2.1.1 Set-valued functions

A *set-valued function* F from X to Y (or a *correspondence*) is a mapping that associates to each point of X a subset of Y , and will be denoted by the notation $F : X \rightrightarrows Y$. If $F(x)$ is a singleton (that is, a set with only one element) for each x , then the set-valued function can be regarded as an usual single-valued function from X to Y .

The notion of continuity of single-valued functions is not immediately extended to set-valued functions: adapting the property of preserving converging sequences yields the notion of *outer semicontinuity*, while adapting the usual $\varepsilon - \delta$ definition (pre-image of any open set is open) yields the notion of *inner semicontinuity*, and these notions are not equivalent in general [55].

To define outer semicontinuity, it is necessary first to define a notion adapting the idea of convergence of sequences for sets.

DEFINITION 2.1 [56] Let $\{S_i\}_{i=1}^{\infty}$ be a sequence of subsets of \mathbb{R}^n . The **outer limit** of this sequence, denoted by $\limsup S_i$, is the set of all accumulation points of sequences of points $x_i \in S_i$.

Based on the property that continuous functions preserve the limit of convergent sequences, we define outer semicontinuity of a set-valued function as follows:

DEFINITION 2.2 [56, p. 102] A set-valued function $F : \mathbb{R}^n \rightrightarrows \mathbb{R}^m$ is **outer semicontinuous at** $x \in \mathbb{R}^n$ if for each sequence $\{x_i\}_{i=1}^{\infty} \in \mathbb{R}^n$ converging to x , the outer limit $\limsup F(x_i)$ is contained in $F(x)$. A set-valued function $F : \mathbb{R}^n \rightrightarrows \mathbb{R}^m$ is **outer semicontinuous (everywhere)** if it is outer semicontinuous at each $x \in \mathbb{R}^n$. Given $S \subseteq \mathbb{R}^n$, F is **outer semicontinuous relative to** S if the set-valued function

$$F \upharpoonright_S (x) := \begin{cases} F(x), & \text{if } x \in S, \\ \emptyset, & \text{if } x \notin S, \end{cases}$$

is outer semicontinuous at each $x \in S$.

In this thesis, we will also be dealing with functions taking values in product of sets. The following lemma will be useful to check the outer semicontinuity of such functions.

Lemma 2.1. Let $F_i : \mathbb{R}^n \rightrightarrows S_i$, $i = 1, \dots, p$, be set-valued functions. Let $F : \mathbb{R}^n \rightrightarrows S_1 \times \dots \times S_p$ be the set-valued function defined by $F(x) = (F_1(x), \dots, F_p(x))$. F is outer semicontinuous (at x , relative to S) if and only if F_i is outer semicontinuous (at x , relative to S) for each $i = 1, \dots, p$.

proof.

Follows directly by the definition of outer semicontinuity using outer limits and from the identity

$$\limsup F(x_i) = \limsup (F_1(x_i), \dots, F_p(x_i)) = (\limsup F_1(x_i), \dots, \limsup F_p(x_i)).$$

■

An alternative and important characterization of outer semicontinuity is related to the fact that the graph of continuous functions are closed sets (see, for instance [57, p. 192]).

Theorem 2.1 *Closed graph theorem*

[55, p. 154] [56, p. 102] A set-valued function $F : \mathbb{R}^n \rightrightarrows \mathbb{R}^m$ is outer semicontinuous if and only if the set

$$\text{Gr}(F) := \{(x, y) : x \in \mathbb{R}^n, y \in F(x)\} \subseteq \mathbb{R}^n \times \mathbb{R}^m, \quad (2.1)$$

defined as the **graph of the set-valued function** F , is closed. Note that the set (2.1) is the natural generalization of the graph of a real-valued function. Moreover, F is outer semicontinuous relative to $S \subseteq \mathbb{R}^n$ if and only if the set $\text{Gr} \upharpoonright_S := \{(x, y) : x \in S, y \in F(x)\}$ is relatively closed in $S \times \mathbb{R}^m$.

By using the closed graph theorem for set-valued functions, it is possible to easily prove that the notion of outer semicontinuity relative to a set is weaker than outer semicontinuity everywhere.

Lemma 2.2. Let $S \subseteq \mathbb{R}^n$. If a set-valued function $F : \mathbb{R}^n \rightrightarrows \mathbb{R}^m$ is outer semicontinuous everywhere, then F is outer semicontinuous relative to S .

proof.

By Theorem 2.1, $\text{Gr}(F)$ is closed, thus $\text{Gr} \upharpoonright_S (F) = \text{Gr}(F) \cap (S \times \mathbb{R}^m)$ is relatively closed in $S \times \mathbb{R}^m$. ■

Based on the fact that the pre-image of open sets by continuous functions are open sets, we define a set-valued function $F : \mathbb{R}^n \rightrightarrows \mathbb{R}^n$ to be **inner semicontinuous** if the set

$$F^{-1}(O) := \{x \in \mathbb{R}^n : F(x) \cap O \neq \emptyset\}$$

is open in \mathbb{R}^n whenever O is an open set of \mathbb{R}^n [55, p. 193].

For the development of this thesis, the notion of outer semicontinuity will be more useful (fortunately, the property of outer semicontinuity is typically easier to verify than inner semicontinuity [55, p. 155]). In particular, the following fact will be used several times on this thesis:

Theorem 2.2

Let $\overline{\text{sgn}}$ be the set-valued function defined as

$$\overline{\text{sgn}}(x) := \begin{cases} \{1\}, & \text{if } x > 0, \\ \{-1\}, & \text{if } x < 0, \\ \{-1, 1\}, & \text{if } x = 0. \end{cases} \quad (2.2)$$

The set-valued function $\overline{\text{sgn}}$ is outer semicontinuous.

proof.

Note that

$$\text{Gr}(\overline{\text{sgn}}) = \{(x, -1) : x < 0\} \cup (\{0\} \times \{-1, 1\}) \cup \{(x, 1) : x > 0\}$$

is a closed set of \mathbb{R}^2 . By Theorem 2.1, $\overline{\text{sgn}}$ is outer semicontinuous. ■

The following modification of this function will also be important for some of the proposed hybrid controllers.

Theorem 2.3

Let $A > 0$. The set-valued function $B : \mathbb{R}^2 \rightrightarrows \mathbb{R}$ defined by

$$B(x, y) := y\overline{\text{sgn}}(x - Ay)$$

is outer semicontinuous.

proof.

Note that the function $y\overline{\text{sgn}}(x - Ay)$ can only take the following values:

$$y\overline{\text{sgn}}(x - Ay) = \begin{cases} \{y\}, & \text{if } x > Ay, \\ \{-y, y\}, & \text{if } x = Ay, \\ \{-y\}, & \text{if } x < Ay. \end{cases}$$

Let $(x, y) \in \mathbb{R}^2$. We will divide the proof in three cases: $x > Ay$, $x < Ay$ and $x = Ay$.

First, suppose that $x > Ay$. In this case, $y\overline{\text{sgn}}(x - Ay) = \{y\}$. Let $\{(x_k, y_k)\}_{k=1}^{\infty}$ be an arbitrary sequence of \mathbb{R}^2 converging to (x, y) . Since $\lim_{k \rightarrow \infty} (x_k, y_k) = (x, y)$, there exists k^* such that for all $k > k^*$,

$$x_k > Ay_k.$$

Consequently, for $k > k^*$, one has that $y_k\overline{\text{sgn}}(x_k - Ay_k) = y_k$ and the accumulation point of this sequence is $\{y\} \subseteq y\overline{\text{sgn}}(x - Ay)$. The case that $x < Ay$ is similar to the previous case. Finally, if $x = Ay$, then $y\overline{\text{sgn}}(x - Ay) = \{-y, y\}$, but for any sequence $\{(x_k, y_k)\}_{k=1}^{\infty}$, one has that $y_k\overline{\text{sgn}}(x_k - Ay_k) \subseteq \{-y, y\}$. ■

Another property that will be interesting to adapt for set-valued maps is that single-valued continuous functions maps compact sets into compact sets. Based on this property, the definition of boundedness of a single-valued function is extended in the set-valued setting with the idea of local boundedness.

DEFINITION 2.3 [55, pp. 157-158] F is **locally bounded** if for any compact set K , there exists $m > 0$ such that $F(K) \subset m\mathbb{B}$, where \mathbb{B} is the closed unit ball in the Euclidean norm of the convenient dimension.

It is important to note that continuous single-valued functions are always locally bounded, since continuous single-valued functions preserve compact sets.

2.1.2 Differential and difference inclusions

A differential inclusion is described by

$$\dot{x} \in F(x(t), t), \quad x(0) = x_0, \quad (2.3)$$

where F is a set-valued function on $\mathbb{R}^n \times \mathbb{R}_+$. At each fixed time, a differential inclusion specifies that the state derivative belongs to a set of possible directions, rather than a specific direction. If F is only a single-valued function, (2.3) is only an ordinary differential equation. The concept of difference inclusion is defined analogously.

Solutions of (2.3) are understood in the **Carathéodory sense**, that is, a solution of (2.3) is an absolutely continuous function such that for almost every t in some interval, the derivative $\frac{d}{dt}x(t)$ exists and is contained in the set $F(t, x(t))$ [58, p. 384]. Roughly speaking, Carathéodory solutions relax the classical requirement that the solution must follow the direction of the vector field (2.3) at all times by allowing (2.3) to be unsatisfied in a set of measure zero (for more details, see [53]).

Differential (difference) inclusions will be of interest to us when dealing with differential (or difference) equations with a discontinuous vector field f (or a discontinuous map g). In these conditions, even if the differential equations not have solutions in the classical sense, there are generalized solutions that represent the physical behavior of the system accurately [59]. In particular, to give an accurate picture of the behavior of the system under small perturbations (in these cases the effect of state perturbations on the solutions can be quite significant since we do not have anymore any guarantee on the continuous dependence of the initial conditions), generalized solutions expressed in terms of set-valued dynamics are used. Given the differential (difference) equation

$$\dot{x} = f(x), \quad (x^+ = g(x))$$

its **Krasovskii regularization** is given by the differential (difference) inclusion

$$\dot{x} \in F(x), \quad (x^+ \in G(x))$$

where

$$F(x) = \bigcap_{\delta > 0} \overline{\text{co}} f(x + \delta\mathbb{B}) \quad (G(x) = \bigcap_{\delta > 0} \overline{g(x + \delta\mathbb{B})}),$$

where \mathbb{B} is the closed unit ball of appropriate dimension and \overline{S} denotes the topological closure of the set S . See Fig. 2.1 for an illustration of the computation of F in a point x^* .

The differential inclusion yielded by Krasovskii regularization introduces additional solutions (some which are pathological) that are meaningful since they arise from arbitrarily small state perturbations that converge to zero asymptotically. Moreover, asymptotic stability in the original system is robust if and only if asymptotic stability holds for the regularized system [60]. For more details, the reader is referred to [55, 58].

In hybrid systems, the presence of state perturbations can dramatically change its behavior: this can occur even if the perturbation is arbitrarily small and *the flow and jump map are smooth* (as will be seen in Section 2.2.3). Due to this, the notion of Krasovskii regularization will be generalized to deal with hybrid systems.

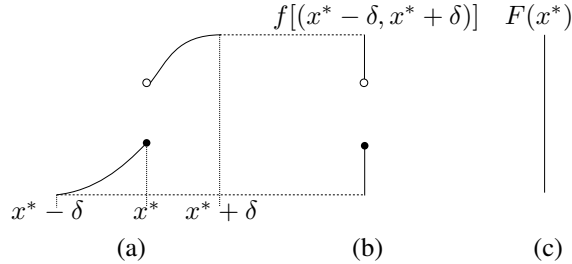


Fig. 2.1: Regularization of a scalar discontinuous function f . (a) Graph of f near a neighborhood of x^* . (b) Image of f near a neighborhood of x^* . (c) Krasovskii regularization of f evaluated at the point x^* .

2.2 DYNAMICAL HYBRID SYSTEMS

Dynamical hybrid systems refers to systems that exhibits both discrete-time and continuous-time behaviors [60, 56]. For instance, a bouncing ball that is dropped from an initial height and bounces has a continuous-time dynamics between each bounce, but as the ball impacts the grounds, its velocity is changed discontinuously according to a inelastic collision rule.

In this work, the framework of [60, 56] will be used to model these systems. Distinguishing features of this hybrid system framework includes allowing for multiple jumps at a time instant, allowing for an infinite number of jumps in a finite amount of time (that is, a Zeno solution), and not insisting on the uniqueness of solutions (which is natural in certain hybrid systems) [61]. Moreover, this framework captures a wide variety of dynamic phenomena and other models for hybrid systems: hybrid automata [62, 63], switched systems [64, 65], sampled-data systems [66] and networked control systems [67] can all be cast in the form of a hybrid system of this framework [60, 56].

The *state* of a hybrid system is a combination of continuous-time states and discrete-time states. The former change continuously, according to a *flow condition*, and the latter change discretely, according to a *jump condition*.

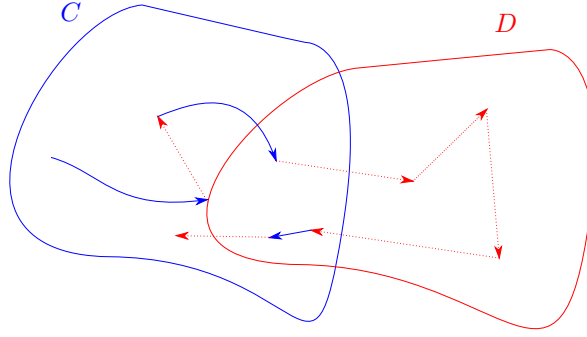


Fig. 2.2: Hybrid trajectory. The blue trajectory represents a continuous evolution (the *flow* of the system) and the red trajectory represents a discrete evolution (the *jump* of the system).

The model of a dynamical hybrid system \mathcal{H} is determined by five objects: the flow map F , the jump map G , a set $M \subseteq \mathbb{R}^n$, the flow set $C \subseteq M$ and the jump set $D \subseteq M$. The state-space of the system will be given by $C \cup D$.

The continuous behavior or *flow* of a hybrid system is modeled by a differential equation $\dot{x} = f(x)$ (or, more general, a differential inclusion $\dot{x} \in F(x)$), which is called the *flow map*, while the discrete behavior or *jumps* is modeled by a difference equation $x^+ = g(x)$ (or, more general, a difference inclusion $x^+ \in G(x)$), which is called the *jump map*. When the current state of system is in the *flow set* C , the transition of the states is done by the flow map, while if the current state of system is in the *jump set* D , the transition of the states is done by the *jump map*. Fig. 2.2 illustrates a possible trajectory realized by the state of a hybrid dynamical system.

In addition, to guarantee the well-posedness of the solutions of the system and to analyze the stability of the system and assure the invariance of this stability regarding state perturbations, we will require some regularity conditions on the data of hybrid systems, called **hybrid basic conditions** [30] (also known as Basic Assumptions in [60, 56]).

DEFINITION 2.4 (hybrid basic conditions) [60, p. 43][30, p. 39] Consider a hybrid system $\mathcal{H} = (C, F, D, G)$ on $M \subseteq \mathbb{R}^n$. The hybrid system \mathcal{H} is said to satisfy the **hybrid basic conditions** if the following conditions are satisfied:

1. $M \subseteq \mathbb{R}^n$ is an open set.
2. C and D are relatively closed sets in M .
3. $F : M \rightrightarrows \mathbb{R}^n$ is outer semicontinuous relative to C and locally bounded on M , and for all $x \in C$, the set $F(x)$ is nonempty and convex.
4. $G : M \rightrightarrows M$ is an outer semicontinuous relative to D and locally bounded on M , and for all $x \in D$, the set $G(x)$ is nonempty.

Remark 2.1. To the best of the author knowledge, the hybrid basic assumptions on Definition 2.4 is the one with the weakest hypothesis in the literature. As will be seen in the future chapters, the hybrid systems presented in this work will satisfy stronger hypothesis that imply the hybrid basic conditions. For instance, all the hybrid

systems in this work will have $M = \mathbb{R}^n$, so condition 1. will be always valid, and in this case, C and D must be closed sets of \mathbb{R}^n to satisfy condition 2.

It also be useful to remark that if F (resp. G) is outer semicontinuous everywhere, then F (resp. G) is outer semicontinuous relative to C (resp. D) by Lemma 2.2. Moreover, if F is a single-valued continuous function, then F satisfies all conditions of condition 3. of Definition 2.4. Similarly, if G is a single-valued continuous function, then G satisfies all conditions of condition 4. of Definition 2.4.

In summary, a hybrid system \mathcal{H} is given by the constrained differential inclusions

$$\mathcal{H} : \begin{cases} \dot{x} \in F(x), & x \in C, \\ x^+ \in G(x), & x \in D. \end{cases} \quad (2.4)$$

Note that the sets C and D are not necessarily disjoint, and when the state is in $C \cap D$, the system can flow or jump: the solutions of a hybrid dynamical system are possibly non-unique. It is also important to remark that $C \cup D = M$ is not necessarily true. In the case the trajectory of the system reach the complement of $C \cup D$ in M , the solution will not be able to evolve forward.

Remark 2.2. Note that by definition, the set M only has to contain the flow set C and the jump set D . The reader can then ask, why not always choose M as the smallest set possible containing C and D , that is, $M = C \cup D$? As will be seen during this thesis, the state-spaces $C \cup D$ of the hybrid systems developed in this thesis will always be a proper closed subset of \mathbb{R}^n . Thus, the choice $M = C \cup D$ implies the violation of condition 1. of Definition 2.4 (note that \mathbb{R}^n is a connected space, so the only simultaneously open and closed subsets of \mathbb{R}^n are the empty set \emptyset and \mathbb{R}^n [57, p. 226]).

The next section will explore with more detail the notion of solution in the context of hybrid dynamical systems.

2.2.1 Solutions to hybrid systems

A solution to a hybrid system will be described simultaneously by its discrete and continuous evolution: one real variable will be used to describe the amount of time passed and another integer variable will describe the number of jumps that have occurred. Thus, a natural choice to parameterize a solution to a hybrid system is to use a subset of $\mathbb{R}_+^* \times \mathbb{N}$. However, not every subset of $\mathbb{R}_+^* \times \mathbb{N}$ will make sense to describe an evolution of a hybrid system: if a solution already jumps twice in the first two seconds, then it will not make sense to ask what is the state of this particular solution after four seconds and the first jump. The next definition states precisely the construction of a time domain in the hybrid system framework.

DEFINITION 2.5 [30, Def. 2.2] A **compact hybrid time domain** is a subset $E \subset \mathbb{R}_+^* \times \mathbb{N}$ such that

$$E = \bigcup_{j=0}^{J-1} ([t_j, t_{j+1}], j)$$

for some finite increasing sequence of times $0 = t_0 \leq t_1 \leq t_2 \leq \dots \leq t_J$. A subset $E \subset \mathbb{R}_+^* \times \mathbb{N}$ is a **hybrid time domain** if for all $(T, J) \in E$, $E \cap ([0, T] \times \{0, 1, \dots, J\})$ is a compact hybrid domain.

Remark 2.3. It is interesting to remark that Definition 2.5 does not exclude solutions that jump more than twice in the same instant of time. It is physical reasonable to consider these solutions. For instance, in a Newton's

cradle with three balls, when the left ball impacts the middle ball, the velocity jumps from 0 to a positive value, but since the middle ball transfers the impact to the right ball in an almost instantaneous time (so it is reasonable to consider in the hybrid model that these two events occurs at the same instant of time), the velocity jumps to 0 again [68].

Given a hybrid system \mathcal{H} , its solutions will be a function from an hybrid time domain to the state-space M satisfying (2.4) in the **Caratheodory sense**: in each interval I^j associated to the j -th jump (that is, an interval I^j such that $I^j \times \{j\} = E \cap (\mathbb{R}_+^* \times \{j\})$), the function $t \mapsto x(t, j)$ is absolutely continuous on each compact subinterval of I^j . On each such I^j , this function is differentiable almost everywhere. Roughly speaking, this means that solution is not required to follow the direction of the vector field at all times, that is, the differential inclusion need not be satisfied on a set of a measure zero.

DEFINITION 2.6 [30, p. 17] Let E be a hybrid time domain. A **hybrid arc** is a function $x : E \rightarrow M$ if E is a **hybrid time domain** and if for each fixed $j \in \mathbb{N}$, the function $t \mapsto x(t, j)$ is locally absolutely continuous on the interval

$$I_j = \{t \in \mathbb{R}_+^* : (t, j) \in E\}.$$

The hybrid time domain E associated to a hybrid arc $x : E \rightarrow M$ will be denoted by $\text{dom}(x)$.

A **solution** to the hybrid system \mathcal{H} given by (2.4) is a hybrid arc satisfying [60, p. 40]

1. $x(0, 0) \in C \cup D$.
2. For each $j \in \mathbb{N}$ such that I_j has non-empty interior,

$$\begin{aligned} \dot{x}(t, j) &\in F(x(t, j)) && \text{for almost all } t \in I_j, \\ x(t, j) &\in C && \text{for all } t \in [\min I_j, \sup I_j]. \end{aligned}$$

3. For each $(t, j) \in E$ such that $(t, j + 1) \in E$,

$$\begin{aligned} x(t, j + 1) &\in G(x(t, j)), \\ x(t, j) &\in D \end{aligned}$$

The following classification of solutions to a hybrid system is important:

DEFINITION 2.7 [30, Definition 2.4] A hybrid arc x that is a solution to the hybrid system \mathcal{H} is called:

- **nontrivial**, if $\text{dom}(x)$ contains at least one point different from $(0, 0)$
- **maximal**, if it cannot be extended, that is, there is no other solution x' whose domain $\text{dom}(x')$ contains $\text{dom}(x)$ as a proper subset and such that $x' \equiv x$ on $\text{dom}(x)$.
- **complete**, if $\text{dom}(x)$ is unbounded.

Existence and uniqueness of solutions of a hybrid system is a more subtle issue for hybrid systems than it is for classical systems: there are reasons to consider models that do not have solutions from some initial conditions and that do not have unique solutions. Nevertheless, the existence of nontrivial solutions from

a point $x_0 \in C \cup D$ amounts to the existence of a classical discrete-time nontrivial solution or a classical continuous-time nontrivial solution. This is stated exactly in the next theorem.

Theorem 2.4

[60, p. 44] Suppose that \mathcal{H} satisfies the **hybrid basic conditions** (see Definition 2.4) and that $x_0 \in \mathbb{R}^n$ is such that $x_0 \in D$ or there exists a nontrivial solution z to $\dot{z} \in F(z)$, $z(0) = x_0$. Then there exists a nontrivial solution x to \mathcal{H} with $x(0, 0) = x_0$.

Regarding the structure of the maximal solutions, we have the following characterization.

Theorem 2.5

[60, p. 44] Suppose that \mathcal{H} satisfies the **hybrid basic conditions** (see Definition 2.4) and for each $x_0 \in C \cup D$ there exists a nontrivial solution to \mathcal{H} starting from x_0 . Let x be a maximal solution to \mathcal{H} . Then exactly one of the following three cases holds:

1. x is complete.
2. x blows up in finite hybrid-time, that is, there exists $T \in \mathbb{R}_+^*$ and $J \in \mathbb{Z}$ such that $(T, J) \notin \text{dom}(x)$ and $\lim_{t \rightarrow T} |x(t, J)| \rightarrow \infty$.
3. x eventually jumps out of $C \cup D$, that is, there exists $T \in \mathbb{R}_+^*$ and $J \in \mathbb{Z}$ such that $(T, J) \in \text{dom}(x)$ and $x(T, J) \notin C \cup D$.

2.2.2 Stability of hybrid systems

As the hybrid controllers for hybrid systems usually include discrete logic variables (such as timers, counters and memory states) that do not converge to a single point, the typical design problem will be of stabilizing a set rather than just a single point. In particular, in the framework of quaternion and dual quaternion we will want to stabilize a set of two points that represents the same rotation (or pose).

In order to do stability analysis, we can use generalizations of classical Lyapunov theorems. In fact, the usual Lyapunov-based control design tools for classical pure continuous-time and pure discrete-time systems (see for instance [69]) can also be generalized for hybrid systems satisfying the hybrid basic conditions. These hybrid Lyapunov tools, however, guarantees a weaker notion of stability that does not require the completeness of all solutions of the hybrid system. This notion of stability is stated in the next definition.

DEFINITION 2.8 [30, Def. 4.1] Given a hybrid system \mathcal{H} with state-space M and a compact set $\mathcal{A} \subseteq M$,

- \mathcal{A} is **pre-stable** if for each $\varepsilon > 0$ there exists $\delta > 0$ such that any solution x to \mathcal{H} with $\|x(0, 0)\|_{\mathcal{A}} \leq \delta$ satisfies $\|x(t, j)\|_{\mathcal{A}} \leq \varepsilon$ for all $(t, j) \in \text{dom}(x)$.
- \mathcal{A} is **pre-attractive** if there exists $\delta > 0$ such that any solution x to \mathcal{H} with $\|x(0, 0)\|_{\mathcal{A}} \leq \delta$ is bounded with respect to M and if x is complete, then $x(t, j) \rightarrow \mathcal{A}$ as $t + j \rightarrow \infty$.

- \mathcal{A} is **pre-asymptotically stable** if its both pre-stable and pre-attractive.
- \mathcal{A} is **asymptotically stable** if it is pre-asymptotically stable and there exists $\delta > 0$ such that any maximal solution x to \mathcal{H} with $\|x(0, 0)\|_{\mathcal{A}} \leq \delta$ is complete.

For a pre-asymptotically stable set \mathcal{A} , the **pre-basin of attraction** (also known as basin of pre-attraction [60]) of \mathcal{A} is the set of all $x \in C \cup D$ from which all solutions are bounded with respect to M and the complete ones converge to \mathcal{A} .

Remark 2.4. Let \mathcal{H} be a hybrid system satisfying the **hybrid basic conditions** (see Definition 2.4). If for each $x \in D$, we have that $\emptyset \neq G(x) \subset C \cup D$, and for each $x \in C$, there exists $\varepsilon > 0$ such that the differential inclusion $\dot{x} \in F(x)$ has a Caratheodory solution in the interval $(0, \varepsilon)$, then all maximal solutions to \mathcal{H} are complete [30, p. 42] and pre-asymptotically stability is equivalent to asymptotically stability.

The next theorem generalizes the classical stability analysis based on Lyapunov functions to the context of hybrid systems. First, we define what is a **Lyapunov function candidate** in the hybrid systems framework.

DEFINITION 2.9 [60, p. 62] Given the hybrid system \mathcal{H} on the state-space $M \subset \mathbb{R}^n$ and the compact set $\mathcal{A} \subset M$, the function $V : M \rightarrow \mathbb{R}$ is a **Lyapunov function candidate** for $(\mathcal{H}, \mathcal{A})$ if:

1. V is continuous and nonnegative on $(C \cup D) \setminus \mathcal{A}$.
2. V is continuously differentiable on an open set \mathcal{O} such that $C \setminus \mathcal{A} \subset \mathcal{O}$.
3. The following limit is satisfied:

$$\lim_{x \rightarrow \mathcal{A}} V(x) = 0.$$

Theorem 2.6

[60, p. 62] Let \mathcal{H} be a hybrid system satisfying the **hybrid basic conditions** (see Definition 2.4) and $\mathcal{A} \subset M$ a compact set satisfying $G(\mathcal{A} \cap D) \subset \mathcal{A}$. If there exists a Lyapunov-function candidate V for $(\mathcal{H}, \mathcal{A})$ such that

1. $\nabla V(x)^T f(x) < 0$ for all $x \in C \setminus \mathcal{A}$, $f \in F(x)$,
2. $V(g(x)) - V(x) < 0$ for all $x \in D \setminus \mathcal{A}$, $g \in G(x) \setminus \mathcal{A}$,

then the set \mathcal{A} is pre-asymptotically stable and the basin of pre-attraction of \mathcal{A} contains every forward invariant, compact set.

Asymptotic stability can also be characterized using a class of functions called comparison functions, and in particular, of a class named \mathcal{KL} -class. Those functions are standard in the analysis of stability and robustness of classical non-hybrid systems [70] and will also be useful in the hybrid setting. Next, we state the definition of \mathcal{KL} -class functions.

DEFINITION 2.10 A continuous function $\beta : \mathbb{R}_+^* \times \mathbb{R}_+^* \rightarrow \mathbb{R}_+^*$ belongs to the set \mathcal{KL} and it is said to be a **\mathcal{KL} -class function** (or shortly, a **\mathcal{KL} -function**) if

- for each $s \geq 0$, the map $r \mapsto \beta(r, s)$ is non-decreasing and zero at zero;
- for each $r \geq 0$, the map $s \mapsto \beta(r, s)$ is non-increasing and tends to zero when s tends to infinity.

The pre-asymptotic stability of a compact set will be described by bounding a proper indicator function, which will be defined next.

DEFINITION 2.11 Let $\mathcal{A} \subset \mathbb{R}^n$ be a compact set and let \mathcal{O} be an open set of \mathbb{R}^n containing \mathcal{A} . A continuous function $\omega : \mathcal{O} \rightarrow \mathbb{R}_{\geq 0}$ is a **proper indicator for \mathcal{A} in \mathcal{O}** if $\omega(x) = 0$ if and only if $x \in \mathcal{A}$ and if $(x_i)_{i \in \mathbb{N}}$ is a sequence in \mathcal{O} with either $\lim x_i = \infty$ or $\lim x_i \in \partial\mathcal{O}$, where $\partial\mathcal{O}$ denotes the boundary of \mathcal{O} , then $\lim \omega(x_i) = \infty$.

The next theorem states the characterization of pre-asymptotic stability of a compact set in terms of \mathcal{KL} functions and a proper indicator function on the compact set. This theorem will be useful to state a robustness result for hybrid systems (see Theorem 2.9).

Theorem 2.7

[60, Theorem 14] Let \mathcal{H} be a hybrid system satisfying the **hybrid basic conditions** (see Definition 2.4) and $\mathcal{A} \subset M$ a pre-asymptotically stable, compact set with basin of pre-attraction given by $\mathcal{B}_{\mathcal{A}}$. Then for each function ω that is a proper indicator for \mathcal{A} on $\mathcal{B}_{\mathcal{A}}$, there exists $\beta \in \mathcal{KL}$ such that each solution x starting in $\mathcal{B}_{\mathcal{A}}$ satisfies

$$\omega(x(t, j)) \leq \beta(\omega(x(0, 0), t + j), \text{ for all } (t, j) \in \text{dom}(x). \quad (2.5)$$

Note that the bound defined by the \mathcal{KL} -function β in (2.5) decreases as the time progress since β is non-decreasing in the second argument. By this and by continuity of β , for any $\varepsilon > 0$ there is a sufficiently large $T \geq 0$ (possibly depending on the solution x) such that $\omega(x(t, j)) < \varepsilon$ for any $t + j \geq T$. Since ω is a proper indicator function for the set \mathcal{A} , this implies that any solution x starting in the basin of pre-attraction of $\mathcal{B}_{\mathcal{A}}$ is nearing the compact set \mathcal{A} as the system evolves.

2.2.3 Generalized solutions and robustness of hybrid systems

In many situations, a control system is affected by perturbations and uncertainties that can possibly destroy the desired behavior for the system. In practice, the sensors of the system are never perfect and in every implemented system, noise arises in the measurements. It is also a common situation that not every physical parameter is exactly known: uncertainties, variations, or disturbances on these physical parameters lead to the called parametric uncertainty of the model. In these settings, the objective of the controller is not only guarantee a good operation in a nominal system, but to guarantee the good operation in a family of systems

possibly arising from these disturbances.

In hybrid systems, the effect of state perturbations on the dynamics can be quite dramatic. In particular, even if the flow map and the jump map are smooth, the asymptotic stability is not robust to perturbations. To illustrate this, consider the hybrid system of Example 2.1.

EXAMPLE 2.1 [60, Example S7] Consider a hybrid system with data given by

$$\begin{aligned} C &= [0, 1], F(x) = -x \text{ for all } x \in C, \\ D &= (1, 2], G(x) = 1 \text{ for all } x \in D. \end{aligned} \tag{2.6}$$

It is interesting to remark that F and G are single-valued continuous functions. Note that a small perturbation in data, namely, closing the set D , changes the globally asymptotic stability of the origin. Indeed, the hybrid system with

$$\begin{aligned} C &= [0, 1], F(x) = -x \text{ for all } x \in C, \\ D &= [1, 2], G(x) = 1 \text{ for all } x \in D. \end{aligned} \tag{2.7}$$

has a solution starting at $x = 1$ that remains at 1 and does not flow to the origin. The same occurs if the flow map of (2.6) is replaced by $G(x) = 1 + \varepsilon$ with $\varepsilon > 0$:

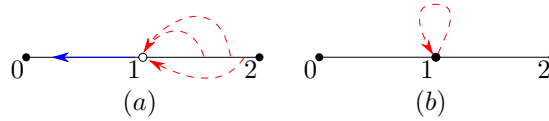


Fig. 2.3: Example of a non-robust hybrid system. The blue continuous arrow represents the flow of the solution and the red dashed arrow represents the jumps of the solution. (a) The origin is globally asymptotically stable in hybrid system given by (2.6). (b) After taking the closure of the jump set, the origin is not more globally asymptotically stable: there is a solution starting at 1 that remains at 1 through an infinite number of jumps.

To take into account these small perturbations that change the dynamics of the system, the analysis is carried on a regularization of the original hybrid system; this regularized hybrid system includes the solutions of the original system and also includes solutions that can arise from arbitrarily small perturbations in the data (C, F, D, G) of the original hybrid system. This regularization is done in a way that generalizes the Krasovskii regularization procedure of Section 2.1.2.

DEFINITION 2.12 [30, Def. 3.10] The **Krasovskii regularization of the hybrid system** \mathcal{H} on state-space M with data (C, F, D, G) is the hybrid system $\hat{\mathcal{H}}$

$$\hat{\mathcal{H}} : \begin{aligned} \dot{x} &\in \hat{F}(x), & x &\in \hat{C}, \\ x^+ &\in \hat{G}(x), & x &\in \hat{D}. \end{aligned} \tag{2.8}$$

with data given by

$$\begin{aligned}\hat{C} &:= \overline{C} \cap M, \\ \hat{F}(x) &:= \bigcap_{\delta > 0} \overline{\text{co}f((x + \delta\mathbb{B}) \cap C)}, \text{ for all } x \in \hat{C}, \\ \hat{D} &:= \overline{D} \cap M, \\ \hat{G}(x) &:= \bigcap_{\delta > 0} \overline{G((x + \delta\mathbb{B}) \cap D)}, \text{ for all } x \in \hat{D}.\end{aligned}$$

Fig. 2.4 illustrates the construction of \hat{C} and \hat{D} by using the Krasovskii regularization.

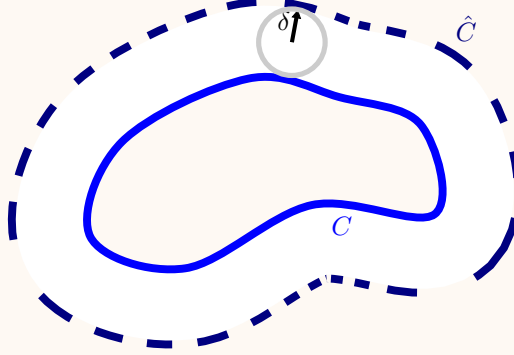


Fig. 2.4: Enlarged set \hat{C} generated by Krasovskii regularization.

Since $C \subset \hat{C}$, $D \subset \hat{D}$, $F(x) \subset \hat{F}(x)$ for all $x \in C$ and $G(x) \subset \hat{G}(x)$ for all $x \in D$, the solutions of \mathcal{H} are also solutions to $\hat{\mathcal{H}}$ (when this is the case we say that the hybrid system $\hat{\mathcal{H}}$ contains \mathcal{H}). The extra solutions of $\hat{\mathcal{H}}$ can be obtained as the limit of solutions perturbed by admissible state perturbations with size converging to zero [30]. Briefly speaking, an appropriately limit of a sequence of solutions to \mathcal{H} generated with state perturbation decreasing in magnitude turns out to be solutions to the regularized hybrid system $\hat{\mathcal{H}}$. Conversely, any solution to the regularized system can be approximated, with arbitrary precision, with solutions to the original system generated with state perturbations [30].

Hybrid systems satisfying the hybrid basic conditions are already regularized. In fact, the Krasovskii regularization is the smallest hybrid system $\hat{\mathcal{H}}$ containing \mathcal{H} that satisfies the hybrid basic conditions [30]. For these systems, there are theoretical and practical guarantees on the robustness of pre-asymptotic stability (we will see it in Theorem 2.9). To state them, we first need to define the concept of σ -perturbation of a hybrid system.

DEFINITION 2.13 [71] Given a hybrid system \mathcal{H} with data (C, F, D, G) and a continuous function $\sigma : \mathbb{R}^n \rightarrow \mathbb{R}_+$, the σ -**perturbation** of \mathcal{H} is the hybrid system \mathcal{H}_σ with data given by

$$\begin{aligned}C_\sigma &:= \{x \in M : (x + \sigma(x)\mathbb{B}) \cap C \neq \emptyset\}, \\ F_\sigma(x) &:= \overline{\text{co}F((x + \sigma(x)\mathbb{B}) \cap C) + \sigma(x)\mathbb{B}} \text{ for all } x \in C_\sigma, \\ D_\sigma &:= \{x \in M : (x + \sigma(x)\mathbb{B}) \cap D \neq \emptyset\}, \\ G_\sigma(x) &:= \{y \in M : y \in g + \sigma(g)\mathbb{B}, \text{ with } g \in G((x + \sigma(x)\mathbb{B}) \cap D)\}, \text{ for all } x \in D_\sigma.\end{aligned}$$

In particular, if $\sigma(x)$ is constant, say, $\sigma(x) = \delta$, then

$$G_\delta(x) = G((x + \delta\mathbb{B}) \cap D) + \delta\mathbb{B}, \text{ for all } x \in D_\delta.$$

Remark 2.5. The mappings F_σ and G_σ may be set valued at points x where $\sigma(x) > 0$, even when F and G are single-valued mappings.

The perturbed system \mathcal{H}_σ contains the unperturbed hybrid system \mathcal{H} , and the extra solutions of \mathcal{H}_σ can be linked to solutions that arise due to parameter variations, measurement noise and external disturbances [60]. For instance, consider an external disturbance d that is bounded in norm by a value $M > 0$. The solutions of

$$\dot{x} = F(x) + d$$

are contained in the set of solutions of $\dot{x} \in F(x) + M\mathbb{B}$. Taking $\sigma(x) = M$, $F(x) + M\mathbb{B} \subset F_\sigma(x)$ for all $x \in C_\sigma$. Thus, the solutions perturbed by external disturbances are contained in the M -perturbation of \mathcal{H} .

A feature of hybrid systems satisfying the basic hybrid conditions (in other words, hybrid systems that are equal to its own Krasovskii regularization) is that pre-asymptotic stability of compact sets are preserved under the presence of small amplitude σ -perturbations. This is stated in the next theorem.

Theorem 2.8

[60, Theorem 15] Let \mathcal{H} be a hybrid system satisfying the **hybrid basic conditions** (see Definition 2.4) and \mathcal{A} be a compact set pre-asymptotically stable with basin of pre-attraction given by $\mathcal{B}_\mathcal{A}$. There exists a continuous function $\sigma : \mathbb{R}^n \rightarrow \mathbb{R}_+^*$ satisfying $\sigma(x) > 0$ for $x \in \mathcal{B}_\mathcal{A}$ such that, for the σ -perturbed hybrid system \mathcal{H}_σ , the compact set \mathcal{A} is pre-asymptotically stable with basin of pre-attraction $\mathcal{B}_\mathcal{A}$.

By Theorem 2.8 there exists a continuous function $\bar{\sigma}$ such that the perturbed system $\mathcal{H}_{\bar{\sigma}}$ still preserves the pre-asymptotic stability of compact sets. Note that if $\sigma(x) \leq \bar{\sigma}(x)$ for all $x \in \mathbb{R}^n$, then the perturbed system \mathcal{H}_σ also preserves the pre-asymptotic stability of compact sets, since the solutions of \mathcal{H}_σ are also solutions of $\mathcal{H}_{\bar{\sigma}}$. In particular, if the hybrid system satisfies the basic assumptions, then its stability is not fragile to admissible state perturbations with size converging to zero.

Note that the previous Theorem 2.8 guarantees robustness of the stability of the system concerning a particular σ -perturbation (the theorem only concludes that there exists a particular function σ such that \mathcal{A} is still pre-asymptotically stable in \mathcal{H}_σ). In this sense, the value of $\sigma(x)$ could be very small for every $x \in \mathbb{R}^n$. What can be said for arbitrary perturbations σ with amplitude $\sigma(x)$ of any size? The next theorem gives a robustness guarantee for σ -perturbations with a constant σ (but with arbitrary amplitude). Roughly speaking, the stability is preserved in a practical sense that solutions that starts close to \mathcal{A} can be made to still stay close to \mathcal{A} within a desired accuracy. Moreover, the solutions can be made to decay in the same rate that the nominal system.

Theorem 2.9

[60, Theorem 17] Let \mathcal{H} be a hybrid system satisfying the **hybrid basic conditions** (see Definition 2.4) and \mathcal{A} be a compact set pre-asymptotically stable with basin of pre-attraction given by $\mathcal{B}_\mathcal{A}$. If there exists $\beta \in KL$ and a proper indicator function ω for \mathcal{A} on $\mathcal{B}_\mathcal{A}$ such that, for all solutions starting in

$\mathcal{B}_{\mathcal{A}}$,

$$\omega(x(t, j)) \leq \beta(\omega(x(0, 0), t + j) \text{ for all } (t, j) \in \text{dom}(x), \quad (2.9)$$

then for each $\varepsilon > 0$ and compact set $K \subseteq \mathcal{B}_{\mathcal{A}}$, there exists $\delta > 0$ such that each solution of the σ -perturbation of \mathcal{H} starting in K satisfies

$$\omega(x(t, j)) \leq \beta(\omega(x(0, 0), t + j) + \varepsilon \text{ for all } (t, j) \in \text{dom}(x). \quad (2.10)$$

The property concluded in this theorem is referred to as semiglobal and practical: *semiglobal* because (2.10) is valid for every compact set $K \subseteq \mathcal{B}_{\mathcal{A}}$ (although not for the entire basin of attraction $\mathcal{B}_{\mathcal{A}}$ if it is not compact), and *practical* because the value of ε can be made small to within a required accuracy. In general, for practical purposes, it will suffice to choose a sufficiently small ε to have a good performance for the system. Fig. 2.5 illustrates Theorem 2.9.

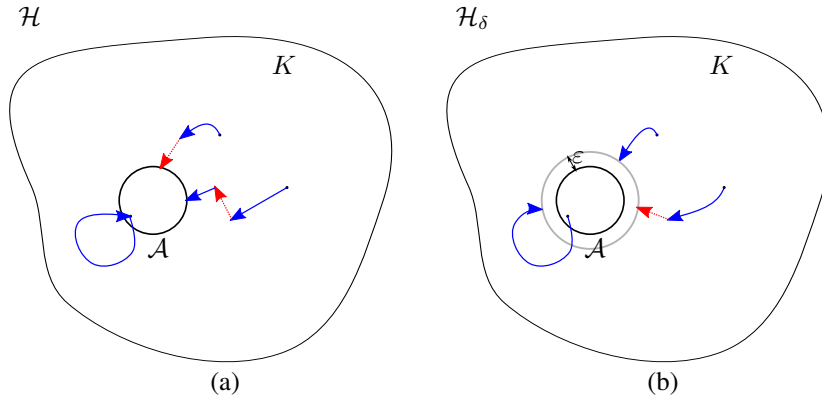


Fig. 2.5: Illustration of the practical stability of Theorem 2.9. (a) Nominal hybrid system \mathcal{H} . (b) Perturbed hybrid system by a constant δ -perturbation.

Note that the estimate given by the \mathcal{KL} -function β guarantees that, when the data of \mathcal{H} is perturbed by a constant δ , every solution of \mathcal{H}_δ is such that it approaches $\mathcal{A} + \varepsilon\mathbb{B}$ when $t + j$, with $(t, j) \in \text{dom}(x)$, grows unbounded. It is also interesting to note that the \mathcal{KL} -function β is the same in (2.9) and in (2.10). This means that the decay rate of β can be still preserved (at least in a practical and semi-global sense) in the perturbed system.

2.3 QUATERNIONS

The quaternion algebra is a four-dimensional **associative division algebra** over \mathbb{R} introduced by Hamilton [72] to algebraically express rotations in the three-dimensional space.

DEFINITION 2.14 The **algebra of quaternions**, whose set is denoted by \mathbb{H} , is the four-dimensional algebra over \mathbb{R} generated by the basis elements, $1, \hat{i}, \hat{j}$ and \hat{k} , whose multiplication is defined pairwise as in Table 2.1.

Table 2.1: Multiplication table of the elements of the canonical basis of \mathbb{H} . The multiplication is not commutative and the multiplication order is row times column.

	1	\hat{i}	\hat{j}	\hat{k}
1	1	\hat{i}	\hat{j}	\hat{k}
\hat{i}	\hat{i}	-1	\hat{k}	$-\hat{j}$
\hat{j}	\hat{j}	$-\hat{k}$	-1	\hat{i}
\hat{k}	\hat{k}	\hat{j}	$-\hat{i}$	-1

As a first comment, it is important to notice that the multiplication of this algebra is not commutative. This is not unreasonable, however, as we will use quaternions to represent rotations in the three-dimensional space and composition of rotations depends on the order that those are done. It is also interesting to note that the quaternions are the only finite dimensional, associative and division algebra over the real numbers which is not commutative (see Appendix A for more details, in special Theorem A.2).

An arbitrary element of \mathbb{H} is spanned by the basis $1, \hat{i}, \hat{j}$ and \hat{k} , and is given by

$$\mathbf{q} := \eta + \hat{i}\mu_1 + \hat{j}\mu_2 + \hat{k}\mu_3 = \begin{bmatrix} \eta \\ \mu_1 \\ \mu_2 \\ \mu_3 \end{bmatrix}$$

where $\eta, \mu_1, \mu_2, \mu_3 \in \mathbb{R}$ are called the **Euler symmetric parameters** or the **Euler-Rodrigues parameters** [73, p.2].

For ease of notation, the quaternion $\mathbf{q} = \eta + \hat{i}\mu_1 + \hat{j}\mu_2 + \hat{k}\mu_3$ may also be denoted as

$$\mathbf{q} = \eta + \boldsymbol{\mu}, \quad \text{with} \quad \boldsymbol{\mu} = \hat{i}\mu_1 + \hat{j}\mu_2 + \hat{k}\mu_3, \quad (2.11)$$

or in terms of its coordinates, as the block vector

$$\mathbf{q} = \begin{bmatrix} \eta \\ \boldsymbol{\mu} \end{bmatrix} = (\eta, \boldsymbol{\mu}), \quad (2.12)$$

where $\eta \in \mathbb{R}$ and $\boldsymbol{\mu} = (\mu_1, \mu_2, \mu_3) \in \mathbb{R}^3$. Both notations are equivalent and will be used interchangeably in this work.

By linearly extending the multiplication defined in Table 2.1, the quaternion multiplication between two arbitrary quaternions $\mathbf{q}_1 = \eta + \boldsymbol{\mu}$ and $\mathbf{q}_2 = \eta' + \boldsymbol{\mu}'$ is explicitly given by

$$\begin{aligned} \mathbf{q}_1 \mathbf{q}_2 &= (\eta + \hat{i}\mu_1 + \hat{j}\mu_2 + \hat{k}\mu_3) (\eta' + \hat{i}\mu'_1 + \hat{j}\mu'_2 + \hat{k}\mu'_3) = \\ &(\eta\eta' - \mu_1\mu'_1 - \mu_2\mu'_2 - \mu_3\mu'_3) + \hat{i}(\eta\mu'_1 + \mu_1\eta' + \mu_2\mu'_3 - \mu_3\mu'_2) \\ &+ \hat{j}(\eta\mu'_2 - \mu_1\mu'_3 + \mu_2\eta' + \mu_3\mu'_1) + \hat{k}(\eta\mu'_3 + \mu_1\mu'_2 - \mu_2\mu'_1 + \mu_3\eta'). \end{aligned} \quad (2.13)$$

In terms of its components, the multiplication (2.13) can also be expressed in block vector notation as

$$\mathbf{q}_1 \mathbf{q}_2 = \begin{bmatrix} \eta \\ \boldsymbol{\mu} \end{bmatrix} \begin{bmatrix} \eta' \\ \boldsymbol{\mu}' \end{bmatrix} = \begin{bmatrix} \eta\eta' - \boldsymbol{\mu}^T \boldsymbol{\mu}' \\ \eta\boldsymbol{\mu}' + \eta'\boldsymbol{\mu} + \boldsymbol{\mu} \times \boldsymbol{\mu}' \end{bmatrix},$$

where the right-hand side is a block vector with the first component in \mathbb{R} and the second component in \mathbb{R}^3 . The notation \times stands for the cross product between two vectors of \mathbb{R}^3 .

An arbitrary quaternion may be decomposed into a **real component** and an **imaginary component**: given $\mathbf{q} \in \mathbb{H}$, we define $\text{Re}(\mathbf{q}) := \eta$ and $\text{Im}(\mathbf{q}) := \boldsymbol{\mu}$. Thus, $\mathbf{q} = \text{Re}(\mathbf{q}) + \text{Im}(\mathbf{q})$. **Pure imaginary quaternions** are the quaternions in the set

$$\mathbb{H}_0 := \{\mathbf{q} \in \mathbb{H} : \text{Re}(\mathbf{q}) = 0\}$$

and they are very convenient to represent vectors of \mathbb{R}^3 within the quaternion formalism by means of the following isomorphism between \mathbb{H}_0 and \mathbb{R}^3 :

$$\mathbf{q} = \hat{i}\mu_1 + \hat{j}\mu_2 + \hat{k}\mu_3 \mapsto \text{vec}(\mathbf{q}) = (\mu_1, \mu_2, \mu_3). \quad (2.14)$$

Both cross product and dot product are defined for elements of \mathbb{H}_0 and they are analogous to their counterparts in \mathbb{R}^3 . More specifically, given $\mathbf{u}, \mathbf{v} \in \mathbb{H}_0$, the dot product is defined as

$$\mathbf{u} \cdot \mathbf{v} := -\frac{\mathbf{u}\mathbf{v} + \mathbf{v}\mathbf{u}}{2}, \quad (2.15)$$

and the cross product is defined by

$$\mathbf{u} \times \mathbf{v} := \frac{\mathbf{u}\mathbf{v} - \mathbf{v}\mathbf{u}}{2}. \quad (2.16)$$

It is direct to verify that $\text{vec}(\mathbf{u})^T \text{vec}(\mathbf{v}) = \mathbf{u} \cdot \mathbf{v}$ and that $\text{vec}(\mathbf{u}) \times \text{vec}(\mathbf{v}) = \mathbf{u} \times \mathbf{v}$. Finally, it is possible to define a multiplication between matrices and pure imaginary quaternions using the vec mapping: the multiplication of a matrix $A \in \mathbb{R}^{3 \times 3}$ by a quaternion $\mathbf{q} \in \mathbb{H}_0$ is the vector quaternion defined as $A\mathbf{q} := \text{vec}^{-1}[A(\text{vec}(\mathbf{q}))]$. When there is no risk of ambiguity, we identify the quaternion $\mathbf{q} \in \mathbb{H}_0$ with its vectorial representation $\text{vec}(\mathbf{q})$ and omit the vec symbol.

2.3.1 Unit quaternions

The quaternions with the most interesting properties are those with unit norm. First, we will define what is a norm in the algebra of quaternions.

DEFINITION 2.15 The **quaternion norm** of $\mathbf{q} = \eta + \boldsymbol{\mu}$ is defined as

$$\|\mathbf{q}\| := \sqrt{\mathbf{q}\mathbf{q}^*},$$

where $\mathbf{q}^* := \eta - \boldsymbol{\mu}$ is the **quaternion conjugate** of \mathbf{q} .

Unit quaternions are defined as the quaternions that lie in the subset of \mathbb{H} given by

$$\mathcal{S}^3 := \{\mathbf{q} \in \mathbb{H} : \|\mathbf{q}\| = 1\}.$$

Consider $\mathbf{q} = \eta + \boldsymbol{\mu}$. As $\|\mathbf{q}\| = 1$ if and only if

$$\mathbf{q}\mathbf{q}^* = \eta^2 + \boldsymbol{\mu} \cdot \boldsymbol{\mu} = \eta^2 + \mu_1^2 + \mu_2^2 + \mu_3^2 = 1,$$

the set \mathcal{S}^3 can be naturally identified with the 3-dimensional unit sphere.

Under quaternion multiplication, the set \mathcal{S}^3 of unit quaternions forms a group whose identity element is 1 and the inverse \mathbf{q}^{-1} of an arbitrary quaternion \mathbf{q} is given by the quaternion conjugate \mathbf{q}^* . In fact, this group has

a natural structure as a manifold for which the group operations are smooth, so it is in fact a Lie group [6]. In this work we will refer to this Lie group by $\text{Spin}(3)$.

Analogously to the way complex numbers are used to represent rotations in the plane [13], unit quaternions can be used to represent rotations in the three-dimensional space. An arbitrary rotation θ around an unit norm axis (n_x, n_y, n_z) is represented by the unit quaternion $r = \cos(\theta/2) + \sin(\theta/2) \mathbf{n}$, where $\mathbf{n} = \text{vec}^{-1}(n_x, n_y, n_z) = \hat{i}n_x + \hat{j}n_y + \hat{k}n_z$. To rotate a vector $v \in \mathbb{R}^3$ by an angle θ about the axis (n_x, n_y, n_z) using the right-hand convention, one first represent v by the pure imaginary quaternion $\mathbf{v} = v_1\hat{i} + v_2\hat{j} + v_3\hat{k}$ using the isomorphism (2.14). Expressing this rotation as the quaternion r , the rotated vector (expressed as a pure imaginary quaternion) is given by $r\mathbf{v}r^*$. This operation is illustrated in Fig. 2.6.

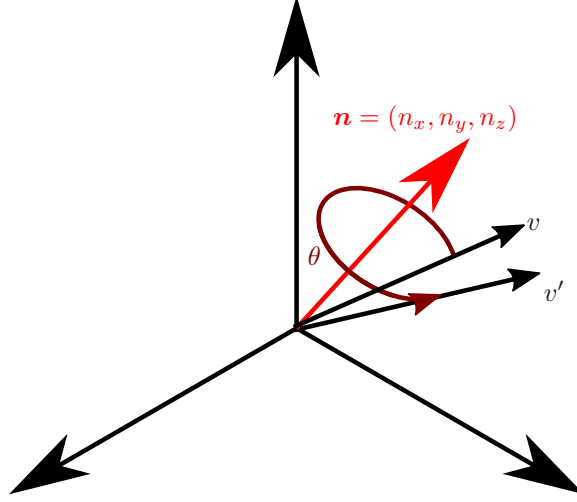


Fig. 2.6: Rotation represented by a unit quaternion $r = \cos(\theta/2) + \sin(\theta/2) \mathbf{n}$. The vector v is rotated an angle θ about the axis (n_1, n_2, n_3) resulting in the vector v' .

Remark 2.6. It is important to remark that the operation $v \mapsto r\mathbf{v}r^*$ can also be interpreted as a coordinate transformation between frames. If frame \mathcal{F}_1 is obtained by rotating \mathcal{F}_0 by a quaternion ρ_1^0 , and $\mathbf{p}^0, \mathbf{p}^1 \in \mathbb{H}_0$ are respectively the quaternion representations of the point \mathbf{p} with respect to the frames \mathcal{F}_0 and \mathcal{F}_1 , then

$$\mathbf{p}^1 = \rho_1^{0*} \mathbf{p}^0 \rho_1^0.$$

Moreover, one can explicitly calculate a rotation matrix $R \in \text{SO}(3)$ from an unit quaternion $q = \eta + \mu$ through Rodrigues' rotation formula [6]:

$$R = I + 2\eta [\mu]_{\times} + 2([\mu]_{\times})^2, \quad (2.17)$$

where $[\mu]_{\times}$ is the matrix representation of the linear operation $v \mapsto \mu \times v$, that is,

$$[\mu]_{\times} := \begin{bmatrix} 0 & -\mu_3 & \mu_2 \\ \mu_3 & 0 & -\mu_1 \\ -\mu_2 & \mu_1 & 0 \end{bmatrix}.$$

The map $\mathcal{R} : \text{Spin}(3) \rightarrow \text{SO}(3)$ which maps q to R according to (2.17) gives a surjective **group homomorphism** between $\text{Spin}(3)$ and $\text{SO}(3)$. This map fails to be a group isomorphism, since q and $-q$ maps to the same rotation matrix—this is the only way it fails to be an isomorphism, however, as the pre-image $\mathcal{R}^{-1}(R)$ is exactly $\{q, -q\}$ [6]. Due to this last property, we say that the unit quaternion group double covers the rotation group $\text{SO}(3)$. In other words, the unit quaternion $-q$ also represents the same rotation associated to q .

2.3.2 Rotation kinematics

Since unit quaternions describe the attitude of a rigid body, they are used to represent a rotation between the body frame and the inertial frame. In this sense, the kinematic equation of a rotation represented by the unit quaternion q is expressed as

$$\dot{q}(t) = \frac{1}{2}q(t)\omega(t), \quad (2.18)$$

where $\omega(t) \in \mathbb{H}_0$ is the quaternion representation of the angular velocity of the rigid body (given in the body frame) in instant t [74]. Although in this thesis we use directly the quaternion product in (2.18), it is interesting to remark that the kinematic equation of rotation can also be expressed in vectorial form in terms of Hamilton operators [74] or in terms of a Jacobian [25]. Moreover, the Jacobian has orthogonality properties which can be used to derive passivity properties that are useful for designing attitude controllers (see [25] for more details).

Remark 2.7. Supposing that $\omega(t) \in \mathbb{H}_0$ for all $t \geq 0$, the differential equation (2.18) is always well-posed for $q(0) \in \text{Spin}(3)$. This is due to the fact that (2.18) defines a left-invariant vector field over $\text{Spin}(3)$ (see [75] for more details, in particular Proposition 5.3.1)

Remark 2.8. The angular velocity ω can be obtained from the quaternion q and its derivative \dot{q} as follows:

$$\omega(\dot{q}) = 2q^{-1}\dot{q}.$$

2.4 DUAL QUATERNIONS

Similarly to how the quaternion algebra was introduced to address rotations in the three-dimensional space, the dual quaternion algebra was introduced by Clifford and Study [76, 77]¹ to describe rigid body movements.

DEFINITION 2.16 The **algebra of dual quaternions**, whose set is denoted by $\underline{\mathbb{H}}$, is generated by the basis elements, $1, \hat{i}, \hat{j}, \hat{k}, \varepsilon, \varepsilon\hat{i}, \varepsilon\hat{j}$ and $\varepsilon\hat{k}$, whose multiplication is defined pairwise as in Table 2.2.

Table 2.2: Multiplication table of the elements of the canonical basis of $\underline{\mathbb{H}}$. The multiplication is not commutative and the multiplication order is row times column.

	1	\hat{i}	\hat{j}	\hat{k}	ε	$\varepsilon\hat{i}$	$\varepsilon\hat{j}$	$\varepsilon\hat{k}$
1	1	\hat{i}	\hat{j}	\hat{k}	ε	$\varepsilon\hat{i}$	$\varepsilon\hat{j}$	$\varepsilon\hat{k}$
\hat{i}	\hat{i}	-1	\hat{k}	$-\hat{j}$	$\varepsilon\hat{i}$	$-\varepsilon$	$\varepsilon\hat{k}$	$-\varepsilon\hat{j}$
\hat{j}	\hat{j}	$-\hat{k}$	-1	\hat{i}	$\varepsilon\hat{j}$	$-\varepsilon\hat{k}$	$-\varepsilon$	$\varepsilon\hat{i}$
\hat{k}	\hat{k}	\hat{j}	$-\hat{i}$	-1	$\varepsilon\hat{k}$	$\varepsilon\hat{j}$	$-\varepsilon\hat{i}$	$-\varepsilon$
ε	ε	$\varepsilon\hat{i}$	$\varepsilon\hat{j}$	$\varepsilon\hat{k}$	0	0	0	0
$\varepsilon\hat{i}$	$\varepsilon\hat{i}$	$-\varepsilon$	$\varepsilon\hat{k}$	$-\varepsilon\hat{j}$	0	0	0	0
$\varepsilon\hat{j}$	$\varepsilon\hat{j}$	$-\varepsilon\hat{k}$	$-\varepsilon$	$\varepsilon\hat{i}$	0	0	0	0
$\varepsilon\hat{k}$	$\varepsilon\hat{k}$	$\varepsilon\hat{j}$	$-\varepsilon\hat{i}$	$-\varepsilon$	0	0	0	0

¹In truth, this is controversial [6]: the construction of dual quaternions is usually attributed to Clifford himself by the kinematic community citing [76], however it seems that the construction was due to Study [77]. The confusion probably arises because in [76] Clifford introduces the biquaternions, also known as double quaternions. The algebra relevant to $\text{SE}(3)$, however, is the dual quaternion algebra, which is also sometimes called the biquaternion algebra.

The basis elements $1, \hat{i}, \hat{j}$ and \hat{k} multiplies as the quaternions (see Table 2.1), and the basis element ε , called the **dual unit**, commutes with every other element of the algebra and is nilpotent, that is, $\varepsilon \neq 0$ and $\varepsilon^2 = 0$.

An arbitrary element \underline{q} of \mathbb{H} can always be written as a sum of a quaternion with another quaternion multiplied by the dual unit ε , that is,

$$\underline{q} = \mathbf{q} + \varepsilon \mathbf{q}', \text{ with } \mathbf{q}, \mathbf{q}' \in \mathbb{H}.$$

Thus, the product of two arbitrary dual quaternions $\underline{q}_1 = \mathbf{q}_1 + \varepsilon \mathbf{q}'_1$ and $\underline{q}_2 = \mathbf{q}_2 + \varepsilon \mathbf{q}'_2$ can be computed by

$$\underline{q}_1 \underline{q}_2 = \mathbf{q}_1 \mathbf{q}_2 + \varepsilon (\mathbf{q}_1 \mathbf{q}'_2 + \mathbf{q}'_1 \mathbf{q}_2).$$

For ease of notation, the dual quaternion

$$\underline{q} = \eta + \hat{i}\mu_1 + \hat{j}\mu_2 + \hat{k}\mu_3 + \varepsilon\eta' + \varepsilon\hat{i}\mu'_1 + \varepsilon\hat{j}\mu'_2 + \varepsilon\hat{k}\mu'_3 \quad (2.19)$$

may also be denoted as

$$\underline{q} = \eta + \boldsymbol{\mu} + \varepsilon(\eta' + \boldsymbol{\mu}'), \quad (2.20)$$

with $\boldsymbol{\mu} = \hat{i}\mu_1 + \hat{j}\mu_2 + \hat{k}\mu_3$ and $\boldsymbol{\mu}' = \hat{i}\mu'_1 + \hat{j}\mu'_2 + \hat{k}\mu'_3$. We can also denote the dual quaternion (2.19) by stacking its coordinates in a block vector:

$$\underline{q} = \begin{bmatrix} \eta \\ \boldsymbol{\mu} \\ \eta' \\ \boldsymbol{\mu}' \end{bmatrix} = (\eta, \boldsymbol{\mu}, \eta', \boldsymbol{\mu}'), \quad (2.21)$$

where in this case $\boldsymbol{\mu}$ and $\boldsymbol{\mu}'$ should be interpreted as (μ_1, μ_2, μ_3) and (μ'_1, μ'_2, μ'_3) by means of the isomorphism (2.14). Both notation (2.20) and (2.21) will be used interchangeably in this work.

By linearly extending the multiplication defined in Table 2.2, the multiplication between two arbitrary quaternions

$$\mathbf{q}_1 = \eta_1 + \boldsymbol{\mu}_1 + \eta'_1 + \boldsymbol{\mu}'_1$$

and

$$\mathbf{q}_2 = \eta_2 + \boldsymbol{\mu}_2 + \eta'_2 + \boldsymbol{\mu}'_2$$

is explicitly given by

$$\begin{bmatrix} \eta_1 \\ \boldsymbol{\mu}_1 \\ \eta'_1 \\ \boldsymbol{\mu}'_1 \end{bmatrix} \begin{bmatrix} \eta_2 \\ \boldsymbol{\mu}_2 \\ \eta'_2 \\ \boldsymbol{\mu}'_2 \end{bmatrix} = \begin{bmatrix} \eta_1 \eta_2 - \boldsymbol{\mu}_1^T \boldsymbol{\mu}_2 \\ \eta_1 \boldsymbol{\mu}_2 + \eta_2 \boldsymbol{\mu}_1 + \boldsymbol{\mu}_1 \times \boldsymbol{\mu}_2 \\ \eta_1 \eta'_2 + \eta'_1 \eta_2 - \boldsymbol{\mu}_1^T \boldsymbol{\mu}'_2 - \boldsymbol{\mu}'_1^T \boldsymbol{\mu}_2 \\ \eta_1 \boldsymbol{\mu}'_2 + \eta'_1 \boldsymbol{\mu}_2 + \eta'_2 \boldsymbol{\mu}_1 + \eta_2 \boldsymbol{\mu}'_1 + \boldsymbol{\mu}_1 \times \boldsymbol{\mu}'_2 + \boldsymbol{\mu}'_2 \times \boldsymbol{\mu}_2 \end{bmatrix}, \quad (2.22)$$

The term defined as $\mathcal{P}(\underline{q}) := \eta + \boldsymbol{\mu}$ is known as the **primary component** of \underline{q} , and the term defined as $\mathcal{D}(\underline{q}) := \varepsilon(\eta' + \boldsymbol{\mu}')$ is known as the **dual component** of \underline{q} . An arbitrary dual quaternion may also be decomposed into a **real component** and an **imaginary component**: given $\underline{q} \in \mathbb{H}$, we define $\mathbf{Re}(\underline{q}) := \eta + \varepsilon\eta'$ and $\mathbf{Im}(\underline{q}) := \boldsymbol{\mu} + \varepsilon\boldsymbol{\mu}'$. Thus, $\underline{q} = \mathbf{Re}(\underline{q}) + \mathbf{Im}(\underline{q})$.

Pure imaginary dual quaternions, also called **dual vector quaternions**, are given by the set

$$\mathbb{H}_0 := \{\underline{q} \in \mathbb{H} : \mathbf{Re}(\underline{q}) = 0\}.$$

As will be seen soon, the pure imaginary dual quaternions are very convenient to represent lines in the spaces and also the twist, which will be defined in (2.30). Both cross product and dot product can be defined for elements of \mathbb{H}_0 by extending the definitions (2.15) and (2.16): given $\underline{u}, \underline{v} \in \mathbb{H}_0$, the dot product is defined as

$$\underline{u} \cdot \underline{v} := -\frac{\underline{uv} + \underline{vu}}{2}, \quad (2.23)$$

and the cross product is defined as

$$\underline{u} \times \underline{v} := \frac{\underline{uv} - \underline{vu}}{2}. \quad (2.24)$$

2.4.1 Unit dual quaternions

Analogously to the quaternions, the dual quaternions with the most interesting properties are those with unit norm. First, we will define what is a norm in the algebra of dual quaternions.

DEFINITION 2.17 Let $\underline{q} \in \mathbb{H}$ and suppose $\underline{q} = \eta + \boldsymbol{\mu} + \varepsilon(\eta' + \boldsymbol{\mu}')$. The **dual quaternion norm** of \underline{q} is defined as

$$\|\underline{q}\| := \begin{cases} \sqrt{(\eta^2 + \|\boldsymbol{\mu}\|^2)} + \varepsilon 2 \frac{(\eta\eta' + \boldsymbol{\mu}^T \boldsymbol{\mu}')}{\sqrt{(\eta^2 + \|\boldsymbol{\mu}\|^2)}}, & \text{if } \mathcal{P}(\underline{q}) \neq 0, \\ 0, & \text{if } \mathcal{P}(\underline{q}) = 0. \end{cases}$$

Remark 2.9. The dual quaternion norm isn't a **norm** in the usual sense. First, the image of the dual quaternion norm is not contained in \mathbb{R} , but in the set

$$\mathbb{D} := \{\underline{q} \in \mathbb{H} : \text{Im}(\mathcal{P}(\underline{q})) = 0 \text{ and } \text{Im}(\mathcal{D}(\underline{q})) = 0\}.$$

Second, it is not positive definite: there exists $\underline{q} \neq 0$ such that $\|\underline{q}\| = 0$. In fact, the set of dual quaternions with zero norm is the non-empty set given by

$$\mathbb{O} := \{\underline{q} \in \mathbb{H} : \mathcal{P}(\underline{q}) = 0\}.$$

Consider $\underline{q} = \eta + \boldsymbol{\mu} + \varepsilon(\eta' + \boldsymbol{\mu}')$. We have that $\|\underline{q}\| = 1$ if and only if

$$\begin{aligned} \eta^2 + \|\boldsymbol{\mu}\|^2 &= 1, \\ \eta\eta' + \boldsymbol{\mu}^T \boldsymbol{\mu}' &= 0. \end{aligned} \quad (2.25)$$

In honor of Study, the set $\underline{\mathcal{S}}$ defined by (2.25) is called **Study quadric** [6].

Under dual quaternion multiplication, the set $\underline{\mathcal{S}}$ of unit dual quaternions forms a Lie group [12], which will be referred as the unit dual quaternions group $\text{Spin}(3) \times \mathbb{R}^3$, whose identity element is 1 and group inverse is the **dual quaternion conjugate** of \underline{q} defined as $\underline{q}^* := \text{Re}(\underline{q}) - \text{Im}(\underline{q})$.

An arbitrary rigid displacement characterized by a rotation represented by a quaternion $\mathbf{q} \in \text{Spin}(3)$, with $\mathbf{q} = \cos(\theta/2) + \sin(\theta/2) \mathbf{n}$, followed by a translation $\mathbf{p} \in \mathbb{H}_0$, with $\mathbf{p} = p_x \hat{i} + p_y \hat{j} + p_z \hat{k}$, is represented by the unit dual quaternion [23, 39]

$$\underline{q} = \mathbf{q} + \varepsilon \frac{1}{2} \mathbf{q} \mathbf{p}. \quad (2.26)$$

Similarly, the rigid motion could also be represented by a translation $\bar{\mathbf{p}}$ followed by a rotation \mathbf{q} [78] resulting in the dual quaternion

$$\underline{q} = \mathbf{q} + \varepsilon \frac{1}{2} \bar{\mathbf{p}} \mathbf{q}. \quad (2.27)$$

The quaternions \bar{p} and p are related by the transformation $\bar{p} = qpq^*$. It is also important to observe that in either (2.26) and (2.27) can be recovered from the dual quaternion \underline{q} . In fact, by taking the dual part of both sides (2.26) yields

$$\mathcal{D}(\underline{q}) = \frac{1}{2}qp,$$

and by multiplying this last equation on the left side by $2q^*$ gives

$$p = 2q^* \mathcal{D}(\underline{q}). \quad (2.28)$$

Similar reasoning can be applied to (2.27) to yield

$$\bar{p} = 2\mathcal{D}(\underline{q})q^*.$$

In this thesis, we will always represent an arbitrary rigid displacement in the form of (2.26).

As is already known, the rotation of a vector \vec{v} to a vector \vec{v}' can be written by means of unit quaternions as the product $v' = qvq^*$, where $v' = \text{vec}^{-1}(\vec{v}')$ and $v = \text{vec}^{-1}(\vec{v})$ are the pure imaginary quaternions representing vectors \vec{v} and \vec{v}' (see Figure 2.6). This form allows the concatenation of rotations to be represented by a simple quaternion product. Unfortunately, no such quaternion representation exists for a general rigid transformation that includes translation. The introduction of dual quaternions allows a rigid-transformation rule as simple as the one for pure rotations; however, not for a vector, but for an arbitrary line in space. It is possible to prove that each line in the three-dimensional space correspond to a dual quaternion by the means of **Plücker coordinates** [6, pp. 115-117]. Briefly, a line l_a in space with direction $\vec{l} \in S^2$ through a point $\vec{p} \in \mathbb{R}^3$ can be represented by the pure imaginary dual quaternion

$$l_a = l + \varepsilon(p \times l),$$

where $l = \text{vec}^{-1}(\vec{l})$ and $p = \text{vec}^{-1}(\vec{p})$ are the quaternion representation of vectors \vec{l} and \vec{p} . The term $(p \times l)$ is called the moment of line l_a .

Let \underline{q} be the dual quaternion representation of the rigid motion $(R, t) \in SO(3) \times \mathbb{R}^3$ (see (2.26)). Applying the rotation R followed by the translation \vec{t} to the line l_a results in a novel line whose direction and moment are respectively the primary and dual part of the pure imaginary dual quaternion [79, p. 6]

$$l'_a = \underline{q}l_a\underline{q}^*.$$

Remark 2.10. It is important to remark that the operation $l \mapsto \underline{q}l\underline{q}^*$ can also be interpreted as a coordinate transformation between frames. If frame \mathcal{F}_1 is obtained by the rigid displacement of the frame \mathcal{F}_0 by a dual quaternion $\underline{\rho}_1^0$, and $l^0, l^1 \in \mathbb{H}_0$ are respectively the pure imaginary dual quaternion representations of the line l with respect to the frames \mathcal{F}_0 and \mathcal{F}_1 , then

$$l^1 = (\underline{\rho}_1^0)^* l^0 \underline{\rho}_1^0.$$

In addition, one can explicitly calculate an element \underline{R} of $SE(3)$ given in its homogeneous representation [80]

$$\underline{R} = \begin{bmatrix} R & p \\ 0 & 1 \end{bmatrix},$$

where R is a rotation and p is the translation vector, from an unit dual quaternion \underline{q} through the mapping

$$\underline{q} = \eta + \mu + \varepsilon(\eta' + \mu') \mapsto \underline{R} = \begin{bmatrix} I + 2\eta[\mu]_{\times} + 2([\mu]_{\times})^2 & 2(\eta\mu' - \eta'\mu - \mu \times \mu') \\ 0 & 1 \end{bmatrix}.$$

Analogously to unit quaternions, the unit dual quaternions group double covers $SE(3)$ and any displacement \underline{q} can also be described by $-\underline{q}$.

2.4.2 Rigid body kinematic equations

Analogously how the unit quaternion describes the kinematic equation of a rotation, the unit dual quaternion \underline{q} can be used to describe the kinematics equation of coupled attitude and position. This is shown in the next lemma.

Lemma 2.3. [78] *The first order kinematic equation of a rigid body motion in the inertial frame is given by^a*

$$\underline{\dot{q}} = \frac{1}{2} \underline{q} \underline{\omega}, \quad (2.29)$$

where $\underline{\omega} \in \mathbb{H}_0$ is the *twist* in body frame given by

$$\underline{\omega} = \omega + \varepsilon [\dot{\mathbf{p}} + \omega \times \mathbf{p}]. \quad (2.30)$$

^aTo lighten the notation, the time dependence will be omitted when it is clear by context.

proof.

The time derivative of (2.26) is

$$2\underline{\dot{q}} = 2\dot{q} + \varepsilon (\dot{q}\mathbf{p} + q\dot{\mathbf{p}}) \quad (2.31)$$

Substituting (2.18) into (2.31),

$$\begin{aligned} 2\underline{\dot{q}} &= 2 \left(\frac{1}{2} q \omega \right) + \varepsilon \left[\left(\frac{1}{2} q \omega \right) \mathbf{p} + q \dot{\mathbf{p}} \right] \\ &= q \omega + \varepsilon \left(q \dot{\mathbf{p}} + \frac{1}{2} q \omega \mathbf{p} \right) \end{aligned} \quad (2.32)$$

$$= q \omega + \varepsilon q \left[\dot{\mathbf{p}} + \left(\frac{1}{2} \omega \mathbf{p} \right) \right] \quad (2.33)$$

$$= q \omega + \varepsilon q \left[\dot{\mathbf{p}} + \left(\omega \times \mathbf{p} + \frac{1}{2} \mathbf{p} \omega \right) \right] \quad (2.34)$$

$$= q \omega + \varepsilon \left[\frac{1}{2} q \mathbf{p} \omega + q (\dot{\mathbf{p}} + \omega \times \mathbf{p}) \right] \quad (2.35)$$

$$= \left(q + \varepsilon \frac{1}{2} q \mathbf{p} \right) [\omega + \varepsilon (\dot{\mathbf{p}} + \omega \times \mathbf{p})]. \quad (2.36)$$

Hence,

$$\underline{\dot{q}} = \frac{1}{2} \underline{q} \underline{\omega}. \quad \blacksquare$$

Remark 2.11. Supposing that $\underline{\omega}(t) \in \mathbb{H}_0$ for all $t \geq 0$, the differential equation (2.18) is always well-posed for

any $\underline{q}(0) \in \text{Spin}(3) \times \mathbb{R}^3$. This is due to the fact that (2.29) defines a left-invariant vector field over $\text{Spin}(3) \times \mathbb{R}^3$ (see [75] for more details, in particular Proposition 5.3.1).

Remark 2.12. The twist $\underline{\omega}$ can be recovered from the dual quaternion \underline{q} and its derivative $\dot{\underline{q}}$ as follows:

$$\underline{\omega} = 2\underline{q}^{-1}\dot{\underline{q}}.$$

It is also interesting to note that (2.30) implies that $\mathcal{D}(\underline{\omega}) = \dot{\underline{p}} + \underline{\omega} \times \underline{p}$, which gives a simple way to recover the velocity from the twist:

$$\dot{\underline{p}} = \mathcal{D}(\underline{\omega}) - \mathcal{P}(\underline{\omega}) \times \underline{p}. \quad (2.37)$$

Remark 2.13. Even using a variable-step solver to solve (2.29), the norm of unit dual quaternion may drift from 1. To avoid numerical errors in the numeric integration of (2.29), [81, pp.36-37] proposes to perform the numeric integration in the tangent space and then project to the dual quaternion group using the following numeric scheme:

$$\underline{x}_k = \exp\left(\frac{T\xi(t)}{2}\right)\underline{x}_{k-1},$$

where $\xi(t) = \omega(t) + \varepsilon(v(t) + p(t) \times \omega(t))$, with $\underline{x}(t) = \underline{r}(t) + \varepsilon\frac{1}{2}\underline{p}(t)\underline{r}(t)$, and T is the integration step.

The remarkable similarity between equations (2.18) and (2.29) is due to the **principle of transference**, whose various forms as stated in [44] can be summarized in mathematical terms as [6, Sec 7.6]: “All representations of the group $\text{SO}(3)$ become representations of $\text{SE}(3)$ when tensored with the dual numbers.” This means that several properties and algebraic identities of $\text{SO}(3)$ and the quaternions can be carried to $\text{SE}(3)$ and the dual quaternions algebra, respectively.

The principle of transference may mislead one to think that every theorem in quaternions can be transformed to another theorem in dual quaternions by a transference process. However, this is not the case, as shown by counterexamples in [44]. Therefore, properties and phenomena related to quaternion motions like topological obstructions and unwinding may not follow by direct use of transference and have to be verified for dual quaternions.

The same can be said in the context of controller design for dual quaternions: although [26] shows that (2.18) has passivity properties similar to (2.29) and that the extension of the passivity approach of [25] from quaternions to dual quaternions is straightforward (for stabilization only, but not tracking), the extension of other control techniques for quaternions to dual quaternions can be complicated. For instance, for designing a Lyapunov-based control one must take into account the dual terms of the dual quaternion and this information can not be extracted directly from Lyapunov functions used for attitude control using quaternion. Indeed, the kinematic controller proposed in Chapter 4 has the same primary part of the kinematic controller proposed in Chapter 5, but the dual part of these kinematic controllers are very different, and is due to this difference in dual part that the latter controller has exponential convergence while the former not.

2.4.3 Rigid body dynamic equations

In classical mechanics, the Newton-Euler equations describe the combined translational and rotational dynamics of a rigid body [82]. The Newton equation gives the translational dynamics while Euler equation gives the rotational dynamics of the rigid-body. Those equations can be combined in a single equation described by dual quaternions.

Considering a coordinate frame whose origin coincides with the body's center of mass, the Newton equation for translational dynamics can be expressed in quaternions by

$$\frac{d(m\dot{\mathbf{p}})}{dt} = \mathbf{f} \quad (2.38)$$

where $\mathbf{p} \in \mathbb{H}_0$ is the quaternion representation of the translation of the rigid-body (expressed in body frame), $\mathbf{f} \in \mathbb{H}_0$ is the quaternion representation of the external force actuating in the rigid body (expressed in body frame) and $m > 0$ is the mass of the body. Supposing that the mass of the rigid-body does not vary with the time (an assumption that is made for the rest of the text), (2.38) simplifies to

$$\ddot{\mathbf{p}} = \frac{\mathbf{f}}{m}, \quad (2.39)$$

Recalling that the multiplication of a matrix $A \in \mathbb{R}^{3 \times 3}$ by a quaternion $\mathbf{q} \in \mathbb{H}_0$ is the vector quaternion $A\mathbf{q} = \text{vec}^{-1}[A(\text{vec}(\mathbf{q}))]$, the Euler equation for rotational dynamics of a rigid body can be expressed by quaternions as

$$\dot{\boldsymbol{\omega}} = J^{-1}([\mathbf{J}\boldsymbol{\omega}]_{\times} \boldsymbol{\omega} + \boldsymbol{\tau}), \quad (2.40)$$

where $\boldsymbol{\omega} \in \mathbb{H}_0$ is the quaternion representation of the angular velocity of the rigid body (expressed in the body frame), $\boldsymbol{\tau} \in \mathbb{H}_0$ is the quaternion representation of external torque actuating in the rigid body (expressed in body frame) and $J \in \mathbb{R}^{3 \times 3}$ is the moment of inertia of the rigid body about the center of mass.

Note that the time derivative of the twist (2.30) is

$$\underline{\dot{\boldsymbol{\omega}}} = \dot{\boldsymbol{\omega}} + \varepsilon(\dot{\boldsymbol{\omega}} \times \mathbf{p} + \boldsymbol{\omega} \times \dot{\mathbf{p}} + \ddot{\mathbf{p}}). \quad (2.41)$$

Substituting (2.39) and (2.40) into (2.41), yields the Newton-Euler equations expressed by a single dual quaternions equation:

$$\underline{\dot{\boldsymbol{\omega}}} = \dot{\boldsymbol{\omega}} + \varepsilon(\dot{\boldsymbol{\omega}} \times \mathbf{p} + \boldsymbol{\omega} \times \dot{\mathbf{p}} + \mathbf{f}/m), \quad (2.42)$$

$$= [J^{-1}(S(\mathbf{J}\boldsymbol{\omega})\boldsymbol{\omega} + \boldsymbol{\tau})] + \varepsilon\{[J^{-1}(S(\mathbf{J}\boldsymbol{\omega})\boldsymbol{\omega} + \boldsymbol{\tau})] \times \mathbf{p} + \boldsymbol{\omega} \times \dot{\mathbf{p}} + \mathbf{f}/m\}. \quad (2.43)$$

With respect to a coordinate frame located at point X that is fixed in the body and not coincident with the center of mass, the Newton-Euler equations assume a more complex form and the translational and angular acceleration are coupled:

$$\begin{aligned} \mathbf{f} &= m\ddot{\mathbf{p}}^X - m[\mathbf{c}]_{\times} \dot{\boldsymbol{\omega}} + m[\boldsymbol{\omega}]_{\times} [\boldsymbol{\omega}]_{\times} \mathbf{c} \\ \boldsymbol{\tau} &= m[\mathbf{c}]_{\times} \ddot{\mathbf{p}}^X + (J - m[\mathbf{c}]_{\times} [\mathbf{c}]_{\times}) \dot{\boldsymbol{\omega}} + [\boldsymbol{\omega}]_{\times} (J - m[\mathbf{c}]_{\times} [\mathbf{c}]_{\times}) \boldsymbol{\omega} \end{aligned}$$

where $\ddot{\mathbf{p}}^X \in \mathbb{H}_0$ is the quaternion representation of the acceleration expressed in the frame located at point X and $\mathbf{c} \in \mathbb{H}_0$ is the quaternion representation of the location of the center of mass expressed in the body frame.

In the following chapters, we will design controllers that considers only the kinematic equation (2.29) (the twist is considered to be an input to the system) and a tracking controller that consider the kinematic equation

(2.29) and also the dynamic² equation (2.43) for the derivative of the twist (the twist is considered to be a state of the system and the inputs are the force and torque). The former controllers can be considered to be a single layer of a more complex controller which generates the twist for the system, while the latter controller is a controller that consider the full dynamic of the system. Controllers that only consider (2.29) will be denominated **kinematic controllers**, and controllers that consider (2.29)-(2.43) will be denominated **dynamic controller**.

²The expression dynamic here should be understood in the mechanics sense, that is, forces and torques are present in the equation.

3

CHALLENGES OF RIGID-BODY POSE STABILIZATION AND PRIOR WORK

3.1 INTRODUCTION

In this chapter, we briefly review the challenges of rigid-body pose stabilization and the disadvantages of previous solutions using memoryless discontinuous-based controllers

3.2 A TOPOLOGICAL OBSTRUCTION TO GLOBAL STABILIZATION BY CONTINUOUS FEEDBACK

It is well known that controllability of a linear system implies its stabilizability—in fact, one can design a smooth feedback to stabilize the system [83]. However, as was pointed out by Brockett, some non-linear systems cannot be asymptotically stabilized by smooth (or even continuous) static state feedback control laws [84]. This is not simply a lack of controllability: it might happen that, while every state can be steered to the origin by some control law, these control laws cannot be stitched together in a continuous manner to yield a globally defined stabilizing feedback [65].

Brockett’s criterion states that the domain of attraction of an asymptotically stable equilibrium must be homeomorphic to \mathbb{R}^n for some n [84] (see also [65, p. 79] for more details). Since a sufficiently small neighborhood of an equilibrium point has the same topological properties as \mathbb{R}^n , this means that such an obstruction to continuous stabilization has nothing to do with the properties of the state space and is instead embedded into the systems equations [65]. While Brockett’s criterion refers to the impossibility of local asymptotic stabilization by a continuous (time-invariant) state feedback, *global* asymptotic stabilization by a continuous state feedback depends strongly on the global topology of the state space \mathcal{M} . More details can be seen in Appendix B.

In scenarios where the state space of the dynamical system is not the Euclidean space \mathbb{R}^n but a general differentiable manifold \mathcal{M} —which is the case of $\text{SE}(3)$ and $\text{Spin}(3) \times \mathbb{R}^3$ —the topology of the state space \mathcal{M} may obstruct the existence of a globally asymptotically stable equilibrium point in any continuous vector field defined on \mathcal{M} : in [27] it is proved that if \mathcal{M} has the structure of a vector bundle over a compact manifold \mathcal{L} , then no continuous vector field on \mathcal{M} has a globally asymptotically stable equilibrium. In particular, this means that it is impossible to design a continuous feedback that globally stabilizes the pose of a rigid body, as in this case the closed-loop system state space manifold $\mathcal{M} = \text{SO}(3) \times \mathbb{R}^3 \times \mathbb{R}^6$ is a trivial bundle over the compact manifold $\text{SO}(3)$. In this work, it is proved that the same topological obstruction is also present in the group of unit dual quaternions since its underlying manifold is a trivial bundle over the unit sphere \mathcal{S}^3 (see Theorem B.3 in Subsection 2.4.2).

To surpass this topological obstruction using continuous controllers, one may try to:

1. stabilize the set of opposite quaternions (respectively dual quaternions) that represents the same attitude

(respectively pose), leading to the problem of unwinding (as will be seen in Subsection 3.3), or

2. use a solution that only guarantees an almost global stabilization (for instance, [43]), which may lead to an undesired equilibrium manifold that even being of null measure can lead to undesirable effects (see [28] for more details).

As will be seen in Subsection 3.4 other options are to use a memoryless discontinuous feedback (leading to the problem of vulnerability to arbitrarily small measurement noises) or to resort to a hybrid strategy with memory (which is the case of this work), which mitigates the unwinding problem while reducing the vulnerability to measurement noises.

3.3 THE UNWINDING PHENOMENA

The unwinding phenomena happens when a rigid body starts arbitrarily close to the desired final attitude and yet unnecessarily rotate through large angles before coming to rest in the desired attitude [9]. Unwinding can be highly undesirable in practical uses, particularly in aerospace applications, since it can lead to unnecessary fuel consumption.

As saw in the previous section, it is impossible to design a continuous feedback that globally stabilizes the attitude of a rigid body, as in this case the state-space of closed-loop system is $\mathcal{M} = \text{SO}(3) \times \mathbb{R}^3$, and this is a trivial bundle over the compact manifold $\text{SO}(3)$. The same can be said for the group of unit quaternions because its underlying manifold is the 3 dimensional sphere \mathcal{S}^3 , which is also a compact manifold. Nevertheless, since the quaternions 1 and -1 represent the same attitude, one may try to design a control law which achieves the asymptotically stability of these points in closed-loop. However, in view of that the Euler characteristic of \mathcal{S}^3 is 0, the Poincaré-Hopf index theorem [85, p. 35] (see Appendix B for more details) rules out the possibility of the existence of a continuous vector field over \mathcal{S}^3 where $\{-1, 1\}$ are asymptotically stable equilibrium points.

An example of this approach is [25], wherein the authors propose a PD controller to solve the attitude tracking problem in the dynamic control scenario. For the case of the stabilization problem, the equilibrium points of the closed-loop system are given by the set

$$\{(\mathbf{q}, \boldsymbol{\omega}) \in \mathcal{S}^3 \times \mathbb{R}^3 : (\mathbf{q}, \boldsymbol{\omega}) \in \{(-1, 0), (1, 0)\}\}. \quad (3.1)$$

By using LaSalle invariance principle, [25] proves that every trajectory of the closed-loop system with this controller converges to the set given in (3.1). This, however, does not imply that each one of these equilibrium points are asymptotically stable: as a corollary of the Poincaré-Hopf index theorem [85, p. 35] (see Appendix B for more details), if there are two equilibrium points in $\mathcal{S}^3 \times \mathbb{R}^3$ and one of these equilibrium points are stable, the other must be unstable. This leads to the problem named as unwinding in the literature [86].

Fig. 3.1 illustrates how unwinding happens and how it is undesirable. Suppose that one wishes to stabilize a rigid body in the final rest attitudes represented by the quaternions 1 and -1 and a controller is designed in such way that the closed-loop vector field in \mathcal{S}^3 has -1 and 1 as equilibrium points. As a result of the above discussion, one of those equilibrium points must be unstable: without loss of generality, assume that point 1 is unstable. If the rigid body starts in an attitude represented by a quaternion A which is very near to 1, the vector field on \mathcal{S}^3 will push the body towards the quaternion -1 instead of promptly stabilizing it at quaternion 1.

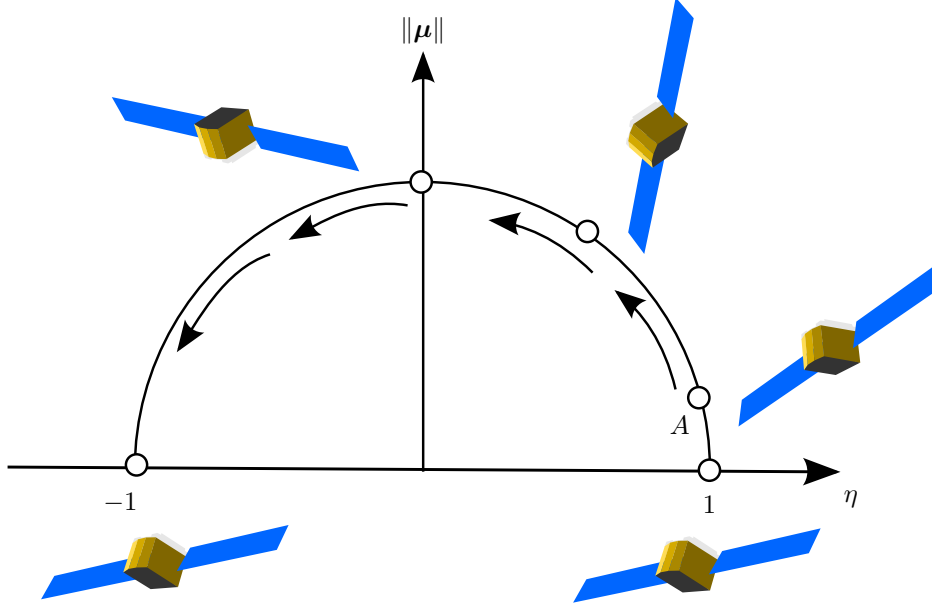


Fig. 3.1: Illustration of unwinding problem using a continuous controller. The unit-norm quaternion $q = \eta + \mu$ represents the current attitude of the satellite illustrated in the figure. Since $\eta^2 + \|\mu\|^2 = 1$, this quaternion is in the unit half-circle of the figure. Supposing that the initial attitude of the satellite is described by quaternion A and point 1 is unstable, the satellite will rotate towards the further equilibrium point -1 , although the quaternions -1 and 1 describe the same attitude.

Due to the two-to-one covering map between $\text{Spin}(3) \times \mathbb{R}^3$ and $\text{SE}(3)$, the unit dual quaternion group is endowed with a double representation for every pose in $\text{SE}(3)$, and the same analysis can be done in the dual quaternion framework. Neglecting the double covering yields to an unwinding-like problem whereby solutions close to the desired pose in $\text{SE}(3)$ may travel farther to the unit dual quaternion representing the same pose [35].

A way to avoid the unwinding problem and also the topological obstruction to global stabilization is to use discontinuous feedback laws (in the sense of [59]): this is the approach done in [87, 88, 89, 90, 91, 92] within the context of quaternions, and in [35, 36, 39, 2] within the context of dual quaternions. This approach, however, has a disadvantage: it is highly sensitive to arbitrarily small amplitude measurement noises. This problem can greatly affect the performance as well the stability of the system, as will be seen in the next section.

3.4 DISCONTINUOUS CONTROLLERS AND THE VULNERABILITY TO SMALL AMPLITUDE MEASUREMENT NOISES PROBLEM

In most applications of control systems, the designer must take into account the presence of noise in the measurements: usually those are yielded from sensors which are frequently corrupted by noise. Neglecting the measurement noise in the design of the control system can degrade the performance of the system and may even lead to instability.

As saw in the Section 3.2, it is impossible to design a continuous feedback that globally stabilizes the pose of a rigid body. Thus, one has to resort to non-continuous feedback: this is done for instance in [35, 36, 39, 2] within the framework of dual quaternions. All of these works, however, use a discontinuous sign-based approach that is very fragile to measurement noise. In fact, in the presence of a small random measurement noise it may happen that, near the discontinuity point, we misjudge which side of this point we are currently on and start moving toward it instead of away from it. If this happens often enough, the solution will oscillate around the discontinuity point and may never reach the origin [65].

Fig. 3.2 illustrates this vulnerability to measurement noise. Suppose one has to stabilize the attitude (respectively pose) of the rigid body in a desired position represented by the quaternions (respectively dual quaternions) -1 and 1 , which represent the same attitude (respectively pose). A naive approach to the problem would be to take the rigid body to 1 if it is nearer to 1 and to take the rigid body to -1 if it is nearer to -1 : in this way, unwinding is avoided. However, suppose noise corrupts the measurement at point A and the sensors falsely output that the system is at point B . This makes the system flow in direction of point 1 instead of -1 , even if it is nearer to point -1 (see Fig. 3.2(a)). If the noise corrupts the measurement again at point B and makes the measure be the point A , then the system will flow in direction of point -1 instead of point 1 (see Fig. 3.2(b)). This could repeat indefinitely, preventing the stability of the system. Note also that points A and B could be very near to each other: this imply that even an arbitrarily small measurement noise of this type could lock the system in a region within A and B , not allowing the system settle at point 1 or -1 .

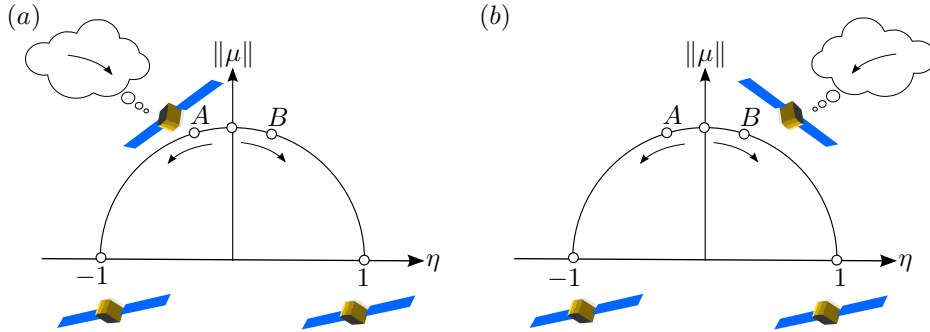


Fig. 3.2: Illustration of chattering problem when using a discontinuous vector field to control the attitude of a satellite. The unit-norm quaternion $q = \eta + \mu$ represents the current attitude of the satellite illustrated in the figure. Since $\eta^2 + \|\mu\|^2 = 1$, this quaternion is in the unit half-circle of the figure. (a) In this state, the real attitude of satellite is described by quaternion A . However, due to noise, the measurement sensor outputs that the satellite is quaternion B , causing it to rotate in the wrong direction. (b) In this state, the real attitude of satellite is described by quaternion B . However, due to noise, the measurement sensor outputs that the satellite is quaternion A , causing it to rotate again in the wrong direction.

At first glance, it seems that the measurement noise discussed above is not natural to occur in an infinite time horizon, but this is not unlikely if one consider a scenario of malicious cyberattacks and sabotages [93, 94]. Moreover, even if the measurement noise corrupt the system during a short finite time horizon, this noise can lead to chattering, that is, undesired oscillations that degrades the performance of the system. Depending on the frequency of these oscillations, the chattering can be very harmful to the system, generating high heat losses in power circuits and high wear of moving mechanical parts.

This vulnerability is even more relevant when dealing with dual quaternion-based controllers: the discontinuity of the controller not only affects the rotation, but may also disturb and deteriorate the trajectory of the

system translation. In this context, extremely small noises may also lead to chattering, performance degradation—and in the worst case, prevent stability.

To illustrate this, consider the discontinuous control law proposed in [36, 35] for the stabilization problem in the kinematic control scenario. In terms of the components of the measured dual quaternion $\underline{q} = \eta + \boldsymbol{\mu} + \varepsilon(\eta' + \boldsymbol{\mu}')$, the control law is a twist feedback given by¹

$$\underline{\boldsymbol{\omega}} = \begin{cases} -2k \left[\text{acos}(\eta) \frac{\boldsymbol{\mu}}{\|\boldsymbol{\mu}\|} + \varepsilon \boldsymbol{v} \right], & \text{if } \eta \geq 0, \\ -2k \left[(\text{acos}(\eta) - \pi) \frac{\boldsymbol{\mu}}{\|\boldsymbol{\mu}\|} + \varepsilon \boldsymbol{v} \right], & \text{if } \eta < 0, \end{cases} \quad (3.2)$$

where $\boldsymbol{v} = \eta \boldsymbol{\mu}' - \eta' \boldsymbol{\mu} - \boldsymbol{\mu} \times \boldsymbol{\mu}'$ and k is a proportional gain.

Albeit this control law avoids unwinding, a careful look reveals a strong sensitivity around attitudes that are up to π away from the desired attitude about some axis—that is, $\eta = 0$. In view of Theorem 2.6 of [29], one can see that such control law isn't robust in the sense that arbitrarily small measurement noises can force η to stay near to 0 for initial conditions within its neighborhood. Indeed, similar to Theorem 3.2 of [28], one can even exhibit an explicit noise signal to persistently trap the system about a fixed pose, thus preventing its stability. To illustrate the sensitivity of pure discontinuous state feedback controllers, we introduce a simple case study in which the trajectory of (2.29) is simulated using the discontinuous control law (3.2) in the presence of a random measurement noise²—the results are shown in Fig. 3.3. As can be seen during the initial 20 seconds, which is the time the noise afflicts the system, the trajectory of the closed-loop system exhibits chattering in the neighborhood of the discontinuity around $\eta = 0$. Furthermore, the chattering influence over the system is not restricted to the trajectory of the attitude and may also impact on the resulting trajectory of the translation, as shown in Fig. 3.3(b). In other words, the lack of robustness of a discontinuous solution may lead to chattering in orientation and to additional disturbances in the translation of the rigid motion in the presence of arbitrarily small random noises.

It is important to remark that this discussion is not exclusive to the kinematic control scenario, and that in Chapter 6 a numerical example where the chattering phenomenon happens for a discontinuous control law (precisely, [2]) proposed to the dynamic control scenario will be shown.

¹The discontinuous kinematic control law in [36, 35] contains a typo that has been fixed in [2]. It is also important to remark that different from (3.2), in [36, 35, 39, 2] the controller is expressed in terms of the logarithm of a unit dual quaternion.

²The simulation has been performed in accordance with the procedures described in Section 4.3 of the next chapter. It is interesting to point out that the choice of the numerical integrator for the simulation is very important, as a bad choice of numerical integration can lead to drifting of the quaternion manifold [95, 96] or numerical chattering [97], which degrades the chattering problem. Following [28], the MATLAB ode45 variable-step numerical integration method was used to perform these simulations.

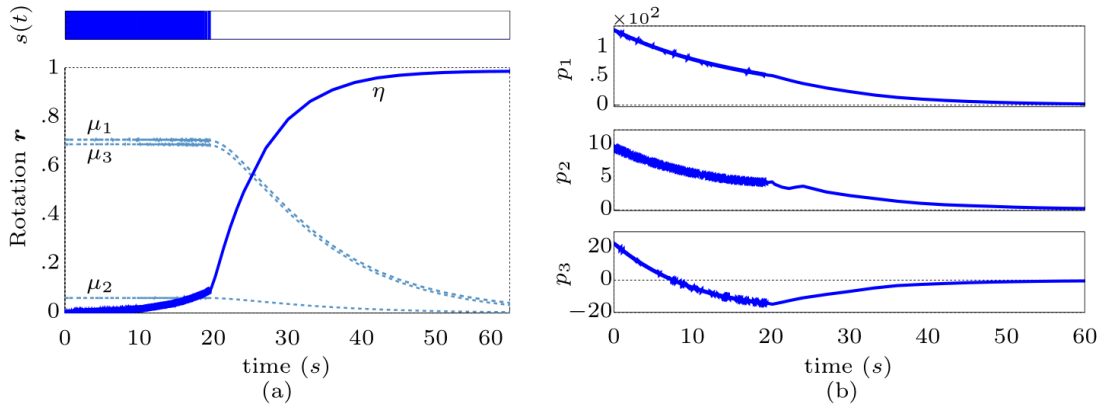


Fig. 3.3: Time-simulation of discontinuous control law (3.2) in presence of a random measurement noise (note that the measurement noise is turned off after 20 seconds of simulation). (a) Trajectory of the rotation unit quaternion $\mathbf{r} = \eta + \boldsymbol{\mu} = \eta + \mu_1 \hat{i} + \mu_2 \hat{j} + \mu_3 \hat{k}$ and switches $s(t)$ along time t . (b) Trajectory of the three-dimensional translation elements $\mathbf{p} = p_1 \hat{i} + p_2 \hat{j} + p_3 \hat{k}$.

4

FIRST PROPOSED HYBRID SOLUTION FOR A ROBUST KINEMATIC CONTROLLER

4.1 INTRODUCTION

In this chapter, the control design problem for globally stabilizing a rigid body coupled rotational and translational kinematics is addressed using the solution published in [17]. Part of the results presented here are also presented in Chapter 6 from Figueredo's thesis [98], who co-authored [17]. Different from [17] and Chapter 6 from [98], the proofs of the theoretical guarantees of the controller proposed in [17] will be presented with more details in this chapter.

The proposed controller copes with the topological constraint inherent from the unit dual quaternion parameterization while also ensuring robustness against measurement noises. To avoid the unwinding phenomenon and the lack of robustness from pure discontinuous solutions, we appeal to the hybrid system formalism of [60, 56] described in Section 2.2 of the preliminaries. To solve the problem of robust global asymptotic stabilization of (2.29), we propose a generalization to the hysteresis-based hybrid control law of [28] that extends the attitude stabilization to render both coupled kinematics—attitude and translation—stable.

The system studied in this chapter is described by the kinematic equation

$$\dot{\underline{q}} = \frac{1}{2} \underline{q} \underline{\omega},$$

where $\underline{q} \in \underline{\mathcal{S}}$ is the state of the system, $\underline{\omega} \in \mathbb{H}_0$ is the input of the system, and the measurement output is

$$y := \underline{q}.$$

4.2 KINEMATIC HYBRID CONTROL LAW FOR ROBUST GLOBAL POSE STABILITY

As will be proved in Theorem 4.1, it is possible to use a Lyapunov-based approach to derive a feedback control law that solves the problem of global stabilization of rigid-body pose. The proposed control law is defined as

$$\underline{\omega}_{f1} := -k_1 h \underline{\mu} - \varepsilon k_2 \eta \underline{\mu}', \quad (4.1)$$

where $k_1, k_2 \in \mathbb{R}_+^*$ are control gains and $h \in \{-1, 1\}$ is a memory state with hysteresis characterized by a constant parameter $\delta \in (0, 1)$. Based on the hysteretic strategy of [28], the memory state h has its dynamics defined by

$$\begin{aligned} \dot{h} &:= 0, & \text{when } (\underline{q}, h) \text{ are such that } h\eta \geq -\delta, \\ h^+ &\in \overline{\text{sgn}}(\eta), & \text{when } (\underline{q}, h) \text{ are such that } h\eta \leq -\delta, \end{aligned} \quad (4.2)$$

where $\overline{\text{sgn}}$ is the set-valued function defined in (2.2).

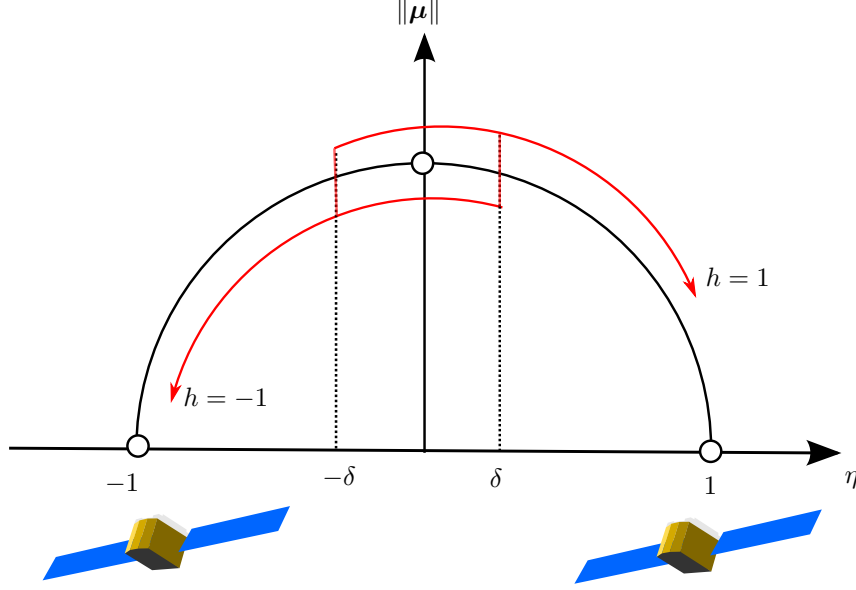


Fig. 4.1: Illustration of the hysteretic control strategy. The unit-norm quaternion $\mathbf{q} = \eta + \boldsymbol{\mu}$ represents the current attitude of the satellite illustrated in the figure. Since $\eta^2 + \|\boldsymbol{\mu}\|^2 = 1$, this quaternion is in the unit half-circle of the figure. The discrete variable h indicates if the target equilibrium should be -1 or 1 . The state variable h will only change according to the hysteretic curve of Fig. 4.2(a).

As illustrated in Fig. 4.1, the idea behind the memory state h is to indicate if the rigid-body should move to the pose described by the unit dual quaternion -1 or should move to the pose described by its opposite dual quaternion, i.e. the unit dual quaternion 1 .

The jump set defined on (4.2) models a hysteretic curve, illustrated by Fig. 4.2(a). The state h will only change its value from -1 to 1 if η gets larger than δ . Similarly, h will only change its value from 1 to -1 if η gets smaller than $-\delta$. Intuitively, this means that if $\eta = 0$, a small change in η will not be sufficient to change the target equilibrium point. It is important to note that if δ tends to 0 , the controller will behave as the discontinuous controller illustrated in Fig. 3.2 of the previous chapter. In this case, when the state variable η is close to 0 , an arbitrary small change of η immediately changes the target equilibrium point causing the problem of chattering, as illustrated by Fig. (b). Moreover, if δ tends to 1 , then the controller will behave as the continuous controller illustrated in Fig. 3.1 of the previous chapter, and will be more prone to suffer an unwinding-like behavior. Thus, the choice of the parameter δ is made considering a trade-off between protection against measurement noises and avoiding unwinding-like behavior.

Denoting the state-space of the hysteretic memory by $X_c := \{-1, 1\}$, let $X_1 := \underline{\mathcal{S}} \times X_c$ and denote $\bar{\mathbf{x}} := (\underline{\mathbf{q}}, h)$. In terms of the hybrid formalism (2.4), the closed loop system made by (2.29), (4.1) and (4.2) is characterized by the hybrid system

$$\bar{\mathcal{H}}_1 : \quad \begin{aligned} \dot{\bar{\mathbf{x}}} &= F(\bar{\mathbf{x}}), & \bar{\mathbf{x}} &\in C, \\ \bar{\mathbf{x}}^+ &\in G(\bar{\mathbf{x}}), & \bar{\mathbf{x}} &\in D, \end{aligned}$$

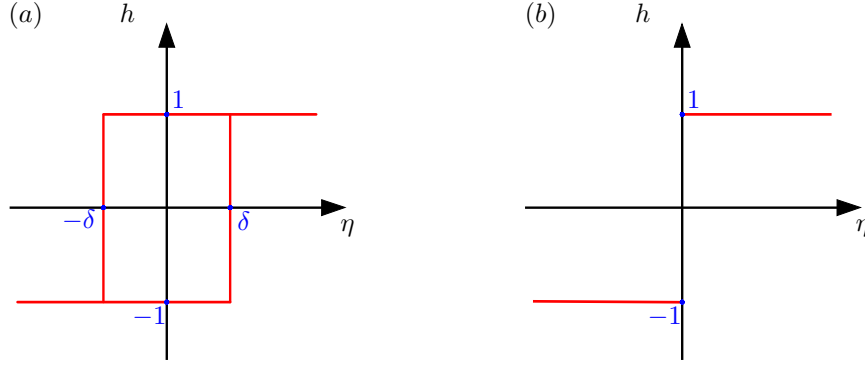


Fig. 4.2: Curves illustrating how the state h changes according to the state variable η . (a) Hysteresis curve for $\delta > 0$. (b) When δ tends to 0, the hysteresis curve will behave as the graph of the sgn function, that is, without memory and with a discontinuity on $\eta = 0$.

with flow map $F : \mathbb{R}^9 \rightarrow \mathbb{R}^9$ and flow set $C \subseteq \mathbb{R}^9$ given by¹

$$F(\underline{q}, h) = \left(\frac{1}{2} \underline{q} \underline{\omega}, 0 \right), \quad C = \{(\underline{q}, h) \in X_1 : h\eta \geq -\delta\}, \quad (4.3)$$

and jump map $G : \mathbb{R}^9 \rightarrow \mathbb{R}^9$ and jump set $D \subseteq \mathbb{R}^9$ given by

$$G(\underline{q}, h) \in (\{\underline{q}\}, \overline{\text{sgn}}(\eta)), \quad D = \{(\underline{q}, h) \in X_1 : h\eta \leq -\delta\}, \quad (4.4)$$

where $\underline{\omega}_{f_1}$ is defined as in (4.1) and h as in (4.2).

The following lemma proves that the hybrid system $\bar{\mathcal{H}}_1$ made by (2.29), (4.1) and (4.2) satisfies the **hybrid basic conditions** (see Definition 2.4), which helps to prove the stability of the system and its robustness.

Lemma 4.1. *The maps F and G , and the sets C and D defined on (4.3)-(4.4) satisfy the following properties:*

1. C and D are closed sets in \mathbb{R}^9 .
2. $F : \mathbb{R}^9 \rightarrow \mathbb{R}^9$ is continuous.
3. $G : \mathbb{R}^9 \rightrightarrows \mathbb{R}^9$ is an outer semicontinuous set-valued mapping, locally bounded and $G(\underline{q}, h)$ is nonempty for each $(\underline{q}, h) \in D$.

proof.

Setting $\delta \in (0, 1)$, consider the continuous map $\tau : \mathbb{R}^9 \rightarrow \mathbb{R}$ given by $\tau(x_1, \dots, x_8, y) = yx_1 + \delta$. The restriction $\tau|_{X_1} : X_1 \rightarrow \mathbb{R}$ of this map to X_1 is also continuous [99, Theorem 8]. Moreover, by the definition of the sets C and D , we have that

$$\begin{aligned} C &= \tau|_{X_1}^{-1}([0, +\infty)), \\ D &= \tau|_{X_1}^{-1}((-\infty, 0]). \end{aligned}$$

¹It is important to observe that we are interpreting (\underline{q}, h) as a block vector of \mathbb{R}^9 using notation (2.21) for \underline{q} . That is why the domain of F is in \mathbb{R}^9 and C is a subset of \mathbb{R}^9 .

Since the preimage of a closed set under a continuous mapping is closed, C and D are closed in X_1 . We also have that X_1 is closed in \mathbb{R}^9 . In fact, consider the continuous functions $p, d : \mathbb{R}^8 \rightarrow \mathbb{R}$ given respectively by

$$\begin{aligned} p(\eta, \mu_1, \mu_2, \mu_3, \eta', \mu'_1, \mu'_2, \mu'_3) &= [\eta, \mu_1, \mu_2, \mu_3][\eta, \mu_1, \mu_2, \mu_3]^T - 1, \\ d(\eta, \mu_1, \mu_2, \mu_3, \eta', \mu'_1, \mu'_2, \mu'_3) &= [\eta, \mu_1, \mu_2, \mu_3][\eta', \mu'_1, \mu'_2, \mu'_3]^T. \end{aligned} \quad (4.5)$$

By the definition of p and d in (4.5), one has that $\underline{S} = p^{-1}(\{0\}) \cap d^{-1}(\{0\})$. Since $\{0\}$ is a closed set of \mathbb{R} , the sets $p^{-1}(\{0\})$ and $d^{-1}(\{0\})$ are closed and their intersections are closed. Thus, \underline{S} is closed in \mathbb{R}^8 . Moreover, the set $\{-1, 1\}$ is closed in \mathbb{R} , therefore the Cartesian product $X_1 = \underline{S} \times X_c$ is closed in \mathbb{R}^9 . Thus, since X_1 is closed in \mathbb{R}^9 , C and D are also closed in \mathbb{R}^9 .

By using (2.22), the map F in terms of vector components $(\eta, \boldsymbol{\mu}, \eta', \boldsymbol{\mu}', h)$ is given by

$$F(\eta, \boldsymbol{\mu}, \eta', \boldsymbol{\mu}', h) = \frac{1}{2} \begin{bmatrix} k_1 h \boldsymbol{\mu} \cdot \boldsymbol{\mu} \\ -\eta k_1 h \boldsymbol{\mu} \\ k_2 \eta \boldsymbol{\mu} \cdot \boldsymbol{\mu}' + k_1 h \boldsymbol{\mu}' \cdot \boldsymbol{\mu} \\ -\eta^2 k_2 \boldsymbol{\mu}' - \eta' k_1 h \boldsymbol{\mu} - k_2 \eta \boldsymbol{\mu} \times \boldsymbol{\mu}' - k_1 h \boldsymbol{\mu}' \times \boldsymbol{\mu} \\ 0 \end{bmatrix}.$$

On the account that each component of F is a polynomial in variables $(\eta, \boldsymbol{\mu}, \eta', \boldsymbol{\mu}', h)$, one has that F is continuous.

We now prove that G is **outer semicontinuous**. By Lemma 2.1 it suffices to prove that each component of G is outer semicontinuous. The map $(\underline{\mathbf{q}}, h) \mapsto \underline{\mathbf{q}}$ is a projection, thus it is continuous [99]. The map $(\underline{\mathbf{q}}, h) \mapsto \overline{\text{sgn}}(\eta)$ is outer semicontinuous by Theorem 2.2. Furthermore, G is **locally bounded** because given any compact set $K \subset \mathbb{R}^9$, one has that $G(K) \subset K \times \{-1, 1\}$. Thus, $G(K)$ is bounded. Finally, by the definition of G , one has that $G(\underline{\mathbf{q}}, h)$ is nonempty for every $(\underline{\mathbf{q}}, h) \in D$. ■

Remark 4.1. Note that Lemma 4.1 implies the **hybrid basic conditions** of Definition 2.4 by Remark 2.1.

Next, we prove that the set $\{\pm 1\}$ is an asymptotically stable set for the closed-loop system.

Theorem 4.1

With feedback $\underline{\omega}$ defined as in (4.1), the set

$$A_1 := \{(\underline{\mathbf{q}}, h) \in X_1 : \underline{\mathbf{q}} = h \underline{\mathbf{1}}\}$$

is globally asymptotically stable for the closed-loop system \mathcal{H} (that is, the system made by (2.29), (4.1) and (4.2)).

proof.

Let us regard the Lyapunov candidate function $V : X_1 \rightarrow \mathbb{R}_+^*$ given by

$$V(\underline{\mathbf{q}}, h) = 2(1 - h\eta) + \eta'^2 + \|\boldsymbol{\mu}'\|^2. \quad (4.6)$$

The term $2(1 - h\eta)$ of the Lyapunov function is based on the kinematic controller of [28], while the

quadratic term $\eta'^2 + \|\boldsymbol{\mu}'\|^2$ is a novel term introduced to also consider the stabilization of the dual part of the dual quaternion. It is interesting to remark that is not necessary to add the quadratic term $\|\boldsymbol{\mu}\|^2$ in (4.6), since when $\eta = 1$ or $\eta = -1$, one has that $\|\boldsymbol{\mu}\|$ must be 0 to respect the unit-norm quaternion restriction given by $\eta^2 + \|\boldsymbol{\mu}\|^2 = 1$.

Since $\eta \in [-1, 1]$ and $h \in \{-1, 1\}$, one has that $(1 - h\eta) \geq 0$. Therefore, V is a positive semidefinite function. The condition $V = 0$ implies $0 \leq 2(1 - h\eta) = -\eta'^2 - \|\boldsymbol{\mu}'\|^2 \leq 0$ which yields $\eta' = 0$, $\boldsymbol{\mu}' = 0$ and $h\eta = 1$, that is, $V = 0$ if and only if $(\underline{\mathbf{q}}, h) \in A$. Hence, V is a positive definite function on X_1 with respect to A . Taking the time-derivative of V yields

$$\begin{aligned}\dot{V} &= -2h\dot{\eta} + 2\eta'\dot{\eta}' + 2\boldsymbol{\mu}' \cdot \dot{\boldsymbol{\mu}}' \\ &= -h^2k_1 \|\boldsymbol{\mu}\|^2 - \eta^2\eta'^2k_2 - \eta^2 \|\boldsymbol{\mu}'\|^2 k_2 \leq 0.\end{aligned}$$

In addition, $\dot{V} = 0$ if and only if $\underline{\mathbf{q}} \in \{\pm 1\}$.

Moreover, V also decreases over jumps of the closed loop system since for $h\eta < -\delta < 0$ one has that

$$V(\underline{\mathbf{q}}, h^+) - V(\underline{\mathbf{q}}, h) = 4h\eta < 0. \quad (4.7)$$

Thus, asymptotically stability of the set A_1 follows from Lemma 4.1 and by Theorem 2.6. It is also important to highlight that the closed-loop differential equation is well-posed [7, Prop. 2.1] as the chosen $\underline{\boldsymbol{\omega}}$ is in the Lie algebra of the Lie group $\text{Spin}(3) \times \mathbb{R}^3$. ■

Remark 4.2. At a first glance, one could imagine that due to the transference principle [44], the extension of rotation stabilizers (e.g., the ones of [45, 28]) to full rigid body stabilizers would be trivial, only requiring the substitution of adequate variables as in (2.18) and (2.29). However, for stability analysis based on Lyapunov functions, this supposition does not even make sense, since a Lyapunov function is a real-valued function and never a dual-number valued function. As a consequence, stabilization in $\text{Spin}(3) \times \mathbb{R}^3$ using dual quaternions required one independent study from the quaternion stabilization analysis in $\text{Spin}(3)$. The necessity of different procedures for quaternion and dual quaternion is also inferred by remembering that due to the fact that $\text{SO}(3)$ is compact and $\text{SE}(3)$ is not, it was required one controller design procedure for each case in [4].

Similarly to the rotation controllers proposed in [28], the proposed pose controller does not exhibit an infinite number of jumps in a finite amount of time, that is, a Zeno behavior [60]. This is shown in the next theorem.

Theorem 4.2

For any compact set $K \subset X_1$, if $\bar{\mathbf{x}}$ is a solution of \mathcal{H} with initial state in K , then the number of jumps is bounded.

proof.

Since V is a hybrid Lyapunov function, it follows that

$$0 \leq V(\bar{\mathbf{x}}(t, j)) \leq V(x(0, j)) \quad (4.8)$$

By (4.7), V decreases exactly $4h\eta$ after a single jump. This means that after the j th jump, V will decrease

by

$$V(\bar{\mathbf{x}}(0, j)) - V(\bar{\mathbf{x}}(0, 0)) = 4h\eta j < -4\delta j. \quad (4.9)$$

Combining inequalities (4.8) and (4.9) gives

$$0 \leq V(\bar{\mathbf{x}}(0, 0)) - 4\delta j. \quad (4.10)$$

Finally, since V is continuous and K is compact, there exists V^* such that $V^* = \max_{x \in K} V$, yielding

$$V(\bar{\mathbf{x}}(0, 0)) - 4\delta j \leq V^* - 4\delta j. \quad (4.11)$$

By combining (4.10) and (4.11), one has that $0 \leq V^* - 4\delta j$, implying that for any solution with initial state in K ,

$$j \leq \left\lceil \frac{V^*}{4\delta} \right\rceil. \quad \blacksquare$$

By Lemma 4.1, the closed-loop hybrid system satisfies the **hybrid basic conditions**. Theorem 2.8 guarantees that the asymptotically stability of set $\{\pm 1\}$ is not fragile with relation to arbitrarily small perturbations on the data of the system. The robustness of the closed-loop system can also be characterized in terms of practical \mathcal{KL} -stability in the presence of constant **σ -perturbations**: given $\rho > 0$, the σ -perturbation, with $\sigma(x) = \rho$, of the hybrid system $\bar{\mathcal{H}}_1$ is

$$\begin{aligned} C_\sigma &:= \{\bar{\mathbf{x}} \in \mathbb{R}^9 : (\bar{\mathbf{x}} + \rho\mathbb{B}) \cap C \neq \emptyset\}, \\ F_\sigma(x) &:= \overline{\text{co}}F((\bar{\mathbf{x}} + \rho\mathbb{B}) \cap C) + \rho\mathbb{B} \text{ for all } \bar{\mathbf{x}} \in C_\rho, \\ D_\sigma &:= \{\bar{\mathbf{x}} \in \mathbb{R}^9 : (x + \rho\mathbb{B}) \cap D \neq \emptyset\}, \\ G_\sigma(x) &:= G((\bar{\mathbf{x}} + \rho\mathbb{B}) \cap D) + \rho\mathbb{B}, \text{ for all } \bar{\mathbf{x}} \in D_\rho. \end{aligned}$$

The resistance of the closed-loop system against these perturbations will be expressed in Theorem 4.3 by bounding the Lyapunov function by a **\mathcal{KL} -class function**. This bound guarantees practical stability for perturbed solutions starting from arbitrarily large subsets of the basin of attraction of $\{\pm 1\}$ [60].

Theorem 4.3

Let V be as in (4.6). Then there exists a class- \mathcal{KL} function β such that for each compact set $K \subset X_1$ and $\Delta > 0$ there exists $\rho^* > 0$ such that for each $\rho \in (0, \rho^*]$, the solutions $\bar{\mathbf{x}}_\rho$ from K of the perturbed system $\bar{\mathcal{H}}_\rho = (C_\rho, F_\rho, D_\rho, G_\rho)$ satisfy

$$V(\bar{\mathbf{x}}_\rho(t, j)) \leq \beta(V(\bar{\mathbf{x}}_\rho(0, 0)), t + j) + \Delta, \quad \forall (t, j) \in \text{dom } \bar{\mathbf{x}}_\rho. \quad (4.12)$$

proof.

We have that V is a **proper indicator function** of the compact set A_1 in X_1 . From Theorem 2.7, there exists a **\mathcal{KL} -function** β such that for all solutions $\bar{\mathbf{x}}$ of $\bar{\mathcal{H}}_1$,

$$V(\bar{\mathbf{x}}(t, j)) \leq \beta(V(\bar{\mathbf{x}}(0, 0)), t + j), \quad \forall (t, j) \in \text{dom } \bar{\mathbf{x}}.$$

From this and from Lemma 4.1, the bound on $V(\bar{\mathbf{x}}_\rho(t, j))$ given by (4.12) follows by Theorem 2.9. \blacksquare

Remark 4.3. It is important to note that \underline{S} is not a compact set, due to the translation components of unit dual quaternions. However, the compact set K of Theorem 4.3 can be chosen as large as the control designer wants, provided it is still compact and is inside X_1 . Thus, Theorem 4.3 guarantees “global” stabilization in a practical sense, since projects of physical systems will naturally have an upper bound to the norm of translations.

Remark 4.4. Differently from the Lyapunov function proposed in [28] for its hybrid kinematic controller, the proposed Lyapunov function (4.6) exploits the non-compactness of the Study quadric \underline{S} : using this property, the Lyapunov function is already a proper indicator function, enabling a direct proof of Theorem 4.3. Explicitly, it is due to the terms $\zeta^2 + \|\mathbf{v}\|^2$ of the proposed Lyapunov that V is a proper indicator function. Only the term $2(1 - h\eta)$, which is exactly the Lyapunov proposed in [28] for kinematic stabilization of \mathcal{S}^3 , does not tend to infinity even in the boundary of \mathcal{S}^3 .

4.3 NUMERICAL SIMULATIONS

In this section, the effectiveness of the proposed hybrid technique for robust global stabilization of the rigid body motion is demonstrated in four different numerical simulations.² The numerical simulations presented here are exactly the same as the numerical simulations of [17] and they will be reproduced here for convenience of the reader. The first simulation considers the robustness of the proposed controller against chattering. The second simulation shows the influence of the design parameter δ in the execution of the controller. The last two simulations consider a more practical situation using a robotic manipulator.

We first illustrate the proposed controller global stability and robustness against measurement noises. To this aim, a simulation is performed using the hybrid feedback controller (4.1), with hysteresis parameter $\delta = 0.3$, and the pure discontinuous controller (3.2) of [36, 35] for the kinematic control scenario using the same proportional gain $k = 0.08$. For this particular scenario, we assume an initial condition,

$$\underline{\mathbf{q}}_0 = 0.001 + \hat{i}0.72 + \hat{j}0.06 + \hat{k}0.69 + \varepsilon \left(-55.15 - \hat{i}2.52 + \hat{j}36.71 - \hat{k}0.59 \right),$$

which was chosen arbitrarily, located in the neighborhood of $\eta = 0$, and a measurement noise over η set to $\mathcal{N}(0, 0.16)$, that is, a Gaussian random variable with zero mean and 0.16 variance. Fig. 3.3 illustrates the result from the discontinuous controller (3.2) whereby one can clearly see the problematic noise influence—for instance, the excess of switches causing chattering for up to 20 seconds and the consequent convergence lag. In contrast, the proposed hybrid feedback controller ensures a robust performance without chattering as shown in Fig. 4.3.

To further highlight the absence of chattering and performance improvements from the hybrid feedback solution (4.1)—regardless of the initial and noise conditions and the control parameters—a second scenario is devised with initial condition

$$\underline{\mathbf{q}}_0 = 0.001 + \hat{i}0.78 + \hat{j}0.57 + \hat{k}0.28 + \varepsilon \left(-1.28 + \hat{i}1.50 - \hat{j}2.44 + \hat{k}0.77 \right)$$

and a zero mean Gaussian measurement noise over η with a 0.1 standard deviation, which was also chosen arbitrarily. The results illustrating the trajectory of η from both the discontinuous and hybrid controllers—set with the same control gain, $k = 2$ —are shown in Fig. 4.4.

²The results of the simulations were computed using MATLAB environment and the DQ_robotics toolbox (<http://dqrobotics.sourceforge.net/>). The code of the simulations are available at <https://htadashi.github.io/code/KFIA15.zip>.

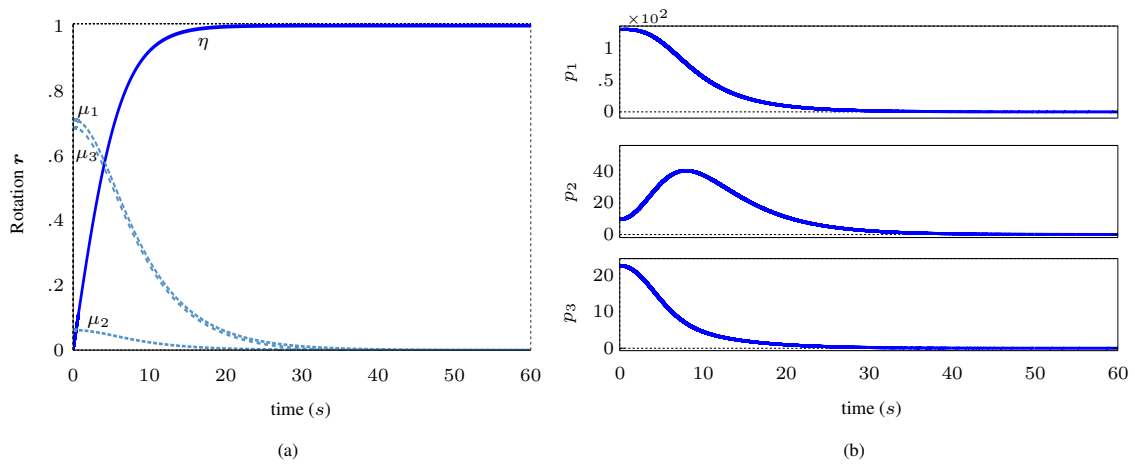


Fig. 4.3: Numerical example for the hybrid controller: (a) Trajectory of the rotation unit quaternion r in terms of η and μ (dashed line). (b) Trajectory of the three-dimensional translation elements $p = p_1\hat{i} + p_2\hat{j} + p_3\hat{k}$.

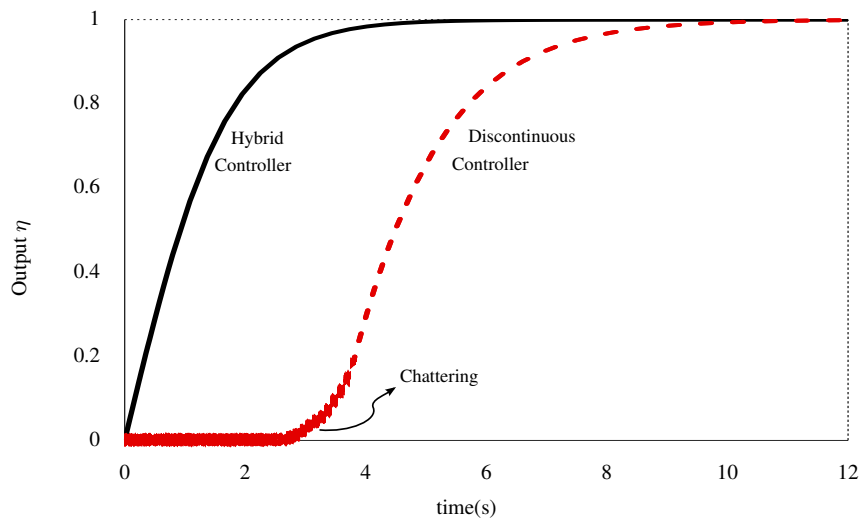


Fig. 4.4: Trajectory of η with hybrid feedback controller (4.1) and discontinuous controller (3.2) over time.

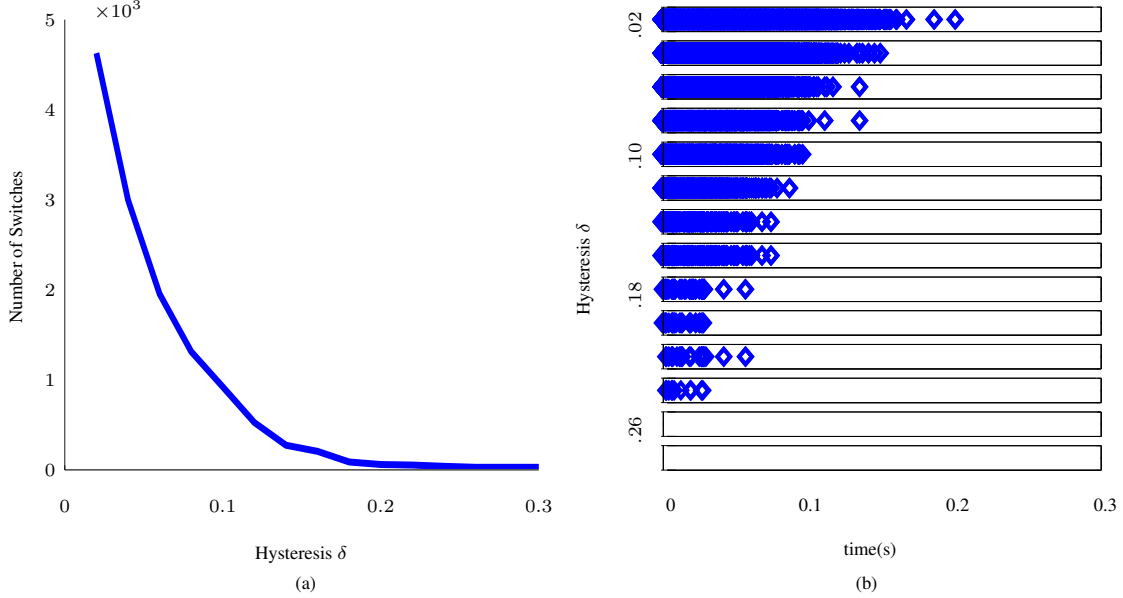


Fig. 4.5: The number of switches with regard to the hysteresis parameter δ is shown in (a), while the switches along time $s(t)$ are illustrated in (b) for different values of δ .

To illustrate the influence of the design parameter δ over the switches along time of the closed-loop system (2.29), a set of simulations is performed using the hybrid controller (4.1) with different values for δ . For these simulations, we assume the same initial condition, control gain, and measurement noise as defined in the former scenario. As shown in Fig. 4.5(a), larger hysteresis parameters yield a smaller number of switches, as one would expect. As shown in Fig. 4.5(b), it is also interesting to highlight that the number of switches tends to decrease along time as η converges to the equilibrium.

Moreover, to elucidate the influence of the hysteresis parameter δ with regard to the unwinding phenomenon, a different scenario is simulated using (4.1) with $\delta = 0.15$ and $\delta = 0.95$ and with a proportional gain $k = 5$. We assume an initial state with η close to -1 and $h = 1$. As shown in Fig. 4.6, very large values of δ may induce the stabilization to $\eta = 1$, which leads to needless motions and control efforts compared to the case of $\delta = 0.15$.

Lastly, as a concluding example, and to assess the effectiveness of the proposed solution in a more practical context, we designed a simple robot manipulator kinematic control task. To this aim, we considered a 6-DOF manipulator, the Comau SMART SiX robot, and two simple control tasks whereby the end-effector of the robot manipulator is regarded as a rigid body and described within the unit dual quaternion framework.³

In the first control setting, the end-effector of the manipulator \underline{q}_m , described within unit dual quaternions framework, is expected to hold the same current configuration—hence, the desired pose $\underline{q}_d = \underline{q}_m$ —in the presence of different sensor readings. In this case, it is rather ordinary to have readings in the antipodal configuration of the current pose, that is, $-\underline{q}_m$. To illustrate the behavior of different controllers—with gain equally set to $k = 5$ —within this particular case, that is, $\underline{q}_d = -\underline{q}_m$, we set the manipulator to a random configuration and sought to stabilize the system using a continuous feedback controller, a discontinuous controller, and the proposed hybrid controller (with $\delta = 0.1$). The simulated result can be observed in Figs. 4.7 and 4.8, which illustrate the rigid motion of the manipulator’s end-effector. Clearly, the continuous feedback controller failed

³Further information on how to describe and map the end-effector’s rigid motion using unit dual quaternions can be found in [23].

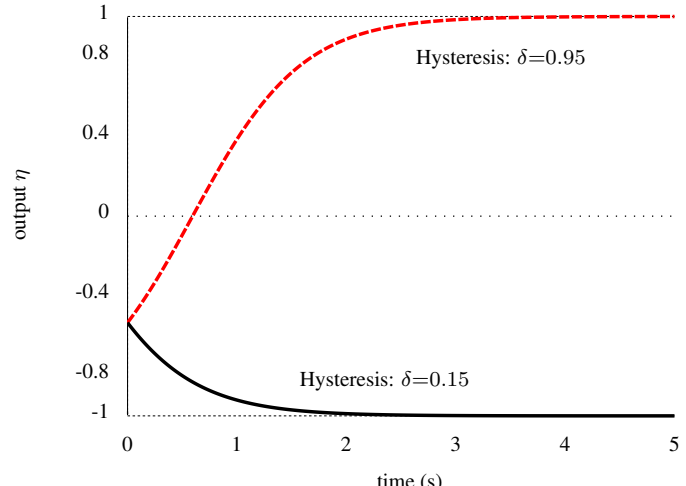


Fig. 4.6: Influence of the hysteresis parameter δ on unwinding— η converges to the farther stable point when the value of δ increases.

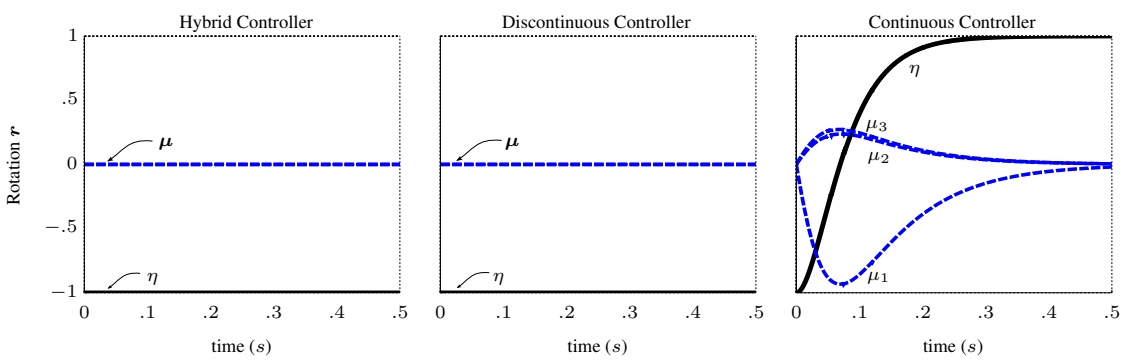


Fig. 4.7: Trajectory of the rotation unit quaternion r in terms of η and μ using the proposed hybrid controller (*left*), the discontinuous controller (*center*), and the continuous feedback controller (*right*). The unwinding phenomenon arises only on the continuous feedback controller.

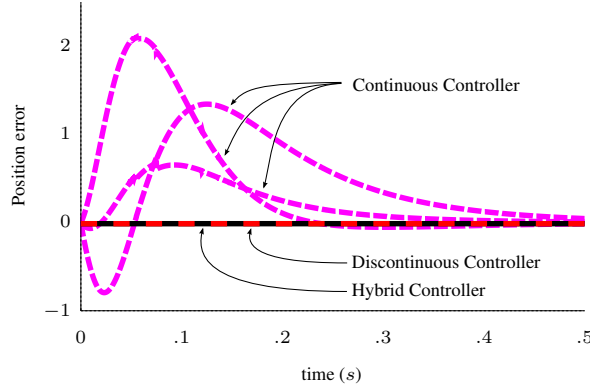


Fig. 4.8: Trajectory of the three-dimensional translation error using the hybrid (*solid line*), the discontinuous (*red dashed line*) and the continuous controller (*magenta dashed line*).

to maintain the same end-effector configuration, exhibiting the unwinding phenomenon which yields needless motions—as observed in Fig. 4.9.⁴ Such phenomena could be avoided by simply enforcing a discontinuous controller or by using the proposed hysteresis-based hybrid control strategy.

Nonetheless, as was observed in Fig. 4.4, the discontinuous sign-based approach is particularly sensitive to measurement noises. Hence, the second control task was devised to illustrate the behavior of the robot manipulator in the presence of measurement noises. In this scenario, both controllers were supposed to take the end-effector pose from an initial pose, represented by $\underline{\mathbf{q}}_0 = -0.31 - \hat{i}0.67 + \hat{j}0.67 - \hat{k}0.05 + \varepsilon(-0.06 - \hat{i}0.31 - \hat{j}0.31 + \hat{k}0.40)$ and corresponding to a rotation angle of $(\pi + 0.63)$ rad around the axis $(-\sqrt{2}/2, -\sqrt{2}/2, 0)$ followed by a translation of $(-0.39, -0.29, -1.09)$, to a desired pose, represented by $\underline{\mathbf{q}}_d = \hat{i}0.707 + \hat{j}0.707 + \varepsilon(0.28 - \hat{i}0.38 + \hat{j}0.38 + \hat{k}0.28)$ and corresponding to a rotation angle of π rad around the axis $(\sqrt{2}/2, \sqrt{2}/2, 0)$ followed by a translation of $(-0.79, 0.00, -1.07)$. The error between these poses are represented by the dual quaternion $\underline{\mathbf{q}}_e = \underline{\mathbf{q}}_m^* \underline{\mathbf{q}}_d$, where $\underline{\mathbf{q}}_m$ is the measured dual quaternion. In addition, the measurement noise over η was set to $\mathcal{N}(0, 0.09)$ and the control gain for both controllers were set to $k = 0.020$ —the hysteresis parameter was set to $\delta = 0.1$. Fig. 4.10 illustrate the rigid motion of the manipulator’s end-effector and the behavior of both controllers. It is easy to see that the problematic noise influence is restricted to the discontinuous controller—resulting in undesired chattering and delaying the closed-loop convergence. As expected, the proposed hybrid solution ensures robust performance, that is, a trajectory without chattering.

4.4 CHAPTER CONCLUSIONS

In this chapter, a kinematic controller for the rigid body stabilization problem was presented. To prove the stability of this controller, a Lyapunov function that exploits the structure of the group of unit dual quaternions was proposed. Moreover, this controller was simulated and compared to the discontinuous controller of Chapter 3. Simulation results show that the proposed controller is robust against measurement noises and, different

⁴Since the discontinuous and hybrid feedback controllers successfully hold the same end-effector pose, the corresponding trajectories of the robot were not shown in this figure because they are constant. A video comparing the trajectories generated by the three different controllers can be seen in <https://youtu.be/F8Ky60J6qHg>.

⁵A video showing the motion of the robot can be seen in the link <https://youtu.be/1RBfPX DVR-Y>.

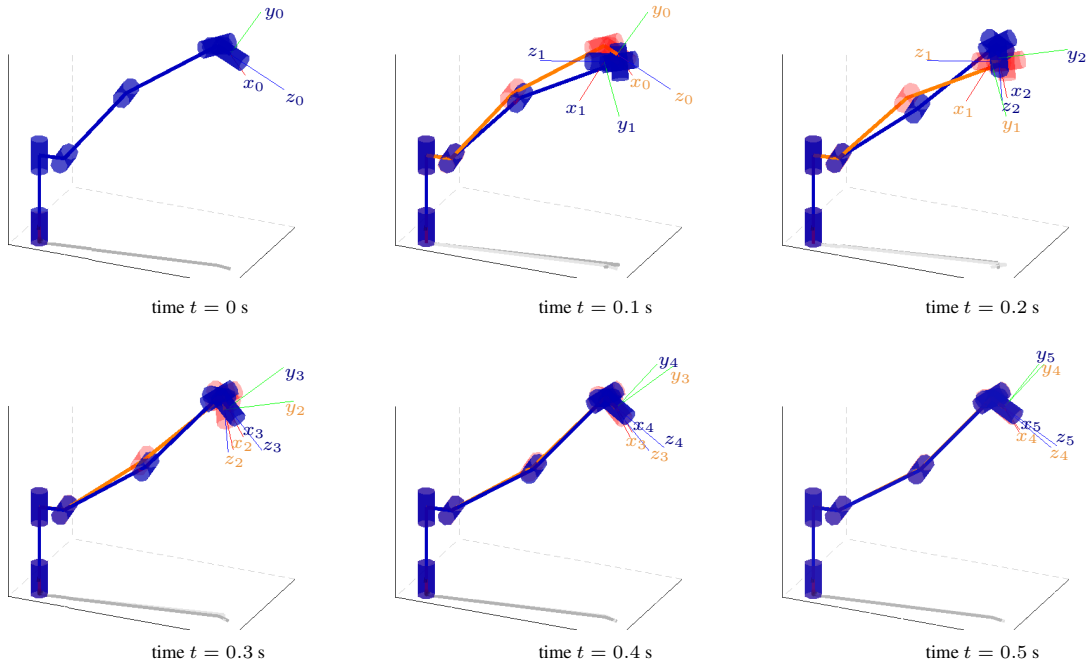


Fig. 4.9: Simulation snapshots of the robotic manipulator using the continuous controller. When the dual quaternion representing the desired robot pose is changed from \underline{q} to $-\underline{q}$ (both represents the same pose), the unwinding phenomenon can be observed. In contrast to maintaining the desired pose, the robotic manipulator goes through unexpected and unnecessary longer motions. In all snapshots, the light red robot represents the initial robot configuration.⁵

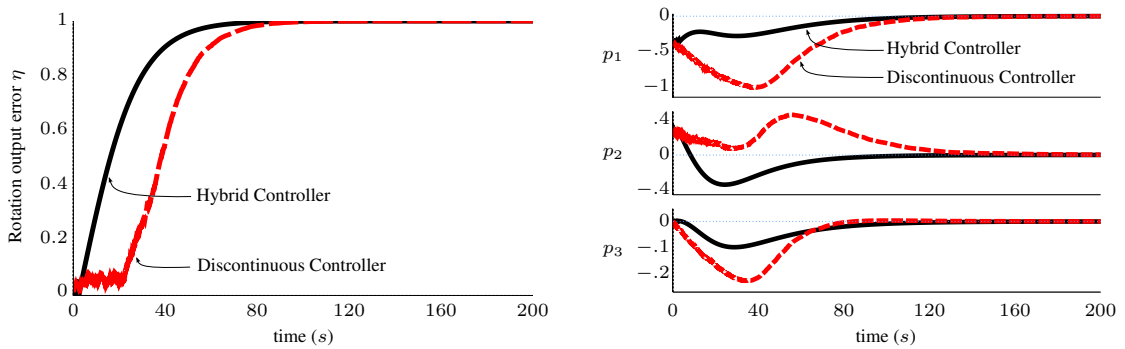


Fig. 4.10: The left figure shows the trajectory of the rotation error in terms of the scalar part η using the hybrid controller (*solid line*) and the discontinuous controller (*red dashed line*). The right figure shows the trajectory of the three-dimensional translation elements $\mathbf{p} = p_1\hat{i} + p_2\hat{j} + p_3\hat{k}$ with reference given in dotted blue line.

from discontinuous-based feedback controllers, it also avoids the problem of sensitivity of the global stabilization property to chattering. The proposed solution was also simulated in a simple robot manipulator kinematic control task to assess the controller in a more practical context. The results of this chapter have been published in [17].

To control the pose of the system, it was assumed that the designer can use the twist as an input to the system (2.29). It should be mentioned that in Chapter 6, this assumption will be dropped and a dynamic controller which considers both the pose and the twist as a state of system will be proposed: in this scenario, the resulting force and torque on the system will be the input. The next chapter will present another kinematic controller that was obtained after the qualification exam of this thesis. This novel kinematic controller will be based in another Lyapunov function which guarantees an exponential rate of convergence.

5

BIMODAL KINEMATIC CONTROLLER WITH EXPONENTIAL CONVERGENCE

5.1 INTRODUCTION

The previous controller presented in the last chapter does not have a theoretical guarantee of an exponential rate of decay for stability. In this chapter, we use a novel Lyapunov function to derive a new controller for the system, and prove that this new proposed controller has an exponential rate of convergence. The hysteretic controller strategy suggested in the previous chapter uses only one state variable $h \in X_c$ (where $X_c = \{-1, 1\}$) to determine the rotation direction so the system is regulated either to -1 or 1 . In this chapter we also use the bimodal hybrid strategy from [32]. It uses two state variables $(h, b) \in X_c \times X_c$ as shown in Fig. 5.1. The state h determines the rotation direction as in the hysteretic controller. The state b is introduced in order to adapt the hysteresis width of the on-off control for state h in such a way that the width gets shorter whenever the attitude gets relatively far from the chattering prone region, that is, the region corresponding to $\eta = 0$. This bimodal strategy spends less energy in average while keeping the same robustness margin [32]. It should be remarked that the novel Lyapunov function introduced in this chapter could also be used with a hysteretic controller with only one state variable to produce a controller with exponential rate of decay for stability.

5.2 BIMODAL CONTROLLER WITH EXPONENTIAL CONVERGENCE

The space-state of the closed-loop system is given by $X_2 := \underline{S} \times X_c \times X_c$, and the state $\bar{x}_2 \in X_2$ is represented by $\bar{x}_2 = (\underline{q}, h, b)$. As will be proved in Theorem 5.1, it is possible to use a Lyapunov-based approach to derive a feedback control law that solves the problem of global stabilization of rigid-body pose and also has exponential rate of convergence. The twist feedback law for the kinematic equation (2.29) is given by

$$\underline{\omega}_{f2} := -k_1 h \underline{\mu} - \varepsilon \left(\frac{k_2}{2} \underline{p} + k_1 h \underline{\mu} \times \underline{p} \right), \quad (5.1)$$

where $k_1, k_2 > 0$ are the controller gains. Compared with the feedback controller of the last chapter (see (4.1)), this controller uses directly the translation of the rigid-body in the dual part.

The closed-loop system is defined by the hybrid system $\overline{\mathcal{H}}_2$ given by

$$\left. \begin{array}{l} \underline{\dot{q}} = \frac{1}{2} \underline{q} \underline{\omega}_{f2} \\ \dot{h} = 0 \\ \dot{b} = 0 \end{array} \right\} \bar{x}_2 \in C_2, \quad (5.2)$$

$$\left. \begin{array}{l} \underline{q}^+ = \underline{q} \\ h^+ \in \overline{\text{sgn}}(\eta - h\delta/2) \\ b^+ \in h \overline{\text{sgn}}(\eta - h\delta/2) \end{array} \right\} \bar{x}_2 \in D_2,$$

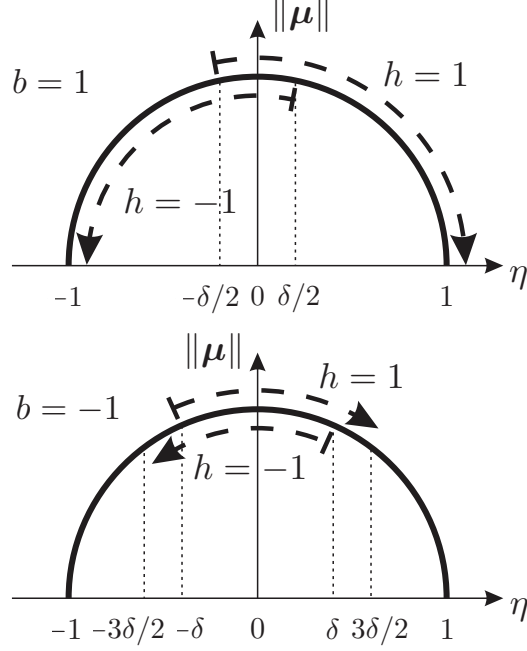


Fig. 5.1: State space representation of the quaternionic part of the bimodal controller. Arrows indicate the direction of the rotation. (Figure based on Fig. 5.2 of [1]).

where the $\overline{\text{sgn}}$ function is defined as in (2.2), and the jump set is given by $D_2 := D_{2a} \cup D_{2b} \cup D_{2c}$, with

$$D_{2a} := \{\bar{\mathbf{x}}_2 \in X_2 : h\eta \leq -\delta\}, \quad (5.3)$$

$$D_{2b} := \{\bar{\mathbf{x}}_2 \in X_2 : b = 1, h\eta \leq -\delta/2\}, \quad (5.4)$$

$$D_{2c} := \{\bar{\mathbf{x}}_2 \in X_2 : b = -1, h\eta \geq 3\delta/2\}, \quad (5.5)$$

and the flow set is $C_2 := \overline{X_2} \setminus \overline{D_2}$, where \overline{K} denotes the topological closure of the set K (see [99] for more details). The jump set D_2 models the varying hysteresis (whose width is regulated according to the discrete state variable b) shown in Fig. 5.1. For more details, the reader is referred to [1].

The following lemma proves that the hybrid system $\overline{\mathcal{H}}_2$ satisfies the **hybrid basic conditions** (see Definition 2.4).

Lemma 5.1. *The maps $F_2 : \mathbb{R}^{10} \rightarrow \mathbb{R}^{10}$ and $G_2 : \mathbb{R}^{10} \rightrightarrows \mathbb{R}^{10}$ given by*

$$F_2(\underline{\mathbf{q}}, h, b) = \left(\frac{1}{2} \underline{\mathbf{q}} \omega_{f_2}, 0, 0 \right), \quad G_2(\underline{\mathbf{q}}, h, b) \in \left(\{\underline{\mathbf{q}}\}, \overline{\text{sgn}}(\eta - h\delta/2), h\overline{\text{sgn}}(\eta - h\delta/2) \right),$$

and the sets C_2 and D_2 satisfy the following properties:

1. C_2 and D_2 are closed sets.
2. F_2 is continuous.
3. G_2 is an outer semicontinuous set-valued mapping, locally bounded and $G_2(\underline{\mathbf{q}}, h, b)$ is nonempty for each $(\underline{\mathbf{q}}, h, b) \in D_2$.

proof.

First we prove that C_2 and D_2 are closed sets: D_2 is the finite union of the sets D_{2a} , D_{2b} and D_{2c} defined in (5.3)-(5.5). Since D_{2a} , D_{2b} and D_{2c} are closed sets (the proof is similar to the proof of Lemma 4.1), D_2 is also a closed set. C_2 is the topological closure of the set $X_2 \setminus D_2$, thus by definition of topological closure, its closed.

Next, we prove that F_2 is continuous. Since $\underline{\omega}_f \in \mathbb{H}_0$, we can write it as $\underline{\omega}_f = \omega_1 + \varepsilon\omega_2$. By using (2.22), the map F in terms of vector components $(\eta, \mu, \eta', \mu', h, b)$ is given by

$$\begin{bmatrix} \dot{\eta} \\ \dot{\mu} \\ \dot{\eta}' \\ \dot{\mu}' \\ \dot{h} \\ \dot{b} \end{bmatrix} = F_2 \begin{bmatrix} \eta \\ \mu \\ \eta' \\ \mu' \\ h \\ b \end{bmatrix} = \frac{1}{2} \begin{bmatrix} -\mu^T \omega_1 \\ \eta_1 \omega_1 + \mu \times \omega_1 \\ -\mu^T \omega_2 - \mu'^T \omega_1 \\ \eta \omega_2 + \eta' \omega_1 + \mu \times \omega_2 + \mu' \times \omega_1 \\ 0 \\ 0 \end{bmatrix}, \quad (5.6)$$

Note that F_2 is a continuous mapping since each of its components are polynomial.

We now prove that G_2 is **outer semicontinuous**. By Lemma 2.1 it suffices to prove that each component of G_2 is outer semicontinuous. The map $(\underline{q}, h) \mapsto \underline{q}$ is a projection, thus it is continuous [99]. The maps $(\underline{q}, h, b) \mapsto \overline{\text{sgn}}(\eta - h\delta/2)$ and $(\underline{q}, h, b) \mapsto h\overline{\text{sgn}}(\eta - h\delta/2)$ are outer semicontinuous by Theorem 2.3. Moreover, given any compact set $K \subset \underline{\mathcal{S}} \times X_c \times X_c$, we have that $G_2(K) \subseteq \underline{\mathcal{S}} \times X_c \times X_c$, thus G_2 is **locally bounded**. Finally, $G_2(\underline{q}, h, b)$ is nonempty for each $(\underline{q}, h, b) \in D_2$ by definition of G_2 and D_2 . ■

Remark 5.1. Note that Lemma 5.1 implies the **hybrid basic conditions** of Definition 2.4 by Remark 2.1.

5.3 STABILITY ANALYSIS OF THE BIMODAL KINEMATIC CONTROLLER

In this section, we prove that the proposed hybrid bimodal control globally exponentially stabilizes the pose of a rigid body even in the presence of measurement noise.

Theorem 5.1

Let $\delta \in (0, 1)$ and $k_1, k_2 > 0$. The compact set $A_2 = \{\bar{\mathbf{x}}_2 \in X_2 : \underline{q} = h\underline{1}, b = 1\}$ is globally exponentially stable for the closed-loop hybrid system $\overline{\mathcal{H}}_2$.

proof.

For easy presentation, let us first consider $\delta \in (0, 2/3]$. Let $\underline{q} := \eta + \mu + \varepsilon(\eta' + \mu')$, and $V_2 : X_2 \rightarrow \mathbb{R}$ be defined as

$$V_2(\bar{\mathbf{x}}_2) = 2(1 - h\eta) + \|\mathbf{p}\|^2/4, \quad (5.7)$$

where $\mathbf{p} = 2\underline{q}^* \mathcal{D}(\underline{q})$ is the translation of the rigid-body represented as a quaternion. As $b = 1$ whenever

$\underline{q} = \pm \mathbf{1}$ and as $\mathbf{p} = \mathbf{0}$ if and only if $\eta' = 0$ and $\boldsymbol{\mu}' = \mathbf{0}$, it follows that $V_2(\bar{\mathbf{x}}_2) > 0$ for $\bar{\mathbf{x}}_2 \in X_2 \setminus A_2$ and $V_2(\bar{\mathbf{x}}_2) = 0$ for $\bar{\mathbf{x}}_2 \in A_2$. Hence, the function V_2 is positive definite on X_2 with respect to A_2 .

Replacing the twist feedback $\underline{\omega}_{f_2}$ given in (5.1) into (2.37) yields

$$\dot{\mathbf{p}} = \mathcal{D}(\underline{\omega}_{f_2}) - \mathcal{P}(\underline{\omega}_{f_2}) \times \mathbf{p} = \frac{k_2}{2} \mathbf{p} + k_1 h \boldsymbol{\mu} \times \mathbf{p} - k_1 h \boldsymbol{\mu} \times \mathbf{p} = \frac{k_2}{2} \mathbf{p}. \quad (5.8)$$

Thus, the time derivative \dot{V}_2 of V_2 is given by

$$\dot{V}_2(\bar{\mathbf{x}}_2) = -2h\eta + \mathbf{p} \cdot \dot{\mathbf{p}}/2 \quad (5.9)$$

$$\stackrel{(5.6)}{=} -2h \left(-\frac{1}{2} \boldsymbol{\mu} \cdot \boldsymbol{\omega} \right) + \mathbf{p} \cdot \dot{\mathbf{p}}/2 \quad (5.10)$$

$$\stackrel{(5.8)}{=} -2h \left(-\frac{1}{2} \boldsymbol{\mu} \cdot \boldsymbol{\omega} \right) + \mathbf{p} \cdot \left(-\frac{k_2}{2} \mathbf{p} \right) / 2 \quad (5.11)$$

$$= h \boldsymbol{\mu} \cdot (-k_1 h \boldsymbol{\mu}) - k_2 \mathbf{p} \cdot \mathbf{p} / 4 \quad (5.12)$$

$$= -k_1 h^2 \boldsymbol{\mu} \cdot \boldsymbol{\mu} - k_2 \|\mathbf{p}\|^2 / 4 \quad (5.13)$$

$$= -k_1 \|\boldsymbol{\mu}\|^2 - k_2 \|\mathbf{p}\|^2 / 4. \quad (5.14)$$

Thus, \dot{V}_2 is negative definite on X_2 with respect to A_2 .

Along jumps, when $\bar{\mathbf{x}}_2 \in D_2$, since $\mathbf{q}^+ = \mathbf{q}$,

$$\Delta V_2(\bar{\mathbf{x}}_2) = V_2(\bar{\mathbf{x}}_2^+) - V_2(\bar{\mathbf{x}}_2) = -2\eta(h^+ - h).$$

Let $D_2 = D_{2a} \cup D_{2b} \cup D_{2c}$, where D_{2a} , D_{2b} and D_{2c} are respectively defined in (5.3), (5.4) and (5.5).

Thus,

$$\Delta V_2(\bar{\mathbf{x}}_2) \begin{cases} \leq -4\delta_a, & \bar{\mathbf{x}}_2 \in D_{2a} \cup D_{2b}, \\ = 0, & \bar{\mathbf{x}}_2 \in D_{2c}, \end{cases}$$

where

$$\delta_a := \begin{cases} \delta, & \text{if } \bar{\mathbf{x}}_2 \in D_{2a} \setminus D_{2b}, \\ \delta/2, & \text{if } \bar{\mathbf{x}}_2 \in D_{2b}. \end{cases}$$

From Lemma 5.1 and Theorem 7.6 of [100], it follows that the compact set A_2 is stable since $\Delta V_2(\bar{\mathbf{x}}_2) \leq 0$ and $\dot{V}_2(\bar{\mathbf{x}}_2) < 0$ for all $\bar{\mathbf{x}}_2 \in X_2$.

To conclude that the set A_2 is globally asymptotically stable, it is necessary to apply Theorem 4.7 of [100] to prove that the set A_2 is the largest invariant set in $W = W_1 \cup W_2$, where $W_1 := \{\bar{\mathbf{x}}_2 \in C_2 : \dot{V}_2(\bar{\mathbf{x}}_2) = 0\}$ and $W_2 := \Delta V_2^{-1}(0) \cap G_2(\Delta V_2^{-1}(0))$, $G_2(\bar{\mathbf{x}}_2) = \bar{\mathbf{x}}_2^+$. It follows that $W_1 = A_2$, $\Delta V_2^{-1}(0) = D_{2c}$ and $G_2(\Delta V_2^{-1}(0)) = \{\bar{\mathbf{x}}_2 \in X_2 : b = 1 \text{ and } h\eta \geq 3\delta/2\}$. Thus, $W_2 = \emptyset$, $W = A_2$ and any solution $\bar{\mathbf{x}}_2(t)$ approaches the largest invariant set A_2 .

The proof is valid for $\delta \in (0, 2/3]$. For the case $\delta \in (2/3, 1)$, the system still behaves as proposed until the first jump. Afterward, it will behave as the hysteretic controller, since b will not change anymore.

Following is the proof that the set A_2 is globally exponentially stable. Using (5.14) and the fact that

the norm of the unit quaternion is 1,

$$\begin{aligned}
\dot{V}_2 &= -k_1(1 - \eta^2) - k_2\|\mathbf{p}\|^2/4 \\
&\leq \max\{-k_1, -k_2\} [(1 - \eta^2) + \|\mathbf{p}\|^2/4] \\
&\leq \max\{-k_1, -k_2\} [(1 - h\eta)(1 + h\eta) + \|\mathbf{p}\|^2/4] \\
&\leq \max\{-k_1, -k_2\} \left[2(1 - h\eta) \frac{(1 + h\eta)}{2} + \|\mathbf{p}\|^2/4 \right] \\
&\leq \max\{-k_1, -k_2\} \left[2(1 - h\eta) \frac{(1 - \delta)}{2} + \|\mathbf{p}\|^2/4 \right] \\
&\leq \max\{-k_1, -k_2\} \frac{(1 - \delta)}{2} [2(1 - h\eta) + \|\mathbf{p}\|^2/4] \\
&\leq \max\{-k_1, -k_2\} \frac{(1 - \delta)}{2} V_2,
\end{aligned}$$

where it was used that $(1 - \eta^2) = (1 - h\eta)(1 + h\eta)$ and that $0 < 1 - \delta \leq 1 + h\eta$. ■

Differently from memoryless discontinuous controllers, the next theorem states that the stability of the set A_2 is not sensitive to arbitrarily small constant σ -perturbations. The proof follows from the same reasoning of Theorem 4.3.

Theorem 5.2

Let V_2 be as in (5.7). Then there exists a class- \mathcal{KL} function β such that for each compact set $K_2 \subset X_2$ and $\Delta > 0$ there exists $\rho^* > 0$ such that for each $\rho \in (0, \rho^*]$, the solutions $\bar{\mathbf{x}}_{2\rho}$ from K_2 of the perturbed system $\bar{\mathcal{H}}_{2\rho}$ satisfy

$$V_2(\bar{\mathbf{x}}_{2\rho}(t, j)) \leq \beta(V_2(\bar{\mathbf{x}}_{2\rho}(0, 0)), t + j) + \Delta, \quad \forall (t, j) \in \text{dom } \bar{\mathbf{x}}_{2\rho}. \quad (5.15)$$

The analysis of either the presence of Zeno solutions (infinite number of jumps in a finite amount of time) or chattering are only related to the rotation. The rotation evolution follows the primary part of (2.29), that is, it follows the same kinematic equation for quaternions (2.18). Replacing (5.1) into (2.18) yields

$$\begin{aligned}
\dot{\mathbf{q}} &= \frac{1}{2}(\eta + \boldsymbol{\mu})(-k_1 h \boldsymbol{\mu}) \\
&= \frac{k_1}{2} h (\|\boldsymbol{\mu}\|^2 - \eta \boldsymbol{\mu}).
\end{aligned}$$

Note that $\dot{\mathbf{q}}$ depends only on \mathbf{q} and the dynamics of h . On the other hand, the dynamics of h and b depend only on η , that is, the body rotation. Hence, we conclude that jumps on state variables h and b depend only on the rotation evolution. Since this dynamics is exactly the same of the bimodal controller of [32], it follows directly from Theorems 3.2 and 3.3 of [32] that no Zeno solutions occur even when constant σ -perturbations (see Definition 2.13) are taken into account, provided that the amplitude of the perturbation is sufficiently small.

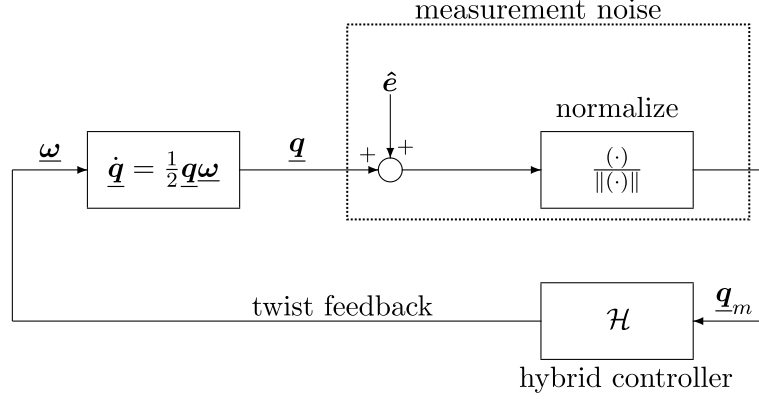


Fig. 5.2: Block diagram of the closed-loop system.

5.4 NUMERICAL SIMULATIONS

This section presents simulation results to compare performance among the novel kinematic controller from this chapter and the hybrid controllers of [17] (Chapter 4) and [38], which uses the twist feedback proposed in [17], but coupled with the bimodal mechanism proposed in [1]. To maintain fairness, all simulated controllers have been implemented with the same control gains $k_1 = 3$ and $k_2 = 1.2$. The hysteresis parameter defined for the controllers was set to $\delta = 0.40$.

The initial pose of the controllers was set to $\mathbf{q}(0) = -0.2 + 0.48\hat{i} + 0.20\hat{j} + 0.83\hat{k}$ and $\mathbf{p}(0) = -0.33\hat{i} - 0.50\hat{j} + 2.94\hat{k}$. The initial discrete state for the hybrid controller of [17] was set to $h(0) = 1$, while the proposed bimodal controller and the bimodal controller of [38] was set to $h(0) = 1$ and $b(0) = 1$. Moreover, to illustrate the robustness of the proposed controller and the performance of all three controllers, measured noise have been included to the value of \mathbf{q} and was calculated as follows: $\mathbf{q}_m = (\mathbf{q} + z\hat{e}) / \|\mathbf{q} + z\hat{e}\|$, $\hat{e} = \mathbf{e} / \|\mathbf{e}\|$, where each component of $\mathbf{e} \in \mathbb{R}^4$ was chosen from a Gaussian distribution of zero mean and unitary standard deviation and $z \in \mathbb{R}$ was chosen from a uniform distribution on the interval $[0, 0.2]$. Following [28], the solver ode45 from MATLAB was used for performing the numerical integration. The block diagram of the closed loop system is illustrated in Fig. 5.2.

The next figures show the results of the simulation of the three controllers, that is, the one from [17], [38] and the proposed controller. In all the legend of the next four figures, $\underline{\omega}_{f1,hys}$ indicates the controller from [17], $\underline{\omega}_{f1,bim}$ indicates the controller from [38] and $\underline{\omega}_{f2,bim}$ indicates the controller proposed in this chapter.

Fig. 5.3 illustrates the evolution of the real primary part of the dual quaternion in each controller. Since the evolution of the rotational parameters for the proposed kinematic controller and for the controller from [38] are the same, they have exactly the same behavior. The controller proposed in [17], however, takes a different direction of rotation from the proposed controller and the controller proposed in [38]. For [17] only, the initial condition belongs to a region of the state space where the control law pulls the rigid body in the direction of the longer rotation.

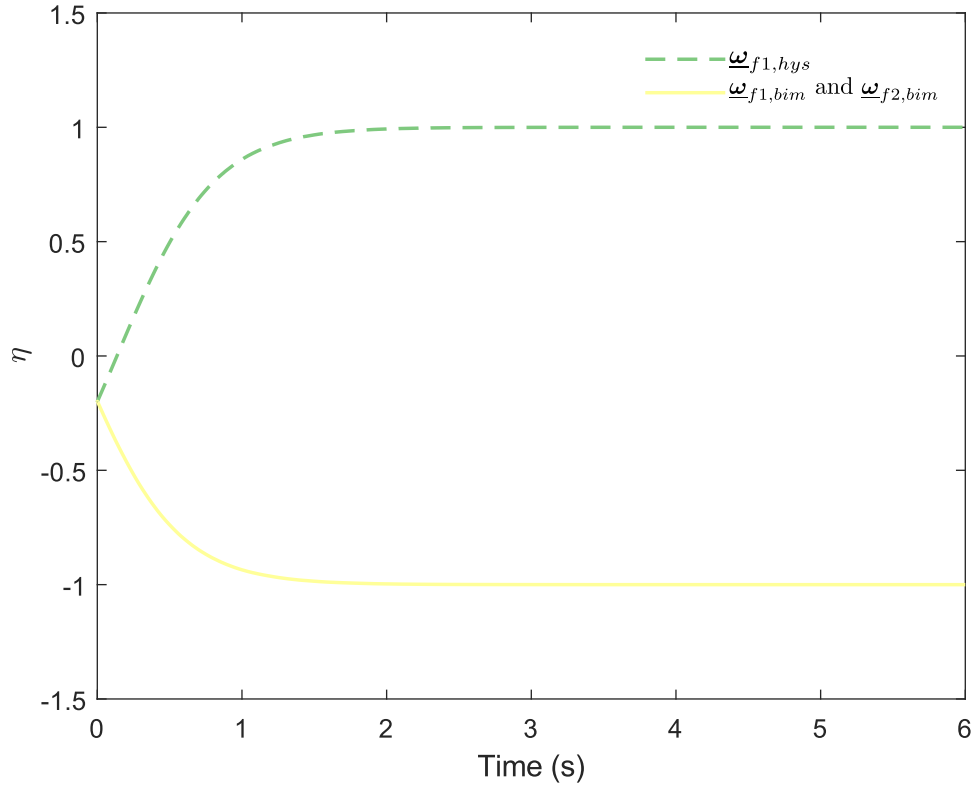


Fig. 5.3: Trajectory of the real primary part of the dual quaternion \underline{q} .

In Fig. 5.4 it is shown the evolution of the norm of the angular velocity of these controllers. Since the primary part of the twist feedback of the proposed controller and the controller of [38] are the same, the rotation movement has the same behavior. It is important to notice that the proposed controller in this chapter and the controller proposed in [38] use less control effort (in terms of the norm of the angular velocity at each time) than the controller suggested in [17].

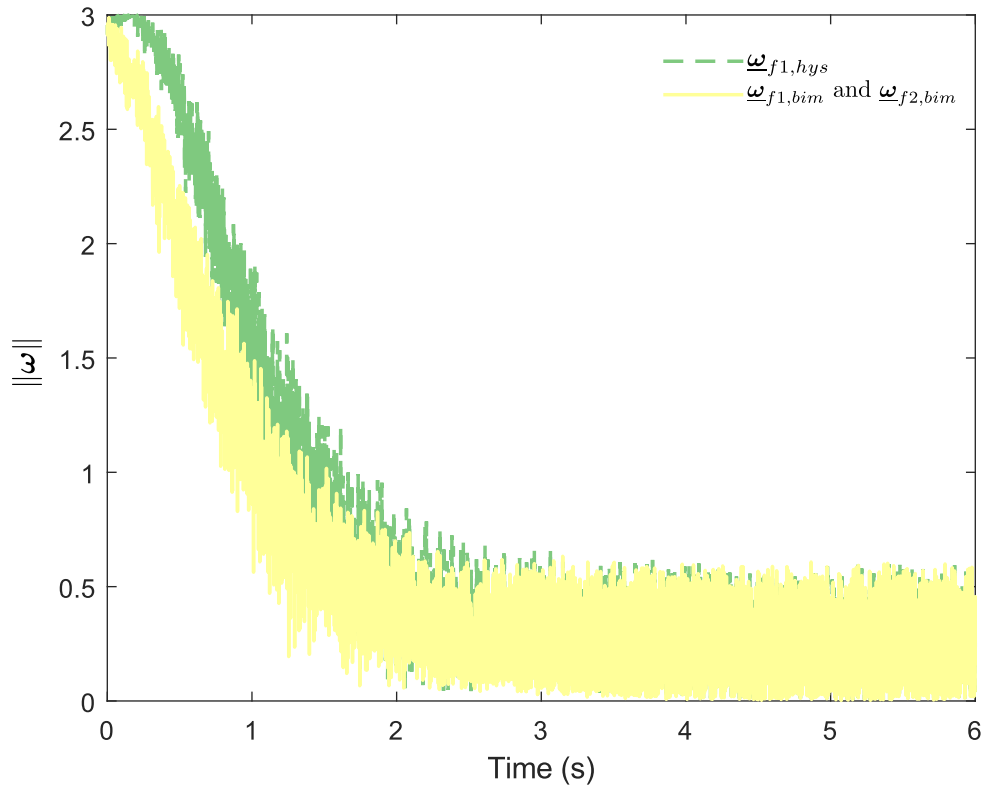


Fig. 5.4: Evolution of the norm of angular velocity ω .

Fig. 5.5 shows the evolution of the rigid-body translation under the three controllers. The variable $p_s = qpq^*$ is the translation expressed in the reference frame. As can be seen in this figure, the proposed controller causes the rigid body to come closer to the origin faster than the hybrid controllers of [38] and [17].

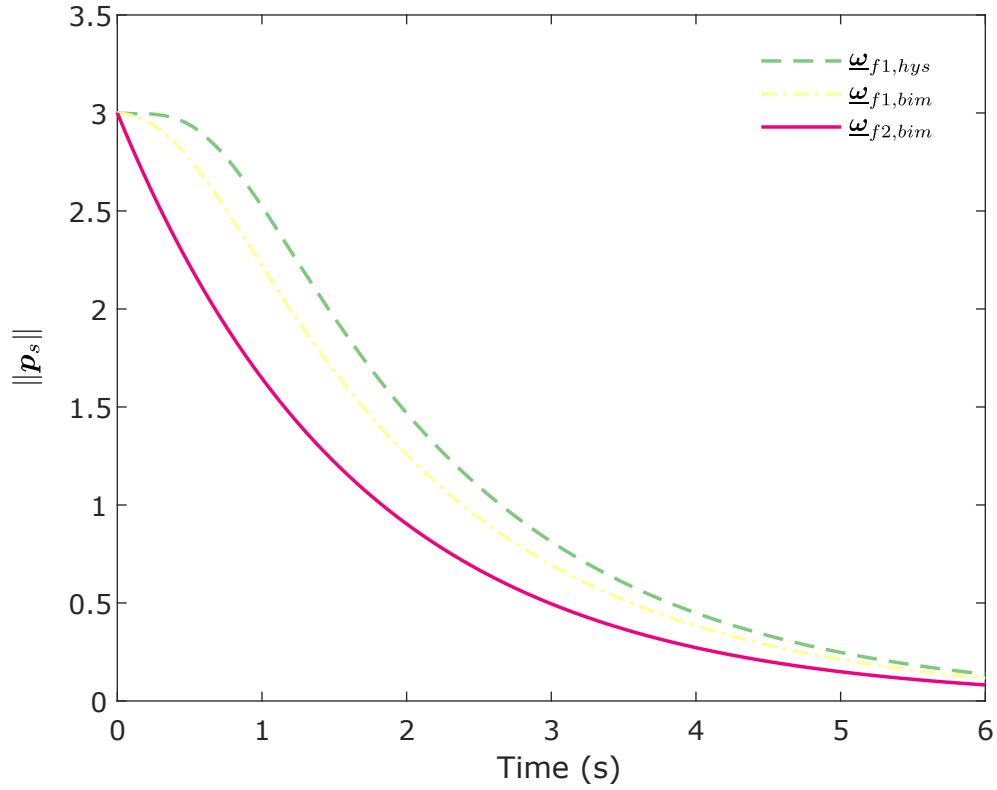


Fig. 5.5: Evolution of the norm of position expressed in the reference frame.

Finally, in Fig. 5.6 it is shown the evolution of the norm of velocity under the three controllers. While the angular velocity norm evolves in the same way for the proposed controller and the controller of [38], the norm of the velocity evolves differently: it is clear from this figure that much less effort is used for the proposed controller. Besides, note that for the proposed controller, $\|\dot{\boldsymbol{p}}\| = (k_2/2)\|\boldsymbol{p}\|$ (from (5.8)) does not depend on \boldsymbol{q} and its measured noise. Thus, differently from the controllers of [17] and [38], the evolution of $\|\dot{\boldsymbol{p}}\|$ it completely chattering free.

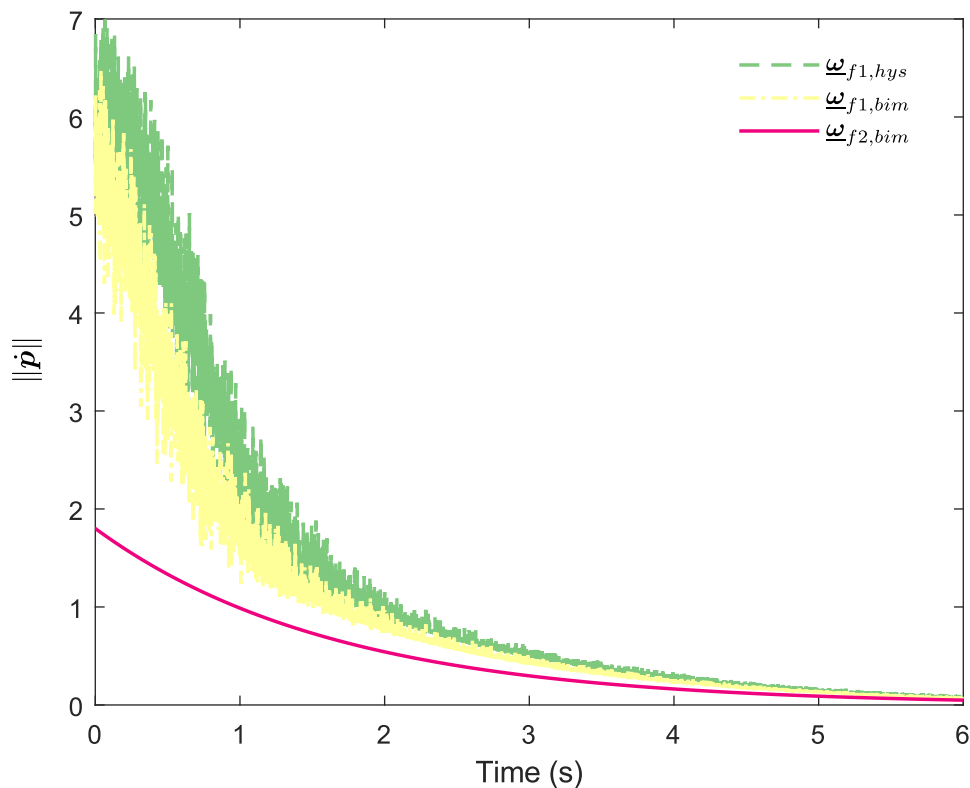


Fig. 5.6: Evolution of the norm of position expressed in the reference frame.

5.5 CHAPTER CONCLUSIONS

This chapter presents a novel control strategy for the motion of rigid bodies that guarantees global stability of the closed-loop kinematics. The result, based on the exploitation of hybrid theory tools and the unit dual quaternion manifold characteristics, enlarges the applicability of hybrid theory improving the closed-loop performance of the rigid body kinematics. In contrast to the existing literature of memoryless discontinuous controllers, the proposed kinematic controller ensures robust global exponential stability of the rigid body kinematics whilst also ensuring that the global attractivity of the stabilization pose does not exhibit chattering. Simulation results show that the proposed controller is robust against measurement noises and, different from memoryless discontinuous-based feedback controllers, it also avoids the problem of sensitivity of the global stabilization property to chattering. Moreover, the numerical simulations show the advantage of the proposed controller over the hybrid kinematic controllers of [17] (presented in the last chapter) and the controller of [38], both of which do not present exponential decaying stability.

To control the pose of the system, it was again assumed that the designer can use the twist as an input to the system (2.29). In the next chapter, this assumption will be dropped and a dynamic controller which considers both the pose and the twist as a state of system will be proposed.

6

HYBRID DYNAMIC CONTROLLER

6.1 INTRODUCTION

In the controllers presented on the previous chapters, the state of the dynamical system was the unit dual quaternion describing the rigid-body pose, and the input was done directly by the twist. On more common scenarios, the input of the system is done by forces and torques actuating in the system, while the complete state of the system is the unit dual quaternion describing the rigid-body pose and the twist.

Moreover, in these scenarios, it is common to have a more general control problem than stabilization that is the tracking problem. The goal of this problem is to design a torque and force feedback such that the pose of the controlled rigid body tracks a desired reference attitude and a reference spatial trajectory. This problem is interesting for example, in the context of a surveillance mission where an unmanned vehicle equipped with a camera is required to scout a predefined trajectory and to film in predefined orientations. In the case that the desired pose to be tracked is described by the constant dual-quaternion 1, the tracking problem yields the particular case of stabilization problem.

This chapter presents a hybrid dynamic controller that solves the tracking problem. As a direct consequence, this controller also solves the stabilization problem by specializing this tracking controller. This is stated on Section 6.5. In the next section, we will derive the dynamics of the tracking problem.

6.2 DYNAMICS OF THE POSE TRACKING PROBLEM

For this problem, we will assume that the current attitude of the rigid-body, represented by quaternion \mathbf{q} , the velocity angular of the system, represented by quaternion $\boldsymbol{\omega}$, and the current translation and velocity of the system, represent by quaternions \mathbf{p} and $\dot{\mathbf{p}}$ are available to measurement. In other words, the vector of measurements are given by

$$y = (\mathbf{q}, \boldsymbol{\omega}, \mathbf{p}, \dot{\mathbf{p}}). \quad (6.1)$$

Let $N > 0$, $P > 0$ and $C \subset \mathbb{R}^3$ be a compact set containing the closed ball $\max\{N, P\}\mathbb{B}$. To derive the pose tracking dynamics, suppose the body should track the following desired bounded reference trajectory given by state $\bar{\mathbf{x}}_d = (\underline{\mathbf{q}}_d, \underline{\boldsymbol{\omega}}_d, \underline{\dot{\mathbf{p}}}_d) \in X_d$, where $X_d := \underline{\mathcal{S}} \times C \times C$ is the state-space of the desired configuration. It is assumed that state x_d to be tracked has the following dynamics:

$$\begin{cases} \underline{\dot{\mathbf{q}}}_d = \frac{1}{2} \underline{\mathbf{q}}_d \underline{\boldsymbol{\omega}}_d, \\ \underline{\dot{\boldsymbol{\omega}}}_d \in N\mathbb{B}, \\ \underline{\ddot{\mathbf{p}}}_d \in P\mathbb{B}, \end{cases} \quad (6.2)$$

where $\underline{\mathbf{q}}_d = \mathbf{q}_d + \varepsilon \frac{1}{2} \mathbf{q}_d \mathbf{p}_d$ is the desired pose, \mathbf{q}_d is the desired attitude, \mathbf{p}_d is the desired translation expressed in the desired frame, and $\underline{\boldsymbol{\omega}}_d = \boldsymbol{\omega}_d + \varepsilon (\dot{\mathbf{p}}_d + \boldsymbol{\omega}_d \times \mathbf{p}_d)$ is the desired twist, $\boldsymbol{\omega}_d$ is the desired angular velocity and $\dot{\mathbf{p}}_d$ is the desired velocity, both of them expressed in the desired frame. Since the dynamic equations will

only make sense if all of its variables are expressed in the same frame (in the particular case, we shall express all the variables in the body frame), it is important to express these variables in the appropriated frame. Suppose that a variable \underline{x}_d is expressed in the desired frame. According to Remark 2.10, one can express \underline{x}_d in the body frame by the variable $\underline{x}_d^b := \underline{q}_e^* \underline{x}_d \underline{q}_e$. The superscript b , in \underline{x}_d^b , means that the variable coordinates are referred to the body frame. It is important to note that $[\dot{x}]^b \neq \frac{d}{dt}[\underline{x}^b]$. To simplify notation, $[\dot{x}]^b$ is denoted as $\underline{\dot{x}}^b$.

We shall define now the error variables, expressed in the body frame. The error variables will be denoted with a subscript e and for convenience will never appear with the superscript b , since those variables always will be expressed in the body frame. Let $\underline{q}_e = \eta_e + \mu_e$ be the attitude error, $\underline{q}_e = \underline{q}_e + \varepsilon \underline{q}'_e$ be the pose error defined as the error between the current configuration \underline{q} and the desired configuration \underline{q}_d , calculated as follows

$$\underline{q}_e = \underline{q}_d^* \underline{q}. \quad (6.3)$$

To obtain the dynamics of the error states, we will derive expressions for $\underline{\dot{q}}_e$ and $\underline{\dot{\omega}}_e$ in function of the states $(\underline{q}_e, \underline{\omega}_e, \underline{q}_d, \omega_d, \dot{p}_d)$. The development of these expressions will follow [101], but for convenience of the reader, we will present here the derivations of these expressions with more details. For the reader interested in the final expression of the pose tracking problem, it is recommended to jump this subsections to subsection 6.2.3.

6.2.1 Dual quaternion error kinematics

In this section, we will derive a equation for $\underline{\dot{q}}_e$ in function of the states \underline{q}_e and $\underline{\omega}_e$. Using (6.3) and substituting (2.26) and (6.2) into it,

$$\begin{aligned} \underline{q}_e &= \left(\underline{q}_d + \varepsilon \frac{1}{2} \underline{q}_d \underline{p}_d \right)^* \left(\underline{q} + \varepsilon \frac{1}{2} \underline{q} \underline{p} \right) \\ &= \left(\underline{q}_d^* - \varepsilon \frac{1}{2} \underline{p}_d \underline{q}_d^* \right) \left(\underline{q} + \varepsilon \frac{1}{2} \underline{q} \underline{p} \right) \end{aligned} \quad (6.4)$$

$$= \underline{q}_d^* \underline{q} + \varepsilon \frac{1}{2} (\underline{q}_d^* \underline{q} \underline{p} - \underline{p}_d \underline{q}_d^* \underline{q}) \quad (6.5)$$

$$= \underline{q}_d^* \underline{q} + \varepsilon \frac{1}{2} [(\underline{q}_d^* \underline{q}) \underline{p} - (\underline{q}_d^* \underline{q}) (\underline{q}_d^* \underline{q})^* \underline{p}_d (\underline{q}_d^* \underline{q})] \quad (6.6)$$

$$= \underline{q}_d^* \underline{q} + \varepsilon \frac{1}{2} \underline{q}_d^* \underline{q} [\underline{p} - (\underline{q}_d^* \underline{q})^* \underline{p}_d (\underline{q}_d^* \underline{q})] \quad (6.7)$$

$$= \underline{q}_e + \varepsilon \frac{1}{2} \underline{q}_e (\underline{p} - \underline{q}_e^* \underline{p}_d \underline{q}_e) \quad (6.8)$$

$$= \underline{q}_e + \varepsilon \frac{1}{2} \underline{q}_e (\underline{p} - \underline{p}_d^b) \quad (6.9)$$

$$= \underline{q}_e + \varepsilon \frac{1}{2} \underline{q}_e \underline{p}_e, \quad (6.10)$$

where

$$\underline{p}_e := \underline{p} - \underline{p}_d^b = \underline{p} - \underline{q}_e^* \underline{p}_d \underline{q}_e \quad (6.11)$$

is the translation error. The time derivative of (6.3) is

$$\underline{\dot{q}}_e = \underline{\dot{q}}_d^* \underline{q} + \underline{q}_d^* \underline{\dot{q}} \quad (6.12)$$

Substituting (2.29) and (6.2) into (6.12), yields

$$\begin{aligned}\dot{\underline{q}}_e &= \left(\frac{1}{2}\underline{q}_d\omega_d\right)^* \underline{q} + \underline{q}_d^* \left(\frac{1}{2}\underline{q}\omega\right) \\ &= \frac{1}{2} \left(\underline{q}_d^*\underline{q}\omega - \omega_d\underline{q}_d^*\underline{q}\right)\end{aligned}\quad (6.13)$$

$$= \frac{1}{2} \left[\left(\underline{q}_d^*\underline{q}\right)\omega - \left(\underline{q}_d^*\underline{q}\right)^* \omega_d \left(\underline{q}_d^*\underline{q}\right) \right] \quad (6.14)$$

$$= \frac{1}{2}\underline{q}_e \left(\omega - \underline{q}_e^*\omega_d\underline{q}_e\right) \quad (6.15)$$

$$= \frac{1}{2}\underline{q}_e \left(\omega - \omega_d^b\right) \quad (6.16)$$

$$= \frac{1}{2}\underline{q}_e \omega_e, \quad (6.17)$$

where

$$\omega_e := \omega - \omega_d^b = \omega - \underline{q}_e^*\omega_d\underline{q}_e \quad (6.18)$$

is the twist error. The state-space of the error states $(\underline{q}_e, \omega_e)$ will be denoted by $X_e := \underline{S} \times \mathbb{H}_0$.

It is interesting to remark the similarity of (6.17) with (2.29), that is, the kinematics of error is the same of the kinematics of the actual state dynamics. It is also interesting to remark that the primary part of $\dot{\underline{q}}_e$ is

$$\begin{aligned}\dot{\underline{q}}_e &= \frac{1}{2}\underline{q}_e \left(\omega - \underline{q}_e^*\omega_d\underline{q}_e\right) \\ &= \frac{1}{2}\underline{q}_e \left(\omega - \omega_d^b\right) \\ &= \frac{1}{2}\underline{q}_e \omega_e^b,\end{aligned}\quad (6.19)$$

where

$$\omega_e := \omega - \omega_d^b = \omega - \underline{q}_e^*\omega_d\underline{q}_e \quad (6.20)$$

is the angular velocity error.

We derive now some expressions for the time derivatives of the translation error that will also be important in the next sections. Applying the time derivative in both sides of (6.11) results in

$$\dot{\underline{p}}_e^b = \dot{\underline{p}} - \dot{\underline{q}}_e^*\underline{p}_d\underline{q}_e - \underline{q}_e^*\dot{\underline{p}}_d\underline{q}_e - \underline{q}_e^*\underline{p}_d\dot{\underline{q}}_e \quad (6.21)$$

Replacing (6.19) and (6.20) in (6.21) yields

$$\begin{aligned}\dot{\underline{p}}_e^b &= \dot{\underline{p}} - \left(\frac{1}{2}\underline{q}_e\omega_e^b\right)^* \underline{p}_d\underline{q}_e - \underline{q}_e^*\dot{\underline{p}}_d\underline{q}_e - \underline{q}_e^*\underline{p}_d\left(\frac{1}{2}\underline{q}_e\omega_e^b\right) \\ &= \dot{\underline{p}} + \frac{1}{2}\omega_e^b\underline{q}_e^*\underline{p}_d\underline{q}_e - \underline{q}_e^*\dot{\underline{p}}_d\underline{q}_e - \underline{q}_e^*\underline{p}_d\left(\frac{1}{2}\underline{q}_e\omega_e^b\right) \\ &= \dot{\underline{p}} - \dot{\underline{p}}_d^b + \frac{1}{2}\omega_e^b\underline{p}_d^b - \frac{1}{2}\underline{p}_d^b\omega_e^b \\ &\stackrel{(2.24)}{=} \dot{\underline{p}} - \dot{\underline{p}}_d^b + \omega_e^b \times \underline{p}_d^b,\end{aligned}\quad (6.22)$$

Applying the time derivative in both sides of (6.22) results in

$$\begin{aligned}\ddot{\underline{p}}_e^b &= \ddot{\underline{p}} - \left(\ddot{\underline{p}}_d^b + \dot{\underline{p}}_d^b \times \omega_e^b\right) + \dot{\omega}_e^b \times \underline{p}_d^b + \omega_e^b \times \left(\dot{\underline{p}}_d^b + \underline{p}_d^b \times \omega_e^b\right) \\ &= \underline{f}/m - \ddot{\underline{p}}_d^b + \dot{\omega}_e^b \times \underline{p}_d^b + 2\omega_e^b \times \dot{\underline{p}}_d^b + \omega_e^b \times \left(\underline{p}_d^b \times \omega_e^b\right).\end{aligned}\quad (6.23)$$

6.2.2 Dynamics of the twist error

In this section we will express the derivative of the twist error $\underline{\omega}_e$ in terms of the states $(\underline{q}_e, \underline{\omega}_e, \underline{q}_d, \omega_d, \dot{\underline{p}}_d)$ and the input variables (τ, \mathbf{f}) , where τ is the quaternion representation of external torque actuating in the rigid body and \mathbf{f} is the quaternion representation of the external force actuating in the rigid body, both expressed in body frame. In order to derive those equations, we first express the desired twist in the body frame in function of the desired translation and the translation error, and the desired angular velocity:

$$\begin{aligned}
\underline{\omega}_d^b &= \underline{q}_e^* \omega_d \underline{q}_e \\
&\stackrel{(6.10)}{=} \left(\underline{q}_e + \varepsilon \frac{1}{2} \underline{q}_e \underline{p}_e \right)^* [\omega_d + \varepsilon (\dot{\underline{p}}_d + \omega_d \times \underline{p}_d)] \left(\underline{q}_e + \varepsilon \frac{1}{2} \underline{q}_e \underline{p}_e \right) \\
&= \left(\underline{q}_e^* - \varepsilon \frac{1}{2} \underline{p}_e \underline{q}_e^* \right) [\omega_d + \varepsilon (\dot{\underline{p}}_d + \omega_d \times \underline{p}_d)] \left(\underline{q}_e + \varepsilon \frac{1}{2} \underline{q}_e \underline{p}_e \right) \\
&= \left\{ \underline{q}_e^* \omega_d + \varepsilon \left[\underline{q}_e^* (\dot{\underline{p}}_d + \omega_d \times \underline{p}_d) - \frac{1}{2} \underline{p}_e \underline{q}_e^* \omega_d \right] \right\} \left(\underline{q}_e + \varepsilon \frac{1}{2} \underline{q}_e \underline{p}_e \right) \\
&= \underline{q}_e^* \omega_d \underline{q}_e + \varepsilon \left[\underline{q}_e^* (\dot{\underline{p}}_d + \omega_d \times \underline{p}_d) - \frac{1}{2} \underline{p}_e \underline{q}_e^* \omega_d \right] \underline{q}_e + \varepsilon \underline{q}_e^* \omega_d \frac{1}{2} \underline{q}_e \underline{p}_e \\
&= \omega_d^b + \varepsilon \left[\underline{q}_e^* \dot{\underline{p}}_d \underline{q}_e + \underline{q}_e^* (\omega_d \times \underline{p}_d) \underline{q}_e - \frac{1}{2} \underline{p}_e (\underline{q}_e^* \omega_d \underline{q}_e) \right] + \varepsilon \frac{1}{2} (\underline{q}_e^* \omega_d \underline{q}_e) \underline{p}_e \\
&= \omega_d^b + \varepsilon \left[\dot{\underline{p}}_d^b + (\underline{q}_e^* \omega_d \underline{q}_e) \times (\underline{q}_e^* \underline{p}_d \underline{q}_e) - \frac{1}{2} \underline{p}_e \omega_d^b \right] + \varepsilon \frac{1}{2} \omega_d^b \underline{p}_e^b \\
&= \omega_d^b + \varepsilon \left(\dot{\underline{p}}_d^b + \omega_d^b \times \underline{p}_d^b + \frac{1}{2} \omega_d^b \underline{p}_e - \frac{1}{2} \underline{p}_e \omega_d^b \right) \\
&\stackrel{(2.24)}{=} \omega_d^b + \varepsilon \left(\dot{\underline{p}}_d^b + \omega_d^b \times \underline{p}_d^b + \omega_d^b \times \underline{p}_e^b \right). \tag{6.24}
\end{aligned}$$

Thus, the twist error given in (6.18) is

$$\begin{aligned}
\underline{\omega}_e &= \underline{\omega} - \underline{\omega}_d^b \\
&\stackrel{(2.30)}{=} \underline{\omega} + \varepsilon (\dot{\underline{p}} + \underline{\omega} \times \underline{p}) - \underline{\omega}_d^b \\
&\stackrel{(6.24)}{=} \underline{\omega} + \varepsilon (\dot{\underline{p}} + \underline{\omega} \times \underline{p}) - \left\{ \omega_d^b + \varepsilon \left[\dot{\underline{p}}_d^b + \omega_d^b \times (\underline{p}_d^b + \underline{p}_e) \right] \right\} \tag{6.25}
\end{aligned}$$

$$= \underline{\omega} - \omega_d^b + \varepsilon \left[\dot{\underline{p}} + \underline{\omega} \times \underline{p} - \dot{\underline{p}}_d^b - \omega_d^b \times (\underline{p}_d^b + \underline{p}_e) \right] \tag{6.26}$$

$$= \underline{\omega}_e + \varepsilon \left[\dot{\underline{p}} + (\underline{\omega}_e + \omega_d^b) \times (\underline{p}_e + \underline{p}_d^b) - \dot{\underline{p}}_d^b - \omega_d^b \times (\underline{p}_d^b + \underline{p}_e) \right] \tag{6.27}$$

$$= \underline{\omega}_e + \varepsilon \left[\dot{\underline{p}} + \underline{\omega}_e \times (\underline{p}_e + \underline{p}_d^b) + \omega_d^b \times (\underline{p}_e + \underline{p}_d^b) - \dot{\underline{p}}_d^b - \omega_d^b \times (\underline{p}_d^b + \underline{p}_e) \right] \tag{6.28}$$

$$= \underline{\omega}_e + \varepsilon \left(\dot{\underline{p}} - \dot{\underline{p}}_d^b + \underline{\omega}_e \times \underline{p}_d^b + \underline{\omega}_e \times \underline{p}_e \right) \tag{6.29}$$

By replacing (6.22) in (6.29), one has that

$$\underline{\omega}_e = \underline{\omega}_e + \varepsilon (\dot{\underline{p}}_e + \underline{\omega}_e \times \underline{p}_e), \tag{6.30}$$

and consequently,

$$\dot{\underline{\omega}}_e = \dot{\underline{\omega}}_e + \varepsilon (\ddot{\underline{p}}_e + \dot{\underline{\omega}}_e \times \underline{p}_e + \underline{\omega}_e \times \dot{\underline{p}}_e). \tag{6.31}$$

We compute (6.31) in two steps: first the primary part, then the dual part. The primary part of (6.31) is

$$\begin{aligned}
\mathcal{P}(\underline{\dot{\omega}}_e) &= \underline{\dot{\omega}}_e \stackrel{(6.20)}{=} \frac{d}{dt} [\boldsymbol{\omega} - \mathbf{q}_e^* \boldsymbol{\omega}_d \mathbf{q}_e] \\
&= \dot{\boldsymbol{\omega}} - \dot{\mathbf{q}}_e^* \boldsymbol{\omega}_d \mathbf{q}_e - \mathbf{q}_e^* \dot{\boldsymbol{\omega}}_d \mathbf{q}_e - \mathbf{q}_e^* \boldsymbol{\omega}_d \dot{\mathbf{q}}_e \\
&= \dot{\boldsymbol{\omega}} + \frac{1}{2} \boldsymbol{\omega}_e \mathbf{q}_e^* \boldsymbol{\omega}_d \mathbf{q}_e - \frac{1}{2} \mathbf{q}_e^* \boldsymbol{\omega}_d \mathbf{q}_e \boldsymbol{\omega}_e \mathbf{q}_e - \mathbf{q}_e^* \dot{\boldsymbol{\omega}}_d \mathbf{q}_e \\
&= \dot{\boldsymbol{\omega}} + \frac{1}{2} \boldsymbol{\omega}_e \boldsymbol{\omega}_d^b - \frac{1}{2} \boldsymbol{\omega}_d^b \boldsymbol{\omega}_e - \mathbf{q}_e^* \dot{\boldsymbol{\omega}}_d \mathbf{q}_e \\
&\stackrel{(2.24)}{=} \dot{\boldsymbol{\omega}} + \boldsymbol{\omega}_e \times \boldsymbol{\omega}_d^b - \dot{\boldsymbol{\omega}}_d^b \\
&\stackrel{(2.40)}{=} J^{-1} ([J\boldsymbol{\omega}]_{\times} \boldsymbol{\omega} + \boldsymbol{\tau}) - \dot{\boldsymbol{\omega}}_d^b + \boldsymbol{\omega}_e \times \boldsymbol{\omega}_d^b \\
&\stackrel{(6.18)}{=} J^{-1} \left([J\boldsymbol{\omega}_e + J\boldsymbol{\omega}_d^b]_{\times} (\boldsymbol{\omega}_e + \boldsymbol{\omega}_d^b) + \boldsymbol{\tau} \right) - \dot{\boldsymbol{\omega}}_d^b - \boldsymbol{\omega}_d^b \times \boldsymbol{\omega}_e \\
&= J^{-1} \left([J\boldsymbol{\omega}_e]_{\times} \boldsymbol{\omega}_e + [J\boldsymbol{\omega}_d^b]_{\times} \boldsymbol{\omega}_e - [\boldsymbol{\omega}_d^b]_{\times} J\boldsymbol{\omega}_e + [J\boldsymbol{\omega}_d^b]_{\times} \boldsymbol{\omega}_d^b + \boldsymbol{\tau} \right) \\
&\quad - \dot{\boldsymbol{\omega}}_d^b + J^{-1} [J\boldsymbol{\omega}_d^b]_{\times} \boldsymbol{\omega}_d^b \\
&= J^{-1} \left([J\boldsymbol{\omega}_e]_{\times} + [J\boldsymbol{\omega}_d^b]_{\times} - [\boldsymbol{\omega}_d^b]_{\times} J - J [\boldsymbol{\omega}_d^b]_{\times} \right) \boldsymbol{\omega}_e \\
&\quad + J^{-1} [J\boldsymbol{\omega}_d^b]_{\times} \boldsymbol{\omega}_d^b - \dot{\boldsymbol{\omega}}_d^b + J^{-1} \boldsymbol{\tau}. \tag{6.32}
\end{aligned}$$

The dual part is

$$\begin{aligned}
\mathcal{D}(\underline{\dot{\omega}}_e) &= \ddot{\mathbf{p}}_e + \dot{\boldsymbol{\omega}}_e \times \mathbf{p}_e + \boldsymbol{\omega}_e \times \dot{\mathbf{p}}_e \\
&\stackrel{(6.23)}{=} \mathbf{f}/m - \ddot{\mathbf{p}}_d^b + \dot{\boldsymbol{\omega}}_e^b \times \mathbf{p}_d^b + 2\boldsymbol{\omega}_e^b \times \dot{\mathbf{p}}_d^b + \boldsymbol{\omega}_e^b \times (\mathbf{p}_d^b \times \boldsymbol{\omega}_e^b) + \dot{\boldsymbol{\omega}}_e^b \times \mathbf{p}_e^b + \boldsymbol{\omega}_e^b \times \dot{\mathbf{p}}_e^b \tag{6.33}
\end{aligned}$$

6.2.3 Full dynamics of tracking problem

By (6.2), (6.12), (6.32) and (6.33), the full dynamics of the problem can be described by the system

$$\dot{\bar{\mathbf{x}}}_e = \begin{bmatrix} \underline{\dot{\mathbf{q}}}_e \\ \underline{\dot{\boldsymbol{\omega}}}_e \\ \underline{\dot{\mathbf{q}}}_d \\ \underline{\dot{\boldsymbol{\omega}}}_d \\ \underline{\dot{\mathbf{p}}}_d \end{bmatrix} \in F_e(\bar{\mathbf{x}}_e, \boldsymbol{\tau}, \mathbf{f}), \tag{6.34}$$

with

$$F_e(\bar{\mathbf{x}}_e, \boldsymbol{\tau}, \mathbf{f}) := \begin{bmatrix} \left\{ \frac{1}{2} \mathbf{q}_e \boldsymbol{\omega}_e \right\} \\ \left\{ \underline{\dot{\boldsymbol{\omega}}}_e \right\} \\ \left\{ \frac{1}{2} \mathbf{q}_d \boldsymbol{\omega}_d \right\} \\ N\mathbb{B} \\ P\mathbb{B} \end{bmatrix},$$

where

$$\begin{aligned}
\underline{\dot{\boldsymbol{\omega}}}_e &= \mathcal{P}(\underline{\dot{\boldsymbol{\omega}}}_e) + \varepsilon \mathcal{D}(\underline{\dot{\boldsymbol{\omega}}}_e) \\
&\stackrel{(6.32)}{=} J^{-1} \left([J\boldsymbol{\omega}_e]_{\times} + [J\boldsymbol{\omega}_d^b]_{\times} - [\boldsymbol{\omega}_d^b]_{\times} J - J [\boldsymbol{\omega}_d^b]_{\times} \right) \boldsymbol{\omega}_e + J^{-1} [J\boldsymbol{\omega}_d^b]_{\times} \boldsymbol{\omega}_d^b - \dot{\boldsymbol{\omega}}_d^b + J^{-1} \boldsymbol{\tau} + \\
&\quad \varepsilon \mathcal{D}(\underline{\dot{\boldsymbol{\omega}}}_e) \\
&\stackrel{(6.33)}{=} J^{-1} \left([J\boldsymbol{\omega}_e]_{\times} + [J\boldsymbol{\omega}_d^b]_{\times} - [\boldsymbol{\omega}_d^b]_{\times} J - J [\boldsymbol{\omega}_d^b]_{\times} \right) \boldsymbol{\omega}_e + J^{-1} [J\boldsymbol{\omega}_d^b]_{\times} \boldsymbol{\omega}_d^b - \dot{\boldsymbol{\omega}}_d^b + J^{-1} \boldsymbol{\tau} + \\
&\quad \varepsilon \left(\mathbf{f}/m - \ddot{\mathbf{p}}_d^b + \dot{\boldsymbol{\omega}}_e^b \times \mathbf{p}_d^b + 2\boldsymbol{\omega}_e^b \times \dot{\mathbf{p}}_d^b + \boldsymbol{\omega}_e^b \times (\mathbf{p}_d^b \times \boldsymbol{\omega}_e^b) + \dot{\boldsymbol{\omega}}_e^b \times \mathbf{p}_e^b + \boldsymbol{\omega}_e^b \times \dot{\mathbf{p}}_e^b \right), \tag{6.35}
\end{aligned}$$

and the inputs are given by the torque $\boldsymbol{\tau}$ and force \boldsymbol{f} . Recalling that each physical pose $(R, \boldsymbol{p}) \in \text{SO}(3) \times \mathbb{R}^3$ is described by a pair of antipodal unit dual quaternions $\pm \underline{\boldsymbol{q}} \in \underline{\mathcal{S}}$, the objective of a tracking controller is to find an appropriate choice of feedback torque $\boldsymbol{\tau}$ and an appropriate choice of feedback force \boldsymbol{f} to stabilize the set

$$\left\{ \bar{\boldsymbol{x}}_e = \left(\underline{\boldsymbol{q}}_e, \underline{\boldsymbol{\omega}}_e, \underline{\boldsymbol{q}}_d, \underline{\boldsymbol{\omega}}_d, \dot{\boldsymbol{p}}_d \right) \in X_e \times X_d : \underline{\boldsymbol{q}}_e = \pm \mathbf{1}, \underline{\boldsymbol{\omega}}_e = \mathbf{0} + \varepsilon \mathbf{0} \right\}. \quad (6.36)$$

In the next section we will see how to make this choice.

6.3 PROPOSED BIMODAL HYBRID DYNAMIC POSE TRACKING CONTROLLER

The proposed dynamic controller strategy adapts the bimodal hybrid controller strategy used in (5.2) for the kinematic control. It will also use two discrete state variables $(h, b) \in X_c \times X_c$ which have the same function as those in (5.2). The state-space of the controlled system is $X_3 := (X_e \times X_d) \times X_c \times X_c$, and the state of the system will be denoted concisely by $\bar{\boldsymbol{x}}_3 = (\bar{\boldsymbol{x}}_e, h, b)$.

The augmented system is given by (6.34), (6.1) and the following bimodal controller dynamics

$$\left. \begin{array}{l} \dot{h} = 0 \\ \dot{b} = 0 \end{array} \right\} \bar{\boldsymbol{x}}_3 \in C_3, \quad (6.37)$$

$$\left. \begin{array}{l} h^+ \in \overline{\text{sgn}}(u_1 - u_2 \delta / 2) \\ b^+ \in u_2 \overline{\text{sgn}}(u_1 - u_2 \delta / 2) \end{array} \right\} \bar{\boldsymbol{x}}_3 \in D_3,$$

where $u_1 \in \mathbb{R}$ and $u_2 \in \mathbb{R}$ are inputs to the controller that will be soon defined, $\overline{\text{sgn}}$ is defined as in (2.2), and the jump set is given by $D_3 := D_{3a} \cup D_{3b} \cup D_{3c}$, with

$$D_{3a} := \{ \bar{\boldsymbol{x}}_3 \in X_3 : h \eta_e \leq -\delta \}, \quad (6.38)$$

$$D_{3b} := \{ \bar{\boldsymbol{x}}_3 \in X_3 : b = 1, h \eta_e \leq -\delta / 2 \}, \quad (6.39)$$

$$D_{3c} := \{ \bar{\boldsymbol{x}}_3 \in X_3 : b = -1, h \eta_e \geq 3\delta / 2 \} \quad (6.40)$$

and the flow set is $C_3 := \overline{X_3 \setminus D_3}$.

The vector of inputs of the augmented system is $U = (\boldsymbol{\tau}, \boldsymbol{f}, u_1, u_2)$ and closed-loop hybrid system is achieved by setting

$$U = (\boldsymbol{\tau}_{fb}, \boldsymbol{f}_{fb}, \eta_e, h), \quad (6.41)$$

where $\boldsymbol{\tau}_{fb}$ is the proposed torque feedback given by

$$\boldsymbol{\tau}_{fb} := -k_1 h \boldsymbol{\mu}_e - [J \boldsymbol{\omega}_d^b]_{\times} \boldsymbol{\omega}_d^b + J \dot{\boldsymbol{\omega}}_d^b - K_{\omega} \boldsymbol{\omega}_e, \quad (6.42)$$

with gains k_1 (a real-valued positive number) and K_{ω} (a symmetric positive definite matrix), and where \boldsymbol{f}_{fb} is the proposed force feedback given by

$$\boldsymbol{f}_{fb} := -\frac{1}{2} k_2 \boldsymbol{p}_e - m \left[-\ddot{\boldsymbol{p}}_d^b + \dot{\boldsymbol{\omega}}_e \times \boldsymbol{p}_d^b + 2\boldsymbol{\omega}_e \times \dot{\boldsymbol{p}}_d^b + \boldsymbol{\omega}_e \times (\boldsymbol{p}_d^b \times \boldsymbol{\omega}_e) \right] - K_{\dot{\boldsymbol{p}}} \dot{\boldsymbol{p}}_e, \quad (6.43)$$

with gains k_2 (a real-valued positive number) and $K_{\dot{\boldsymbol{p}}}$ (a symmetric positive definite matrix).

It will be shown in the next section that the set

$$A_3 = \left\{ \bar{\boldsymbol{x}}_3 \in X_3 : \underline{\boldsymbol{q}}_e = h \mathbf{1}, \underline{\boldsymbol{\omega}}_e = \mathbf{0}, b = 1 \right\}. \quad (6.44)$$

is globally asymptotically stable under the closed-loop dynamics.

6.4 DYNAMICS STABILITY ANALYSIS

In this section, we prove that the proposed hybrid bimodal tracking control globally asymptotically stabilizes the pose of a rigid body even in the presence of measurement noise. Replacing the proposed controller input (6.41) on (6.35) yields the primary and dual part of $\dot{\omega}_e$ in closed loop:

$$\mathcal{P}(\dot{\omega}_e) = J^{-1} \left\{ \left[[J\omega_e]_{\times} + [J\omega_d^b]_{\times} - [\omega_d^b]_{\times} J - J [\omega_d^b]_{\times} \right] \omega_e - k_1 h \mu_e - K_{\omega} \omega_e \right\}, \quad (6.45)$$

$$\mathcal{D}(\dot{\omega}_e) = -\frac{1}{2} k_2 \mathbf{p}_e / m - K_{\dot{\mathbf{p}}} \dot{\mathbf{p}}_e / m + \dot{\omega}_e \times \mathbf{p}_e + \omega_e \times \dot{\mathbf{p}}_e. \quad (6.46)$$

By using (6.45) and (6.46) in (6.34), and combining the dynamics of (6.34) and the dynamics of the bimodal strategy (6.37), the closed-loop system $\overline{\mathcal{H}}_3$ has flow set C_3 , jump set D_3 , and the following flow map F_3 and jump set G_3 :

$$F_3(\bar{\mathbf{x}}_3, h, b) := \begin{bmatrix} \left\{ \frac{1}{2} \mathbf{q}_e \omega_e \right\} \\ \left\{ \dot{\omega}_e \right\} \\ \left\{ \frac{1}{2} \mathbf{q}_d \omega_d \right\} \\ \text{NB} \\ \text{PB} \\ \{0\} \\ \{0\} \end{bmatrix},$$

$$G_3(\bar{\mathbf{x}}_3, h, b) := \begin{bmatrix} \left\{ \mathbf{q}_e \right\} \\ \left\{ \omega_e \right\} \\ \left\{ \mathbf{q}_d \right\} \\ \left\{ \omega_d \right\} \\ \left\{ \dot{\mathbf{p}}_d \right\} \\ \overline{\text{sgn}}(\eta_e - h\delta/2) \\ h \overline{\text{sgn}}(\eta_e - h\delta/2) \end{bmatrix}.$$

As will be seen in Lemma 6.1, the closed-loop hybrid system $\overline{\mathcal{H}}_3$ satisfies the **hybrid basic conditions** (see Definition 2.4).

Lemma 6.1. *The maps F_3 and G_3 , and the sets C_3 and D_3 satisfy the following properties:*

1. C_3 and D_3 are closed sets.
2. F_3 is outer semicontinuous, locally bounded, and $F_3(\bar{\mathbf{x}}_3, h, b)$ is nonempty and convex for each $(\bar{\mathbf{x}}_3, h, b) \in C_3$.
3. G_3 is outer semicontinuous, locally bounded and $G_3(\bar{\mathbf{x}}_3, h, b)$ is nonempty for each $(\bar{\mathbf{x}}_3, h, b) \in D_3$.

proof.

First we prove that C_3 and D_3 are closed sets: D_3 is the finite union of the sets D_{3a} , D_{3b} and D_{3c} defined in (5.3)-(5.5). Since D_{3a} , D_{3b} and D_{3c} are closed sets (the proof is similar to the proof of Lemma 4.1), D_3 is also a closed set. C_3 is the topological closure of the set $X_3 \setminus D_3$, thus by definition of topological

closure, its closed.

To prove that F_3 is outer semicontinuous, it suffices to prove that each component of F_3 is outer semicontinuous (see Lemma 2.1). By the use of the same argument of Lemma 5.1, one can show that the maps $(\bar{x}_3, h, b) \mapsto \frac{1}{2}\underline{q}_e \underline{\omega}_e$ and $(\bar{x}_3, h, b) \mapsto \frac{1}{2}\underline{q}_d \underline{\omega}_d$ are continuous (and thus, outer semicontinuous). The map $(\bar{x}_3, h, b) \mapsto 0$ is also continuous, since it is a constant function. Finally, by using (6.45) and 6.46 it is possible to prove that $(\bar{x}_3, h, b) \mapsto \underline{\dot{\omega}}_e$ is also continuous.

The graphs of the maps $(\bar{x}_3, h, b) \mapsto N\mathbb{B}$ and $(\bar{x}_3, h, b) \mapsto P\mathbb{B}$ are, respectively, $X_3 \times N\mathbb{B}$ and $X_3 \times P\mathbb{B}$. Since the product of closed sets are closed, both of these sets are closed. It follows by Theorem 2.1 that these maps are outer semicontinuous. Thus, all components of F_3 are outer semicontinuous, and consequently, F_3 is outer semicontinuous. $F_3(\bar{x}_3, h, b)$ is also convex-valued for any $(\bar{x}_3, h, b) \in X_3$, since its components are single-valued maps (thus, sets consisting of only a point) or the maps $(\bar{x}_3, h, b) \mapsto N\mathbb{B}$ and $(\bar{x}_3, h, b) \mapsto P\mathbb{B}$. These last two maps are also convex-valued, since the set $r\mathbb{B}$ is convex for any $r > 0$. Moreover, $F_3(\bar{x}_3, h, b)$ is nonempty for each $(\bar{x}_3, h, b) \in C_3$ by definition of F_3 and C_3 .

We prove now that G_3 is outer semicontinuous. All of the maps $(\bar{x}_3, h, b) \mapsto \{\underline{q}_e\}$, $(\bar{x}_3, h, b) \mapsto \{\underline{\omega}_e\}$, $(\bar{x}_3, h, b) \mapsto \{\underline{q}_d\}$, $(\bar{x}_3, h, b) \mapsto \{\underline{\omega}_d\}$ and $(\bar{x}_3, h, b) \mapsto \{\dot{p}_d\}$ are projections, thus are continuous [99]. The maps $(\bar{x}_3, h, b) \mapsto \overline{\text{sgn}}(\eta_e - h\delta/2)$ and $(\bar{x}_3, h, b) \mapsto h\overline{\text{sgn}}(\eta_e - h\delta/2)$ are outer semicontinuous by Theorem 2.3. Since each component of G_3 is outer semicontinuous, it follows that G_3 is outer semicontinuous by Lemma 2.1. Moreover, any compact set K of X_3 is contained in a set of the format $K_1 \times X_c \times X_c$, where K_1 is a compact set. By definition of G_3 , we have that $G_3(K) \subseteq G_3(K_1 \times X_c \times X_c) \subseteq K_1 \times X_c \times X_c$. Thus, G_3 is **locally bounded** on X_3 . Finally, $G_3(\bar{x}_3, h, b)$ is nonempty for each $(\bar{x}_3, h, b) \in D_3$ by definition of G_3 and D_3 . ■

Remark 6.1. Note that Lemma 6.1 implies the **hybrid basic conditions** of Definition 2.4 by Remark 2.1.

The next theorem proves the stability of the closed-loop hybrid system $\overline{\mathcal{H}}_3$.

Theorem 6.1

Let $\delta \in (0, 1)$ and $k_1, k_2 > 0$. The compact set A_3 defined in (6.44), is globally asymptotically stable for the closed-loop hybrid system $\overline{\mathcal{H}}_3$.

proof.

For simplifying the presentation, let us first consider $\delta \in (0, 2/3]$. Let $V_3 : X_3 \rightarrow \mathbb{R}$ be defined as

$$V_3(\bar{x}_3) = 2k_1(1 - h\eta_e) + k_2\|\underline{p}_e\|^2/4 + \frac{1}{2}\underline{\omega}_e^T J \underline{\omega}_e + \frac{1}{2}m\dot{\underline{p}}_e^T \dot{\underline{p}}_e. \quad (6.47)$$

The first two terms of (6.47) is based on the Lyapunov proposed for the kinematic controller of the previous chapter (see (5.7)). The third term is the angular energy of the error system and is commonly used in attitude tracking problems (for instance, [102, 25]), and the last term is the kinetic energy of the error system. The last two terms have also been used in the Lyapunov proposed in [26].

Due to the same reasoning of Theorem 5.1, and that $\underline{\omega}_e = 0$ if and only if $\omega_e = 0$ and $\dot{p}_e = 0$, it follows that $V_3(\bar{x}_3) > 0$ for $\bar{x}_3 \in X_3 \setminus A_3$ and $V_3(\bar{x}_3) = 0$ for $\bar{x}_3 \in A_3$. Hence, V_3 is positive definite on X_3 with respect to A_3 .

The time derivative \dot{V}_3 of V_3 is given by

$$\dot{V}_3(\bar{\mathbf{x}}_3) = -2k_1 h \dot{\eta}_e + k_2 \mathbf{p}_e \cdot \dot{\mathbf{p}}_e / 2 + (J\boldsymbol{\omega}_e) \cdot \dot{\boldsymbol{\omega}}_e + m \dot{\mathbf{p}}_e \cdot \ddot{\mathbf{p}}_e \quad (6.48)$$

Using (6.32), (6.23) and the fact that

$$A := \left([J\boldsymbol{\omega}_e]_{\times} + [J\boldsymbol{\omega}_d^b]_{\times} - [\boldsymbol{\omega}_d^b]_{\times} J - J [\boldsymbol{\omega}_d^b]_{\times} \right)$$

is skew-symmetric, one has that

$$\begin{aligned} \dot{V}_3(\bar{\mathbf{x}}_3) &= -2k_1 h \dot{\eta}_e + k_2 \mathbf{p}_e \cdot \dot{\mathbf{p}}_e / 2 + \dot{\boldsymbol{\omega}}_e \cdot (J\boldsymbol{\omega}_e) + m \dot{\mathbf{p}}_e \cdot \ddot{\mathbf{p}}_e \\ &\stackrel{(6.32)}{=} -2k_1 h \dot{\eta}_e + k_2 \mathbf{p}_e \cdot \dot{\mathbf{p}}_e / 2 + \left[J^{-1} A \boldsymbol{\omega}_e + J^{-1} \left([J\boldsymbol{\omega}_d^b]_{\times} \boldsymbol{\omega}_d^b - J \dot{\boldsymbol{\omega}}_d^b + \boldsymbol{\tau} \right) \right] \cdot (J\boldsymbol{\omega}_e) + m \dot{\mathbf{p}}_e \cdot \ddot{\mathbf{p}}_e \\ &= -2k_1 h \dot{\eta}_e + k_2 \mathbf{p}_e \cdot \dot{\mathbf{p}}_e / 2 + \left[\left([J\boldsymbol{\omega}_d^b]_{\times} \boldsymbol{\omega}_d^b - J \dot{\boldsymbol{\omega}}_d^b + \boldsymbol{\tau} \right) \right] \cdot (\boldsymbol{\omega}_e) + m \dot{\mathbf{p}}_e \cdot \ddot{\mathbf{p}}_e \\ &\stackrel{(6.19)}{=} -2k_1 h \left(-\frac{1}{2} \boldsymbol{\mu}_e \cdot \boldsymbol{\omega}_e \right) + k_2 \mathbf{p}_e \cdot \dot{\mathbf{p}}_e / 2 + \left[[J\boldsymbol{\omega}_d^b]_{\times} \boldsymbol{\omega}_d^b - J \dot{\boldsymbol{\omega}}_d^b + \boldsymbol{\tau} \right] \cdot \boldsymbol{\omega}_e + m \dot{\mathbf{p}}_e \cdot \ddot{\mathbf{p}}_e \\ &= -2k_1 h \left(-\frac{1}{2} \boldsymbol{\mu}_e \cdot \boldsymbol{\omega}_e \right) + k_2 \mathbf{p}_e \cdot \dot{\mathbf{p}}_e / 2 + \left[[J\boldsymbol{\omega}_d^b]_{\times} \boldsymbol{\omega}_d^b - J \dot{\boldsymbol{\omega}}_d^b + \boldsymbol{\tau} \right] \cdot \boldsymbol{\omega}_e + m \dot{\mathbf{p}}_e \cdot \ddot{\mathbf{p}}_e \\ &\stackrel{(6.23)}{=} -2k_1 h \left(-\frac{1}{2} \boldsymbol{\mu}_e \cdot \boldsymbol{\omega}_e \right) + k_2 \mathbf{p}_e \cdot \dot{\mathbf{p}}_e / 2 + \left[[J\boldsymbol{\omega}_d^b]_{\times} \boldsymbol{\omega}_d^b - J \dot{\boldsymbol{\omega}}_d^b + \boldsymbol{\tau} \right] \cdot \boldsymbol{\omega}_e + \\ &\quad m \dot{\mathbf{p}}_e \cdot \left[\mathbf{f} / m - \ddot{\mathbf{p}}_d^b + \dot{\boldsymbol{\omega}}_e \times \mathbf{p}_d^b + 2\boldsymbol{\omega}_e \times \dot{\mathbf{p}}_d^b + \boldsymbol{\omega}_e \times (\mathbf{p}_d^b \times \boldsymbol{\omega}_e^b) \right] \\ &= k_1 h \boldsymbol{\mu}_e \cdot \boldsymbol{\omega}_e + \left[[J\boldsymbol{\omega}_d^b]_{\times} \boldsymbol{\omega}_d^b - J \dot{\boldsymbol{\omega}}_d^b + \boldsymbol{\tau} \right] \cdot \boldsymbol{\omega}_e + \\ &\quad k_2 \mathbf{p}_e \cdot \dot{\mathbf{p}}_e / 2 + m \left[\mathbf{f} / m - \ddot{\mathbf{p}}_d^b + \dot{\boldsymbol{\omega}}_e \times \mathbf{p}_d^b + 2\boldsymbol{\omega}_e \times \dot{\mathbf{p}}_d^b + \boldsymbol{\omega}_e \times (\mathbf{p}_d^b \times \boldsymbol{\omega}_e) \right] \cdot \dot{\mathbf{p}}_e \\ &= \left[k_1 h \boldsymbol{\mu}_e + [J\boldsymbol{\omega}_d^b]_{\times} \boldsymbol{\omega}_d^b - J \dot{\boldsymbol{\omega}}_d^b + \boldsymbol{\tau} \right] \cdot \boldsymbol{\omega}_e + \\ &\quad \left\{ m \left[-\ddot{\mathbf{p}}_d^b + \dot{\boldsymbol{\omega}}_e \times \mathbf{p}_d^b + 2\boldsymbol{\omega}_e \times \dot{\mathbf{p}}_d^b + \boldsymbol{\omega}_e \times (\mathbf{p}_d^b \times \boldsymbol{\omega}_e) \right] + k_2 \mathbf{p}_e / 2 + \mathbf{f} \right\} \cdot \dot{\mathbf{p}}_e \end{aligned}$$

Using the proposed controller feedbacks (6.42) and (6.43) yields

$$\begin{aligned} \dot{V}_3(\bar{\mathbf{x}}_3) &= -K_{\dot{\mathbf{p}}} \dot{\mathbf{p}}_e \cdot \dot{\mathbf{p}}_e - K_{\boldsymbol{\omega}} \boldsymbol{\omega}_e \cdot \boldsymbol{\omega}_e \\ &= -K_{\dot{\mathbf{p}}} \|\dot{\mathbf{p}}_e\|^2 - K_{\boldsymbol{\omega}} \|\boldsymbol{\omega}_e\|^2. \end{aligned}$$

Thus, \dot{V}_3 is negative semidefinite on X_3 with respect to A_3 . Along jumps, when $\bar{\mathbf{x}}_3 \in D_3$, since $\mathbf{q}_e^+ = \mathbf{q}_e$,

$$\Delta V_3(\bar{\mathbf{x}}_3) = V_3(\bar{\mathbf{x}}_3^+) - V_3(\bar{\mathbf{x}}_3) = -2\eta_e(h^+ - h).$$

Let $D_3 = D_{3a} \cup D_{3b} \cup D_{3c}$, where D_{3a} , D_{3b} and D_{3c} are respectively defined in (6.38), (6.39) and (6.40).

Thus,

$$\Delta V_3(\bar{\mathbf{x}}_3) = \begin{cases} \leq -4\delta_a, & \bar{\mathbf{x}}_3 \in D_{3a} \cup D_{3b}, \\ 0, & \bar{\mathbf{x}}_3 \in D_{3c}, \end{cases}$$

where $\delta_a = \delta$ for $\bar{\mathbf{x}}_3 \in D_{3a} \setminus D_{3b}$ and $\delta_a = \delta/2$ for $\bar{\mathbf{x}}_3 \in D_{3b}$.

From Lemma 6.1 and by Theorem 7.6 of [100], it follows that the compact set A_3 is stable since $\Delta V_3(\bar{\mathbf{x}}_3) \leq 0$ and $\dot{V}_3(\bar{\mathbf{x}}_3) \leq 0$ for all $\bar{\mathbf{x}}_3 \in X_3$.

To conclude that the set A_3 is globally asymptotically stable, it is necessary to apply Theorem 4.7 of [100] to prove that the set A_3 is the largest invariant set in $W = W_1 \cup W_2$, where $W_1 := \{\bar{x}_3 \in C_3 : \dot{V}_3(\bar{x}_3) = 0\}$ and $W_2 := \Delta V_3^{-1}(0) \cap G_3(\Delta V_3^{-1}(0))$, with $G_3(\bar{x}_3) := \bar{x}_3^+$. It follows that $\Delta V_3^{-1}(0) = D_{3c}$ and

$$G_3(\Delta V_3^{-1}(0)) = \{\bar{x}_3 \in X_3 : b = 1, h\eta_e \geq 3\delta/2\}.$$

Thus, $W_2 = \emptyset$ and

$$W = W_1 = \{\bar{x}_3 \in X_3 : \dot{p}_e = \mathbf{0} \text{ and } \omega_e = \mathbf{0} \text{ and } (h\eta_e \geq -\delta) \text{ and } (b = -1 \text{ or } h\eta_e \geq -\delta/2) \text{ and } (b = 1 \text{ or } h\eta_e \leq 3\delta/2)\}.$$

From (6.45) and (6.46), the only way to keep $\omega_e \equiv \mathbf{0}$ and $\dot{p}_e \equiv \mathbf{0}$ is when $\mu_e = \mathbf{0}$ and $p_e = \mathbf{0}$. This means $\underline{q}_e = \pm \mathbf{1}$. Using the restriction $h\eta_e \geq -\delta$, it follows that $\underline{q}_e = h\mathbf{1}$ and using the other two restrictions, $b = 1$. Thus, any solution $\bar{x}_3(t)$ approaches the largest invariant set A_3 . This controller restricts parameter δ to $(0, 2/3]$. For the case $\delta \in (2/3, 1)$, the system still behaves as proposed until the first jump. Afterward, it will behave as the hysteretic controller with only one mode, since b will not change anymore. ■

Differently from memoryless discontinuous controllers, the next theorem states that the stability of the set A_3 is not sensitive to arbitrarily small constant σ -perturbations. The proof follows from the same reasoning of Theorem 4.3.

Theorem 6.2

Let V_3 be as in (6.47). There exists a class- \mathcal{KL} function β such that for each compact set $K_3 \subset X_3$ and $\Delta > 0$ there exists $\rho^* > 0$ such that for each $\rho \in (0, \rho^*]$, the solutions $\bar{x}_{3\rho}$ from K_3 of the perturbed system $\bar{\mathcal{H}}_{3\rho}$ satisfy

$$V_3(\bar{x}_{3\rho}(t, j)) \leq \beta(V_3(\bar{x}_{3\rho}(0, 0)), t + j) + \Delta, \forall (t, j) \in \text{dom } \bar{x}_{3\rho}. \quad (6.49)$$

It was proved in the end of Section 5.3 that the analysis of either the presence of Zeno solutions (infinite number of jumps in a finite amount of time) or chattering are only related to the rotation quaternion. The same idea applies here, and as corollary, no Zeno solutions occur even when constant σ -perturbations (see Definition 2.13) are taken into account, provided that the amplitude of the perturbation is sufficiently small.

6.5 STABILIZING CONTROLLER

The stabilization problem is a particular case of the tracking problem with $\mathbf{q}_d = \mathbf{1}$, $\omega_d = \mathbf{0}$, $\dot{\omega}_d = \mathbf{0}$, $p_d = \mathbf{0}$, $\dot{p}_d = \mathbf{0}$ and $\ddot{p}_d = \mathbf{0}$. In this case, the dynamics of the system is simply described by (2.29) and (2.43), that is,

$$\begin{aligned} \dot{\underline{q}} &= \frac{1}{2} \underline{q} \omega, \\ \dot{\underline{\omega}} &= [J^{-1}(S(J\omega)\omega + \tau)] + \varepsilon \{ [J^{-1}(S(J\omega)\omega + \tau)] \times p + \omega \times \dot{p} + f/m \}, \end{aligned} \quad (6.50)$$

where the states of the system are given by $(\underline{q}, \underline{\omega}) \in X$, and the input are made by force \mathbf{f} and torque \mathbf{q} . The state-space of the system coupled with the controller is $X_{3s} := X \times X_c \times X_c$, with the states denoted concisely by $\bar{\mathbf{x}}_{3s} := (\underline{q}, \underline{\omega}, h, b)$. The stabilizing controller is given by the dynamics

$$\left. \begin{array}{l} \dot{h} = 0 \\ \dot{b} = 0 \end{array} \right\} \bar{\mathbf{x}}_{3s} \in C_{3s}, \quad (6.51)$$

$$\left. \begin{array}{l} h^+ \in \overline{\text{sgn}}(u_1 - u_2\delta/2) \\ b^+ \in u_2 \overline{\text{sgn}}(u_1 - u_2\delta/2) \end{array} \right\} \bar{\mathbf{x}}_{3s} \in D_{3s},$$

with the jump set given by $D_{3s} := D_{3as} \cup D_{3bs} \cup D_{3cs}$, with

$$D_{3as} := \{\bar{\mathbf{x}}_{3s} \in X_{3s} : h\eta \leq -\delta\}, \quad (6.52)$$

$$D_{3bs} := \{\bar{\mathbf{x}}_{3s} \in X_{3s} : b = 1, h\eta \leq -\delta/2\}, \quad (6.53)$$

$$D_{3cs} := \{\bar{\mathbf{x}}_{3s} \in X_{3s} : b = -1, h\eta \geq 3\delta/2\} \quad (6.54)$$

and the flow set is $C_{3s} := \overline{X_{3s} \setminus D_{3s}}$. As a corollary of Theorem 6.1, by using the feedback torque and force given by

$$\begin{aligned} \boldsymbol{\tau}_{fb} &= -k_1 h \boldsymbol{\mu} - K_\omega \boldsymbol{\omega}, \\ \mathbf{f}_{fb} &= -\frac{1}{2} k_2 \mathbf{p} - K_{\dot{\mathbf{p}}} \dot{\mathbf{p}}, \end{aligned}$$

and $(u_1, u_2) = (\eta_e, h)$, the set

$$A_{3s} := \{(\underline{q}, \underline{\omega}, h, b) \in X \times X_c \times X_c : \underline{q} = h \underline{\mathbf{1}}, \underline{\omega} = \mathbf{0}, b = 1\}$$

is globally stable under the combined dynamics of (6.50)-(6.51).

6.6 NUMERICAL SIMULATIONS

In this section, the proposed dynamic controller is compared with the dynamic controller of [2] in the presence and absence of measurement noise in \mathbf{q} . The initial pose in both scenarios was set to $\mathbf{q}(0) = -0.01 + 0.09\hat{i} + 0.76\hat{j} + 0.64\hat{k}$ and $\mathbf{p}(0) = 0.19\hat{i} - 1.09\hat{j} + 2.79\hat{k}$. The inertial matrix of the rigid body expressed in the body frame is $J = \text{diag}\left(\begin{bmatrix} 1 & 0.63 & 0.85 \end{bmatrix}\right)$ and the mass of the rigid body is $m = 1$. The controller parameters of [2] were also set as in [2]. The proposed dynamic controller parameters were set to $k_1 = 3$, $k_2 = 120$, $K_\omega = 1.2I$ and $K_{\dot{\mathbf{p}}} = 100I$. The initial discrete states of the proposed controller were set to $h(0) = 1$ and $b(0) = 1$.

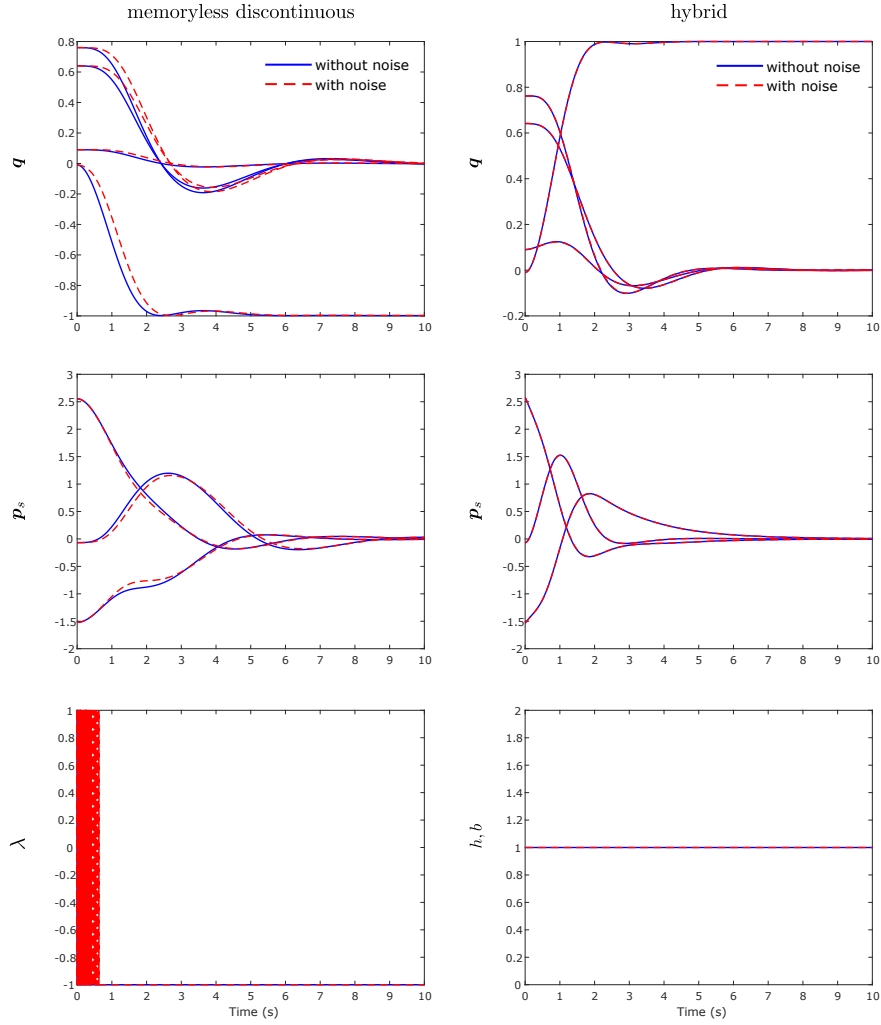


Fig. 6.1: Comparison between dynamic controllers in the presence (red dashed line) and absence (blue solid line) of disturbances. The left graphics show the time evolution of the dynamic controller proposed in [2] and the right graphics show the time evolution of the proposed dynamic controller.

Fig. 6.1 compares the time evolution of the rotation quaternion and the translation expressed in the reference frame. It illustrates how measurement noise influences the behavior of a memoryless discontinuous controller such as the one suggested in [2], especially the rotation. The procedure to add the measurement noise to simulations is the same as the one of Section 5.4. Following the suggestion of [103], a implicit numerical integrator (ode23 in MATLAB) was used to simulate the controller of [2] to avoid the additional chattering caused by numerical errors. It is important to remark that the simulation was also made using the ode45 numerical integrator of MATLAB, and the graphics of the figures did not change.

The discrete state variable for both controllers is also shown in this figure. The λ variable is used as the switching variable of the dynamic controller from [2]. While in the absence of noise scenario the λ variable is constant and equal to -1 , in the presence of noise, it chatters and causes a lag in the rotation evolution. This is not the case of the discrete states h and b of the proposed hybrid dynamic controller, which does not change.

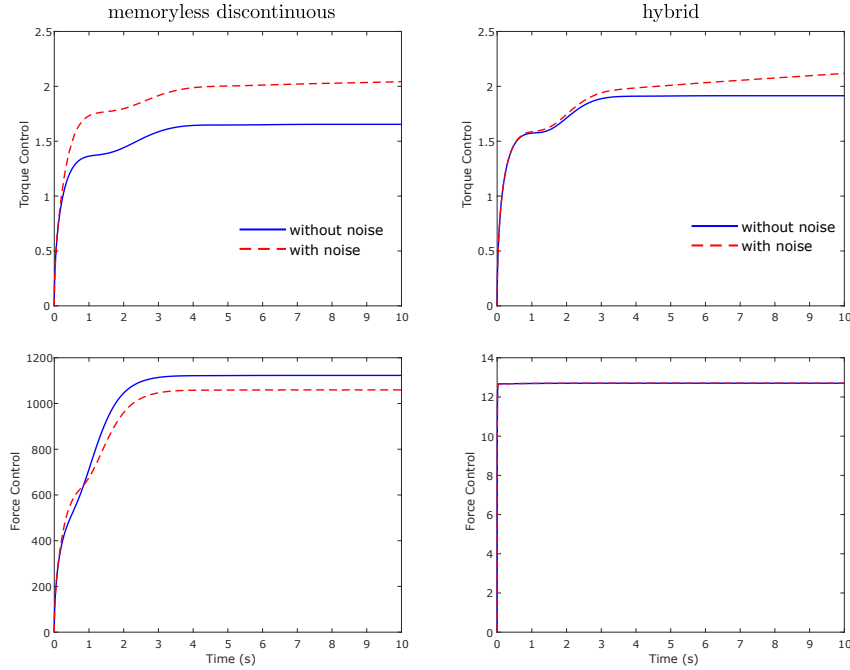


Fig. 6.2: Compared total control effort (force and torque) between proposed dynamic hybrid controller (right plot) and the memoryless discontinuous controller of [2] (left plot).

In addition of achieving a better performance and successfully avoiding chattering due to noise, the proposed hybrid controller also demands considerably less control effort compared to [2]. Fig. 6.2 compares the use of control effort for both controllers—herein, the control effort related to the required torque is calculated by $\sqrt{\int_0^t \tau_{fb}^T(s) \tau_{fb}(s) ds}$, whilst the force by $\sqrt{\int_0^t f_{fb}^T(s) f_{fb}(s) ds}$. While the presence of noise causes a significant difference in both overall torque and force employed in the controller of [2], it has little effect over the proposed controller. Moreover, even in absence of external disturbances, the memoryless discontinuous controller of [2] requires more force compared to the proposed hybrid controller.

6.7 CHAPTER CONCLUSIONS

This chapter presents a novel tracking controller which consider the complete dynamics of rigid-body, that is, which considers the twist not as an input, but as a state of the system. Compared with the dynamic controllers of [28, 31], the proposed dynamic controller controls both the attitude and the coupled translational dynamics. Moreover, the quaternion-based controllers proposed in [28] has a drawback in the scenario of systems with restricted energy storage and power supply, such as satellites: some initial attitudes yields unnecessary longer rotation trajectories, leading to a higher average settling time and/or energy consumption. As discussed in [17], the energy consumption of the system is aggravated when the translation movement is also considered. To address this problem, the proposed dynamic controller extends the bimodal strategy proposed in last chapter to the dynamic setting. This technique allows a trade-off in terms of cost between a memoryless discontinuous controller and the hysteretic-based controllers proposed in [28, 17]. To illustrate the advantage of the proposed hybrid dynamic controller, numeric comparisons contrast it with the memoryless discontinuous dynamic

controller of [2]. As seen in the simulations, only the controller of [2] suffers from rotation lag, induced by chattering in the presence of small magnitude measurement noises.

7

CONCLUSION

This thesis presented novel hybrid control strategies for the motion of rigid bodies that guarantee global stability and also simultaneously mitigates chattering and unwinding problems. The result, based on the exploitation of hybrid theory tools and the unit dual quaternion manifold characteristics, enlarges the applicability of hybrid theory to non-Euclidean manifolds and improves the closed-loop performance of the rigid body kinematics and dynamics, which is critical to real-world applications. Furthermore, due to the high applicability of pose controllers, it is expected that the results presented here to be relevant to the control of manipulators, mobile robots, satellite and spacecraft tracking and stabilization problems.

In addition, the controllers presented in this thesis open the doors to further investigations and extensions that are important and whose results may have several practical consequences. For instance, one possible line of research would be to extend the proposed controllers in this thesis to the cooperative control of multi-agent systems, that is, the simultaneous control of many autonomous systems cooperating together in order to perform a task: a large number of unmanned aerial vehicles may have as a objective to synchronize their pose or to form certain patterns of positioning between them. Such missions are very important, for example, in military strategies and tactics. Moreover, as the task is distributed to many autonomous agents, the cooperative control paradigm provides a high redundancy and can prevent the possibility of compromising an entire task because of a failure in a single agent. Therefore, the cooperative control architecture is a scalable and flexible solution that can excel at tasks where high fault tolerance is desired. Examples of such tasks include risky scenarios such as the removal of explosive mines in minefields and the exploration of hazardous environments such as the damaged Fukushima nuclear power plants in Japan [104]. Another reason to use the cooperative control paradigm is that it may be impracticable to set up a structure to control the pose of the robots in a centralized mode due to the location of the task, as in the cases of space or submarine exploration. In the case of space exploration, it is worth mentioning the possibility of using multiple independent space telescopes to form a stellar interferometer and achieve unprecedented image resolutions, advancing the state of the art of astronomy [105].

Another further work would be to enhance the dynamic control law proposed in Chapter 6. It is important to note that the control law presented in this chapter depends on full knowledge of the inertial parameters of the model (that is, the mass and the inertia matrix of rigid body expressed in some frame). In many practical situations, the inertial parameters of the system are not available a priori or they are time-varying (for instance, a rocket will have a considerable loss of mass since the fuel will be expelled during flight). Thus, a controller which does not require the knowledge of inertial parameters such as the one proposed in [25, 106] for attitude-only control or an adaptive solution such as the ones proposed in [41, 43] for pose control is highly desirable. To the best of the author knowledge, no hybrid solution has been proposed in this context.

Finally, the proposed dynamic controller in Chapter 6 requires that the linear and velocity measurements are available. This may not be true in some practical situations, due to a sensor malfunction or simply because the vehicles or manipulators are not equipped with linear or angular velocity sensors. This justifies the investigation of hybrid pose controllers that are free of angular and velocity measurements, such as the **non**-hybrid approaches made in [25] for attitude-only control using quaternion and [26] for pose control using dual quaternions.

APPENDIX

A

ALGEBRAIC STRUCTURES

In this appendix one can have a quick glance of definitions and properties of some algebraic structures that may be used during the reading of this book.

DEFINITION A.1 (Group) [107, p.31] A **group** $(G, \diamond, 1_G)$ is defined by a set G , a single binary operation $\diamond : G \times G \rightarrow G$ (named the *group operation*), and a element $1_G \in G$ (the *identity element*) that satisfies the following axioms:

G1 [Associative] For all $a, b, c \in G$ we have

$$(a \diamond b) \diamond c = a \diamond (b \diamond c);$$

G2 [Identity Operation] For all $a \in G$, we have

$$a \diamond 1_G = 1_G \diamond a = a;$$

G3 [Inverse Element] For all $a \in G$, there exists an inverse element in G (denoted by a^{-1}) such that

$$a \diamond a^{-1} = a^{-1} \diamond a = 1_G.$$

Remark A.1. To simplify notation, groups are usually referred only by the pair (G, \diamond) or the set G .

The follow properties are valid for all groups:

Proposition A.1. [107, p.29] *The identity of the group is unique.*

Proposition A.2. [107, p.31] *For all $g \in G$, there exists an unique inverse element g^{-1} .*

Groups whose operation behave nicely with regard to commutativity have a special name.

DEFINITION A.2 (Abelian Group) [107, p.41] A group (G, \diamond) is called an **Abelian^a group** if for all $a, b \in G$ the following property is valid:

Ab1 [Commutative Law] For all $a, b \in G$ we have $a \diamond b = b \diamond a$.

^aIn homage to the mathematician Niels Henrik Abel who studied the relationship between some groups and impossibility of solving quintic equations by radicals.

Some maps between groups are special in the sense that they preserve the group operation. This is made

precise in definition.

DEFINITION A.3 (Group Homomorphism) [107, p.58] A map $\phi : (G, \diamond, \epsilon) \rightarrow (H, \circ, e)$ between group is called a **group homomorphism** if it satisfies:

H1 For all $a, b \in G$, we have $\phi(a \diamond b) = \phi(a) \circ \phi(b)$.

As the group operation is preserved, the identity element is also preserved by homomorphisms:

Proposition A.3. [107, p. 59] *If $\phi : (G, \diamond, \epsilon) \rightarrow (H, \circ, e)$ is a homomorphism, then $\phi(\epsilon) = e$ and $\phi(g^{-1}) = \phi^{-1}(g)$ for all $g \in G$.*

DEFINITION A.4 [107, p.37] If a is a bijective map, the group homomorphism is said to be an **isomorphism**. Two groups G and H are **isomorphic** if there exists an isomorphism between G and H . If this occurs, we denote $G \simeq H$ to indicate that they are isomorphic.

DEFINITION A.5 (Subgroup) [107, p.31] A subgroup $(H, \diamond, 1_H)$ of $(G, \diamond, 1_G)$ is a subset of G that is also a group under the same group operation – we use the notation $H \leq G$ to indicate that H is a subgroup of G .

Some examples of groups comes from special sets of matrices:

EXAMPLE A.1 The group $GL(n, \mathbb{R})$ made by invertible $n \times n$ real matrices and whose operation is the multiplication between matrices.

EXAMPLE A.2 The subgroup $SO(n)$ of $GL(n, \mathbb{R})$. The underlying set of this subgroup is made by orthogonal matrices with unitary determinant. The subgroup operation is multiplication between matrices.

It is interesting to note that these groups in the last examples have a differentiable structure, in the sense that $GL(n, \mathbb{R})$ and $SO(n)$ are real smooth manifolds. Moreover, the multiplication map between matrices and the map that sends a matrix to its inverse are compatible with the differentiable structure of these manifolds. Groups having these smoothness properties are known as **Lie groups**. Other important Lie groups that are used in this thesis is the Lie group of the unit quaternions [6] and the Lie group of the unit norm dual quaternions [12]. For more details of Lie groups and its applications in control theory and robotics, the reader is referred to [6, 7].

Another important algebraic structure is that of a vector space over a field. First, it is necessary to define a field.

DEFINITION A.6 [107, p.91] A field $(\mathbb{F}, \oplus, \otimes, 1_{\mathbb{F}}, 0_{\mathbb{F}})$ consists of a set \mathbb{F} with functions $\oplus, \otimes : G \times G \rightarrow G$ and elements $0_{\mathbb{F}}, 1_{\mathbb{F}} \in \mathbb{F}$ satisfying the following properties:

F1 $(\mathbb{F}, \oplus, 0_{\mathbb{F}})$ is an Abelian group (see Definition A.2).

F2 $(\mathbb{F} - \{0_{\mathbb{F}}\}, \otimes, 1_{\mathbb{F}})$ is an Abelian group (see Definition A.2).

F3 The operation \otimes must distribute with the operation \oplus , that is, for all $x, y, z \in \mathbb{F}$:

$$x \otimes (y \oplus z) = (x \otimes y) \oplus (x \otimes z).$$

F4 $0_{\mathbb{F}} \otimes x = x \otimes 0_{\mathbb{F}}$ for any $x \in \mathbb{F}$.

DEFINITION A.7 (Vector Space) [107, p.165] A vector space V over a field $(\mathbb{F}, \oplus, \otimes, 1_{\mathbb{F}}, 0_{\mathbb{F}})$ is the 4-tuple $(V, +, \cdot, 0_V)$ such that $0_V \in V$ and the functions $+: V \times V \rightarrow V$ (known as **addition between vectors**) and $\cdot: \mathbb{F} \times V \rightarrow V$ (known as **product by scalar**) satisfies the following properties:

V1 $(V, +, 0_V)$ is an Abelian group (see Definition A.2).

V2 The scalar product must distribute with the addition between vectors, that is, for all $v, w \in V$ and $\alpha \in \mathbb{F}$:

$$\alpha \cdot (v + w) = \alpha \cdot v + \alpha \cdot w.$$

V3 The operation of \oplus in \mathbb{F} must distribute with the scalar product also, that is, for all $\alpha, \beta \in \mathbb{F}$ and $v \in V$:

$$(\alpha \oplus \beta) \cdot v = \alpha \cdot v + \beta \cdot v.$$

V4 There is a kind of associative property between the scalar product and the operation \otimes of \mathbb{F} , that is, for all $\alpha, \beta \in \mathbb{F}$ and $v \in V$:

$$\alpha \cdot (\beta \cdot v) = (\alpha \otimes \beta) \cdot v.$$

V5 The multiplicative identity of \mathbb{F} must satisfy for all $v \in V$:

$$1_{\mathbb{F}} \cdot v = v.$$

If the field can be implied by context, it is common to omit it. A vector space may be equipped with a well-behaved function that measures the size of the vector, in the sense that a vector can be greater or smaller than other vectors.

DEFINITION A.8 (Normed Vector Space) [108, p.275] A normed vector space is a vector space equipped with a function $\|\cdot\| : V \rightarrow \mathbb{R}$ denominated as **norm** such that the following are satisfied:

N1 [Positive Definiteness] The norm must be **positive definite**, that is, for all $x \in V - \{0_V\}$ we have

$$\|x\| > 0.$$

N2 [Positive Scalability] The norm must be compatible with the scalar product in the sense that for all $\alpha \in \mathbb{F}$ and $x \in V$ we have

$$\|\alpha x\| = |\alpha| \|x\|,$$

where $|\cdot| : \mathbb{F} \rightarrow \mathbb{R}$ is a chosen norm in \mathbb{F} .

N3 [Triangle Inequality] The **triangle inequality** must hold, i.e.: for all $x, y \in V$,

$$\|x + y\| \leq \|x\| + \|y\|.$$

The vector space may also have a richer structure equipping it with an operation of multiplication between the vectors - such is the case of the cross product between vectors in \mathbb{R}^3 , for example.

DEFINITION A.9 (Algebra) [109] An algebra \mathcal{A} over a field \mathbb{F} is a vector space over the same field equipped with a bilinear function $\square : \mathcal{A} \times \mathcal{A} \rightarrow \mathcal{A}$, where **bilinear** means that the function must obey the following property:

A1 [Bilinearity] For all $x, y, z \in \mathcal{A}$ and $\alpha, \beta \in \mathbb{F}$ we have:

$$(\alpha \cdot x + \beta \cdot y) \square z = \alpha \cdot (x \square z) + \beta \cdot (y \square z) \text{ and } z \square (\alpha \cdot x + \beta \cdot y) = \alpha \cdot (z \square x) + \beta \cdot (z \square y).$$

An algebra is called an **associative algebra** when the function \square is associative, and it is called a **division algebra** if for any element $a \in \mathcal{A}$ and any non-zero element $b \in \mathcal{A}$ there exists precisely one element $x \in \mathcal{A}$ with $a = bx$ and precisely one element $y \in \mathcal{A}$ such that $a = yb$.

In order to represent rotations in three dimensions in a similar way that complex numbers represent rotations in the plane, it is naturally to ask if it is possible to have an algebra with dimension 3 over the field of real numbers that extends the complex numbers. As showed in the next proposition, the answer is no:

Theorem A.1

[110, pp. 3-4] An algebra over the field of real numbers with dimension 3 that extends the complex numbers does not exist.

proof.

Suppose the contrary and let $(1, i, j)$ be a basis of such algebra, such that $i^2 = -1$. Since the multiplication in an algebra is closed, we have that

$$ij = \alpha_0 + \beta_0 i + \gamma_0 j, \tag{A.1}$$

with $\alpha_0, \beta_0, \gamma_0 \in \mathbb{R}$. Multiplying both sides in the left by i :

$$-j = i^2 j = i(ij) = i(\alpha_0 + \beta_0 i + \gamma_0 j) = \alpha_0 i - \beta_0 + \gamma_0 \underbrace{ij}_{(A.1)}.$$

Substituting ij by $\alpha_0 + \beta_0 i + \gamma_0 j$:

$$(\alpha_0 \gamma_0 - \beta_0) + (\alpha_0 + \beta_0 \gamma_0) i + (\gamma_0^2 + 1) j = 0,$$

which implies that $\gamma_0^2 + 1 = 0$, contradicting that $\gamma_0 \in \mathbb{R}$. ■

As discussed in the Chapter 2, the algebra of quaternions does extend the complex numbers and can be used to represent rotations in the three-dimensional space. The quaternions can also be uniquely be characterized by being the only finite dimensional, associative and division algebra over the real numbers which is not commutative. This is the content of Frobenius' Theorem:

Theorem A.2

The only associative and division algebras over the real numbers are (up to isomorphism) the field of real numbers, the field of complex numbers and the algebra of the quaternions. [110, p.21-24]

proof.

Let D be a n -dimensional division algebra^a over \mathbb{R} . For $n = 1$, D is equivalent to the field of real numbers. Thus, suppose that $n > 1$.

Since $n > 1$, the set $D \cap \mathbb{R}^C$ is not empty and thus exists $a \in D$ such that $a \notin \mathbb{R}$. For such a , we claim that there exists $\gamma, \delta \in \mathbb{R}$ such that $[1/\gamma (a + \delta)]^2 = -1$. Indeed, the $n + 1$ elements $1, a, a^2, \dots, a^n$ are linearly independent over \mathbb{R} , that is, it is possible to write

$$\alpha_0 + \alpha_1 a + \alpha_2 a^2 + \dots + \alpha_n a^n \quad (\alpha_i \in \mathbb{R})$$

where not every α_i is 0. Let f be the polynomial defined as

$$f(x) = \alpha_0 + \alpha_1 x + \alpha_2 x^2 + \dots + \alpha_n x^n.$$

By the fundamental theorem of algebra, f splits as a product of linear or quadratic factors with real coefficients, that is

$$f(x) = f_1(x) \dots f_r(x).$$

Since $f(a) = f_1(a) \dots f_r(a) = 0$ and D is a division algebra, it follows that a can't be the root of a linear factor, because

$$a - r = 0 \quad (r \in \mathbb{R})$$

implies that $a \in \mathbb{R}$ which contradicts that $a \notin \mathbb{R}$. Hence, a is the root of a quadratic polynomial, say

$$a^2 + \alpha a + \beta = 0 \quad (\alpha, \beta \in \mathbb{R}).$$

Thus, for $\delta = \alpha/2$ we have that $(a + \delta)^2 = \delta^2 - \beta$; Since $a \notin \mathbb{R}$, the discriminant of the quadratic polynomial is

$$\Delta := \alpha^2 - 4\beta = 4\delta^2 - 4\beta = 4(\delta^2 - \beta) < 0,$$

which implies that $\delta^2 - \beta < 0$. In other words, $(a + \delta)^2 = -\gamma^2$ where $\gamma \in \mathbb{R}$, $\gamma \neq 0$ and the claim follows.

For $n = 2$, by the claim it is possible to choose a basis $1, I$ for D over \mathbb{R} such $I^2 = -1$. Thus, for this case D is isomorphic to the field of complex numbers.

Suppose now that $n > 2$. By using again the claim, we can choose a basis $1, I, J, \dots$ of D over \mathbb{R} such that

$$I^2 = -1, J^2 = -1, \dots$$

Thus, $I + J$ and $I - J$ satisfies quadratic equations, say:

$$\begin{aligned} (I + J)^2 + \alpha_1 (I + J) + \beta_1 &= 0, \\ (I - J)^2 + \alpha_2 (I - J) + \beta_2 &= 0. \end{aligned} \tag{A.2}$$

Summing both equations:

$$(\alpha_1 + \alpha_2)I + (\alpha_1 - \alpha_2)J + \beta_1 + \beta_2 - 4 = 0.$$

Since $1, I, J$ are linearly independent, $\alpha_1 = \alpha_2 = 0$. Thus, from (A.2):

$$(I + J)^2 + \beta_1 = I^2 + IJ + JI + J^2 + \beta_1 = IJ + JI + \beta_1 - 2 = 0 \implies IJ + JI = 2 - \beta_1 \in \mathbb{R}.$$

Defining μ as the real number $\mu := \frac{1}{2}(IJ + JI)$ and using again (A.2), we have that:

$$(I + J)^2 = 2\mu - 2, (I - J)^2 = -2\mu - 2.$$

Since $I + J$ and $I - J$ are not real numbers, we have that $\pm 2\mu - 2 < 0$. Consequently:

$$1 - \mu^2 = \frac{1}{4}(2\mu - 2)(-2\mu - 2) > 0.$$

Let

$$i = I, j = \frac{J + \mu I}{\sqrt{1 - \mu^2}}.$$

Therefore,

$$i^2 = -1, j^2 = -1, ij = ji$$

and $1, i, j, \dots$ forms a basis of D over \mathbb{R} .

The product ij can't be written as a linear combination of $1, i, j$, for otherwise we would have a contradiction (cf. Theorem A.1). Thus $n \geq 4$ and $k := ij$ can be considered as the fourth element of the basis. Hence, if $n = 4$, D is isomorphic to the algebra of quaternions.

Suppose now that $n > 4$. Thus D has a fifth element of the basis ℓ such that $\ell^2 = -1$. As before,

$$i\ell + \ell i = \mu_1, j\ell + \ell j = \mu_2, k\ell + \ell k = \mu_3$$

where μ_1, μ_2 and μ_3 are real numbers. Thus,

$$\ell k = \ell(ij) = (\ell i)j = (\mu_1 - i\ell)j = \mu_1 j - i(\mu_2 - j\ell) = \mu_1 j - \mu_2 i + k\ell.$$

Summing ℓk in both sides, it is obtained:

$$2\ell k = \mu_1 j - \mu_2 i + \mu_3.$$

Multiplying over k in the right, it follows that

$$-2\ell = \mu_1 i + \mu_2 j + \mu_3 k,$$

contradicting the fact that ℓ is linearly independent of i, j, k . ■

^aTo lighten the notation, along this proof it is assumed that algebra refers to an associative algebra.

Some special algebras are related to Lie groups and are called Lie algebras. Its definition is given next.

DEFINITION A.10 (Lie algebra) [109] A Lie Algebra \mathfrak{g} is an algebra such that its multiplication between vectors, entitled by **Lie bracket** and usually denoted by $[\cdot, \cdot]$, satisfies the following additional identities:

LA1 [Skew-symmetry] For every $x \in \mathfrak{g}$,

$$[x, x] = 0_{\mathbb{F}}$$

LA2 [Jacobi Identity] For every $x, y, z \in \mathfrak{g}$,

$$[x, [y, z]] + [y, [z, x]] + [z, [x, y]] = 0_{\mathbb{F}}$$

Familiar examples are the Euclidean space \mathbb{R}^3 with the multiplication given by the cross product and $\text{GL}(n, \mathbb{R})$ with the **commutator** between matrices A and B given by $[A, B] = AB - BA$.

Lie's fundamental theorems describe a relation between Lie groups and Lie algebras. In particular, any Lie group gives rise to a canonically determined Lie algebra (concretely, the tangent space at the identity); and, conversely, for any finite-dimensional Lie algebra there is a corresponding connected Lie group (Lie's third theorem) [111]. In the next examples we shall see how compute the Lie algebras of the Lie groups $\text{Spin}(3)$ and $\text{Spin}(3) \times \mathbb{R}^3$.

EXAMPLE A.3 Let $\mathbf{q} \in \text{Spin}(3)$ be a curve be given by $\mathbf{q} = \eta + \boldsymbol{\mu}$. Since $\mathbf{q} \in \text{Spin}(3)$, we have that $\mathbf{q}^* \mathbf{q} = 1$. Thus,

$$\dot{\mathbf{q}}^* \mathbf{q}$$

B

RESULTS ON TOPOLOGY

In this appendix, some topological definitions and results that are related to this thesis are presented. In this section, by a **manifold** it is meant a smooth, positive dimensional, connected manifold without boundary [109]. The following definitions we will also be used: a **homeomorphism** is a continuous and invertible map between topological spaces (in particular, manifolds) such that its inverse is also continuous. A **diffeomorphism** between manifolds is a differentiable and invertible map whose inverse is also differentiable.

B.1 THE IMPOSSIBILITY OF A GLOBAL THREE DIMENSIONAL PARAMETERIZATION FOR $SO(3)$ WITHOUT SINGULAR POINTS

In this section we prove that is impossible to have a *global* 3-dimensional parameterization *without* singular points for the rotation group. To find a 1 – 1 global parameterization of the rotation group using k parameters it is necessary to embed the rotation group $SO(3)$ in the Euclidean space \mathbb{R}^k , that is, to find a differentiable 1 – 1 map with differentiable inverse which carries $SO(3)$ into \mathbb{R}^k , and use the image points as representatives of the rotation matrices. As a corollary of the next theorem, we will see that there is no diffeomorphism between $SO(3)$ and \mathbb{R}^3 .

Theorem B.1 *Brouwer's theorem on the invariance of domain*

[112, p. 254] If U is an open subset of \mathbb{R}^n and $f : U \rightarrow \mathbb{R}^n$ is an injective continuous map, then $V = f(U)$ is open and f is a homeomorphism between U and V .

Corollary B.1. [15] *There is no diffeomorphism between \mathbb{R}^3 and $SO(3)$.*

proof.

Since $SO(3)$ is a 3-dimensional manifold, each point $r \in SO(3)$ has a neighborhood U_r which is homeomorphic to an open subset of \mathbb{R}^3 . If there were a homeomorphism $h : SO(3) \rightarrow \mathbb{R}^3$, then $h(U_r)$ would be open in \mathbb{R}^3 by Brouwer's theorem, so $h(SO(3))$, being the union of all $h(U_r)$ for $r \in SO(3)$, would be open in \mathbb{R}^3 . But $SO(3)$ is compact, and h is continuous, so $h(SO(3))$ should be compact. This contradicts with the fact that no Euclidean space contains an open compact subset, so there can exist no such homeomorphism. As a consequence, there is also no diffeomorphism between $SO(3)$ and \mathbb{R}^3 . ■

B.2 A TOPOLOGICAL OBSTRUCTION TO GLOBAL STABILITY

In this section we consider continuous vector fields f defined on manifolds \mathcal{L} such that the initial value problem

$$\dot{x}(t) = f(x(t)), x(0) \in \mathcal{L},$$

is well-posed. In this case, this vector field defines a continuous map $\psi : [0, \infty) \times \mathcal{L} \rightarrow \mathcal{L}$ satisfying

$$\begin{aligned}\psi(0, x) &= x, \\ \psi(t, (\psi(\tau, x))) &= \psi(t + \tau, x),\end{aligned}$$

for all $t, \tau \in [0, \infty)$ and $x \in \mathcal{L}$. This map is called a **semiflow** of the system and it is a generalization of the idea of state transition matrix for linear systems [113].

To connect the existence of global stabilizing feedbacks with the topology of the system, the notion of contractibility of the state space manifold will be defined next.

DEFINITION B.1 A set (resp. manifold) \mathcal{L} is a **contractible set (resp. manifold)** if there exists a point $x_0 \in \mathcal{L}$ and a continuous mapping $H : [0, 1] \times \mathcal{L} \rightarrow \mathcal{L}$ such that $H(0, x) = x$ and $H(1, x) = x_0$ for all $x \in \mathcal{L}$. In case of existence, the map H is said to be a **homotopy**.

Intuitively, a contractible set is one that can be continuously shrunk to a point x_0 within that set. For dimensions 1 and 2, contractible manifolds are very easy to describe: all contractible manifolds are homeomorphic to a *open* ball with the correspondent dimension. However, in higher dimensions this characterization is not true anymore: already in dimension 3 there is a manifold that is contractible but not homeomorphic to a ball in \mathbb{R}^3 [114].

As we will see in the next theorem, contractibility of state-space is a necessary condition for the system to be globally asymptotically stable.

Theorem B.2

Consider a continuous-time system $\dot{x} = f(x)$ defined on some state space $\mathcal{L} \subseteq \mathbb{R}^n$. If the system is globally asymptotically stable, then \mathcal{L} is a contractible set.

The homotopy mapping H can be constructed in a natural way using the semiflow ψ of the system:

$$H(t, x) = \begin{cases} \psi(-\ln(1-t), x), & t \in [0, 1), \\ x_0, & t = 1. \end{cases}$$

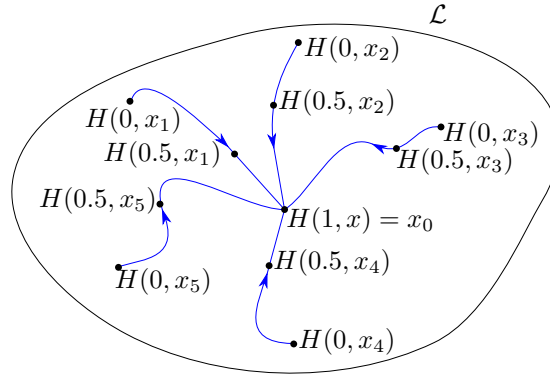


Fig. B.1: Homotopy mapping H induced by the semi-flow of the system in a neighborhood of the global equilibrium point x_0 . The map is illustrated for points x_1, \dots, x_5 at times $t = 0$ and $t = 0.5$. At time $t = 1$, the map $x \mapsto H(1, x)$ is equal to the constant map x_0 .

The last theorem restricts the class of manifolds that can be the state-space of a (continuous) globally asymptotically stable system. In particular, the next theorem states that no compact non-trivial (that is, made by more than one point) manifold (such as the case of S^3 , the underlying manifold of the unit quaternion group) has a continuous vector field with a globally asymptotically stable equilibrium point.

Theorem B.3

[115, p. 83] Let M be a manifold whose underlying set is not a single point. If M is compact, then M is not contractible.

When dealing with feedback, the closed-loop state space is augmented: for instance, in the case of kinematic attitude control, the open-loop state space is $SO(3)$ and the closed-loop state space is $SO(3) \times \mathbb{R}^3$. The latter is a first example of a real vector bundle over the $SO(3)$.

DEFINITION B.2 A (real) vector bundle is a triple (E, B, π) consisting of topological spaces E (total space), B (base space) and a continuous surjective map $\pi: E \rightarrow B$ such that

- For each point $x \in B$, the preimage (also called **fiber**) of π at x has the structure of a vector space over the field of reals. That is, the set $E_x := \pi^{-1}(x)$ is a vector space over \mathbb{R} .
- (**Local trivialization**) At any point $x \in B$, there exists a neighborhood U of x and **homeomorphism** $\Phi: \pi^{-1}(U) \rightarrow U \times \mathbb{R}^k$ satisfying
 - $\text{Pr}_U \circ \Phi = \pi$, where $\text{Pr}_U: U \times \mathbb{R}^k \rightarrow \mathbb{R}^k$ is the projection $(x, y) \mapsto x$.
 - for each $q \in U$, $\Phi|_{E_q}: E_q \rightarrow \{q\} \times \mathbb{R}^k$ is a vector space isomorphism.

Remark B.1. When there is no possibility of confusion, we will indicate vector bundles only by the total space E and say that E is a vector bundle over the base space B .

The local trivialization condition in the definition of vector bundle express that every vector bundle, at least *locally*, has the structure of a product $X \times \mathbb{R}^n$, where X is the base space. When the vector bundle has the

product structure *globally*, we have a first example of a vector bundle.

EXAMPLE B.1 The product space $X \times \mathbb{R}^k$ with the projection $\pi: X \times \mathbb{R}^k \rightarrow X$ is a vector bundle with $E = X \times \mathbb{R}^k$ and $B = X$. This vector bundle is called the **trivial bundle** over X . If $X = S^1$ and $k = 1$, the trivial bundle can be identified with a cylinder, as illustrated in Fig. B.2.

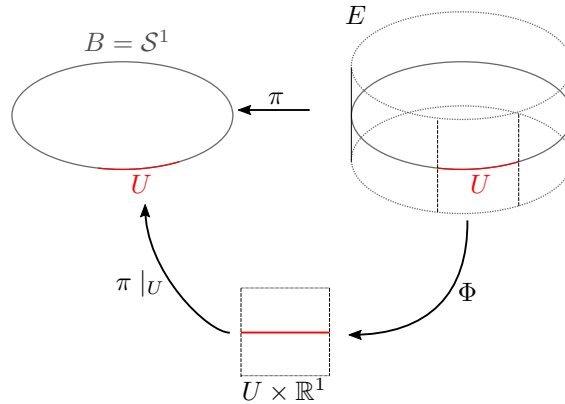


Fig. B.2: Example of a vector bundle: the trivial bundle given by $S^1 \times \mathbb{R}$.

The next example is a vector bundle which is locally equivalent to the trivial bundle given by $S^1 \times \mathbb{R}$, but globally has a different topological structure.

EXAMPLE B.2 The **Möbius bundle**, illustrated in Fig. B.3, is an example of a vector bundle which is not the trivial bundle.

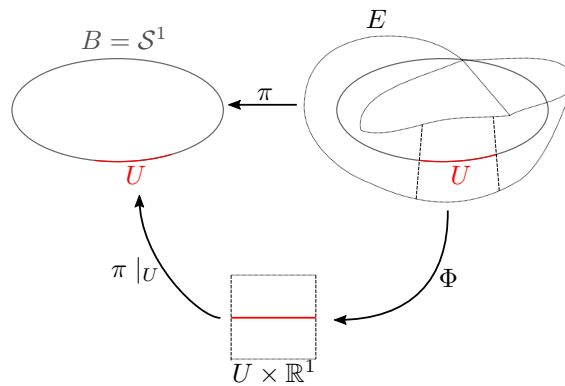


Fig. B.3: Möbius bundle.

The Möbius bundle and the cylinder are not homeomorphic: cutting the base circle from the cylinder results in a disconnected space, but cutting the base circle from the Möbius strip results in a connected space, as shown in Fig. B.4.

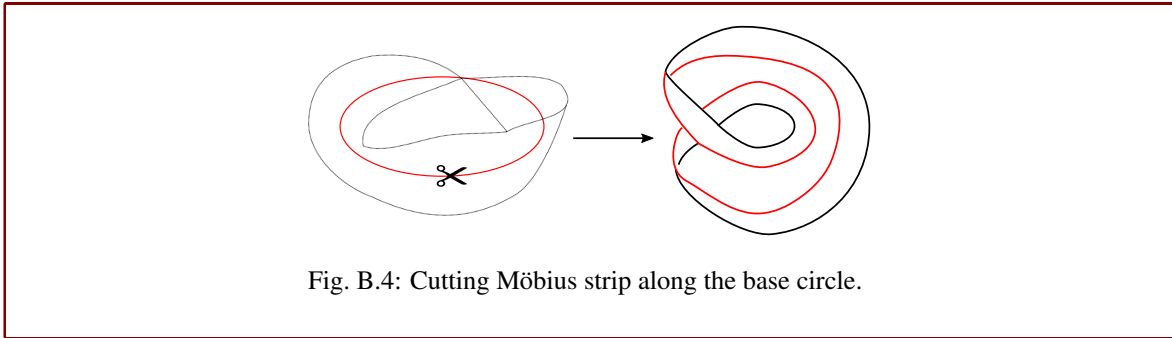


Fig. B.4: Cutting Möbius strip along the base circle.

The next theorem from [27] generalizes Theorem B.2 for vector bundles whose base space are compact manifolds: if the a vector bundle built over this compact manifold has a globally asymptotically stable equilibrium point, it would be possible to induce a globally asymptotically stable equilibrium point on the the compact manifold, contradicting Theorem B.3. This is illustrated in Fig. B.5 for the case that E is the cylinder.

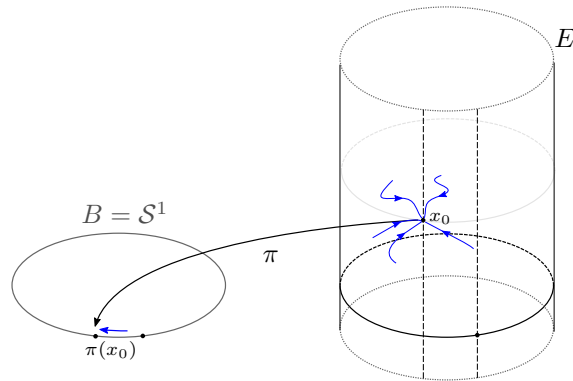


Fig. B.5: Semi-flow induced in the base space by the semi-flow on the bundle.

Theorem B.4

[27] Let \mathcal{M} be a manifold of dimension m and consider a continuous vector field f on \mathcal{M} . Suppose $\pi : \mathcal{M} \rightarrow \mathcal{L}$ is a vector bundle over \mathcal{L} , where \mathcal{L} is a compact, r -dimensional manifold with $r \leq m$. Then there exists no equilibrium point of f that is globally asymptotically stable.

As a corollary from Theorem B.4, continuous vector fields over $SE(3)$ cannot have a global asymptotic equilibrium point. This fact is proved next.

Corollary B.2. *If f is a continuous vector field defined on $SE(3)$, then there exists no equilibrium point of f that is globally asymptotically stable.*

proof.

The underlying manifold of Lie group $SE(3)$ is $SO(3) \times \mathbb{R}^3$, which can be seen as a trivial bundle over $SO(3)$, that is the vector bundle $\pi : SO(3) \times \mathbb{R}^3 \rightarrow SO(3)$. By Theorem B.4 there is no equilibrium point of f that is globally asymptotically stable. ■

The same obstruction for global asymptotic stability by means of continuous vector fields is present on $\text{Spin}(3) \times \mathbb{R}^3$. This is stated and proved in Corollary B.3.

Corollary B.3. *Let f be a continuous vector field defined on the underlying manifold $\underline{\mathcal{S}}$ of the Lie group of unit dual quaternions. Then there exists no equilibrium point of f that is globally asymptotically stable.*

proof.

For an arbitrary unit dual quaternion element $\underline{q} \in \underline{\mathcal{S}}$, with $\underline{q} = \mathbf{q} + \varepsilon \mathbf{q}' = \eta + \boldsymbol{\mu} + \varepsilon(\eta' + \boldsymbol{\mu}')$, it is possible to verify by direct calculation that the constraint $\mathbf{q}\mathbf{q}'^* + \mathbf{q}'\mathbf{q}^* = 0$ implies

$$\eta\eta' + \boldsymbol{\mu} \cdot \boldsymbol{\mu}' = 0. \quad (\text{B.1})$$

Furthermore, since $\|\mathbf{q}\| = 1$, then \mathbf{q} lies in \mathcal{S}^3 . In addition, \mathbb{H} is isomorphic to \mathbb{R}^4 as a vector space, which implies that $\mathbf{q}' \in \mathbb{H}$ lies in a three-dimensional hyperplane, with \mathbf{q} being its normal vector, due to constraint (B.1). In this sense, $\underline{\mathcal{S}}$ can be regarded as the product manifold $\mathcal{S}^3 \times \mathbb{R}^3$ [116].

The product $\mathcal{S}^3 \times \mathbb{R}^3$ equipped with the projection $\mathcal{S}^3 \times \mathbb{R}^3 \rightarrow \mathcal{S}^3$ given by $\underline{q} \mapsto \mathbf{q}$ yields a vector bundle $\mathcal{S}^3 \times \mathbb{R}^3$ onto \mathcal{S}^3 , namely the trivial bundle [109]. Since \mathcal{S}^3 is compact, it follows from Theorem B.4 that there is no equilibrium point of any continuous vector field f that is globally asymptotically stable. ■

Remark B.2. Corollaries B.2 and B.3 extends to any rigid transformation with some rotational degrees of freedom, as it is still possibly to write the state space as a vector bundle over the compact rotational manifold.

B.3 POINCARÉ-HOPF INDEX THEOREM

In the last section was demonstrated the impossibility of the existence of a point of equilibrium which is globally asymptotically stable. In this section, Poincaré-Hopf index theorem will be used to characterize the type of the equilibrium point (or points) of a vector field [117, p.63]. The index of an isolated zero of a vector field is an integer that helps to describe the behavior of the vector field around this zero.

DEFINITION B.3 [118, p. 309] Consider a continuous vector field v defined on an oriented Euclidean plane and suppose its zeros are finite and isolated. Consider a small oriented circle C around a zero, say x_0 , such that no other zeros lie inside this circle (nor in the boundary). Consider a point p in the boundary of this circle. As the point p traverses the circle in the positive direction, the vector $v(p)$ will also rotate continuously during the motion. When the point returns to its original position, so does the vector, but in doing so, it may complete several revolutions in one direction or the other. The number of revolutions it undergoes is called the **index** of x_0 , and it is denoted by $\text{ind}_{v,C,p}(x_0)$. In computing the index a revolution is counted positive if the vector rotates in the direction given by the orientation of the plane and negative in the opposite case.

It is possible to prove that the index is independent of the circle C and the initial point p chosen in Definition B.3. Because of this, we denote the index of x_0 by simply $\text{ind}_v(x_0)$. In the plane, the index takes the value -1 if x_0 is a saddle-like equilibrium point and takes value $+1$ if x_0 is a source or sink-like equilibrium point.

This is illustrated in Fig. B.6.

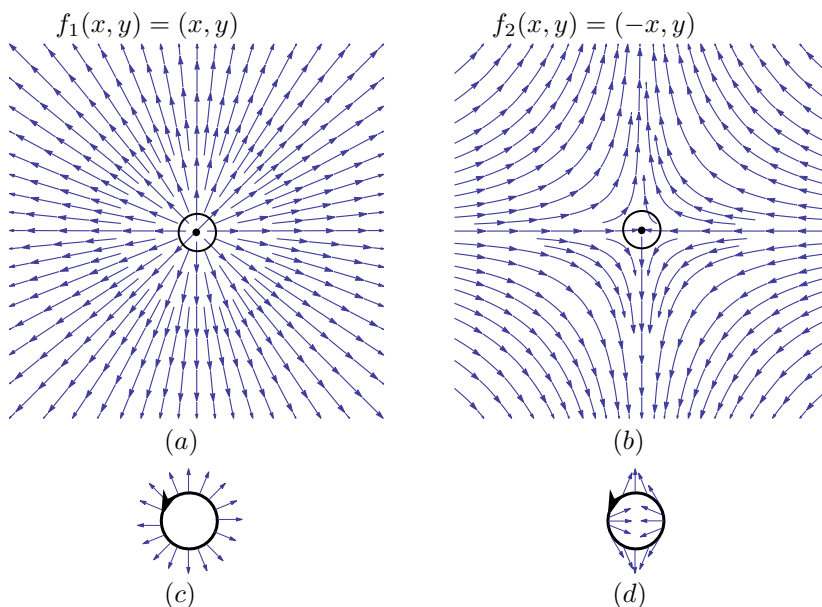


Fig. B.6: Vector fields on \mathbb{R}^2 and computation of its indices. All of the vector fields has an unique isolated equilibrium point in $(0, 0)$. (a) Vector field defined by $f_1(x, y) := (x, y)$. The equilibrium point can be seen to be unstable and source-like. (b) Vector field defined by $f_2(x, y) := (-x, y)$. The equilibrium point can be seen to be unstable and saddle-like. (c) Computation of $\text{ind}_{f_1}(0, 0)$: following the vector field f_1 counterclockwise along a circle gives a single complete revolution counterclockwise, thus $\text{ind}_{f_1}(0, 0) = 1$. (d) Computation of $\text{ind}_{f_2}(0, 0)$: following the vector field f_2 counterclockwise along a circle gives a single complete revolution clockwise, thus $\text{ind}_{f_2}(0, 0) = -1$.

The idea of index can be generalized to vector fields defined on manifolds (for more details of the construction, see [85, p. 34]). In the same way, if the index is -1 , the equilibrium point associated to the vector fields is a saddle point, and if the index is $+1$, it is a source or sink point. The next theorem, Poincaré-Hopf index theorem, can be used to relate a topological property, the Euler characteristic [109, p. 433], to the sum of indexes of zeros of a vector field.

Theorem B.5 Poincaré-Hopf theorem

[85, pg.35] Let M be a compact orientable manifold and v a continuous vector field defined on M with p isolated zeros given by x_1, \dots, x_p . The following formula is valid:

$$\sum_{i=1}^p \text{ind}_v(x_i) = \chi(M)$$

where $\chi(M)$ is the Euler characteristic of M .

By examining vector fields in a sufficiently small neighborhood of a source or a sink, we see that sources and sinks contribute integer amounts (the index) to the total, and they must all sum to 0. In the case of S^3 , we have that its Euler characteristic $\chi(S^3) = 0$ (for details, see [109]). This implies that if a continuous vector field on S^3 has two equilibrium points and one of the equilibrium points is asymptotic stable (corresponding to

a sink equilibrium point and a positive index), then the another equilibrium point must have a negative index, that is, it must be unstable (it is a source-like equilibrium point or a saddle-like equilibrium point).

In the context of the attitude stabilization problem for the kinematic control scenario, the closed-loop state space is \mathcal{S}^3 . This implies the non-existence of a continuous static controller that guarantees that the only equilibrium points for the closed-loop system are -1 and 1 , and with both of them simultaneously asymptotically stable. For dynamic controllers, the state-space is $\mathcal{S}^3 \times \mathbb{R}^3$, a non-compact manifold. While Theorem B.5 does not applies directly to non-compact manifolds¹, it still can be used to show that the unwinding problem remains even in the scenario of dynamic control. In fact, it is impossible to have a continuous vector field in $\mathcal{S}^3 \times \mathbb{R}^3$ with equilibrium points given by

$$\{(\mathbf{q}, \omega) \in \mathcal{S}^3 \times \mathbb{R}^3 : (\mathbf{q}, \omega) \in \{(-1, 0), (1, 0)\}\}$$

and both of them asymptotically stable. Indeed, suppose for the sake of contradiction that X is such continuous vector field and define $S_0 := \{(\mathbf{q}, \omega) \in \mathcal{S}^3 \times \mathbb{R}^3 : (\mathbf{q}, \omega) \in \mathcal{S}^3 \times \{0\}\}$. Note that $X|_{S_0}$ is a continuous vector field (the restriction of any continuous vector field is continuous) over the compact set S_0 , whose Euler characteristic is 0. By applying Theorem B.5 the result follows.

Finally, the same reasoning can be applied to the case of pose control using dual quaternions, where the state-space is $\underline{\mathcal{S}}$ (in the case of kinematic control) or $\underline{\mathcal{S}} \times \mathbb{R}^6$ (in the case of dynamic control).

¹Albeit not used here, it is interesting to remark that there is a generalization of Poincaré-Hopf theorem for non-compact manifolds. For more details, see [119].

C

PUBLISHED ARTICLES RELATED TO THE THESIS

During the doctorate, the following papers related to the theme of the thesis have been published:

- H. T. Kussaba, L. F. Figueredo, J. Y. Ishihara, and B. V. Adorno, “Hybrid Kinematic Control for Rigid Body Pose Stabilization using Dual Quaternions,” *Journal of the Franklin Institute*, vol. 354, no. 7, pp. 2769–2787, 2017
- P. P. M. Magro, H. T. M. Kussaba, L. F. Figueredo, and J. Y. Ishihara, “Dual quaternion-based bimodal global control for robust rigid body pose kinematic stabilization,” in *Proceedings of 2017 American Control Conference*, Seattle, USA, 2017, pp. 1205–1210

The published and submitted papers related to the thesis can be found in the next pages of this appendix.



Available online at www.sciencedirect.com

ScienceDirect

Journal of the Franklin Institute 354 (2017) 2769–2787

www.elsevier.com/locate/jfranklin



Hybrid kinematic control for rigid body pose stabilization using dual quaternions

Hugo T.M. Kussaba^{a,*}, Luis F.C. Figueredo^a, João Y. Ishihara^{a,1},
Bruno V. Adorno^b

^aDepartment of Electrical Engineering, University of Brasília (UnB), 70910-900 Brasília, DF, Brazil

^bDepartment of Electrical Engineering, Federal University of Minas Gerais (UFMG), 31270-010 Belo Horizonte, MG, Brazil

Received 30 October 2015; received in revised form 5 December 2016; accepted 26 January 2017

Available online 3 February 2017

Abstract

In this paper, we address the rigid body pose stabilization problem using dual quaternion formalism. We propose a hybrid control strategy to design a switching control law with hysteresis in such a way that the global asymptotic stability of the closed-loop system is guaranteed and such that the global attractivity of the stabilization pose does not exhibit chattering, a problem that is present in all discontinuous-based feedback controllers. Using numerical simulations, we illustrate the problems that arise from existing results in the literature—as unwinding and chattering—and verify the effectiveness of the proposed controller to solve the robust global pose stability problem.

© 2017 The Franklin Institute. Published by Elsevier Ltd. All rights reserved.

1. Introduction

Rigid body motion and its control have been extensively investigated in the last 40 years because of its applications in the theory of mechanical systems, such as robotic manipulators,

* Corresponding author.

E-mail addresses: kussaba@lara.unb.br, tadasho@gmail.com (H.T.M. Kussaba).

¹ A portion of this work was completed while the author was with Department of Electrical Engineering, University of California, Los Angeles (UCLA), 90095 California.

satellites and mobile robots. Research has largely focused on the study of models and control strategies in the Lie group of rigid body motions $SE(3)$ and its subgroup $SO(3)$ of proper rotations [1–4].

Although it is usual to design attitude and rigid motion controllers for mechanical systems respectively using rotation matrices and homogeneous transformation matrices (HTM) [3], it has been noted by some authors that a non-singular representation, namely the unit quaternion group $Spin(3)$ for rotations and the unit dual quaternions $Spin(3) \times \mathbb{R}^3$ for rigid motions can bring computational advantages [4–6].

In scenarios where the state space of the dynamical system is not the Euclidean space \mathbb{R}^n but a general differentiable manifold \mathcal{M} —which is the case of $SE(3)$ and $Spin(3) \times \mathbb{R}^3$ —some difficulties in designing a stabilizing closed-loop controller may arise. For instance, the topology of \mathcal{M} may obstruct the existence of a globally asymptotically stable equilibrium point in any continuous vector field defined on \mathcal{M} : in [1] it is proved that if \mathcal{M} has the structure of a vector bundle over a compact manifold \mathcal{L} , then no continuous vector field on \mathcal{M} —indeed, nor in \mathcal{L} —has a globally asymptotically stable equilibrium. In particular, this means that it is impossible to design a continuous feedback that globally stabilizes the pose of a rigid body, as in this case the closed-loop system state space manifold is a trivial bundle over the compact manifold $SO(3)$. The same topological obstruction is also present in the group of unit dual quaternions since its underlying manifold is a trivial bundle over the unit sphere \mathcal{S}^3 (see Theorem 1 in Section 2.3).

On the other hand, due to the two-to-one covering map $Spin(3) \times \mathbb{R}^3 \rightarrow SE(3)$, the unit dual quaternion group is endowed with a double representation for every pose in $SE(3)$. Neglecting the double covering yields to the problem of unwinding whereby solutions close to the desired pose in $SE(3)$ may travel farther to the antipodal unit dual quaternion representing the same pose [7]. There are few works on unwinding avoidance in the context of pose stabilization using unit dual quaternions [7–10]. All of them are based on a discontinuous sign-based feedback approach.

As shown by [11] for the particular case of $Spin(3)$, the discontinuous sign-based approach may, however, be particularly sensitive to measurement noises, and despite achieving global stability, global attractivity properties may be detracted with arbitrarily small measurement noises. As one would expect, the same happens with $Spin(3) \times \mathbb{R}^3$ and this will be shown in Theorem 1.

As verified in Section 3, in $Spin(3) \times \mathbb{R}^3$ the lack of robustness is even more relevant as the discontinuity of the controller not only affects the rotation, but may also disturb and deteriorate the trajectory of the system translation. In this context, even extremely small noises may lead to chattering, performance degradation—and in the worst case, prevent stability. Summing up, despite the solid contributions in the literature on dual quaternion based controllers in the context of rigid body motion stabilization, tracking, and multi-agent coordination [7–10,12–15], control of manipulators and human–robot interaction [16–21], and satellite and spacecraft tracking [22–24], it is important to emphasize that existing pose controllers are either stable only locally (as we show in Section 2) or have lack of robustness in the sense that they are sensitive to arbitrarily small measurement noises (as we illustrate in Section 5). In other words, the topological constraints from $Spin(3) \times \mathbb{R}^3$, most of them inherited from $SE(3)$, still pose a challenge—the extension from results on attitude control to the problem of pose control is not trivial—and there exists no result in the literature that ensures **robust** global stability.

1.1. Contributions

In this paper, a generalized robust hybrid control strategy for the global stabilization of rigid motion kinematics within unit dual quaternions framework is proposed. The strategy stems from the idea of the hybrid kinematic control law with hysteresis switching proposed in [11] to solve the non-robustness issue for quaternions. It is important to emphasize that, albeit some algebraic identities in quaternion algebra can be easily carried over to the dual quaternion algebra by the principle of transference [4,25], the proposed generalization does not follow by the principle of transference. In fact, counterexamples shown in [25] illustrate the failure of the transfer principle outside the algebraic realm.

In summary, whereas unit quaternions are used to model only attitude and perform a double cover for the Lie group $SO(3)$, unit dual quaternions model the coupled attitude and position and perform a double cover for the Lie group $SE(3)$. The necessity of different procedures for quaternion and dual quaternion stems from their different topologies and group structures. For example, the unit quaternion group is a compact manifold, whereas the unit dual quaternion group is not a compact manifold. This reflects in the use of distinct approaches to controller design (see for instance [3]). It is also interesting to highlight that due to $SO(3)$ being compact, it has a natural bi-invariant metric, but the same cannot be said from $SE(3)$ as it does not possess any bi-invariant metric. The unit dual quaternion group is not a subgroup from $Spin(3)$ —it is indeed the other way around—and boundedness, geodesic distance, norm properties, and other manifold features that are valid on \mathcal{S}^3 cannot be directly carried to $Spin(3) \times \mathbb{R}^3$. In this sense, the extension of control results to $Spin(3) \times \mathbb{R}^3$ is not trivial, which is reflected by the gap between quaternion based results and dual quaternion based controllers—where the double covering map is often neglected [6,12–15]. To overcome this context, we introduce a novel Lyapunov function that exploits the algebraic constraints inherent from the unit dual quaternion manifold, and a new robust hybrid stabilization controller for rigid motion using $Spin(3) \times \mathbb{R}^3$ is derived.

1.2. Notation

Lowercase bold letters represent quaternions, such as \mathbf{q} . Underlined lower case bold letters represent dual quaternions, such as $\underline{\mathbf{q}}$. The following notations will also be used:

\mathbb{R}	set of real numbers;
$\mathbb{R}_{\geq 0}$	set of non-negative real numbers;
\mathbb{B}	closed unit ball in the Euclidean norm;
\mathbb{H}	set of quaternions;
\mathbb{H}_0	set of pure imaginary quaternions;
$\mathbb{H} \otimes \mathbb{D}$	set of dual quaternions;
$SO(3)$	3-dimensional Lie group of rotations;
$SE(3)$	3-dimensional Lie group of rigid body motions;
$Spin(3)$	Lie group of unit norm quaternions;
$Spin(3) \times \mathbb{R}^3$	Lie group of unit norm dual quaternions;
\mathcal{S}^3	underlying manifold of unit norm quaternions;
$\underline{\mathcal{S}}$	underlying manifold of unit norm dual quaternions;
\mathcal{KL}	class of continuous functions $\beta : \mathbb{R}_{\geq 0} \times \mathbb{R}_{\geq 0} \rightarrow \mathbb{R}_{\geq 0}$ such that for each fixed s , the function $\beta(r, s)$ is strictly increasing and $\beta(0, s) = 0$ and for each fixed r , the function $\beta(r, s)$ is decreasing and $\lim_{s \rightarrow \infty} \beta(r, s) = 0$;

$\ \cdot \ $	Euclidean norm;
$\mathbf{u} \cdot \mathbf{v}$	dot product between pure imaginary quaternions \mathbf{u} and \mathbf{v} ;
$\mathbf{u} \times \mathbf{v}$	cross product between pure imaginary quaternions \mathbf{u} and \mathbf{v} ;
$\overline{\text{co}}(\cdot)$	closure of the convex hull;
$X + Y$	Minkowski sum between the sets X and Y ;
x^+	denotes the next state of the hybrid system after a jump;

2. Preliminaries

In this section, we provide for the reader basic concepts and a brief theoretical background regarding quaternions and dual quaternion representation for rigid body motion. We also present the topological constraints—which affect any mathematical structure that represents rigid motion—imposed by dual quaternions.

2.1. Quaternions

The quaternion algebra is a four-dimensional associative division algebra over \mathbb{R} introduced by Hamilton [26] to algebraically express rotations in the three-dimensional space. The elements $1, \hat{i}, \hat{j}, \hat{k}$ are the basis of this algebra, satisfying

$$\hat{i}^2 = \hat{j}^2 = \hat{k}^2 = \hat{i}\hat{j}\hat{k} = -1,$$

and the set of quaternions is defined as

$$\mathbb{H} \triangleq \{\eta + \hat{i}\mu_1 + \hat{j}\mu_2 + \hat{k}\mu_3 : \eta, \mu_1, \mu_2, \mu_3 \in \mathbb{R}\}.$$

Consider a quaternion $\mathbf{q} = \eta + \hat{i}\mu_1 + \hat{j}\mu_2 + \hat{k}\mu_3$; for ease of notation, it may be denoted as

$$\mathbf{q} = \eta + \boldsymbol{\mu}, \quad \text{with} \quad \boldsymbol{\mu} = \hat{i}\mu_1 + \hat{j}\mu_2 + \hat{k}\mu_3.$$

In addition, it may be decomposed into a real component and an imaginary component: $\text{Re}(\mathbf{q}) \triangleq \eta$ and $\text{Im}(\mathbf{q}) \triangleq \boldsymbol{\mu}$, such that $\mathbf{q} = \text{Re}(\mathbf{q}) + \text{Im}(\mathbf{q})$. The quaternion conjugate is given by $\mathbf{q}^* \triangleq \text{Re}(\mathbf{q}) - \text{Im}(\mathbf{q})$. Pure imaginary quaternions are given by the set

$$\mathbb{H}_0 \triangleq \{\mathbf{q} \in \mathbb{H} : \text{Re}(\mathbf{q}) = 0\}$$

and are very convenient to represent vectors of \mathbb{R}^3 within the quaternion formalism by means of a trivial isomorphism, which implies $\mathbb{H}_0 \cong \mathbb{R}^3$. Both cross product and dot product are defined for elements of \mathbb{H}_0 and they are analogous to their counterparts in \mathbb{R}^3 . More specifically, given $\mathbf{u}, \mathbf{v} \in \mathbb{H}_0$, the dot product is defined as

$$\mathbf{u} \cdot \mathbf{v} \triangleq -\frac{\mathbf{uv} + \mathbf{vu}}{2},$$

and the cross product is given by

$$\mathbf{u} \times \mathbf{v} \triangleq \frac{\mathbf{uv} - \mathbf{vu}}{2}.$$

The quaternion norm is defined as $\|\mathbf{q}\| \triangleq \sqrt{\mathbf{q}\mathbf{q}^*}$. Unit quaternions are defined as the quaternions that lie in the subset

$$\mathcal{S}^3 \triangleq \{\mathbf{q} \in \mathbb{H} : \|\mathbf{q}\| = 1\}.$$

The set \mathcal{S}^3 forms, under multiplication, the Lie group Spin(3), whose identity element is 1 and group inverse is given by the quaternion conjugate q^* .

Analogously to the way complex numbers are used to represent rotations in the plane, unit quaternions represent rotations in the three-dimensional space. Indeed, an arbitrary rotation θ around an axis $\mathbf{n} = \hat{i}n_x + \hat{j}n_y + \hat{k}n_z$ is represented by the unit quaternion $\mathbf{r} = \cos(\theta/2) + \sin(\theta/2)\mathbf{n}$. Furthermore, since the unit quaternion group double covers the rotation group SO(3), the unit quaternion $-\mathbf{r}$ also represents the same rotation associated to \mathbf{r} [4].

2.2. Dual quaternions

Similarly to how the quaternion algebra was introduced to address rotations in the three-dimensional space, the dual quaternion algebra was introduced by Clifford and Study [27,28] to describe rigid body movements. This algebra is constituted by the set

$$\mathbb{H} \otimes \mathbb{D} \triangleq \{ \mathbf{q} + \varepsilon \mathbf{q}' : \mathbf{q}, \mathbf{q}' \in \mathbb{H} \},$$

where ε is called the dual unit and is nilpotent—that is, $\varepsilon \neq 0$, but $\varepsilon^2 = 0$. Given $\underline{\mathbf{q}} = \eta + \mu + \varepsilon(\eta' + \mu')$, we define $\text{Re}(\underline{\mathbf{q}}) \triangleq \eta + \varepsilon\eta'$ and $\text{Im}(\underline{\mathbf{q}}) \triangleq \mu + \varepsilon\mu'$, such that $\underline{\mathbf{q}} = \text{Re}(\underline{\mathbf{q}}) + \text{Im}(\underline{\mathbf{q}})$. The dual quaternion conjugate is $\underline{\mathbf{q}}^* \triangleq \text{Re}(\underline{\mathbf{q}}) - \text{Im}(\underline{\mathbf{q}})$.

Under dual quaternion multiplication, the subset of dual quaternions

$$\underline{\mathcal{S}} \triangleq \{ \mathbf{q} + \varepsilon \mathbf{q}' \in \mathbb{H} \otimes \mathbb{D} : \|\mathbf{q}\| = 1, \mathbf{q}\mathbf{q}'^* + \mathbf{q}'\mathbf{q}^* = 0 \}, \tag{1}$$

forms a Lie group [14] called unit dual quaternions group Spin(3) \times \mathbb{R}^3 , whose identity is 1 and group inverse is the dual quaternion conjugate.

An arbitrary rigid displacement characterized by a rotation $\mathbf{r} \in \text{Spin}(3)$, with $\mathbf{r} = \cos(\theta/2) + \sin(\theta/2)\mathbf{n}$, followed by a translation $\mathbf{p} \in \mathbb{H}_0$, with $\mathbf{p} = p_x\hat{i} + p_y\hat{j} + p_z\hat{k}$, is represented by the unit dual quaternion [5,9]²

$$\underline{\mathbf{q}} = \mathbf{r} + \varepsilon \frac{1}{2} \mathbf{r} \mathbf{p}.$$

The unit dual quaternions group double covers SE(3) and thus any displacement $\underline{\mathbf{q}}$ can also be described by $-\underline{\mathbf{q}}$.

2.3. Description of rigid motion and topological constraints

Since unit quaternions describe the attitude of a rigid body, they are used to represent a rotation between the body frame and the inertial frame. In this sense, the kinematic equation of a rotation represented by the unit quaternion \mathbf{q} is expressed as

$$\dot{\mathbf{q}} = \frac{1}{2} \mathbf{q} \boldsymbol{\omega}, \tag{2}$$

where $\boldsymbol{\omega} \in \mathbb{H}_0$ is the angular velocity given in the body frame [30].

Similarly, the unit dual quaternion $\underline{\mathbf{q}}$ describes the coupled attitude and position. The first order kinematic equation of a rigid body motion in the inertial frame is given by

$$\dot{\underline{\mathbf{q}}} = \frac{1}{2} \underline{\mathbf{q}} \boldsymbol{\omega}, \tag{3}$$

² Similarly, the rigid motion could also be represented by a translation $\bar{\mathbf{p}}$ followed by a rotation \mathbf{r} [29] resulting in the dual quaternion $\underline{\mathbf{q}} = \mathbf{r} + (1/2)\varepsilon\bar{\mathbf{p}}\mathbf{r}$. Both $\bar{\mathbf{p}}$ and \mathbf{p} are related by $\bar{\mathbf{p}} = \mathbf{r}\mathbf{p}\mathbf{r}^*$.

where $\underline{\omega}$ is the twist in body frame given by

$$\underline{\omega} = \omega + \varepsilon[\dot{p} + \omega \times p]. \quad (4)$$

The remarkable similarity between Eqs. (2) and (3) is due to the principle of transference, whose various forms as stated in [25] can be summarized in modern terms as [4, Sec 7.6]: “All representations of the group $SO(3)$ become representations of $SE(3)$ when tensored with the dual numbers.” This means that several properties and algebraic identities of $SO(3)$ and the quaternions can be carried to $SE(3)$ and the dual quaternions algebra, respectively.

The principle of transference may mislead one to think that every theorem in quaternions can be transformed to another theorem in dual quaternions by a transference process. However, this is not the case, as shown by counterexamples in [25]. Therefore, properties and phenomena related to quaternion motions like topological obstructions and unwinding may not follow by direct use of transference and have to be verified for dual quaternions.

We first verify that $Spin(3) \times \mathbb{R}^3$ presents an obstruction for the global asymptotic stability of a continuous vector field on its underlying manifold.

Theorem 1. *Let f be a continuous vector field defined on the underlying manifold \underline{S} of the Lie group of unit dual quaternions. Then there exists no equilibrium point of f that is globally asymptotically stable.*

Proof. For an arbitrary unit dual quaternion element $\underline{q} \in \underline{S}$, with $\underline{q} = q + \varepsilon q' = \eta + \mu + \varepsilon(\eta' + \mu')$, as defined in Eq. (1), it is possible to verify by direct calculation that the constraint $qq^{*} + q'q'^{*} = 0$ implies

$$\eta\eta' + \mu \cdot \mu' = 0. \quad (5)$$

Furthermore, since $\|q\| = 1$, then q lies in \mathcal{S}^3 . In addition, \mathbb{H} is isomorphic to \mathbb{R}^4 as a vector space, which implies that $q' \in \mathbb{H}$ lies in a three-dimensional hyperplane, with q being its normal vector, due to constraint Eq. (5). In this sense, \underline{S} can be regarded as the product manifold $\mathcal{S}^3 \times \mathbb{R}^3$ [31].

The product $\mathcal{S}^3 \times \mathbb{R}^3$ equipped with the projection $\mathcal{S}^3 \times \mathbb{R}^3 \rightarrow \mathcal{S}^3$ given by $\underline{q} \mapsto q$ yields a vector bundle $\mathcal{S}^3 \times \mathbb{R}^3$ onto \mathcal{S}^3 , namely the trivial bundle [32]. Since \mathcal{S}^3 is compact, it follows from Theorem 1 of [1] (for the reader's convenience, this theorem is reproduced in Theorem 8 of the Appendix) that there is no equilibrium point of any continuous vector field f that is globally asymptotically stable. \square

3. Prior work on pose stabilization

Due to the topological constraint described in Theorem 1, there is no continuous state feedback controller on \underline{S} that can globally asymptotically stabilize (Eq. (3)) to a rest configuration. Indeed, the two-to-one covering map from $Spin(3) \times \mathbb{R}^3$ to $SE(3)$ renders a closed-loop system with two distinct equilibria q_e and $-q_e$.

Since both $\pm q_e$ correspond to the same configuration in $SE(3)$, solutions neglecting the double cover (see, for example, [12–15,17,18]) are expected to exhibit the unwinding phenomenon [1], that is, solutions starting arbitrarily close to the desired pose in $SE(3)$ —represented by both stable and unstable points in $Spin(3) \times \mathbb{R}^3$ —may travel to the farther stable point instead to the nearest unstable point (see, for example, Fig. 5). The sole contributions in the sense of avoiding the unwinding and stabilizing (Eq. (3)) to the set $\{\pm 1\}$ are

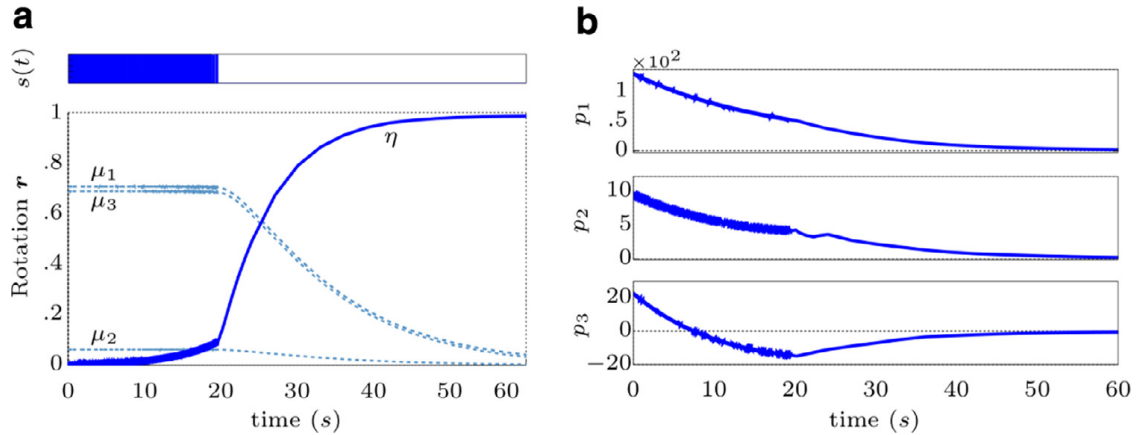


Fig. 1. (a) Trajectory of the rotation unit quaternion r in terms of η and μ (dashed line) with switches along time between the discontinuous control laws in Eq. (6) represented by $s(t)$. (b) Trajectory of the three-dimensional translation elements $p = p_1\hat{i} + p_2\hat{j} + p_3\hat{k}$.

based on a pure discontinuous control law introduced in [7–9]. In terms of the components of $\underline{q} = \eta + \mu + \varepsilon(\eta' + \mu')$, this discontinuous control law is given by³

$$\underline{\omega} = \begin{cases} -2k \left[\text{acos}(\eta) \frac{\mu}{\|\mu\|} + \varepsilon v \right], & \text{if } \eta \geq 0, \\ -2k \left[(\text{acos}(\eta) - \pi) \frac{\mu}{\|\mu\|} + \varepsilon v \right], & \text{if } \eta < 0, \end{cases} \quad (6)$$

where $v = \eta\mu' - \eta'\mu - \mu \times \mu'$ and k is a proportional gain.

Albeit this control law avoids unwinding, a careful look reveals a strong sensitivity around attitudes that are up to π away from the desired attitude about some axis—that is, $\eta = 0$. In view of Theorem 2.6 of [33], one can see that such control law isn't robust in the sense that arbitrarily small measurement noises can force η to stay near to 0 for initial conditions within its neighborhood. Indeed, similar to Theorem 3.2 of [11], one can even exhibit an explicit noise signal to persistently trap the system about a fixed pose, thus preventing its stability. To illustrate the sensitivity of pure discontinuous state feedback controllers, we introduce a simple case study in which the trajectory of Eq. (3) is simulated using the discontinuous control law (Eq. (6)) in the presence of a random measurement noise⁴—the results are shown in Fig. 1. The trajectory of the closed-loop system exhibits chattering in the neighborhood of the discontinuity—that lies in $\eta = 0$ —as a result of the measurement noise. The performance degradation stems from infinitely fast switches in Eq. (6). Furthermore, the chattering influence over the system is not restricted to the attitude error and may also impact on the resulting trajectory of the translation, as shown in Fig. 1(b). In this sense, the lack of robustness of a discontinuous solution may lead to chattering in orientation and to additional disturbances in the translation of the rigid motion in the presence of arbitrarily small random noises.

³ The discontinuous kinematic control law in [7–9] contains a typo that has been fixed in [10]. Different from Eq. (6), in [7–10] the controller is expressed in terms of the logarithm of a unit dual quaternion.

⁴ The simulation has been performed in accordance with the procedures described in Section 5.

4. Kinematic hybrid control law for robust global pose stability

In this section, we address the control design problem for globally stabilizing a rigid body coupled rotational and translational kinematics with no representation singularities. The proposed solution copes with the topological constraint inherent from the $\text{Spin}(3) \times \mathbb{R}^3$ parametrization while also ensuring robustness against measurement noises.

To avoid the unwinding phenomenon and the lack of robustness from pure discontinuous solutions, we appeal to the hybrid system formalism of [34]. This formalism combines both continuous-time and discrete-time dynamics and is useful to formally analyze hysteresis-based control laws, such as the proposed solution. A hybrid system is given by the constrained differential inclusions

$$\begin{aligned} \dot{x} &\in F(x), & x &\in C, \\ x^+ &\in G(x), & x &\in D, \end{aligned} \quad (7)$$

where x^+ denotes the next state of the hybrid system after a jump. The flow map F and the jump map G are set-valued functions, respectively, modeling the continuous and the discrete time dynamics of the system. The flow set C and the jump set D are the respective sets where the evolution occur. The following concepts of set-valued analysis will also be used: a set-valued mapping F is outersemicontinuous if its graph is closed and F is locally bounded—that is, if for any compact set K , there exists $m > 0$ such that $F(K) \subset m\mathbb{B}$, where \mathbb{B} is the closed unit ball in the Euclidean space of the convenient dimension [35]. For more details, the reader is referred to [34,36].

To solve the problem of robust global asymptotic stabilization of Eq. (3), we propose a generalization to the hysteresis-based hybrid control law of [11] that extends the attitude stabilization to render both coupled kinematics—attitude and translation—stable. The proposed control law is defined as

$$\underline{\omega} \triangleq -k_1 h \underline{\mu} - \varepsilon k_2 \eta \underline{\mu}', \quad (8)$$

where $k_1, k_2 \in \mathbb{R}_+^*$ are control gains and $h \in \{-1, 1\}$ is a memory state with hysteresis characterized by a parameter $\delta \in (0, 1)$. The memory state h has its dynamics defined by

$$\begin{aligned} \dot{h} &\triangleq 0, & \text{when } (\underline{q}, h) \text{ are such that } h\eta &\geq -\delta, \\ h^+ &\in \overline{\text{sgn}}(\eta), & \text{when } (\underline{q}, h) \text{ are such that } h\eta &\leq -\delta, \end{aligned} \quad (9)$$

where $\overline{\text{sgn}}$ is the set-valued function defined as

$$\overline{\text{sgn}}(s) \triangleq \begin{cases} \{1\}, & s > 0, \\ \{-1\}, & s < 0, \\ \{-1, 1\}, & s = 0. \end{cases}$$

In terms of the hybrid formalism (Eq. (7)), the closed loop system made by Eqs. (3), (8) and (9) is characterized as

$$\begin{aligned} F(\underline{q}, h) &= \left(\frac{1}{2} \underline{q} \underline{\omega}, 0 \right), C = \{(\underline{q}, h) \in (\text{Spin}(3) \times \mathbb{R}^3) \times \{-1, 1\} : h\eta \geq -\delta\}, \\ G(\underline{q}, h) &\in (\underline{q}, \overline{\text{sgn}}(\eta)), D = \{(\underline{q}, h) \in (\text{Spin}(3) \times \mathbb{R}^3) \times \{-1, 1\} : h\eta \leq -\delta\}, \end{aligned} \quad (10)$$

where $\underline{\omega}$ is defined as in Eq. (8) and h as in Eq. (9).

Consider $\underline{\mu} = \hat{i}\mu_1 + \hat{j}\mu_2 + \hat{k}\mu_3$ and $\underline{\mu}' = \hat{i}\mu'_1 + \hat{j}\mu'_2 + \hat{k}\mu'_3$. The map from $\mathbb{H} \otimes \mathbb{D}$ to \mathbb{R}^8 given by

$$\underline{q} = \eta + \boldsymbol{\mu} + \varepsilon(\eta' + \boldsymbol{\mu}') \mapsto \text{vec}(\underline{q}) = [\eta, \mu_1, \mu_2, \mu_3, \eta', \mu'_1, \mu'_2, \mu'_3]^T \tag{11}$$

is a vector space isomorphism whose inverse will be denoted by $\underline{\text{vec}}$.

The Hamilton operator [5,31] provides a matrix representation for the algebraic multiplication through the map $\overset{+}{\mathbf{H}} : \mathbb{H} \otimes \mathbb{D} \rightarrow \mathbb{R}^{8 \times 8}$ satisfying

$$\text{vec}(\underline{q}_1 \underline{q}_2) = \overset{+}{\mathbf{H}}(\underline{q}_1) \text{vec}(\underline{q}_2) \tag{12}$$

for any $\underline{q}_1, \underline{q}_2 \in \mathbb{H} \otimes \mathbb{D}$. Explicitly, the Hamilton operator is given by

$$\underline{q} = \mathbf{q} + \varepsilon \mathbf{q}' \mapsto \overset{+}{\mathbf{H}}(\underline{q}) = \begin{bmatrix} \overset{+}{\mathbf{H}}_4(\mathbf{q}) & 0_4 \\ \overset{+}{\mathbf{H}}_4(\mathbf{q}') & \overset{+}{\mathbf{H}}_4(\mathbf{q}) \end{bmatrix},$$

where $\overset{+}{\mathbf{H}}_4 : \mathbb{H} \rightarrow \mathbb{R}^{4 \times 4}$ is the map

$$\mathbf{q} = \eta + \hat{i}\mu_1 + \hat{j}\mu_2 + \hat{k}\mu_3 \mapsto \overset{+}{\mathbf{H}}_4(\mathbf{q}) = \begin{bmatrix} \eta & -\mu_1 & -\mu_2 & -\mu_3 \\ \mu_1 & \eta & -\mu_3 & \mu_2 \\ \mu_2 & \mu_3 & \eta & -\mu_1 \\ \mu_3 & -\mu_2 & \mu_1 & \eta \end{bmatrix}.$$

Let $\mathbf{x} = (x_1, \dots, x_8) \in \mathbb{R}^8$ and $y \in \mathbb{R}$. Based on Eqs. (11) and (12), the maps F and G of Eq. (10) induce the function $\vec{F} : \mathbb{R}^9 \rightarrow \mathbb{R}^9$ and the set-valued mapping $\vec{G} : \mathbb{R}^9 \rightrightarrows \mathbb{R}^9$ given by

$$\vec{F}(\mathbf{x}, y) = \left(\frac{1}{2} \overset{+}{\mathbf{H}}(\underline{\text{vec}}(\mathbf{x})) \text{vec}(\underline{\omega}), 0 \right), \quad \vec{G}(\mathbf{x}, y) \in (\mathbf{x}, \overline{\text{sgn}}(x_1)), \tag{13}$$

where

$$\text{vec}(\underline{\omega}) = [0, -k_1 h x_2, -k_1 h x_3, -k_1 h x_4, 0, -k_2 x_1 x_6, -k_2 x_1 x_7, -k_2 x_1 x_8]^T.$$

Similarly, the sets C and D of Eq. (10) induce the subsets \vec{C} and \vec{D} of \mathbb{R}^9 given by

$$\begin{aligned} \vec{C} &= \{(\mathbf{x}, y) \in \mathbb{R}^8 \times \mathbb{R} : (\mathbf{x}, y) \in \underline{\mathcal{S}} \times \{-1, 1\} \text{ and } yx_1 \geq -\delta\}, \\ \vec{D} &= \{(\mathbf{x}, y) \in \mathbb{R}^8 \times \mathbb{R} : (\mathbf{x}, y) \in \underline{\mathcal{S}} \times \{-1, 1\} \text{ and } yx_1 \leq -\delta\}. \end{aligned} \tag{14}$$

The following lemma proves that the hybrid system induced by Eqs. (3), (8) and (9) satisfies some properties which helps to prove the stability of the system and its robustness.

Lemma 2. *The maps \vec{F} and \vec{G} defined on Eq. (13) and the sets \vec{C} and \vec{D} defined on Eq. (14) satisfy the following properties:*

1. \vec{C} and \vec{D} are closed sets in \mathbb{R}^9 .
2. $\vec{F} : \mathbb{R}^9 \rightarrow \mathbb{R}^9$ is continuous.
3. $\vec{G} : \mathbb{R}^9 \rightrightarrows \mathbb{R}^9$ is an outer semicontinuous set-valued mapping, locally bounded and $\vec{G}(\mathbf{x}, h)$ is nonempty for each $(\mathbf{x}, h) \in \vec{D}$.

Proof. The proof is based on Lemma 5.1 of [11]. Setting $\delta \in (0, 1)$, consider the continuous map $\tau : \mathbb{R}^9 \rightarrow \mathbb{R}$ given by $\tau(x_1, \dots, x_8, y) = yx_1 + \delta$. The restriction $\tau|_{\underline{\mathcal{S}} \times \{-1, 1\}} : \underline{\mathcal{S}} \times \{-1, 1\} \rightarrow \mathbb{R}$ of this map to $\underline{\mathcal{S}} \times \{-1, 1\}$ is also continuous [37, Theorem 8].

Moreover, by the definition of the sets \vec{C} and \vec{D} , we have that

$$\vec{C} = \tau|_{\underline{S} \times \{-1, 1\}}^{-1}([0, +\infty)),$$

$$\vec{D} = \tau|_{\underline{S} \times \{-1, 1\}}^{-1}((-\infty, 0]).$$

Since the preimage of a closed set under a continuous mapping is closed, \vec{C} and \vec{D} are closed in $\underline{S} \times \{-1, 1\}$. We also have that $\underline{S} \times \{-1, 1\}$ is closed in \mathbb{R}^9 . In fact, consider the continuous functions $p, d : \mathbb{R}^8 \rightarrow \mathbb{R}$ given respectively by

$$p(\eta, \mu_1, \mu_2, \mu_3, \eta', \mu'_1, \mu'_2, \mu'_3) = [\eta, \mu_1, \mu_2, \mu_3][\eta, \mu_1, \mu_2, \mu_3]^T - 1,$$

$$d(\eta, \mu_1, \mu_2, \mu_3, \eta', \mu'_1, \mu'_2, \mu'_3) = [\eta, \mu_1, \mu_2, \mu_3][\eta', \mu'_1, \mu'_2, \mu'_3]^T.$$

By the definition of p and d , $\underline{S} = p^{-1}(\{0\}) \cap d^{-1}(\{0\})$. Since $\{0\}$ is a closed set of \mathbb{R} , the sets $p^{-1}(\{0\})$ and $d^{-1}(\{0\})$ are closed and their intersections are closed. Thus, \underline{S} is closed in \mathbb{R}^8 . Moreover, the set $\{-1, 1\}$ is closed in \mathbb{R} , therefore the Cartesian product $\underline{S} \times \{-1, 1\}$ is closed in \mathbb{R}^9 .

Since $\underline{S} \times \{-1, 1\}$ is closed in \mathbb{R}^9 , \vec{C} and \vec{D} are also closed in \mathbb{R}^9 . On the account that each component of \vec{F} is a polynomial, the map \vec{F} is continuous.

The graph of the set-valued mapping \vec{G} is given by $\{(\mathbf{x}, y, z) : z \in \vec{G}(\mathbf{x}, y)\} = \mathbb{R}^8 \times \mathbb{R} \times \mathbb{R}^8 \times \{-1, 1\}$. Since this set is closed, it follows by definition that \vec{G} is outer semicontinuous.⁵

Furthermore, \vec{G} is locally bounded because given any compact set $K \subset \mathbb{R}^9$, $\vec{G}(K) \subset K \times \{-1, 1\}$ and thus $\vec{G}(K)$ is bounded. Finally, by the definition of \vec{G} , $\vec{G}(\mathbf{x}, y)$ is nonempty for every $(\mathbf{x}, y) \in \vec{D}$. \square

Theorem 3. With $\underline{\omega}$ defined as in Eq. (8), the equilibrium points of the closed loop system made by Eqs. (3), (8) and (9) are ± 1 and the set $\{\pm 1\}$ is asymptotically stable.

Proof. Using the control law Eqs. (8)–(9) in Eq. (3), the closed-loop system is

$$\begin{aligned} \dot{\underline{q}} &= \dot{\eta} + \dot{\boldsymbol{\mu}} + \varepsilon(\dot{\eta}' + \dot{\boldsymbol{\mu}}'), \quad \text{with } \dot{\eta} = \frac{1}{2}k_1h\|\boldsymbol{\mu}\|^2, \\ \dot{\boldsymbol{\mu}} &= -\frac{1}{2}\eta k_1h\boldsymbol{\mu}, \quad \dot{\eta}' = \frac{1}{2}(k_1h + k_2\eta)\boldsymbol{\mu}' \cdot \boldsymbol{\mu}, \\ \dot{\boldsymbol{\mu}}' &= \frac{1}{2}[(k_1h - k_2\eta)\boldsymbol{\mu} \times \boldsymbol{\mu}' - k_1h\eta'\boldsymbol{\mu} - k_2\eta^2\boldsymbol{\mu}']. \end{aligned} \quad (15)$$

To find the equilibria of Eq. (15), note that $\dot{\underline{q}} = 0$ implies $\boldsymbol{\mu} = 0$. From the unit sphere constraint (Eq. (1)), it also follows that $\eta = \pm 1$ whereby we can find that $\boldsymbol{\mu}' = 0$. In this context, the constraint (Eq. (5)) also renders $\eta' = 0$. Hence, the set of equilibrium points of Eq. (15) is the set $\{\pm 1\}$.

To study the stability of the set of equilibrium points $\{\pm 1\}$, let us regard the Lyapunov candidate function

$$V(\underline{q}, h) = 2(1 - h\eta) + \eta^2 + \|\boldsymbol{\mu}'\|^2. \quad (16)$$

Since $\eta \in [-1, 1]$ and $h \in \{-1, 1\}$, one has that $(1 - h\eta) \geq 0$. Therefore, V is a positive semidefinite function. The condition $V = 0$ implies $0 \leq 2(1 - h\eta) = -\eta^2 - \|\boldsymbol{\mu}'\|^2 \leq 0$ which yields $\eta' = 0$, $\boldsymbol{\mu}' = 0$ and $h\eta = 1$, that is, $\underline{q} = \pm 1$. Hence, V is a positive definite function.

⁵ The graph of a set-valued mapping $F : X \rightrightarrows Y$ is defined by $\{(x, y) \in X \times Y : x \in X, y \in F(x)\}$. F is outer semicontinuous if its graph is a closed set of $X \times Y$ [11].

Taking the time-derivative of V and using (15) yields

$$\begin{aligned} \dot{V} &= -2h\dot{\eta} + 2\eta'\dot{\eta}' + 2\boldsymbol{\mu}' \cdot \dot{\boldsymbol{\mu}}' \\ &= -h^2k_1\|\boldsymbol{\mu}\|^2 - \eta^2\eta'^2k_2 - \eta^2\|\boldsymbol{\mu}'\|^2k_2 \leq 0. \end{aligned}$$

In addition, $\dot{V} = 0$ if and only if $\underline{\mathbf{q}} \in \{\pm 1\}$. Moreover, V also decreases over jumps of the closed loop system since for $h\eta < -\delta < 0$ one has that

$$V(\underline{\mathbf{q}}, h^+) - V(\underline{\mathbf{q}}, h) = 4h\eta < 0.$$

Thus, asymptotically stability of the set $\{\pm 1\}$ follows from Lemma 2 and by Theorem 20 of [34]. It is also important to highlight that the closed-loop differential equation is well-posed [38, Prop. 2.1] as $\underline{\omega}$ is in the Lie algebra of $\text{Spin}(3) \times \mathbb{R}^3$. \square

Remark 4. At a first glance, one could imagine that due to the transference principle [25], the extension of rotation stabilizers (e.g., the ones of [11,39]) to full rigid body stabilizers would be trivial, only requiring the substitution of adequate variables as in Eqs. (2) and (3). However, for stability analysis based on Lyapunov functions, this supposition doesn't even make sense, since a Lyapunov function is a real-valued function and never a dual-number valued function. As a consequence, stabilization in $\text{Spin}(3) \times \mathbb{R}^3$ using dual quaternions required one independent study from the quaternion stabilization analysis in $\text{Spin}(3)$. The necessity of different procedures for quaternion and dual quaternion is also inferred by remembering that due to the fact that $\text{SO}(3)$ is compact and $\text{SE}(3)$ is not, it was required one controller design procedure for each case in [3].

Similarly to the rotation controllers proposed in [11], the proposed pose controller doesn't exhibit Zeno behavior [34]. This is shown in the next lemma.

Lemma 5. *For any compact set $K \subset \mathbf{S} \times \{-1, 1\}$, if x is a solution of Eqs. (3), (8) and (9) with initial state in K , then the number of jumps is bounded.*

Proof. Similar to Theorem 5.3 of [11]. \square

The stability robustness will be characterized by the system's resistance against α -perturbations: given $\alpha > 0$, the α -perturbation of the hybrid system given by \vec{F}, \vec{G} as in Eq. (13), and \vec{C}, \vec{D} as in Eq. (14), is given by

$$\begin{aligned} \vec{C}_\alpha &\triangleq \{x \in \mathbb{R}^9 : (x + \alpha\mathbb{B}) \cap \vec{C} \neq \emptyset\}, \\ \vec{F}_\alpha(x) &\triangleq \overline{\text{co}} \vec{F}((x + \alpha\mathbb{B}) \cap \vec{C}) + \alpha\mathbb{B}, \text{ for all } x \in \vec{C}_\alpha, \\ \vec{D}_\alpha &\triangleq \{x \in \mathbb{R}^9 : (x + \alpha\mathbb{B}) \cap \vec{D} \neq \emptyset\}, \\ \vec{G}_\alpha(x) &\triangleq \{v \in \mathbb{R}^9 : v \in g + \alpha\mathbb{B}, g \in \vec{G}((x + \alpha\mathbb{B}) \cap \vec{D})\}, \text{ for all } x \in \vec{D}_\alpha, \end{aligned}$$

where $\overline{\text{co}}X$ denotes the closure of the convex hull of the set X . These perturbations, as illustrated in [34], include both measurement and modeling error.

The lack of sensitivity to these perturbations will be expressed in Theorem 6 by bounding the Lyapunov function by a class- \mathcal{KL} function. This bound guarantees practical stability for perturbed solutions starting from arbitrarily large subsets of the basin of attraction of $\{\pm 1\}$ [34].

Theorem 6. Let V be as in Eq. (16). Then there exists a class- \mathcal{KL} function β such that for each compact set $K \subset \underline{\mathcal{S}} \times \{-1, 1\}$ and $\Delta > 0$ there exists $\alpha^* > 0$ such that for each $\alpha \in (0, \alpha^*]$, the solutions x_α from K of the perturbed system $\mathcal{H}_\alpha = (\vec{C}_\alpha, \vec{F}_\alpha, \vec{D}_\alpha, \vec{G}_\alpha)$ satisfy

$$V(x_\alpha(t, j)) \leq \beta(V(x_\alpha(0, 0)), t + j) + \Delta, \quad \forall (t, j) \in \text{dom } x_\alpha$$

Proof. We have that V is a proper indicator function⁶ of the compact set $\{(1, 1), (-1, -1)\}$ in $\underline{\mathcal{S}} \times \{-1, 1\}$. From [34, Theorem 14], there exists a class- \mathcal{KL} function β such that for all solutions x of $\underline{\mathcal{S}} \times \{-1, 1\}$,

$$V(x(t, j)) \leq \beta(V(x(0, 0)), t + j), \quad \forall (t, j) \in \text{dom } x.$$

From this and from Lemma 2, the \mathcal{KL} bound on $V(x_\alpha(t, j))$ follows now by [34, Theorem 17]. \square

Remark 7. Differently from the Lyapunov function proposed in [11] for its hybrid kinematic controller, the proposed Lyapunov function (Eq. (16)) exploits the non-compactness of $\underline{\mathcal{S}}$ to be a proper indicator function, enabling the direct proof of Theorem 6.

5. Numerical simulations

In this section, the effectiveness of the proposed hybrid technique for robust global stabilization of the rigid body motion is demonstrated in four different numerical simulations.⁷ The first simulation considers the robustness of the proposed controller against chattering. The second simulation shows the influence of the design parameter δ in the execution of the controller. The last two simulations consider a more practical situation using a robotic manipulator.

We first illustrate the proposed controller global stability and robustness against measurement noises. To this aim, a simulation is performed using the hybrid feedback controller (Eq. (8)), with hysteresis parameter $\delta = 0.3$, and the pure discontinuous controller (Eq. (6))—using the same proportional gain $k = 0.08$. For this particular scenario, we assume an initial condition, $\underline{q}_0 = 0.001 + \hat{i}0.72 + \hat{j}0.06 + \hat{k}0.69 + \varepsilon(-55.15 - \hat{i}2.52 + \hat{j}36.71 - \hat{k}0.59)$, which was chosen arbitrarily, located in the neighborhood of $\eta = 0$, and a measurement noise over η set to $\mathcal{N}(0, 0.16)$, that is, a Gaussian random variable with zero mean and 0.16 variance. Fig. 1 illustrates the result from the discontinuous controller (Eq. (6)) whereby one can clearly see the problematic noise influence—for instance, the excess of switches causing chattering for up to 20 s and the consequent convergence lag. In contrast, the proposed hybrid feedback controller ensures a robust performance without chattering as shown in Fig. 2.

To further highlight the absence of chattering and performance improvements from the hybrid feedback solution (Eq. (8))—regardless the initial and noise conditions and the control parameters—a second scenario is devised with initial condition $\underline{q}_0 = 0.001 + \hat{i}0.78 + \hat{j}0.57 + \hat{k}0.28 + \varepsilon(-1.28 + \hat{i}1.50 - \hat{j}2.44 + \hat{k}0.77)$ and a zero mean Gaussian measurement noise over η with a 0.1 standard deviation, which was also chosen arbitrarily. The results illustrating the

⁶ Following [36, p. 145], a proper indicator function of a compact set \mathcal{A} in an open set $\mathcal{O} \supseteq \mathcal{A}$ is a continuous function on \mathcal{O} which is positive definite with respect to \mathcal{A} and such that it tends to infinity as its argument tends to infinity or to the boundary of \mathcal{O} .

⁷ The results of the simulations were computed using MATLAB environment and the DQ_robotics toolbox (<http://dqrobotics.sourceforge.net/>).

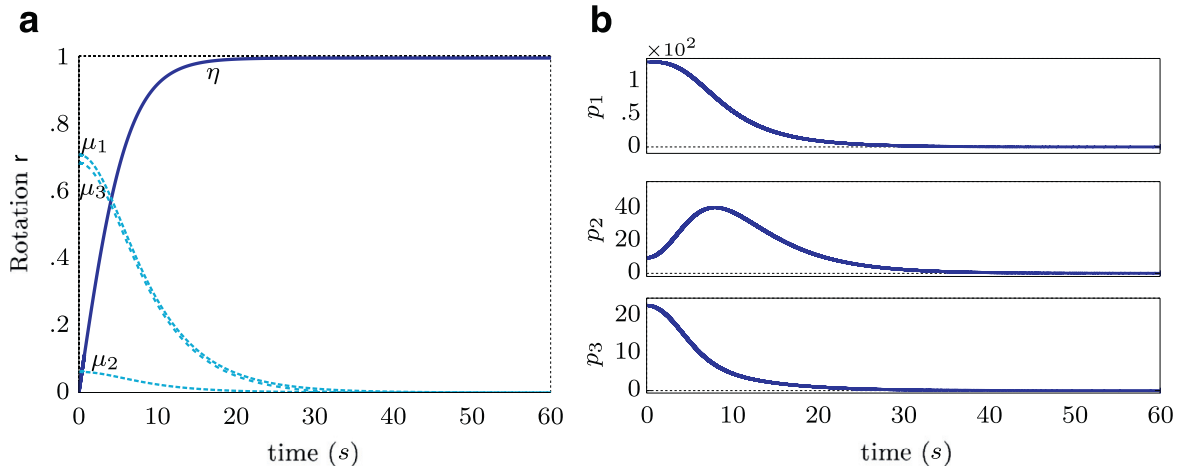


Fig. 2. Numerical example for the hybrid controller: (a) Trajectory of the rotation unit quaternion r in terms of η and μ (dashed line). (b) Trajectory of the three-dimensional translation elements $p = p_1\hat{i} + p_2\hat{j} + p_3\hat{k}$.

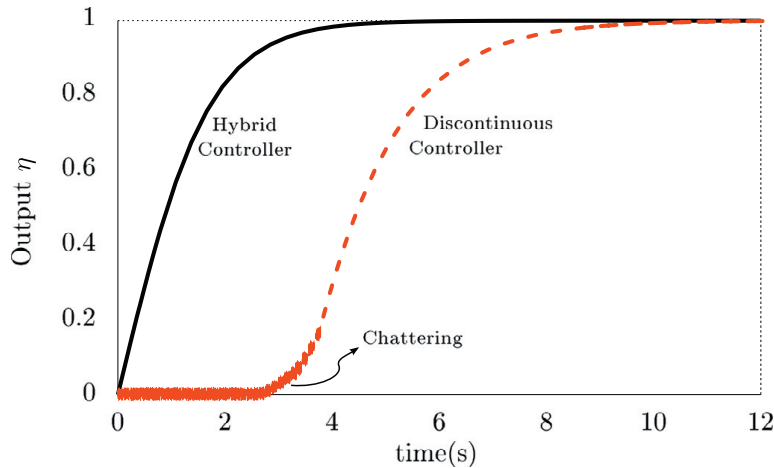


Fig. 3. Trajectory of η with hybrid feedback controller (Eq. (8)) and discontinuous controller (Eq. (6)) over time.

trajectory of η from both the discontinuous and hybrid controllers—set with the same control gain, $k = 2$ —are shown in Fig. 3.

To illustrate the influence of the design parameter δ over the switches along time of the closed-loop system (Eq. (3)), a set of simulations is performed using the hybrid controller (Eq. (8)) with different values for δ . For these simulations, we assume the same initial condition, control gain, and measurement noise as defined in the former scenario. As shown in Fig. 4(a), larger hysteresis parameters yield a smaller number of switches, as one would expect. As shown in Fig. 4(b), it is also interesting to highlight that the number of switches tends to decrease along time as η converges to the equilibrium.

Moreover, to elucidate the influence of the hysteresis parameter δ with regard to the unwinding phenomenon, a different scenario is simulated using Eq. (8) with $\delta = 0.15$ and $\delta = 0.95$ and with a proportional gain $k = 5$. We assume an initial state with η close to -1 and $h = 1$. As shown in Fig. 5, very large values of δ may induce the stabilization to $\eta = 1$, which leads to needless motions and control efforts compared to the case of $\delta = 0.15$. Lastly, as a concluding example, and to assess the effectiveness of the proposed solution in

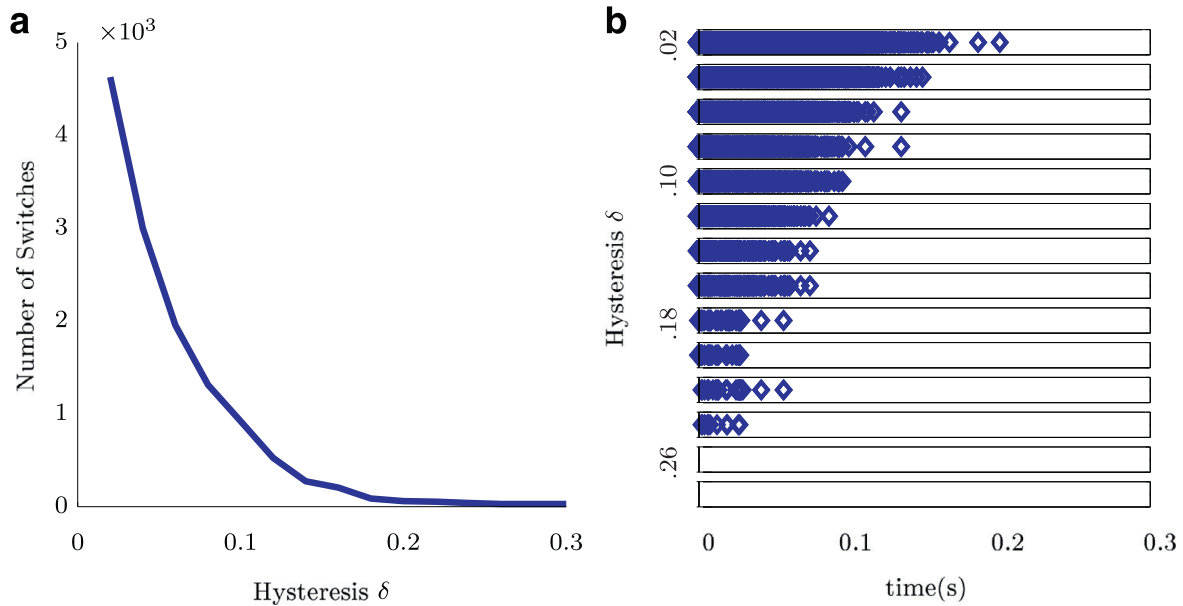


Fig. 4. The number of switches with regard to the hysteresis parameter δ is shown in (a), while the switches along time $s(t)$ are illustrated in (b) for different values of δ .

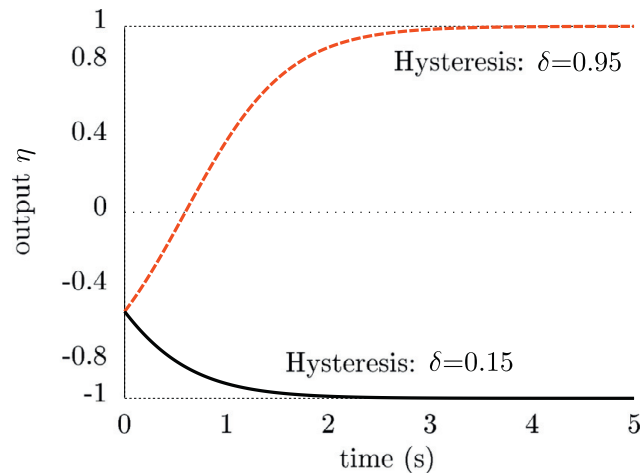


Fig. 5. Influence of the hysteresis parameter δ on unwinding— η converges to the farther stable point when the value of δ increases.

a more practical context, we designed a simple robot manipulator kinematic control task. To this aim, we considered a 6-DOF manipulator, the Comau SMART SiX robot, and two simple control tasks whereby the end-effector of the robot manipulator is regarded as a rigid body and described within the unit dual quaternion framework.⁸

In the first control setting, the end-effector of the manipulator \underline{q}_m , described within unit dual quaternions framework, is expected to hold the same current configuration—hence, the desired pose $\underline{q}_d = \underline{q}_m$ —in the presence of different sensor readings. In this case, it is rather ordinary to have readings in the antipodal configuration of the current pose, that is, $-\underline{q}_m$.

⁸ Further information on how to describe and map the end-effector’s rigid motion using unit dual quaternions can be found in [5].

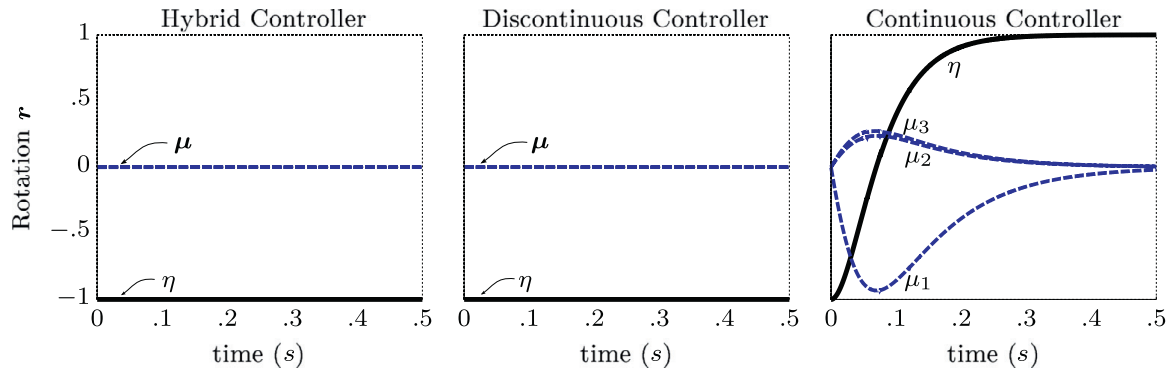


Fig. 6. Trajectory of the rotation unit quaternion r in terms of η and μ using the proposed hybrid controller (left), the discontinuous controller (center), and the continuous feedback controller (right). The unwinding phenomenon arises only on the continuous feedback controller.

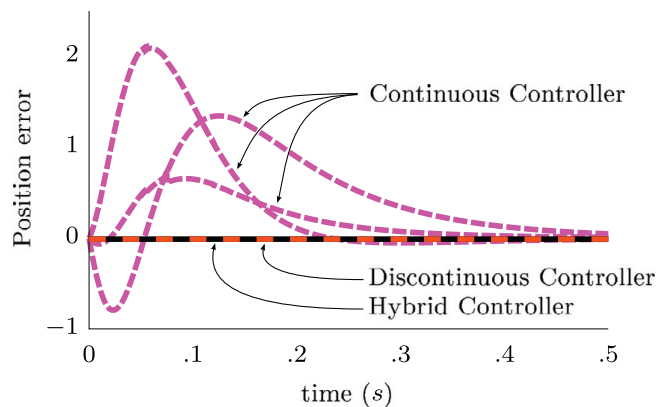


Fig. 7. Trajectory of the three-dimensional translation error using the hybrid (solid line), the discontinuous (red dashed line) and the continuous controller (magenta dashed line). (For interpretation of the references to colour in this figure legend, the reader is referred to the web version of this article.)

To illustrate the behavior of different controllers—with gain equally set to $k = 5$ —within this particular case, that is, $\underline{q}_d = -\underline{q}_m$, we set the manipulator to a random configuration and sought to stabilize the system using a continuous feedback controller, a discontinuous controller, and the proposed hybrid controller (with $\delta = 0.1$). The simulated result can be observed in Figs. 6 and 7, which illustrate the rigid motion of the manipulator's end-effector. Clearly, the continuous feedback controller failed to maintain the same end-effector configuration, exhibiting the unwinding phenomenon which yields needless motions—as observed in Fig. 8.^{9,10} Such phenomena could be avoided by simply enforcing a discontinuous controller or by using the proposed hysteresis-based hybrid control strategy.

Nonetheless, as observed in Fig. 3, the discontinuous sign-based approach is particularly sensitive to measurement noises. Hence, the second control task was devised to illustrate the behavior of the robot manipulator in the presence of measurement noises. In this scenario, both controllers were supposed to take the end-effector pose from an initial pose, represented

⁹ Since the discontinuous and hybrid feedback controllers successfully hold the same end-effector pose, the corresponding trajectories of the robot were not shown in this figure because they are constant. A video comparing the trajectories generated by the three different controllers can be seen in the supplementary material.

¹⁰ A video showing the motion of the robot is included in the supplementary material.

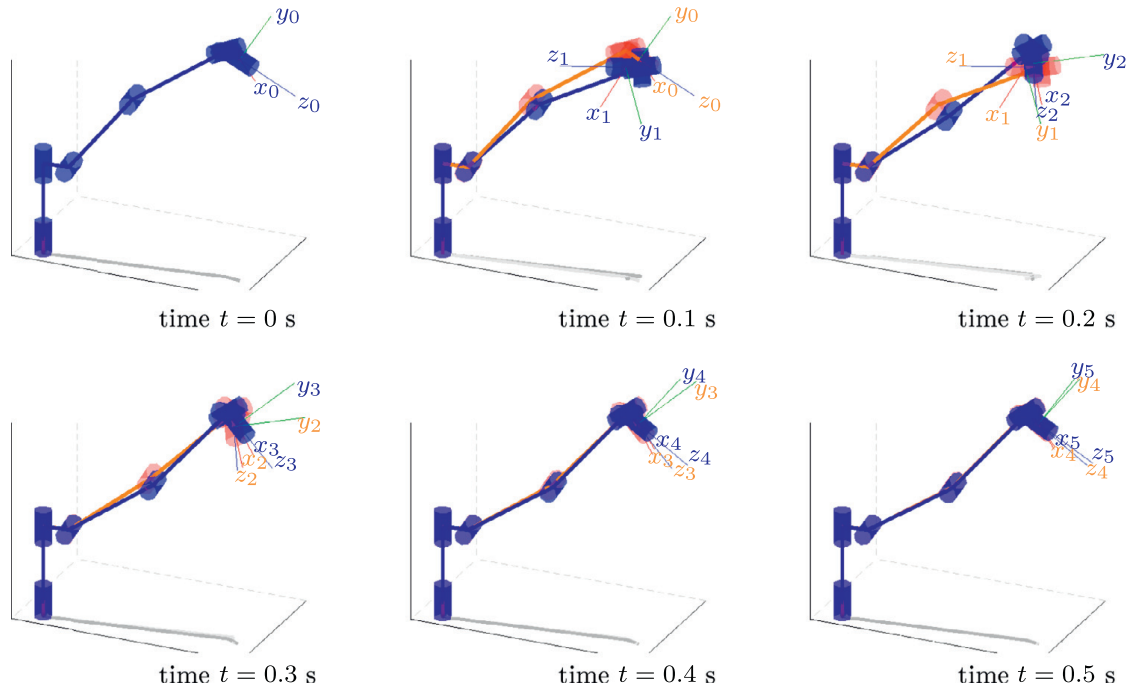


Fig. 8. Simulation snapshots of the continuous controller, when the desired robot pose, represented by \underline{q} , is changed to the same pose, but now represented by $-\underline{q}$. The unwinding phenomenon can be observed in contrast to maintaining the desired pose. In all snapshots, the light red robot represents the initial robot configuration. (For interpretation of the references to colour in this figure legend, the reader is referred to the web version of this article.)

by $\underline{q}_0 = -0.31 - \hat{i}0.67 + \hat{j}0.67 - \hat{k}0.05 + \varepsilon(-0.06 - \hat{i}0.31 - \hat{j}0.31 + \hat{k}0.40)$ and corresponding to a rotation angle of $(\pi + 0.63)$ rad around the axis $(-\sqrt{2}/2, -\sqrt{2}/2, 0)$ followed by a translation of $(-0.39, -0.29, -1.09)$, to a desired pose, represented by $\underline{q}_d = \hat{i}0.707 + \hat{j}0.707 + \varepsilon(0.28 - \hat{i}0.38 + \hat{j}0.38 + \hat{k}0.28)$ and corresponding to a rotation angle of π rad around the axis $(\sqrt{2}/2, \sqrt{2}/2, 0)$ followed by a translation of $(-0.79, 0.00, -1.07)$. The error between these poses are represented by the dual quaternion $\underline{q}_e = \underline{q}_m^* \underline{q}_d$, where \underline{q}_m is the measured dual quaternion. In addition, the measurement noise over η was set to $\mathcal{N}(0, 0.09)$ and the control gain for both controllers were set to $k = 0.020$ —the hysteresis parameter was set to $\delta = 0.1$. Fig. 9 illustrate the rigid motion of the manipulator's end-effector and the behavior of both controllers. It is easy to see that the problematic noise influence is restricted to the discontinuous controller—resulting in undesired chattering and delaying the closed-loop convergence. As expected, the proposed hybrid solution ensures robust performance, that is, a trajectory without chattering.

6. Conclusion

In this paper, a kinematic controller for the rigid body stabilization problem was presented. To prove the stability of this controller, a Lyapunov function that exploits the structure of the group of unit dual quaternions was proposed. Moreover, this controller was simulated and compared to another kinematic controller based on dual quaternions that has recently been presented in the literature. Simulation results show that the proposed controller is robust against measurement noises and, different from discontinuous-based feedback controllers, it

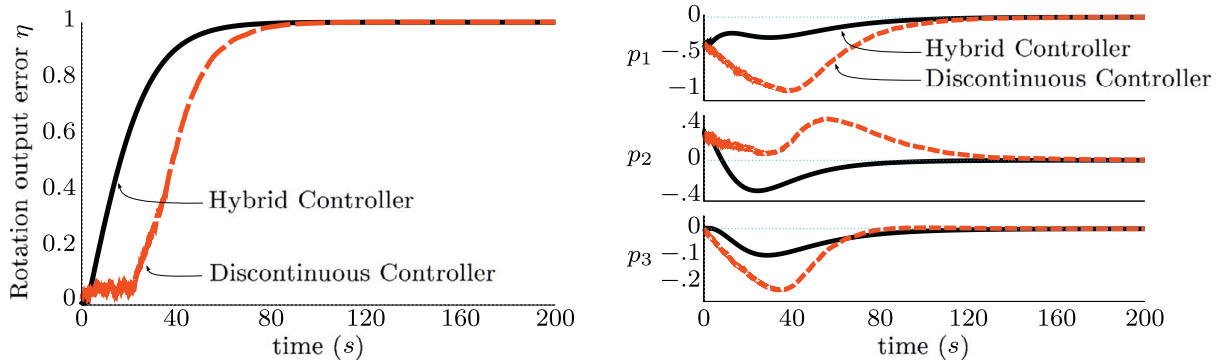


Fig. 9. The left figure shows the trajectory of the rotation error in terms of the scalar part η using the hybrid (solid line) and the discontinuous controller (red dashed line). The right figure shows the trajectory of the three-dimensional translation elements $\mathbf{p} = p_1\hat{i} + p_2\hat{j} + p_3\hat{k}$ with reference given in dotted blue line. (For interpretation of the references to colour in this figure legend, the reader is referred to the web version of this article.)

also avoids the problem of sensitivity of the global stabilization property to chattering. The proposed solution was also simulated in a simple robot manipulator kinematic control task to assess the controller in a more practical context.

In other scenarios it is possible that the input to the system is done by torques and forces instead of the generalized velocity. Further work will aim to incorporate the inertial parameters in the controller design.

Acknowledgments

This work is partially supported by the Coordination for the Improvement of Higher Education (CAPES), by the Brazilian National Council for Technological and Scientific Development (CNPq grant numbers are 456826/2013-0 and 312627/2013-0), and by Fundação de Amparo à Pesquisa do Estado de Minas Gerais (FAPEMIG grant number is APQ-00967-14). We are also grateful to Paulo Percio Mota Magro for the discussions relevant to this work.

Appendix

Theorem 8 [1]. *Let \mathcal{M} be a manifold of dimension m and consider a continuous vector field f on \mathcal{M} . Suppose $\pi : \mathcal{M} \rightarrow \mathcal{L}$ is a vector bundle on \mathcal{L} , where \mathcal{L} is a compact, r -dimensional manifold with $r \leq m$. Then there exists no equilibrium of f that is globally asymptotically stable.*

Supplementary material

Supplementary material associated with this article can be found, in the online version, at [10.1016/j.jfranklin.2017.01.028](https://doi.org/10.1016/j.jfranklin.2017.01.028).

References

- [1] S.P. Bhat, D.S. Bernstein, A topological obstruction to continuous global stabilization of rotational motion and the unwinding phenomenon, *Syst. Contr. Letts.* 39 (1) (2000) 63–70.

- [2] N.A. Aspragathos, J.K. Dimitros, A comparative study of three methods for robot kinematics, *IEEE Trans. Syst. Man Cybern. B* 28 (2) (1998) 135–145.
- [3] F. Bullo, R.M. Murray, Proportional Derivative (PD) Control on the Euclidean Group, Technical Report, Caltech/CDS 95–010, California Institute of Technology, 1995.
- [4] J.M. Selig, *Geometric Fundamentals of Robotics*, Monographs in Computer Science, second, Springer, 2007.
- [5] B.V. Adorno, Two-arm Manipulation: From Manipulators to Enhanced Human–Robot Collaboration, Laboratoire d’Informatique, de Robotique et de Microélectronique de Montpellier (LIRMM) - Université Montpellier 2, Montpellier, France, 2011 Ph.D. thesis.
- [6] X. Wang, H. Zhu, On the comparisons of unit dual quaternion and homogeneous transformation matrix, *Adv. Appl. Clifford Algebras* 24 (1) (2014) 213–229.
- [7] D.-P. Han, Q. Wei, Z.-X. Li, Kinematic control of free rigid bodies using dual quaternions, *Int. J. Autom. Comput.* 5 (3) (2008a) 319–324.
- [8] D. Han, Q. Wei, Z. Li, A dual-quaternion method for control of spatial rigid body, in: *Proc. 2008 IEEE Int. Conf. Networking, Sensing and Control*, 2008b, pp. 1–6.
- [9] D. Han, Q. Wei, Z. Li, W. Sun, Control of oriented mechanical systems: a method based on dual quaternion, in: *Proc. 17th IFAC World Congr.*, 2008c, pp. 3836–3841.
- [10] X. Wang, C. Yu, Unit dual quaternion-based feedback linearization tracking problem for attitude and position dynamics, *Syst. Contr. Lett.* 62 (3) (2013) 225–233.
- [11] C.G. Mayhew, R.G. Sanfelice, A.R. Teel, Quaternion-based hybrid control for robust global attitude tracking, *IEEE Trans. Autom. Contr.* 56 (11) (2011) 2555–2566.
- [12] X. Wang, C. Yu, Feedback linearization regulator with coupled attitude and translation dynamics based on unit dual quaternion, in: *Proc. 2010 IEEE Int. Symp. Intelligent Control*, 2010, pp. 2380–2384.
- [13] X. Wang, C. Yu, Unit-dual-quaternion-based PID control scheme for rigid-body transformation, in: *Proc. 18th IFAC World Congr.*, 2011, pp. 9296–9301.
- [14] X. Wang, D. Han, C. Yu, Z. Zheng, The geometric structure of unit dual quaternion with application in kinematic control, *J. Math. Anal. Appl.* 389 (2) (2012a) 1352–1364.
- [15] X. Wang, C. Yu, Z. Lin, A dual quaternion solution to attitude and position control for rigid-body coordination, *IEEE Trans. Robot.* 28 (5) (2012b) 1162–1170.
- [16] B.V. Adorno, P. Fraitse, S. Druon, Dual position control strategies using the cooperative dual task-space framework, in: *Proc. 2010 IEEE/RSJ Int. Conf. Intell. Robots Syst.*, 2010, pp. 3955–3960.
- [17] H.-L. Pham, V. Perdereau, B.V. Adorno, P. Fraitse, Position and orientation control of robot manipulators using dual quaternion feedback, in: *Proc. 2010 IEEE/RSJ Int. Conf. Intell. Robots Syst.*, 2010, pp. 658–663.
- [18] L.F.C. Figueredo, B.V. Adorno, J.Y. Ishihara, G.A. Borges, Robust kinematic control of manipulator robots using dual quaternion representation, in: *Proc. 2013 IEEE Int. Conf. Rob. Autom.*, 2013, pp. 1949–1955.
- [19] L.F.C. Figueredo, B.V. Adorno, J.Y. Ishihara, G.A. Borges, Switching strategy for flexible task execution using the cooperative dual task-space framework, in: *Proc. 2014 IEEE/RSJ Int. Conf. Intell. Robots Syst.*, 2014, pp. 1703–1709.
- [20] B.V. Adorno, A.P.L. Bó, P. Fraitse, Kinematic modeling and control for human–robot cooperation considering different interaction roles, *Robotica* 33 (2) (2015) 314–331.
- [21] M.M. Marinho, L.F.C. Figueredo, B.V. Adorno, A dual quaternion linear-quadratic optimal controller for trajectory tracking, in: *Proc. 2015 IEEE/RSJ Int. Conf. Intell. Robots Syst.*, 2015, pp. 4047–4052.
- [22] N. Filipe, P. Tsotras, Simultaneous position and attitude control without linear and angular velocity feedback using dual quaternions, in: *Proc. 2013 Amer. Control Conf.*, 2013, pp. 4808–4813.
- [23] N. Filipe, P. Tsotras, Adaptive position and attitude-tracking controller for satellite proximity operations using dual quaternions, *J. Guid. Control Dynam.* 38 (4) (2014) 566–577.
- [24] N. Filipe, M. Kontitsis, P. Tsotras, Extended Kalman filter for spacecraft pose estimation using dual quaternions, *J. Guid. Control Dynam.* 38 (9) (2015) 1625–1641.
- [25] D.P. Chevaller, On the transference principle in kinematics: its various forms and limitations, *Mech. Mach. Theory* 31 (1) (1996) 57–76.
- [26] W.R. Hamilton, On quaternions, or on a new system of imaginaries in algebra: copy of a letter from Sir William R. Hamilton to John T. Graves, esq. on quaternions, *Philos. Mag.* 25 (3) (1844) 489–495.
- [27] W.K. Clifford, A preliminary sketch of biquaternions, *Proc. London Math. Soc.* iv (64/65) (1873) 381–395.
- [28] E. Study, Von den bewegungen und umlegungen, *Math. Ann.* 39 (4) (1891) 441–565.
- [29] Y. Wu, X. Hu, D. Hu, T. Li, J. Lian, Strapdown inertial navigation system algorithms based on dual quaternions, *IEEE Trans. Aerosp. Electron. Syst.* 41 (1) (2005) 110–132.

- [30] J.C.K. Chou, Quaternion kinematic and dynamic differential equations, *IEEE Trans. Robot. Automat.* 8 (1) (1992) 53–64.
- [31] J.M. McCarthy, *Introduction to Theoretical Kinematics*, MIT Press, 1990.
- [32] J.M. Lee, *Introduction to Smooth Manifolds*, Springer, 2013.
- [33] R.G. Sanfelice, M.J. Messina, S. Emre Tuna, A.R. Teel, Robust hybrid controllers for continuous-time systems with applications to obstacle avoidance and regulation to disconnected set of points, in: *Proc. 2006 Amer. Control Conf.*, 2006, pp. 3352–3357.
- [34] R. Goebel, R.G. Sanfelice, A.R. Teel, Hybrid dynamical systems, *IEEE Control Syst.* 29 (2) (2009) 28–93.
- [35] R.T. Rockafellar, R.J.-B. Wets, *Variational Analysis*, second, Springer, 2004.
- [36] R. Goebel, R.G. Sanfelice, A.R. Teel, *Hybrid Dynamical Systems: Modeling, Stability, and Robustness*, Princeton University Press, 2012.
- [37] W. Basener, *Topology and Its Applications*, Pure and Applied Mathematics: A Wiley Series of Texts, Monographs and Tracts, Wiley, 2013.
- [38] Y.L. Sachkov, Control theory on Lie groups, *J. Math. Sci.* 156 (3) (2009) 381–439.
- [39] F. Bullo, R.M. Murray, A. Sarti, *Control on the Sphere and Reduced Attitude Stabilization*, Technical Report, Caltech/CDS 95–005, California Institute of Technology, 1995.

Dual quaternion-based bimodal global control for robust rigid body pose kinematic stabilization

Paulo P. M. Magro, Hugo T. M. Kussaba, Luis F. C. Figueredo and João Y. Ishihara

Abstract—A hybrid bimodal controller for rigid body pose stabilization within the group of unit norm dual-quaternions is proposed in this paper. Using two binary logic state variables, this hysteresis-based controller represents a middle term solution between the memoryless discontinuous controller and the fixed-width hysteretic one. The proposed strategy is novel within the dual-quaternions framework and addresses three common difficulties that appears in the literature of pose and attitude stabilization: global stability, robustness against chattering and against unwinding. The efficacy and performance of the proposed controller are illustrated with numerical examples.

I. INTRODUCTION

In the study of aerospace and robotic systems, the Lie groups of rigid body motions SE(3) and its subgroup SO(3) of proper rotations arise naturally. Stemming from the seminal work of [1] about control theory on general Lie groups, much of the literature has been devoted to the control of systems defined on SO(3) and SE(3). Although it is usual to design controllers for these systems using matrices to represent elements of these Lie groups [2], [3], it has been noted by some authors that controllers designed using another type of representation, namely, the unit quaternions for SO(3) and the unit dual quaternions for SE(3), may have advantages regarding computational time and storage requirements [4], [5].

It is important to note that since in this cases the state space of a dynamical system is not the Euclidean space \mathbb{R}^n but a general manifold, some difficulties to design a stabilizing controller to the system can arise. For instance, the topology of the manifold may be an obstacle to the existence of a global asymptotically stable equilibrium point in any continuous vector field defined on the manifold [6]. In particular, it is impossible to design a continuous feedback that globally stabilizes the attitude of a rigid body [6].

To avoid this topological obstruction in SO(3), one should resort to non-continuous feedback: this is what was done, for instance, in [7], [8]. As noted in [9], however, non-hybrid strategies are prone to chattering and are not robust to arbitrarily small measurement noise since it is impossible to use pure discontinuous state feedback to achieve robust global asymptotic stabilization of a disconnected set of points [10].

To tackle the problem of robust global attitude control, a quaternion-based hybrid controller with hysteretic memory was suggested in [9]. However, the cost for using the

hysteretic controller is longer rotation trajectories for some initial attitudes leading to a higher average settling time or energy consumption. For satellites and other systems with limited energy, this problem is yet more critical [11].

The aforementioned problems also occur in the dual quaternion framework, as the Lie group of unit dual quaternions is a double cover for the Lie group of rigid body motions SE(3) [12], [13]. Moreover, in [13] it was verified that the lack of robustness in the context of dual quaternions is even more important, as the discontinuity of the controller not only affects the rotation of the rigid body, but may also degrade the trajectory of its translation. The problem of energy consumption also aggravates in this context, as the coupled translation and rotation movements consume more energy. Thus, to address the robust global stability problem of rigid bodies we propose a hybrid control law, called bimodal, that extends the hysteretic controller suggested by [13] and represents a compromise in terms of cost between the memoryless discontinuous controller and the hysteretic one.

II. PRELIMINARY

A. Quaternion

The quaternion algebra is a four dimensional associative division algebra over \mathbb{R} invented by Hamilton [14], which naturally extends the algebra of complex numbers. The elements $1, \hat{i}, \hat{j}, \hat{k}$ are the basis of this algebra, satisfying

$$\hat{i}^2 = \hat{j}^2 = \hat{k}^2 = \hat{i}\hat{j}\hat{k} = -1$$

and the set of quaternions is defined as

$$\mathbb{H} \triangleq \left\{ \mathbf{q} = \eta + \mu_1 \hat{i} + \mu_2 \hat{j} + \mu_3 \hat{k} : \eta, \mu_1, \mu_2, \mu_3 \in \mathbb{R} \right\}.$$

For ease of notation, it may be denoted as

$$\mathbf{q} = \eta + \boldsymbol{\mu}, \quad \text{with } \boldsymbol{\mu} = \mu_1 \hat{i} + \mu_2 \hat{j} + \mu_3 \hat{k}$$

In addition, it may be decomposed into a real component and an imaginary component: $\Re(\mathbf{q}) \triangleq \eta$ and $\Im(\mathbf{q}) \triangleq \boldsymbol{\mu}$ such that $\mathbf{q} = \Re(\mathbf{q}) + \Im(\mathbf{q})$. The quaternion conjugate is given by $\mathbf{q}^* \triangleq \Re(\mathbf{q}) - \Im(\mathbf{q})$.

The multiplication of two quaternions $\mathbf{q}_1 = \eta_1 + \boldsymbol{\mu}_1$ and $\mathbf{q}_2 = \eta_2 + \boldsymbol{\mu}_2$ is given by

$$\mathbf{q}_1 \mathbf{q}_2 = (\eta_1 \eta_2 - \boldsymbol{\mu}_1 \cdot \boldsymbol{\mu}_2) + (\eta_1 \boldsymbol{\mu}_2 + \eta_2 \boldsymbol{\mu}_1 + \boldsymbol{\mu}_1 \times \boldsymbol{\mu}_2).$$

Pure imaginary quaternions are given by the set

$$\mathbb{H}_0 \triangleq \{ \mathbf{q} \in \mathbb{H} : \Re(\mathbf{q}) = 0 \}$$

which are very convenient to represent vectors of \mathbb{R}^3 .

This work is partially supported by the Brazilian agencies CAPES, CNPq and FINATEC. The authors are with the Department of Electrical Engineering, University of Brasília, UnB, 70910-900, Brasília, DF, Brazil, ppmmagro@uol.com.br, htksussaba@ieec.org, figueredo@ieec.org, ishihara@ene.unb.br.

The quaternion norm is defined as $\|\mathbf{q}\| \triangleq \sqrt{\mathbf{q}\mathbf{q}^*}$. Unit quaternions are defined as the quaternions that lie in the subset

$$\mathcal{S}^3 \triangleq \{\mathbf{q} \in \mathbb{H} : \|\mathbf{q}\| = 1\}, \quad \mathbf{1} = 1 + 0\hat{i} + 0\hat{j} + 0\hat{k}.$$

The set \mathcal{S}^3 forms, under multiplication, the Lie group Spin(3), whose identity element is $\mathbf{1}$ and group inverse is given by the quaternion conjugate \mathbf{q}^* . As the unit quaternions \mathbf{q} and $-\mathbf{q}$ represent the same rotation, the unit quaternion group double covers the rotation group SO(3).

B. Dual Quaternions

Similarly to how the quaternion algebra was introduced to address rotations in the three-dimensional space, the dual quaternion algebra was introduced by Clifford [15] and Study [16] to describe rigid body movements. This algebra is constituted by the set

$$\mathbb{H} \triangleq \{\mathbf{q} + \varepsilon\mathbf{q}' : \mathbf{q}, \mathbf{q}' \in \mathbb{H}\},$$

where \mathbf{q} and \mathbf{q}' are called the primary part and the dual part of the dual quaternion and ε is called the dual unit which is nilpotent—that is, $\varepsilon \neq 0$ and $\varepsilon^2 = 0$. Given $\underline{\mathbf{q}} = \boldsymbol{\eta} + \boldsymbol{\mu} + \varepsilon(\boldsymbol{\eta}' + \boldsymbol{\mu}')$, we define $\Re(\underline{\mathbf{q}}) \triangleq \boldsymbol{\eta} + \varepsilon\boldsymbol{\eta}'$ and $\Im(\underline{\mathbf{q}}) \triangleq \boldsymbol{\mu} + \varepsilon\boldsymbol{\mu}'$, such that $\underline{\mathbf{q}} = \Re(\underline{\mathbf{q}}) + \varepsilon\Im(\underline{\mathbf{q}})$. The dual quaternion conjugate is $\underline{\mathbf{q}}^* \triangleq \Re(\underline{\mathbf{q}}) - \varepsilon\Im(\underline{\mathbf{q}})$.

The multiplication of two dual quaternions $\underline{\mathbf{q}}_1 = \mathbf{q}_1 + \varepsilon\mathbf{q}'_1$ and $\underline{\mathbf{q}}_2 = \mathbf{q}_2 + \varepsilon\mathbf{q}'_2$ is given by

$$\underline{\mathbf{q}}_1\underline{\mathbf{q}}_2 = \mathbf{q}_1\mathbf{q}_2 + \varepsilon(\mathbf{q}_1\mathbf{q}'_2 + \mathbf{q}'_1\mathbf{q}_2).$$

The subset of dual quaternions

$$\underline{\mathcal{S}} = \{\mathbf{q} + \varepsilon\mathbf{q}' \in \mathbb{H} : \|\mathbf{q}\| = 1, \mathbf{q}\mathbf{q}'^* + \mathbf{q}'\mathbf{q}^* = \mathbf{0}\} \quad (1)$$

forms a Lie group [17] called unit dual quaternions group, whose identity is $\underline{\mathbf{1}} = \mathbf{1} + \varepsilon\mathbf{0}$, $\mathbf{0} = 0 + 0\hat{i} + 0\hat{j} + 0\hat{k}$ and group inverse is the dual quaternion conjugate.

An arbitrary rigid displacement characterized by a rotation $\mathbf{q} \in \text{Spin}(3)$, followed by a translation $\mathbf{p} \in \mathbb{H}_0$, with $\mathbf{p} = p_x\hat{i} + p_y\hat{j} + p_z\hat{k}$, is represented by the unit dual quaternion [12], [18]

$$\underline{\mathbf{q}} = \mathbf{q} + \varepsilon\frac{1}{2}\mathbf{q}\mathbf{p}.$$

As the displacement $\underline{\mathbf{q}}$ is equally described by $-\underline{\mathbf{q}}$, the unit dual quaternions group double covers SE(3).

C. Rigid Motion Description

Using Hamilton convention [19], let \mathbf{q} represent the rigid-body attitude $R \in \text{SO}(3)$, defined as the relative rotation of a body-fixed frame to a reference frame. The quaternion kinematic equation is

$$\dot{\mathbf{q}} = \frac{1}{2}\mathbf{q}\boldsymbol{\omega}, \quad (2)$$

where $\boldsymbol{\omega} \in \mathbb{H}_0$ is the angular velocity expressed in the body frame [18].

Similarly, the unit dual quaternion $\underline{\mathbf{q}}$ describe the coupled attitude and position. The kinematic equation of a rigid body motion is given by [18]

$$\dot{\underline{\mathbf{q}}} = \frac{1}{2}\underline{\mathbf{q}}\boldsymbol{\omega}, \quad (3)$$

where $\boldsymbol{\omega}$ is called twist and is given by

$$\boldsymbol{\omega} = \boldsymbol{\omega} + \varepsilon[\dot{\mathbf{p}} + \boldsymbol{\omega} \times \mathbf{p}] \quad (4)$$

and \mathbf{p} is the translation expressed in the body frame.

Let $\underline{\mathbf{q}} \triangleq \mathbf{q} + \varepsilon\mathbf{q}'$ and $\boldsymbol{\omega} \triangleq \boldsymbol{\omega} + \varepsilon\boldsymbol{\omega}'$. It is straightforward to notice that (3) embodies both equation (2) and $\dot{\mathbf{p}} = \boldsymbol{\omega}' - \boldsymbol{\omega} \times \mathbf{p}$.

III. HYBRID POSE CONTROL

The problem of robust and global pose stabilization of rigid-bodies is not simple. Firstly, there is no continuous feedback controller capable of globally asymptotically stabilizing an equilibrium point on the manifold of the unit dual quaternion group $\underline{\mathcal{S}}$ [13].

Secondly, $\underline{\mathcal{S}}$ double covers SE(3), that is, $\underline{\mathbf{q}}$ and $-\underline{\mathbf{q}}$ corresponds to the same pose in SE(3), and this leads, when a continuous dual quaternion based controller is used, to a phenomenon similar to “unwinding” in SO(3) [6]: the body may start at rest arbitrarily close to the desired final pose and yet travel to the farther stable point before coming to rest.

Lastly, even using a (memoryless) discontinuous state feedback, it is impossible to achieve robust global asymptotic stabilization of a disconnected set of points resulted from the double covering of the SE(3)[9], [10].

There are few works on unwinding avoidance in the context of pose stabilization using unit dual quaternions [12], [20], [21], [22]. All of them are based on a discontinuous feedback approach and are prone to chattering for initial conditions arbitrarily close to the discontinuity.

Inspired on the hysteresis-based hybrid control of [9] applied only to attitude control stabilization, [13] extended it to render both coupled kinematics—attitude and translation—stable.

According to [9], there is a price to pay for robust global asymptotic stabilization of attitude using the hysteretic controller—a region in the state space where the hybrid control law pulls the rigid body in the direction of a longer rotation. The pose controller suggested by [13] inherits the same behavior. We propose a hybrid control law, called bimodal, devised to reduce this price. Actually, the bimodal control halves the hysteresis width in certain situations and is a middle term solution between the hysteretic hybrid control and the discontinuous control (equivalent to the hysteretic control with zero-width hysteresis). This control may be especially useful in applications which use low-cost sensors and requires larger hysteresis width due to attitude measurement noise magnitude. For such applications, the standard deviation in attitude error may reach 10° [23].

A. Hybrid Hysteretic Controller

The hysteretic controller strategy for plant (3), suggested by [13], uses only one state variable $h \in X_c \triangleq \{-1, 1\}$ that determines the rotation direction so the system is regulated either to -1 or 1 (see Fig. 1).

The state of the system is represented by $x_1 = (\underline{q}, h) \in X_1 \triangleq \underline{\mathcal{S}} \times X_c$. The controller is given by the feedback law

$$\underline{\omega} \triangleq -k_1 h \underline{\mu} - \varepsilon k_2 \eta \underline{\mu}', \quad (5)$$

where $k_1, k_2 > 0$ are the control gains and the dynamics¹ of h is defined by

$$\begin{aligned} \dot{h} &= 0 & x_1 \in C_1 &\triangleq \{x_1 \in X_1 : h\eta \geq -\delta\}, \\ h^+ &\in \overline{\text{sgn}}(\eta) & x_1 \in D_1 &\triangleq \{x_1 \in X_1 : h\eta \leq -\delta\}, \end{aligned} \quad (6)$$

where h^+ is the value associated to h just after the state transition and

$$\overline{\text{sgn}}(\eta) = \begin{cases} \{1\}, & \eta > 0, \\ \{-1\}, & \eta < 0, \\ \{-1, 1\}, & \eta = 0. \end{cases}$$

The parameter $\delta \in (0, 1)$ represents the hysteresis half-width and provides robustness against chattering caused by noise in the output measurement. Note that, as commented in Section II-C, the primary part of (3) equals (2). As a consequence, the rotation evolves as the control suggested by [9]. When $h\eta$ gets negative, the feedback determines that the body rotates in the longer rotation direction until a safe distance is achieved to prevent chattering, i.e., until $h\eta \leq -\delta$.

The closed-loop hybrid system, denoted as $\overline{\mathcal{H}}_1$, is formed of equations (3), (5) and (6).

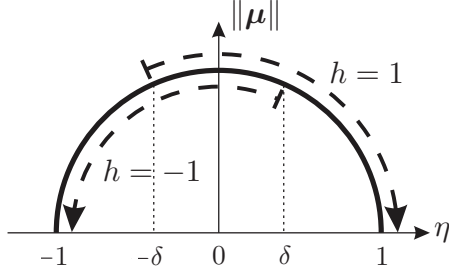


Fig. 1. State space representation of the hysteretic controller (with one state variable h). Arrows indicate the direction of the rotation so the attitude is regulated to 1 or -1 .

B. Hybrid Bimodal Controller

The proposed bimodal controller strategy uses two state variables $(h, m) \in X_c \times X_c$ as shown in Fig. 2. The state h determines the rotation direction as in the hysteretic controller. The state m is introduced in order to adapt the hysteresis width $\delta_a \in \{\delta/2, \delta\}$ of the on-off control for state h in such a way that the width gets shorter whenever the attitude is relatively far from the chattering prone region ($\eta = 0$).

¹Along the text, the dynamics representations follows the hybrid systems framework of [24].

Let the state of the system be represented by $x_2 = (\underline{q}, h, m) \in X_2 \triangleq \underline{\mathcal{S}} \times X_c \times X_c$. The bimodal controller is given by the feedback law (5) and the dynamics of h and m are defined by

$$\begin{aligned} \dot{h} &= 0 \\ \dot{m} &= 0 \end{aligned} \left. \vphantom{\begin{aligned} \dot{h} \\ \dot{m} \end{aligned}} \right\} x_2 \in C_2, \quad (7)$$

$$\left. \begin{aligned} h^+ &\in \overline{\text{sgn}}(\eta - h\delta/2) \\ m^+ &\in h \overline{\text{sgn}}(\eta - h\delta/2) \end{aligned} \right\} x_2 \in D_2,$$

$$\begin{aligned} C_2 &\triangleq \{x_2 \in X_2 : (h\eta \geq -\delta) \text{ and} \\ &(m = -1 \text{ or } h\eta \geq -\delta/2) \text{ and } (m = 1 \text{ or } h\eta \leq 3\delta/2)\}, \\ D_2 &\triangleq \{x_2 \in X_2 : (h\eta \leq -\delta) \text{ or} \\ &(m = 1 \text{ and } h\eta \leq -\delta/2) \text{ or } (m = -1 \text{ and } h\eta \geq 3\delta/2)\}, \end{aligned}$$

where m^+ and h^+ are values associated to m and h , respectively, just after state transition. Note that $C_2 = X_2 \setminus D_2$.

The closed-loop hybrid system, denoted as $\overline{\mathcal{H}}_2$, is formed of equations (3), (5) and (7).

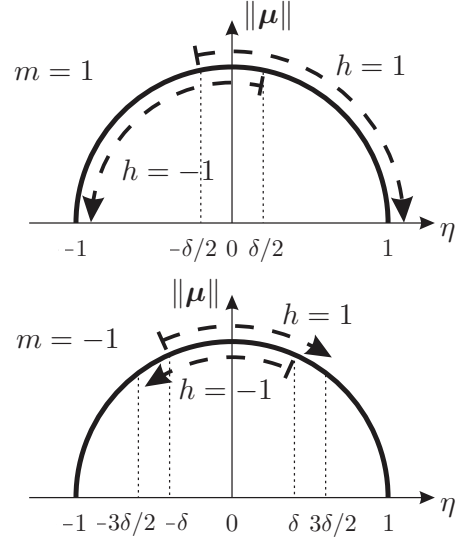


Fig. 2. State space representation of the bimodal controller (with two state variables, h and m). Arrows indicate the direction of the rotation so the attitude is regulated to 1 or -1 .

IV. STABILITY ANALYSIS

In this section, we prove that the proposed hybrid bimodal control globally asymptotically stabilizes the pose of a rigid body even in the presence of measurement noise.

Theorem 4.1: Let $\delta \in (0, 1)$ and $k_1, k_2 > 0$. The compact set A_2 defined below (8), is globally asymptotically stable for the closed-loop hybrid system $\overline{\mathcal{H}}_2$.

$$A_2 = \{x_2 \in X_2 : \underline{q} = h\underline{1}, m = 1\}. \quad (8)$$

Proof: For easy presentation, let us first consider $\delta \in (0, 2/3]$. Let $\underline{q} \triangleq \eta + \underline{\mu} + \varepsilon(\eta' + \underline{\mu}')$ and $V : X_2 \rightarrow \mathbb{R}$,

$$V(x_2) = 2(1 - h\eta) + \|\underline{p}\|^2/4. \quad (9)$$

As $m = 1$ whenever $\underline{q} = \pm\underline{1}$ and as $\underline{p} = \mathbf{0}$ if and only if $\eta' = 0$ and $\underline{\mu}' = \mathbf{0}$, we have that $V(x_2) > 0$ for $x_2 \in$

$X_2 \setminus A_2$ and $V(x_2) = 0$ for $x_2 \in A_2$. Hence function V is positive definite on X_2 with respect to A_2 .

The time derivative \dot{V} of V is given by

$$\dot{V}(x_2) = -2h\dot{\eta} + \mathbf{p} \cdot \dot{\mathbf{p}}/2 \quad (10)$$

$$= -h^2 k_1 \|\boldsymbol{\mu}\|^2 - k_2 \eta \mathbf{p} \cdot \boldsymbol{\mu}'/2 \quad (11)$$

$$= -k_1 \|\boldsymbol{\mu}\|^2 - k_2 \eta (\mathbf{q}^* \mathbf{q}') \cdot \boldsymbol{\mu}' \quad (12)$$

$$= -k_1 \|\boldsymbol{\mu}\|^2 - k_2 \eta^2 (\eta'^2 + \|\boldsymbol{\mu}'\|^2) \quad (13)$$

So, \dot{V}_2 is negative definite on X_2 with respect to A_2 . Besides, observing that the time derivative of $\|\mathbf{p}\|^2$ is lower than or equal to zero, we can conclude that the distance of the body along time always decreases, except when $\eta = 0$.

Along jumps, when $x_2 \in D_2$, since $\underline{\mathbf{q}}^+ = \underline{\mathbf{q}}$,

$$\Delta V(x_2) = V(x_2^+) - V(x_2) = -2\eta(h^+ - h).$$

Let $D_2 = D_{2a} \cup D_{2b} \cup D_{2c}$, where

$$D_{2a} \triangleq \{x_2 \in X_2 : h\eta \leq -\delta\}, \quad (14)$$

$$D_{2b} \triangleq \{x_2 \in X_2 : m = 1 \text{ and } h\eta \leq -\delta/2\}, \quad (15)$$

$$D_{2c} \triangleq \{x_2 \in X_2 : m = -1 \text{ and } h\eta \geq 3\delta/2\}. \quad (16)$$

Thus,

$$\Delta V(x_2) = \begin{cases} \leq -4\delta_a, & x_2 \in D_{2a} \cup D_{2b}, \\ 0, & x_2 \in D_{2c}, \end{cases}$$

where $\delta_a = \delta$ for $x_2 \in D_{2a} \setminus D_{2b}$ and $\delta_a = \delta/2$ for $x_2 \in D_{2b}$.

From Theorem 7.6 of [25], it follows that the compact set A_2 is stable since $\Delta V(x_2) \leq 0$ and $\dot{V}(x_2) < 0$ for all $x_2 \in X_2$.

To conclude that the set A_2 is globally asymptotically stable, it is necessary to apply Theorem 4.7 of [25] to prove that the set A_2 is the largest invariant set in $W = W_1 \cup W_2$, where $W_1 \triangleq \{x_2 \in C_2 : \dot{V}(x_2) = 0\}$ and $W_2 \triangleq \Delta V^{-1}(0) \cap G_2(\Delta V^{-1}(0))$, $G_2(x_2) \triangleq x_2^+$. It follows that $W_1 = A_2$, $\Delta V^{-1}(0) = D_{2c}$ and $G_2(\Delta V^{-1}(0)) = \{x_2 \in X_2 : m = 1 \text{ and } h\eta \geq 3\delta/2\}$. Thus, $W_2 = \emptyset$, $W = A_2$ and any solution $x_2(t)$ approaches the largest invariant set A_2 .

This controller restricts parameter δ to $(0, 2/3]$. For the case $\delta \in (2/3, 1)$, the system still behaves as proposed until the first jump. Afterward, it will behave as the hysteretic controller, since m will remain fixed thereafter. ■

Following we will show that the analysis of either the presence of Zeno solutions (infinite number of jumps in a finite amount of time) or chattering are only related to the rotation.

The rotation evolution follows the primary part of (3). As pointed out in Section II-C, it follows the same kinematic equation for quaternions (2). Substituting (5) into (2),

$$\begin{aligned} \dot{\mathbf{q}} &= \frac{1}{2}(\eta + \boldsymbol{\mu})(-k_1 h \boldsymbol{\mu}) \\ &= \frac{1}{2}(k_1 h \|\boldsymbol{\mu}\|^2 - k_1 h \eta \boldsymbol{\mu}). \end{aligned}$$

Note that $\dot{\mathbf{q}}$ depends only on \mathbf{q} and the dynamics of h . On the other hand, the dynamics of h and m depend only on

the body rotation (η). Hence, we conclude not only that the rotation is independent of the translation but also that jumps on state variables h and m depend only on the rotation evolution.

The proof that no Zeno solutions occur even when ‘‘outer perturbations’’—that includes both measurement and modeling errors [26], [9] are taken into account—is similar to the proofs of Theorem 5.3 and Theorem 5.4 of [9] and will not be proved here.

A. Chattering Analysis

Due to noise present in measurements, chattering is possible to occur when jumps map the state back into the jump set, i.e., when $G_2(D_2) \cap D_2 \neq \emptyset$, $G_2(x_2) = x_2^+$. As the number of discrete states is higher than one, h and m , the immediate consecutive jumps must also be analyzed to make sure the following states are mapped to the jump set again. Considering that the output \mathbf{q} is corrupted by noise of maximum magnitude α , the verification should be concentrated on intersections $G_2^\alpha(D_2^\alpha) \cap D_2^\alpha$, $G_2^\alpha(G_2^\alpha(D_2^\alpha) \cap D_2^\alpha) \cap D_2^\alpha$, and so on until a loop or an empty set is achieved, where G_2^α and D_2^α are the sets G_2 and D_2 , respectively, expanded to accommodate noise of maximum magnitude α as exemplified in [26, Example 5.3].

Theorem 4.2: Let $\alpha > 0$, $\delta > 2\alpha$, $\delta \in (0, 1)$. Then, either $G_2^\alpha(D_2^\alpha) \cap D_2^\alpha = \emptyset$, or $G_2^\alpha(G_2^\alpha(D_2^\alpha) \cap D_2^\alpha) \cap D_2^\alpha = \emptyset$ for system $\overline{\mathcal{H}}_2$.

This proof is not presented here due to space restrictions. The theorem affirms that after two jumps, at most, the state is mapped outside the jump set and no loop (chattering) occurs.

V. NUMERICAL SIMULATIONS

This section presents simulation² results to compare performance among the discontinuous controller, the hysteretic controller, and the proposed bimodal controller. To this aim, two different scenarios considering an initial pose defined in a region near 180° away from the desired attitude have been depicted whereby the different behavior is expected.

To maintain fairness, all simulated controllers have been implemented with the same control gains $k_1 = 1$ and $k_2 = 1$. The initial state of the hysteretic controller has been set to $h(0) = 1$ and the ones of the bimodal controller were set to $h(0) = 1$, $m(0) = 1$. The hysteresis parameter defined both for the hysteretic and bimodal controllers was set to $\delta = 0.4$. Please note that by setting the hysteresis parameter to $\delta = 0$ yields a discontinuous control law.

Moreover, to illustrate the robustness of the proposed controller and the performance of all three controllers, additional measured noise have been included to the value of \mathbf{q} (\mathbf{q}_m) and was calculated as follows: $\mathbf{q}_m = (\mathbf{q} + b\hat{\mathbf{e}}) / \|\mathbf{q} + b\hat{\mathbf{e}}\|$, $\hat{\mathbf{e}} = \mathbf{e} / \|\mathbf{e}\|$, where each component of $\mathbf{e} \in \mathbb{R}^4$ was chosen from a Gaussian distribution of zero mean and unitary standard deviation and $b \in \mathbb{R}$ was chosen from a uniform distribution on the interval $[0, 0.2]$.

²All simulations have been performed in MATLAB ambient, using ordinary differential equation solver with variable integration step (ode45) restricted to a maximum step of 1 ms.

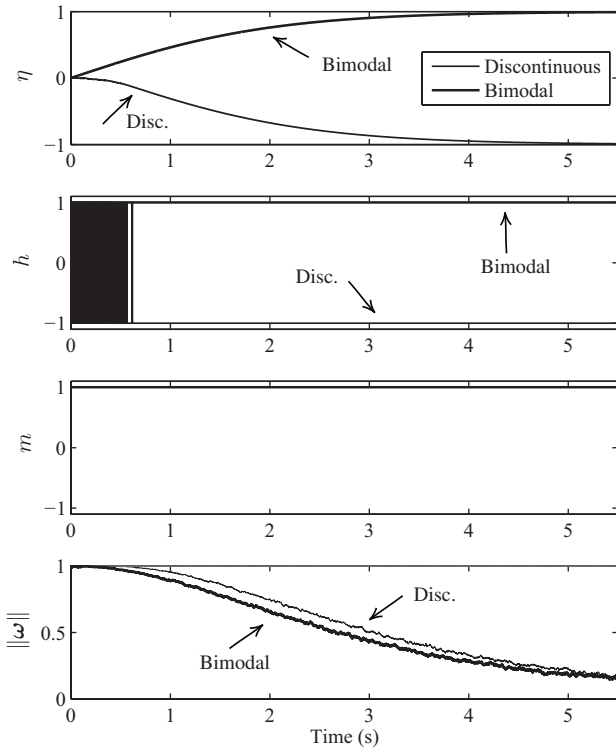


Fig. 3. Rotation comparison between the discontinuous and bimodal controllers.

In the first scenario, the performance of the proposed bimodal controller is investigated against perturbations on the measurement signal and compared to the discontinuous controller. The initial pose in this case was set to $\mathbf{q}(0) = 0 + (1\hat{i} + 2\hat{j} + 3\hat{k})/\sqrt{14}$ and $\mathbf{p}(0) = -0.24\hat{i} + 1.76\hat{j} + 6.2\hat{k}$. Figs. 3 and 4 illustrate the results from both controllers. Clearly, the chattering phenomenon occurs solely when using the discontinuous control law whereby the resulting controller takes more than 0.5 s to set the final equilibrium point (in this case to -1)—in other words, it takes a considerable amount of time to travel away from its discontinuity at $\eta = 0$. The translation \mathbf{p} was also affected. During the period of chattering, the system got stuck around the initial conditions resulting in a convergence lag. The proposed bimodal controller, on the other hand, presents a robust response as expected for both rotation and translation convergence.

The last scenario compares the state evolution between the hysteretic and the bimodal controller. To investigate the liability of the controllers to being pulled to the direction of longer rotation, the initial conditions were $\mathbf{q}(0) = -0.2 + \sqrt{1 - 0.2^2}(1\hat{i} + 2\hat{j} + 3\hat{k})/\sqrt{14}$ and $\mathbf{p}(0) = -0.24\hat{i} + 1.76\hat{j} + 6.2\hat{k}$. The consequence of such initial conditions is that it belongs to the hysteresis region from the hysteretic controller and therefore the result from such controller travels to the further antipodal equilibrium. As shown in Figs. 5 and 6, the hysteretic and bimodal controllers made the rigid body take a different direction of rotation from the beginning. Regarding the energy spent, if we take the area below the graph of the angular velocity norm, $\|\omega\|$, it is possible to affirm that the

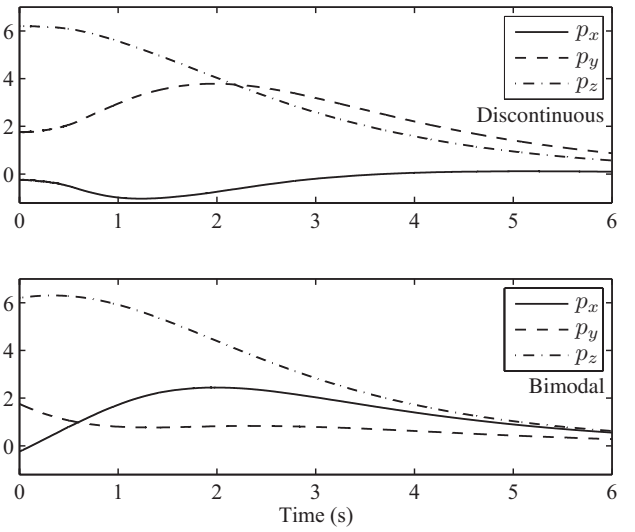


Fig. 4. Evolution of the translation components of $\mathbf{p} = p_x\hat{i} + p_y\hat{j} + p_z\hat{k}$ for the discontinuous and bimodal controllers.

bimodal controller spent less energy.

VI. CONCLUSIONS

This work presented a novel control strategy for robust global rigid body kinematic stabilization using a dual quaternion framework. To address the topological obstruction to global stability inherent to any rigid body representation—which renders the unwinding phenomenon in the case of unit quaternions and unit dual quaternions—this paper exploited an hybrid control technique based on hysteresis, which ensures solution without chattering, in addition to introducing a novel state memory variable that reduces the liability of having the solution trajectory travel to the farther antipodal equilibrium.

REFERENCES

- [1] R. W. Brockett, "System theory on group manifolds and coset spaces," *SIAM J. Control*, vol. 10, no. 2, pp. 265–284, 1972.
- [2] F. Bullo and R. M. Murray, "Proportional derivative (PD) control on the Euclidean group," California Institute of Technology, Technical Report Caltech/CDS 95–010, May 1995.
- [3] F. Bullo, R. M. Murray, and A. Sarti, "Control on the sphere and reduced attitude stabilization," California Institute of Technology, Technical Report Caltech/CDS 95–005, Jan. 1995.
- [4] J. Funda, R. H. Taylor, and R. P. Paul, "On homogeneous transforms, quaternions, and computational efficiency," *IEEE Trans. Robot. Automat.*, vol. 6, no. 3, pp. 382–388, 1990.
- [5] J. M. Selig, *Geometric Fundamentals of Robotics*, 2nd ed., ser. Monographs in Computer Science. Springer, 2007.
- [6] S. P. Bhat and D. S. Bernstein, "A topological obstruction to continuous global stabilization of rotational motion and the unwinding phenomenon," *Syst. Control Lett.*, vol. 39, no. 1, pp. 63–70, 2000.
- [7] D. Fragopoulos and M. Innocenti, "Stability considerations in quaternion attitude control using discontinuous Lyapunov functions," *IEE Proc.-Control Theory Appl.*, vol. 151, no. 3, pp. 253–258, 2004.
- [8] R. Kristiansen, P. J. Nicklasson, and J. T. Gravdahl, "Satellite attitude control by quaternion-based backstepping," *IEEE Trans. Contr. Syst. Technol.*, vol. 17, no. 1, pp. 227–232, 2009.
- [9] C. Mayhew, R. Sanfelice, and A. Teel, "Quaternion-based hybrid control for robust global attitude tracking," *IEEE Trans. Autom. Control*, vol. 56, no. 11, pp. 2555–2566, Nov. 2011.

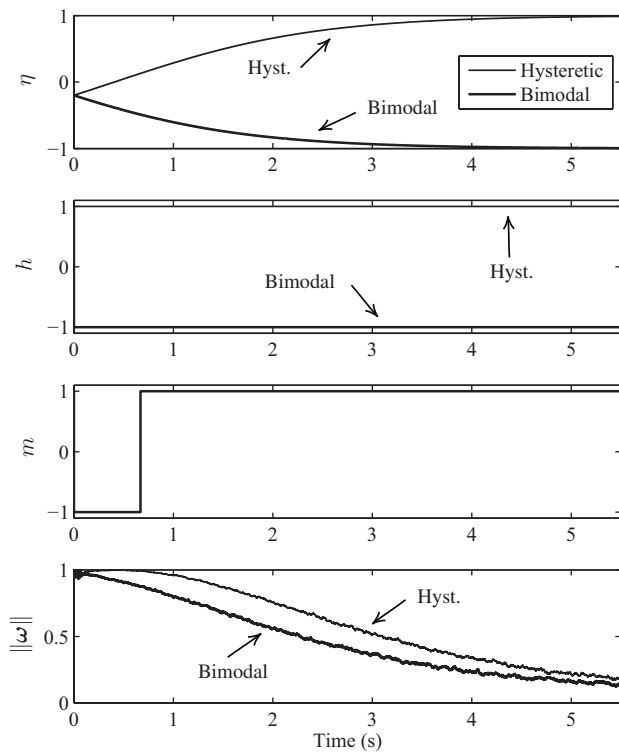


Fig. 5. Rotation comparison between the hysteretic and bimodal controllers.

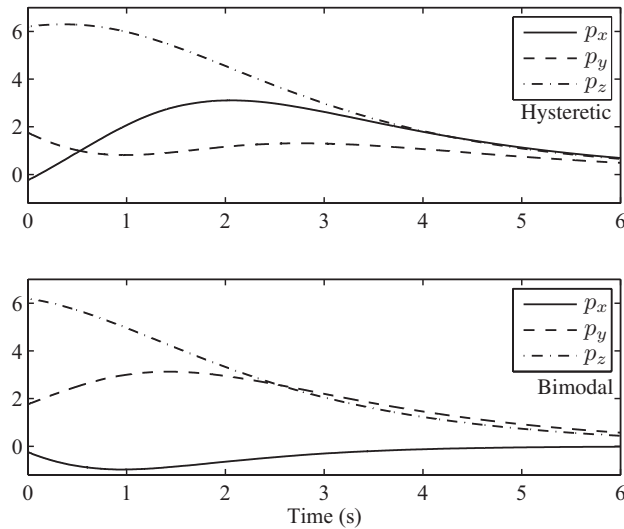


Fig. 6. Evolution of the translation components of $\mathbf{p} = p_x \hat{i} + p_y \hat{j} + p_z \hat{k}$ for the hysteretic and bimodal controllers.

- [10] R. Sanfelice, M. Messina, S. Emre Tuna, and A. Teel, "Robust hybrid controllers for continuous-time systems with applications to obstacle avoidance and regulation to disconnected set of points," in *Amer. Control Conf.*, 2006, pp. 3352–3357.
- [11] A. Fu, E. Modiano, and J. Tsitsiklis, "Optimal energy allocation and admission control for communications satellites," *IEEE/ACM Trans. Netw.*, vol. 11, no. 3, pp. 488–500, Jun. 2003.
- [12] D.-P. Han, Q. Wei, and Z.-X. Li, "Kinematic control of free rigid bodies using dual quaternions," *Int. J. Autom. Comput.*, vol. 5, no. 3, pp. 319–324, 2008.
- [13] H. T. M. Kussaba, L. F. C. Figueredo, J. Y. Ishihara, and B. V. Adorno, "Hybrid kinematic control for rigid body pose stabilization using dual quaternions," *J. Franklin Inst.*, 2017, to be published.
- [14] W. R. Hamilton, "On quaternions, or on a new system of imaginaries in algebra: Copy of a letter from Sir William R. Hamilton to John T. Graves, esq. on quaternions," *Philos. Mag.*, vol. 25, no. 3, pp. 489–495, 1844.
- [15] W. K. Clifford, "A preliminary sketch of biquaternions," in *Proc. London Math. Soc.*, 1871, pp. 381–395.
- [16] E. Study, "Von den bewegungen und umlegungen," *Mathematische Annalen*, vol. 39, no. 4, pp. 441–565, 1891.
- [17] X. Wang, D. Han, C. Yu, and Z. Zheng, "The geometric structure of unit dual quaternion with application in kinematic control," *J. Math. Anal. Appl.*, vol. 389, no. 2, pp. 1352–1364, 2012.
- [18] Y. Wu, X. Hu, D. Hu, T. Li, and J. Lian, "Strapdown inertial navigation system algorithms based on dual quaternions," *IEEE Trans. Aerosp. Electron. Syst.*, vol. 41, no. 1, pp. 110–132, 2005.
- [19] J. Solà, "Quaternion kinematics for the error-state kf," p. 73, 2016. [Online]. Available: <https://hal.archives-ouvertes.fr/hal-01122406v4/document>
- [20] D. Han, Q. Wei, and Z. Li, "A dual-quaternion method for control of spatial rigid body," in *Proc. 2008 IEEE Int. Conf. Networking, Sensing and Control*, 2008, pp. 1–6.
- [21] D. Han, Q. Wei, Z. Li, and W. Sun, "Control of oriented mechanical systems: A method based on dual quaternion," in *Proc. 17th IFAC World Congr.*, 2008, pp. 3836–3841.
- [22] X. Wang and C. Yu, "Unit dual quaternion-based feedback linearization tracking problem for attitude and position dynamics," *Syst. Contr. Letts.*, vol. 62, no. 3, pp. 225–233, 2013.
- [23] D. Gebre-Egziabher, G. H. Elkaim, J. D. Powell, and B. W. Parkinson, "A gyro-free quaternion-based attitude determination system suitable for implementation using low cost sensors," in *Position Location and Navigation Symposium, IEEE 2000*, 2000, pp. 185–192.
- [24] R. Goebel, R. Sanfelice, and A. Teel, "Hybrid dynamical systems," *IEEE Control Syst. Mag.*, vol. 29, no. 2, pp. 28–93, Apr. 2009.
- [25] R. Sanfelice, R. Goebel, and A. Teel, "Invariance principles for hybrid systems with connections to detectability and asymptotic stability," *IEEE Trans. Autom. Control*, vol. 52, no. 12, pp. 2282–2297, Dec. 2007.
- [26] R. Goebel and A. Teel, "Solutions to hybrid inclusions via set and graphical convergence with stability theory applications," *Automatica*, vol. 42, no. 4, pp. 573–587, 2006.

Bibliography

- [1] P. P. M. Magro, “Bimodal hybrid control of rigid-body attitude based on unit quaternions,” Ph.D. dissertation, 2017, available at <http://repositorio.unb.br/handle/10482/31311>.
- [2] X. Wang and C. Yu, “Unit dual quaternion-based feedback linearization tracking problem for attitude and position dynamics,” *Systems & Control Letters*, vol. 62, no. 3, pp. 225–233, 2013.
- [3] R. W. Brockett, “System theory on group manifolds and coset spaces,” *SIAM Journal on Control*, vol. 10, no. 2, pp. 265–284, 1972.
- [4] F. Bullo and R. M. Murray, “Proportional derivative (PD) control on the Euclidean group,” California Institute of Technology, Technical Report Caltech/CDS 95–010, May 1995.
- [5] J. M. Selig, “Lie groups and Lie algebras in robotics,” in *Computational Noncommutative Algebra and Applications*. Springer, 2004, pp. 101–125.
- [6] ———, *Geometric Fundamentals of Robotics*, 2nd ed., ser. Monographs in Computer Science. Springer, 2007.
- [7] Y. L. Sachkov, “Control theory on Lie groups,” *Journal of Mathematical Sciences*, vol. 156, no. 3, pp. 381–439, 2009.
- [8] M. Koldychev and C. Nielsen, “Local observers on linear Lie groups with linear estimation error dynamics,” *IEEE Transactions on Automatic Control*, vol. 59, no. 10, pp. 2772–2777, 2014.
- [9] N. A. Chaturvedi, A. K. Sanyal, and H. N. McClamroch, “Rigid-body attitude control: using rotation matrices for continuous, singularity-free control laws,” *IEEE Contr. Syst. Mag*, vol. 31, no. 3, pp. 30–51, 2011.
- [10] S. Li, S. Ding, and Q. Li, “Global set stabilization of the spacecraft attitude control problem based on quaternion,” *International Journal of Robust and Nonlinear Control*, vol. 20, no. 1, pp. 84–105, 2010.
- [11] F. A. Goodarzi, D. Lee, and T. Lee, “Geometric adaptive tracking control of a quadrotor unmanned aerial vehicle on se (3) for agile maneuvers,” *Journal of Dynamic Systems, Measurement, and Control*, vol. 137, no. 9, p. 091007, 2015.
- [12] X. Wang, D. Han, C. Yu, and Z. Zheng, “The geometric structure of unit dual quaternion with application in kinematic control,” *Journal of Mathematical Analysis and Applications*, vol. 389, no. 2, pp. 1352–1364, 2012.
- [13] I. Yaglom, *Complex numbers in geometry*. Academic Press, 1968.
- [14] N. A. Chaturvedi, A. K. Sanyal, and H. N. McClamroch, “Rigid-body attitude control: using rotation matrices for continuous, singularity-free control laws,” *IEEE Control Systems Magazine*, vol. 31, no. 3, pp. 30–51, 2011.
- [15] J. Stueelpnagel, “On the parametrization of the three-dimensional rotation group,” *SIAM Review*, vol. 6, no. 4, pp. 422–430, 1964.

- [16] H. Hopf, "Systeme symmetrischer Bilinearformen und euklidische Modelle der projektiven Räume," in *Selecta Heinz Hopf*. Springer Berlin Heidelberg, 1964, pp. 107–118.
- [17] H. T. Kussaba, L. F. Figueredo, J. Y. Ishihara, and B. V. Adorno, "Hybrid Kinematic Control for Rigid Body Pose Stabilization using Dual Quaternions," *Journal of the Franklin Institute*, vol. 354, no. 7, pp. 2769–2787, 2017.
- [18] N. A. Aspragathos and J. K. Dimitros, "A Comparative Study of Three Methods for Robot Kinematics," *IEEE Transactions on Systems, Man, and Cybernetics, Part B: Cybernetics*, vol. 28, no. 2, pp. 135–145, jan 1998.
- [19] S. Berkane and A. Tayebi, "On the design of synergistic potential functions on $SO(3)$," in *Proceedings of the 54th IEEE Conference on Decision and Control*, 2015, pp. 270–275.
- [20] —, "Construction of synergistic potential functions on $SO(3)$ with application to velocity-free hybrid attitude stabilization," *IEEE Transactions on Automatic Control*, vol. 62, no. 1, pp. 495–501, 2017.
- [21] J. Funda, R. Taylor, and R. Paul, "On homogeneous transforms, quaternions, and computational efficiency," *IEEE Transactions on Robotics and Automation*, vol. 6, no. 3, pp. 382–388, jun 1990.
- [22] X. Wang and H. Zhu, "On the comparisons of unit dual quaternion and homogeneous transformation matrix," *Advances in Applied Clifford Algebras*, vol. 24, no. 1, pp. 213–229, 2014.
- [23] B. V. Adorno, "Two-arm manipulation: From manipulators to enhanced human-robot collaboration," Ph.D. dissertation, Laboratoire d'Informatique, de Robotique et de Microélectronique de Montpellier (LIRMM) - Université Montpellier 2, Montpellier, France, 2011.
- [24] A.-N. Sharkawy and N. Aspragathos, "A comparative study of two methods for forward kinematics and Jacobian matrix determination," in *2017 International Conference on Mechanical, System and Control Engineering (ICMSC)*, 2017.
- [25] F. Lizarralde and J. T. Wen, "Attitude control without angular velocity measurement: A passivity approach," *IEEE Transactions on Automatic Control*, vol. 41, no. 3, pp. 468–472, 1996.
- [26] N. Filipe and P. Tsiotras, "Simultaneous position and attitude control without linear and angular velocity feedback using dual quaternions," in *Proceedings of the 2013 American Control Conference*, 2013, pp. 4808–4813.
- [27] S. P. Bhat and D. S. Bernstein, "A topological obstruction to continuous global stabilization of rotational motion and the unwinding phenomenon," *Systems & Control Letters*, vol. 39, no. 1, pp. 63–70, 2000.
- [28] C. G. Mayhew, R. G. Sanfelice, and A. R. Teel, "Quaternion-based hybrid control for robust global attitude tracking," *IEEE Transactions on Automatic Control*, vol. 56, no. 11, pp. 2555–2566, 2011.
- [29] R. G. Sanfelice, M. J. Messina, S. Emre Tuna, and A. R. Teel, "Robust hybrid controllers for continuous-time systems with applications to obstacle avoidance and regulation to disconnected set of points," in *Proceedings of the 2006 American Control Conference*, 2006, pp. 3352–3357.
- [30] R. G. Sanfelice, "Robust hybrid control systems," Ph.D. dissertation, Electrical and Computer Engineering, 2007, <https://hybrid.soe.ucsc.edu/files/preprints/20.pdf>.
- [31] C. G. Mayhew and A. R. Teel, "Synergistic hybrid feedback for global rigid-body attitude tracking on $SO(3)$," *IEEE Transactions on Automatic Control*, vol. 58, no. 11, pp. 2730–2742, 2013.

- [32] P. P. M. Magro, J. Y. Ishihara, and H. C. Ferreira, “Robust global bimodal rest-to-rest attitude control of rigid body using unit quaternion,” *Journal of the Franklin Institute*, vol. 354, no. 7, pp. 2769–2787, 2017.
- [33] J. P. Hespanha and A. S. Morse, “Stabilization of nonholonomic integrators via logic-based switching,” *Automatica*, vol. 35, no. 3, pp. 385–393, 1999.
- [34] C. Prieur and A. Astolfi, “Robust stabilization of chained systems via hybrid control,” *IEEE Transactions on Automatic Control*, vol. 48, no. 10, pp. 1768–1772, 2003.
- [35] D.-P. Han, Q. Wei, and Z.-X. Li, “Kinematic control of free rigid bodies using dual quaternions,” *International Journal of Automation and Computing*, vol. 5, no. 3, pp. 319–324, 2008.
- [36] D. Han, Q. Wei, and Z. Li, “A dual-quaternion method for control of spatial rigid body,” in *Proceedings of the 2008 IEEE International Conference on Networking, Sensing and Control*, 2008, pp. 1–6.
- [37] C. G. Mayhew, R. G. Sanfelice, and A. R. Teel, “On path-lifting mechanisms and unwinding in quaternion-based attitude control,” *IEEE Transactions on Automatic Control*, vol. 58, no. 5, pp. 1179–1191, 2013.
- [38] P. P. M. Magro, H. T. M. Kussaba, L. F. Figueredo, and J. Y. Ishihara, “Dual quaternion-based bimodal global control for robust rigid body pose kinematic stabilization,” in *Proceedings of 2017 American Control Conference*, Seattle, USA, 2017, pp. 1205–1210.
- [39] D. Han, Q. Wei, Z. Li, and W. Sun, “Control of oriented mechanical systems: A method based on dual quaternion,” in *Proceedings of the 17th IFAC World Congress*, 2008, pp. 3836–3841.
- [40] J. Wang, H. Liang, Z. Sun, S. Zhang, and M. Liu, “Finite-time control for spacecraft formation with dual-number-based description,” *Journal of Guidance, Control, and Dynamics*, vol. 35, no. 3, pp. 950–962, 2012.
- [41] N. Filipe and P. Tsiotras, “Adaptive position and attitude-tracking controller for satellite proximity operations using dual quaternions,” *Journal of Guidance, Control, and Dynamics*, vol. 38, no. 4, pp. 566–577, 2014.
- [42] H. Gui and G. Vukovich, “Finite-time output-feedback position and attitude tracking of a rigid body,” *Automatica*, vol. 74, pp. 270–278, 2016.
- [43] —, “Dual-quaternion-based adaptive motion tracking of spacecraft with reduced control effort,” *Non-linear Dynamics*, vol. 83, no. 1-2, pp. 597–614, 2016.
- [44] D. P. Chevallier, “On the transference principle in kinematics: its various forms and limitations,” *Mechanism and Machine Theory*, vol. 31, no. 1, pp. 57–76, 1996.
- [45] F. Bullo, R. M. Murray, and A. Sarti, “Control on the sphere and reduced attitude stabilization,” California Institute of Technology, Technical Report Caltech/CDS 95–005, Jan. 1995.
- [46] H. T. M. Kussaba, R. A. Borges, and J. Y. Ishihara, “A new condition for finite time boundedness analysis,” *Journal of the Franklin Institute*, vol. 352, no. 12, pp. 5514–5528, dec 2015.
- [47] H. T. M. Kussaba, J. Y. Ishihara, and R. A. Borges, “Uniform versions of Finsler’s lemma,” in *Proceedings of the 54th IEEE Conference on Decision and Control*. IEEE, dec 2015, pp. 7292–7297.

- [48] —, “Finite time boundedness and stability analysis of discrete time uncertain systems,” in *Proceedings of the 54th IEEE Conference on Decision and Control*. IEEE, dec 2015, pp. 5972–5977.
- [49] H. T. M. Kussaba, R. A. Borges, and J. Y. Ishihara, “Parameter-Dependent Filter with Finite Time Boundedness Property for Continuous-Time LPV Systems,” in *Proceedings of XVII Latin American Conference on Automatic Control*, Medellín, Colombia, 2016, pp. 189–194.
- [50] J. Y. Ishihara, H. T. M. Kussaba, and R. A. Borges, “Existence of continuous or constant Finsler’s variables for parameter-dependent systems,” *IEEE Transactions on Automatic Control*, vol. 62, no. 8, pp. 4187–4193, aug 2017.
- [51] G. V. Smirnov, *Introduction to the theory of differential inclusions*. American Mathematical Soc., 2002, vol. 41.
- [52] J.-P. Aubin and A. Cellina, *Differential inclusions: set-valued maps and viability theory*. Springer Science & Business Media, 2012, vol. 264.
- [53] A. F. Filippov, *Differential equations with discontinuous righthand sides: control systems*. Springer Science & Business Media, 2013, vol. 18.
- [54] M. Marques, *Differential inclusions in nonsmooth mechanical problems: Shocks and dry friction*. Birkhäuser, 2013, vol. 9.
- [55] R. T. Rockafellar and R. J.-B. Wets, *Variational analysis*, 2nd ed. Springer, 2004.
- [56] R. Goebel, R. G. Sanfelice, and A. R. Teel, *Hybrid Dynamical Systems: modeling, stability, and robustness*. Princeton University Press, 2012.
- [57] H. H. Sohrab, *Basic real analysis*. Springer, 2003, vol. 231.
- [58] J.-P. Aubin and H. Frankowska, *Set-valued analysis*. Springer Science & Business Media, 2009.
- [59] J. Cortes, “Discontinuous dynamical systems,” *IEEE control Systems*, vol. 28, no. 3, 2008.
- [60] R. Goebel, R. G. Sanfelice, and A. R. Teel, “Hybrid dynamical systems,” *IEEE Control Systems*, vol. 29, no. 2, pp. 28–93, 2009.
- [61] C. Cai, A. R. Teel, and R. Goebel, “Smooth Lyapunov functions for hybrid systems part II:(pre) asymptotically stable compact sets,” *IEEE Transactions on Automatic Control*, vol. 53, no. 3, pp. 734–748, 2008.
- [62] L. Tavernini, “Differential automata and their discrete simulators,” *Nonlinear Analysis: Theory, Methods & Applications*, vol. 11, no. 6, pp. 665–683, 1987.
- [63] J. Lygeros, K. H. Johansson, S. N. Simic, J. Zhang, and S. S. Sastry, “Dynamical properties of hybrid automata,” *IEEE Transactions on Automatic Control*, vol. 48, no. 1, pp. 2–17, 2003.
- [64] D. Liberzon and A. S. Morse, “Basic problems in stability and design of switched systems,” *IEEE Control systems*, vol. 19, no. 5, pp. 59–70, 1999.
- [65] D. Liberzon, *Switching in systems and control*. Springer Science & Business Media, 2012.
- [66] S. Lall and G. Dullerud, “An LMI solution to the robust synthesis problem for multi-rate sampled-data systems,” *Automatica*, vol. 37, no. 12, pp. 1909–1922, 2001.

- [67] G. C. Walsh, H. Ye, and L. G. Bushnell, “Stability analysis of networked control systems,” vol. 10, no. 3, pp. 438–446, 2002.
- [68] A. J. Van Der Schaft and J. M. Schumacher, *An introduction to hybrid dynamical systems*. Springer London, 2000, vol. 251.
- [69] W. M. Haddad and V. Chellaboina, *Nonlinear dynamical systems and control: a Lyapunov-based approach*. Princeton University Press, 2008.
- [70] C. M. Kellett, “A compendium of comparison function results,” *Mathematics of Control, Signals, and Systems*, vol. 26, no. 3, pp. 339–374, 2014.
- [71] R. Goebel and A. R. Teel, “Solutions to hybrid inclusions via set and graphical convergence with stability theory applications,” *Automatica*, vol. 42, no. 4, pp. 573–587, 2006.
- [72] W. R. Hamilton, “On quaternions, or on a new system of imaginaries in algebra: Copy of a letter from Sir William R. Hamilton to John T. Graves, esq. on quaternions,” *Philosophical Magazine*, vol. 25, no. 3, pp. 489–495, 1844.
- [73] F. L. Markley, “Attitude Error Representations for Kalman Filtering,” in *Proc. of AAS/AIAA Astrodynamics Specialist Conference*, 2001, p. 15.
- [74] J. C. K. Chou, “Quaternion kinematic and dynamic differential equations,” *IEEE Transactions on Robotics and Automation*, vol. 8, no. 1, pp. 53–64, 1992.
- [75] G. Rudolph and M. Schmidt, *Differential geometry and mathematical physics: Part I. Manifolds, Lie Groups and Hamiltonian Systems*. Springer, 2012.
- [76] W. K. Clifford, “A preliminary sketch of biquaternions,” *Proceedings of the London Mathematical Society*, vol. iv, no. 64/65, pp. 381–395, 1873.
- [77] E. Study, “Von den bewegungen und umlegungen,” *Mathematische Annalen*, vol. 39, no. 4, pp. 441–565, 1891.
- [78] Y. Wu, X. Hu, D. Hu, T. Li, and J. Lian, “Strapdown inertial navigation system algorithms based on dual quaternions,” *IEEE Transactions on Aerospace and Electronic Systems*, vol. 41, no. 1, pp. 110–132, 2005.
- [79] K. Daniilidis, “Hand-Eye Calibration Using Dual Quaternions,” *The International Journal of Robotics Research*, vol. 18, no. 3, pp. 286–298, feb 2010.
- [80] R. M. Murray and S. S. Sastry, *A mathematical introduction to robotic manipulation*. CRC press, 1994.
- [81] B. Adorno, “Robot Kinematic Modeling and Control Based on Dual Quaternion Algebra – Part I: Fundamentals,” Tech. Rep., 2017, <https://hal.archives-ouvertes.fr/hal-01478225v1>.
- [82] H. Asada and J.-J. Slotine, *Robot analysis and control*. John Wiley & Sons, 1986.
- [83] E. D. Sontag, *Mathematical control theory: deterministic finite dimensional systems*. Springer Science & Business Media, 2013, vol. 6.
- [84] R. W. Brockett, “Asymptotic stability and feedback stabilization,” in *Differential Geometric Control Theory*. Birkhauser, 1983, pp. 181–191.

- [85] J. W. Milnor, *Topology from the differentiable viewpoint*. Univ. Virginia Press, 1965.
- [86] D. E. Koditschek, “Application of a new Lyapunov function to global adaptive attitude tracking,” in *Proceedings of the 27th IEEE Conference on Decision and Control*, vol. 1, 1988, pp. 63–68.
- [87] B. Wie and P. M. Barba, “Quaternion feedback for spacecraft large angle maneuvers,” *Journal of Guidance, Control, and Dynamics*, vol. 8, no. 3, pp. 360–365, 1985.
- [88] S. Salcudean, “A globally convergent angular velocity observer for rigid body motion,” *IEEE Transactions on Automatic Control*, vol. 36, no. 12, pp. 1493–1497, 1991.
- [89] O.-E. Fjellstad and T. I. Fossen, “Quaternion feedback regulation of underwater vehicles,” in *Proceedings of the 3rd IEEE Conference on Control Applications*, vol. 2, 1994, pp. 857–862.
- [90] J. Thienel and R. M. Sanner, “A coupled nonlinear spacecraft attitude controller and observer with an unknown constant gyro bias and gyro noise,” *IEEE Transactions on Automatic Control*, vol. 48, no. 11, pp. 2011–2015, 2003.
- [91] D. Fragopoulos and M. Innocenti, “Stability considerations in quaternion attitude control using discontinuous Lyapunov functions,” *IEE Proceedings - Control Theory and Applications*, vol. 151, no. 3, pp. 253–258, 2004.
- [92] R. Kristiansen, P. J. Nicklasson, and J. T. Gravdahl, “Satellite attitude control by quaternion-based backstepping,” *IEEE Transactions on Control Systems Technology*, vol. 17, no. 1, pp. 227–232, 2009.
- [93] A. A. Cardenas, S. Amin, and S. Sastry, “Secure control: Towards survivable cyber-physical systems,” in *Proceedings of the 28th International Conference on Distributed Computing Systems Workshops*, 2008, pp. 495–500.
- [94] J. Hu, J. Shen, and D. Lee, “Resilient stabilization of switched linear control systems against adversarial switching,” *IEEE Transactions on Automatic Control*, vol. 62, no. 8, pp. 3820–3834, 2017.
- [95] R. A. Mayo, “Relative quaternion state transition relation,” *Journal of Guidance, Control, and Dynamics*, vol. 2, no. 1, pp. 44–48, 1979.
- [96] P. E. Crouch and R. Grossman, “Numerical integration of ordinary differential equations on manifolds,” *Journal of Nonlinear Science*, vol. 3, no. 1, pp. 1–33, 1993.
- [97] O. Huber, V. Acary, B. Brogliato, and F. Plestan, “Implicit discrete-time twisting controller without numerical chattering: Analysis and experimental results,” *Control Engineering Practice*, vol. 46, pp. 129–141, 2016.
- [98] L. F. d. C. Figueredo, “Kinematic control based on dual quaternion algebra and its application to robot manipulators,” Ph.D. dissertation, 2016, available at <http://repositorio.unb.br/handle/10482/21834>.
- [99] W. Basener, *Topology and Its Applications*, ser. Pure and Applied Mathematics: A Wiley Series of Texts, Monographs and Tracts. Wiley, 2013.
- [100] R. Sanfelice, R. Goebel, and A. R. Teel, “Invariance principles for hybrid systems with connections to detectability and asymptotic stability,” *IEEE Transactions on Automatic Control*, vol. 52, no. 12, pp. 2282–2297, Dec. 2007.

- [101] X. Wang and C. Yu, “Unit dual quaternion-based feedback linearization tracking problem for attitude and position dynamics,” *Systems & Control Letters*, vol. 62, no. 3, pp. 225–233, mar 2013.
- [102] J.-Y. Wen and K. Kreutz-Delgado, “The attitude control problem,” *IEEE Transactions on Automatic Control*, vol. 36, no. 10, pp. 1148–1162, 1991.
- [103] O. Huber, V. Acary, and B. Brogliato, “Analysis of explicit and implicit discrete-time equivalent-control based sliding mode controllers,” INRIA, Research Report RR-8383, Oct. 2013, available at <https://hal.inria.fr/hal-00875209>.
- [104] K. Nagatani, S. Kiribayashi, Y. Okada, K. Otake, K. Yoshida, S. Tadokoro, T. Nishimura, T. Yoshida, E. Koyanagi, M. Fukushima, and S. Kawatsuma, “Emergency response to the nuclear accident at the fukushima daiichi nuclear power plants using mobile rescue robots,” *Journal of Field Robotics*, vol. 30, no. 1, pp. 44–63, 2013.
- [105] S.-J. Chung, U. Ahsun, J.-J. Slotine, and D. Miller, “Application of synchronization to cooperative control and formation flight of spacecraft,” in *AIAA Guidance, Navigation and Control Conference and Exhibit*, 2007, p. 6861.
- [106] A. Abdessameud and A. Tayebi, “Attitude synchronization of a group of spacecraft without velocity measurements,” *IEEE Transactions on Automatic Control*, vol. 54, no. 11, pp. 2642–2648, 2009.
- [107] N. Jacobson, *Basic Algebra I*, 2nd ed. W.H. Freeman and Company, 1985.
- [108] C. Meyer, *Matrix Analysis and Applied Linear Algebra*, ser. Matrix Analysis and Applied Linear Algebra. Society for Industrial and Applied Mathematics, 2000.
- [109] J. M. Lee, *Introduction to Smooth Manifolds*, 2nd ed., ser. Graduate Texts in Mathematics. Springer New York, 2013.
- [110] B. Felzenszwalb, *Álgebras de Dimensão Finitas*. Rio de Janeiro, Brasil: Instituto de Matemática Pura e Aplicada, 1979.
- [111] J. J. Duistermaat and J. A. Kolk, *Lie groups*. Springer Science & Business Media, 2012.
- [112] K. Sakai, *Geometric aspects of general topology*. Springer, 2013.
- [113] N. P. Bhatia and O. Hájek, *Local semi-dynamical systems*. Springer, 2006, vol. 90.
- [114] D. Gabai, “The Whitehead manifold is a union of two Euclidean spaces,” *Journal of Topology*, vol. 4, no. 3, pp. 529–534, 2011.
- [115] V. Guillemin and A. Pollack, *Differential topology*. American Mathematical Society, 2010, vol. 370.
- [116] J. M. McCarthy, *Introduction to Theoretical Kinematics*. MIT Press, 1990.
- [117] D. E. Koditschek, “Application of a new Lyapunov function to global adaptive attitude tracking,” in *Proceedings of the 27th IEEE Conference on Decision and Control*, vol. 1, Austin, TX, dec 1988, pp. 63–68.
- [118] V. I. Arnold, “Ordinary differential equations,” 1992.
- [119] A. Cima, F. Manosas, and J. Villadelprat, “A poincaré-hopf theorem for noncompact manifolds,” *Topology*, vol. 37, no. 2, pp. 261–277, 1998.

Index

- Abelian group, 80
- Algebra, 83
- Associative algebra, 83

- Closed graph theorem, 10
- Conjugate
 - of dual quaternion, 29
 - of quaternion, 25
- Contractible manifold, 88

- Division algebra, 83
- Dual component, 28
- Dual unit, 28

- Euler symmetric parameters, 24
- Euler-Rodrigues parameters, 24

- Field, 82

- Graph of set-valued function, 10
- Group, 80
- Group homomorphism, 81

- Hybrid arc, 16
- Hybrid basic conditions, 14
- Hybrid time domain, 15

- Imaginary component
 - of dual quaternion, 28
 - of quaternion, 25
- Index, 92
- Inner semicontinuous, 10

- \mathcal{KL} -class function, 19
- Krasovskii regularization
 - of a differential (difference) equation, 12
 - of a hybrid system, 20

- Lie algebra, 86
- Lie group, 81
- Local trivialization, 89
- Locally bounded, 12
- Lyapunov function candidate, 18

- Möbius bundle, 90

- Norm
 - of dual quaternion, 29
 - of quaternion, 25

- Outer limit, 9
- Outer semicontinuous, 9

- Plücker coordinates, 30
- Poincaré-Hopf theorem, 93
- Pre-asymptotically stable, 17
- Pre-attractive, 17
- Pre-stable, 17
- Primary component, 28
- Principle of transference, 32
- Proper indicator, 19
- Pure imaginary dual quaternions, 28

- Real component
 - of dual quaternion, 28
 - of quaternion, 25
- Rodrigues' rotation formula, 26

- σ -perturbation, 21
- solution in Carathéodory sense, 12
- Study quadric, 29
- Subgroup, 81

- Trivial bundle, 90
- Twist, 31

- Unit quaternions, 25

- Vector bundle, 89
- Vector space, 82
 - Normed, 82